DIVERSITY AND POTENTIAL GEOCHEMICAL FUNCTIONS OF PROKARYOTES IN HOT SPRINGS OF THE UZON CALDERA, KAMCHATKA

by

WEIDONG ZHAO

(Under the Direction of Chuanlun L Zhang and Christopher S Romanek)

ABSTRACT

Hot springs are modern analogs of ancient hydrothermal systems where life may have emerged and evolved. Autotrophic microorganisms play a key role in regulating the structure of microbial assemblage and associated biochemical processes in hot springs. This dissertation aims to elucidate the diversity, abundance and ecological functions of multiple groups of chemoautotrophs that use diverse energy sources including CO, NH_3, and H_2 in terrestrial hot springs of the Uzon Caldera, Kamchatka (Far East Russia).

This dissertation consists of seven chapters.

Chapter 1 reviews studies in geochemistry and microbiology of studied area.

Chapter 2 reports H_2, CO_2, CH_4 and CO contents and the $\delta^{13}C$ values in vent gas samples. The gases were determined to be thermogenic with small temporal but large spatial variations among the springs investigated. Chemical and partial isotope equilibria between CO_2 and CH_4 may be attained in the subsurface at elevated temperature.

Chapter 3 shows the distribution of bacteria was spatially heterogeneous whereas that of archaea was related to geographic features. Cluster analyses group bacterial and archaeal communities according to their similarities of lipid compositions. Hydrogen-utilizing *Aquificales* appeared to be dominant in two of the four bacterial groups, but was outnumbered by presumably *Cyanobacteria-Thermotogae* or *Proteobacteria-Desulfurobacterium* types in the other two groups. The lipid data also suggest the

existence of possibly three types of archaea with each type producing one of GDGT-0, GDGT-1, and GDGT-4 as the main membrane lipids, respectively.

Chapters 4 and 5 describe a novel aerobic, thermophilic and alkalitolerant bacterium *Caldalkalibacillus uzonensis*, which tolerated >90% headspace CO but cannot utilize CO as carbon and energy sources.

Chapter 6 focuses on the study of carbon isotope fractionation associated with carbon fixation by an anaerobic CO oxidizing hydrogenogen *Carboxydothermus hydrogenoformans*. It reveals that a feedback system tends to hold the $\delta^{13}C$ value constant among CO, CO_2 and biomass. A steady state point and associated carbon isotope fractionations ($\varepsilon_{A\text{-}B} = \delta_A - \delta_B$) were hypothesized to be 18‰ for the CO_2-CO system, 2‰ for the bulk biomass-CO_2 system, and -20‰ for the CO-biomass system.

Chapter 7 reports the diversity and distribution of ammonia-oxidizing archaea (AOA) in hot springs of the Uzon Caldera. A patchy presence of AOA and the absence of AOB (ammonia-oxidizing bacteria) were observed through PCR based surveys. AOA diversity correlated to abundances of archaea or crenarchaeota but was not directly correlated to temperature or chemical variables.

INDEX WORDS: Kamchatka, hot springs, PLFA, GDGT, hydrogen-oxidizing bacterium, *Aquificales*, CO-oxidizing bacterium, ammonia-oxidizing archaea, AOA, CO_2 fixation, carbon stable isotopes, isotope fractionation, pathways, *Carboxydothermus hydrogenoformans*, *Caldalkalibacillus uzonensis*

DIVERSITY AND POTENTIAL GEOCHEMICAL FUNCTIONS OF PROKARYOTES IN HOT SPRINGS OF THE UZON CALDERA, KAMCHATKA

by

WEIDONG ZHAO

B.S. Peking University, P. R. China, 1997

M.S. The Institute of Oceanology, Chinese Academy of Sciences, P. R. China, 2000

A Dissertation Submitted to the Graduate Faculty of The University of Georgia in Partial Fulfillment of the Requirements for the Degree

DOCTOR OF PHILOSOPHY

ATHENS, GEORGIA

2008

DIVERSITY AND POTENTIAL ECOLOGICAL FUNCTIONS OF PROKARYOTES IN HOT SPRINGS OF THE UZON CALDERA, KAMCHATKA

by

WEIDONG ZHAO

Major Professors:	Chuanlun L Zhang Christopher S Romanek
Committee:	Juergen Wiegel Gary Mills Ming-Yi Sun

Electronic Version Approved:

Maureen Grasso
Dean of the Graduate School
The University of Georgia
August 2008

DEDICATION

This work is dedicated to my wife Xiaozhen, who has been a constant source of unwavering love, concern, support and strength through all these years.

ACKNOWLEDGEMENTS

I would like to thank my major advisors Dr. Chuanlun Zhang and Dr. Christopher Romanek for the guidance and instilling in me the qualities of being a good scientist. Their insightful comments and constructive criticisms at different stages of my research have been the major driving force to a high standard research. A special thank goes to my committee member Dr. Juergen Wiegel. He has been an excellent mentor who taught me many concepts and techniques of microbiology. It has been a wonderful experience working in his lab during the first half term of my graduate studies. I would like to thank my other committee members Dr. Gary Mills and Dr. Ming-Yi Sun for supporting my research by providing timely advices and access to instrumentation available in their labs.

I am indebted to many US and Russian colleagues. I thank Dr. Ann Pearson and Yundan Pi (Harvard University) for helping with the archaeal lipid analysis, Dr. Tatyana Sokolova and Dr. Elizaveta Osmolovskaya of Institute of Microbiology, Russia, and Dr. Frank Robb and Steve Techtmann of University of Maryland for providing me strains of bacteria. I thank Dr. Douglas Crowe (Geology, UGA) for providing me the site maps, Dr. Mary Ann Moran for allowing me to use her lab space in one of my projects and helps throughout my graduate study, and Dr. Paul Schroeder (Geology, UGA) for sharing the sampling logs. Special thanks are due to all people who participated in the field expeditions to Uzon Caldera, Kamchatka from 2003 to 2006, which made available the samples for my dissertation.

I thank Qi (Ellen) Ye, Zhiyong Huang, Yiliang Li, Heather Brant, Julie Fiser, Noelle Garvin, Morris Jones, Yong-Jing Lee, Isaac Wagner, Noha Mesbah and Elizabeth Burgess for their supports and friendships.

Finally, I appreciate the financial support from the National Science Foundation and the Department of Energy of the United States.

TABLE OF CONTENTS

Page

ACKNOWLEDGEMENTS v

LIST OF TABLES vii

LIST OF FIGURES ix

INTRODUCTION 1

CHAPTER

1. LITERATURE REVIEW: GEOCHEMISTRY AND MICROBIOLOGY OF HOT SPRINGS IN KAMCHATKA, RUSSIA 3
2. GEOCHEMISTRY OF REDUCED GASES AND CARBON DIOXIDE IN KAMCHATKA HOT SPRINGS 20
3. LIPIDS AND STABLE CARBON ISOTOPES IN HOT SPRINGS OF THE UZON CALDERA, KAMCHATKA: IMPLICATIONS FOR MICROBIAL COMMUNITY DYNAMICS 38
4. *THERMALKALIBACILLUS UZONENSIS* GEN. NOV. SP. NOV., A NOVEL AEROBIC ALKALITOLERANT THERMOPHILIC BACTERIUM ISOLATED FROM A HOT SPRING IN THE UZON CALDERA, KAMCHATKA 86
5. *CALDALKALIBACILLUS UZONENSIS* SP. NOV., AND EMENDED DESCRIPTION OF THE GENUS *CALDALKALIBACILLUS* 109
6. STABLE CARBON ISOTOPE FRACTIONATION ASSOCIATED WITH CARBON FIXATION BY CHEMOLITHOAUTOTROPHIC ANAEROBIC CO-OXIDIZING BACTERIUM *CARBOXYDOTHERMUS HYDROGENOFORMANS* 116
7. AMMONIA-OXIDIZING ARCHAEA IN KAMCHATKA HOT SPRINGS 138

CONCLUSIONS 171

LIST OF TABLES

Page

Table 1.1. Gas composition, surface water temperature and dominant minerals of hot springs in Kamchatka 11

Table 1.2. Thermophilic bacteria isolated from Kamchatka hot springs 12

Table 1.3. Archaea isolated from Kamchatka hot springs. 13

Table 2.1. Gas composition in vent gas samples collected in 2005 and 2006 27

Table 2.2. Carbon isotope values of gas samples collected in 2005 and 2006 28

Table 3.1. Sample identification and description 58

Table 3.2. Mole% of 13 major phospholipid fatty acids from Kamchatka samples 59

Table 3.3. Results of SIMPER analysis showing similarity of PLFA between samples in each group identified by the cluster analysis 60

Table 3.4. Results of SIMPER analysis showing primary contributors (cumulative contribution >90%) to dissimilarities between groups 61

Table 3.5. A subset of samples used for BIOENV routine with six environmental variables. 62

Table 3.6. GDGT compositions of hot spring samples from the Uzon Caldera 63

Table 3.7. Similarity of GDGT composition between samples in group G0 to G6. 64

Table 3.8. Results of SIMPER analysis of archaeal GDGT showing primary contributors (cumulative contribution >90%) to dissimilarities between groups. 65

Table 3.9. $\delta^{13}C$ values of PLFAs, bulk organic matter and hot spring vent CO_2 analyzed in this study. 66

Table S3.1. The best seven correlations between lipid distribution patterns and environmental variable combinations revealed by the BIOENV routine in Primer V5 program 74

Table S3.2. ANOSIM of PLFA sample groups using temperature data 75

Table 4.1. Differentiating characteristics of strain JW/WZ-YB58^T and other related *Firmicutes* species 100

Table 4.2. Membrane fatty-acid composition of strain JW/WZ-YB58^T and other related species 101

Table 5.1. Differentiating characteristics of strain JW/WZ-YB58^T and other related *Firmicutes* species 113

Table 6.1. The head space gas compositions and $\delta^{13}C$ values for CO and CO_2 over the course of incubation for the experiment one 128

Table 6.2. The head space gas compositions and $\delta^{13}C$ values for CO and CO_2 at the beginning and terminal time points of the incubation for the experiment two 129

Table 6.3. $\delta^{13}C$ values of bulk biomass, CO, and CO_2 for the experiments one and two, and instantaneous enrichment between CO and CO_2 ($\varepsilon_{CO\text{-}CO_2}$) at the end of the experiments. 130

Table 7.1. Physicochemisty of sampling sites 155

Table 7.2. Statistics of amoA gene clone libraries. 156

Table 7.3. S-LIBSHUFF comparison of amoA gene clone libraries 157

LIST OF FIGURES

PAGE

Fig 1.1. Map of Kamchatka peninsula, most volcanic activities were located in central and eastern Kamchatka volcanic belt 14

Fig 2.1. H_2 composition in vent gas samples. 29

Fig 2.2. CH_4 composition in vent gas samples 30

Fig 2.3. CO_2 composition in vent gas samples 31

Fig 2.4. CO composition in vent gas samples. 32

Fig 2.5. Correlation of CH_4 and H_2 gas contents in vent gas samples 33

Fig 2.6. Upper panel, a) diagram showing typical range of $\delta^{13}C$ values of biogenic and thermogenic CH_4 and CO_2. Bottom panel, b) same plot at larger scale with computed carbon isotope equilibrium lines from 200 to 500°C 34

Fig 2.7. Comparison of measured values of $\Delta^{13}C$ for the CO_2-CH_4 system versus log (X_{CH4}/X_{CO2}) for gas samples collected from the Uzon Caldera in 2005 and 2006 35

Fig 3.1. Map of sampling sites. (a) Satellite area map of the Uzon Caldera. Arrow indicates the sampling area. (b) Detailed map of sampling sites at the EETF and CETF. 67

Fig 3.2. Hierarchical cluster tree of PLFAs. 69

Fig 3.3. Hierarchical cluster tree of GDGTs 70

Fig 3.4. Variation of GDGT species between groups defined by the hierarchical cluster analysis. Upper panel, GDGT-1, -2 and -3; bottom panel, GDGT-0 and -4. 71

Fig 3.5. Non-metric multidimensional scaling (MDS) analysis of the five most abundant GDGTs 72

Fig 3.6. $\delta^{13}C$ values of PLFAs and their predicted ranges for different carbon fixation pathway relative to $\delta^{13}C$ values of CO_2. 73

Fig 4.1. Phase-contrast microphotograph of strain JW/WZ-YB58^T. 102

Fig 4.2. Electron micrographs. a, scanning electron microscopy revealing retarded peritrichous flagellation (arrow head) and an uneven cell surface. b, transmission electron microscopy revealing organized internal features as well as several circular electron dense bodies of unknown function and nature in each cell 103

Fig 4.3. Phylogenetic tree based on 16S rRNA gene sequences. Comparison between strain JW/WZ-YB58^T and other related, mainly alkaliphilic and thermophilic species. 104

Fig 5.1. Phylogenetic tree for 16S rDNA sequences of *Caldalkalibacillus uzonensis* JW/WZ-YB58^T (DQ221694) and other related, mainly alkaliphilic and thermophilic species 114

Fig 6.1. Proposed acetyl-CoA pathway for the CO-oxidizing hydrogenogenic bacterium *Carboxydothermus hydrogenoformans* based on the genome sequence of *C. hydrogenoformans* Z2901 and KEGG pathway database. 131

Fig 6.2. Optical density of *C. hydrogenoformans* cultures and changes in carbon isotope compositions of head space CO and CO_2 in Experiment 1 132

Fig 6.3. Optical density of *C. hydrogenoformans* cultures and changes in the carbon isotope compositions of head space CO and CO_2 for experiment 2 133

Fig 6.4. A hypothetical feedback system for the CO and CO_2 fixation by *C. hydrogenothermus*. Isotope enrichment factor (ε) associated with each process is labeled in the pink square 134

Fig 7.1. Deduced amino acid trees of archaeal *amo*A gene obtained from hot springs in the Uzon Caldera. Only representative OTUs (<95% sequence identity) are shown 159

Fig 7.2. Relative distribution of *amo*A gene clones in the three phylogenetic clusters 160

Fig 7.3. Abundances of total archaea and crenarchaeota in each sample determined by Q-PCR. 161

Fig 7.4. Inverse linear correlation between the Shannon's diversity index of AOA phylotypes and 16S rRNA gene copies of total archaea and crenarchaeota. 162

Fig 7.5. a) Normalized GDGT compositions of the bulk environmental samples; b) Cluster analysis of the GDGT composition 164

INTRODUCTION

Hot springs are modern analogs of ancient hydrothermal systems where life may have emerged and evolved. Autotrophic microorganisms play a key role in regulating the structure of microbial assemblages and associated biochemical processes in hot springs. This dissertation aims to elucidate the diversity, abundance and ecological functions of multiple groups of chemolithoautotrophs that use diverse energy sources including CO, NH_3, and H_2 in hot springs of the Uzon Caldera, Kamchatka (Far East Russia). Our current understanding of these topics is incomplete, therefore, multiple approaches including stable isotopes, lipid biomarkers, cultivation, and gene clone libraries were employed to investigate different aspects of the autotrophic community in the hot springs.

This dissertation consists of eight chapters. Chapter 1 reviews studies in geochemistry and microbiology in Kamchatka hot springs conducted during the past thirty years. Chapter 2 reports H_2, CO_2, CH_4 and CO contents and $\delta^{13}C$ values for vent gas samples collected during 2005 and 2006 field trips. Temporal and spatial variations in gas chemistry were examined. The origin of the vent gases and attainment of chemical and isotope equilibria between CO_2 and CH_4 in the subsurface were discussed.

Chapter 3 discusses the microbial community dynamics in Kamchatka hot springs using integrated lipid and stable isotope approaches. With the aid of statistics, membrane lipids of bacterial phospholipid fatty acids (PLFAs) and archaeal glycerol alkyl glycerol tetraethers (GDGTs) were used as semi-quantitative proxies to examine taxonomic and metabolic diversities, compare the similarity of microbial communities between sites, and gain insight into the temporal and spatial variations of community structures in a variety of hot springs. Carbon fixation pathways used by dominant microorganisms in different bacterial community types were predicted using carbon isotope analysis of PLFAs.

Chapters 4 to 6 focus on microbial CO-oxidation. Chapters 4 and 5 describe a novel aerobic, thermophilic and alkalitolerant, CO-insensitive bacterium *Caldalkalibacillus uzonensis*, which was isolated from a bacterial mat collected from the Zavarzin II spring in 2004. Chapter 6 is centered on

carbon isotope fractionation associated with carbon fixation by a model anaerobic CO oxidizing and H_2 producing bacterium *Carboxydothermus hydrogenoformans*. Using a series of batch cultures, changes in carbon isotope compositions of CO, CO_2, and biomass were monitored over the course of multiple incubations. A carbon fixation mechanism with associated isotope fractionations between the carbon bearing species (CO, CO_2 and bulk biomass) is proposed based on the acetyl-CoA pathway.

Chapter 7 reports on the diversity and distribution of ammonia-oxidizing archaea (AOA) in hot springs of the Uzon Caldera, Kamchatka. The phylogenetic distribution of AOA in a variety of hot springs was examined by PCR amplification of putative archaeal *amo*A genes. Relationships between the phylogeny of AOA operational taxonomic units (OTUs) and environmental variables or quantities of archaea and crenarchaeota are investigated.

Finally a conclusion section highlights main findings of this dissertation.

CHAPTER 1

LITERATURE REVIEW:

GEOCHEMISTRY AND MICROBIOLOGY OF HOT SPRINGS IN KAMCHATKA, RUSSIA*

* Zhao, W. D., Romanek, C. S., Mills, G., Wiegel, J. and Zhang, C. L., 2005. Geological Journal of Chinese Universities 11(2), 217-223
Reprinted here with permission of publisher

ABSTRACT

Kamchatka is one of the most active regions of volcanism in the world because it is located in the transitional zone where the Eurasian plate, North American plate and Pacific plates meet. As a result, Kamchatka has numerous hydrothermal systems, which constantly release geothermal gases and fluids out to the earth surface. Geothermal gases such as N_2 and CO_2 may prevail in the outflows but H_2, CH_4 and H_2S also occur frequently. Hot spring waters in Kamchatka may have multiple origins including meteoric and magmatic water. The temperature of these hot springs ranges from ~20°C to greater than 90°C. Water chemistry also varies dramatically with pH ranging from 3.1 to 9.8. Hydrothermal fluids are dominated by NaCl-type of water and may contain various dissolved constituents including K^+, H_3BO_3, H_4SiO_4, Ca^{2+}, and SO_4^{2-}. Volcanic ore-formation prevails in the high thermal activity regions in Kamchatka and precipitates may be dominated by silica crusts, sulfur and Hg-Sb-As-FeS deposits. Oils are also generated in the region and dominated by n-alkanes.

More than 24 novel thermophilic microorganisms have been isolated from hot springs in Kamchatka. Most of these isolates are heterotrophs; however, autotrophs may be equally abundant depending on the spring conditions. Collectively, these organisms may play important roles in biogeochemical cycling of carbon, nitrogen, sulfur and iron in the hydrothermal system. Culture-independent approaches and quantitative methods are now employed to enhance our understanding of the ecology and biogeochemical functions of microorganisms in Kamchatka hot springs.

Keywords: Hot springs, geochemistry, microbiology, Kamchatka

GEOLOGY AND CHEMISTRY OF HYDROTHERMAL SYSTEMS IN KAMCHATKA

The Kamchatka Peninsula in the Far East Russia is the north-western unit of the Pacific Ring of Fire, which is located on a unique transitional zone where the Eurasian plate, North American plate and Pacific plate meet. The convergence of these plates creates high seismic activities and broad volcanic and hydrothermal systems in Kamchatka, which is about 370,000 square kilometers in area (Fig 1.1). There are over 30 active volcanoes and numerous hot springs and most of them are located in central and eastern Kamchatka. In eastern Kamchatka, they may be subdivided in five areas: Geyser Valley, Uzon Caldera,

Academii Nauk caldera, Pauzhetka and Kireunckaya (Karpov, unpublished data). In particular, the Uzon Caldera and Geyser Valley systems located along a collapsed caldera are the best described hydrothermal system in the area.

Volcanic activity releases geothermal fluids containing large amounts of gases generated through both biotic and abiotic processes. In Kamchatka, free N_2 and CO_2 prevail in the outflows but H_2, CH_4 and H_2S also occur frequently (Dymkin *et al.* 1988). The gas composition appears to correspond to the specific water chemistry and surface water temperature (Table 1.1). In addition, aromatic hydrocarbons and alkenes are present in fumaroles, which may be generated through thermal degradation of organic matter (Capaccioni *et al.*, 1993).

The origin of the water can be determined based on the stable isotopes of hydrogen and oxygen. Values of δD and $\delta^{18}O$ that fall along the meteoric line having a slope of 8 are characteristic of meteoric water, whereas values that fall off the line may be modified by other processes, for example, evaporation or mixing (Clark and Fritz, 1997). The δD of the hot springs values fall in the range of -119‰ to -74‰ and the $\delta^{18}O$ fall in the range of -16‰ to -2‰ (Jones *et al.*, 2004; Karpov *et al.* 2000). These values suggest that waters in these hot springs are predominantly meteoric water in origin with some dominated by magmatic water, which typically have a window of $\delta^{18}O$ 3‰ to 11‰ and δD -94‰ to -40‰ (Clark and Fritz, 1997). Because magmatic water usually co-occurs with magmatic gas emissions, the isotope data also indicate that some waters having H_2S contain the magmatic components while waters dominated by N_2, CH_4 and CO_2 are practically free of magmatic components (Cheshko, 1994).

Spring waters in Kamchatka also vary in pH (3.1 to 9.8). Chemical composition in the venting water varies with the geographical origin and the maximal surface-temperature of the spring. For example, the Geyser Valley-Uzon Caldera systems are dominated by high-temperature outflow springs, which are enriched in sodium chloride, silicic acid and boron (Karpov and Naboko, 1990). However, the salt concentration of Uzon Caldera system is twice as high as that of Geyser Valley system (Karpov, unpublished data). Based on the temperature of venting water and the dominant chemical composition, five hydrochemical types are distinguished: Na-Cl-hyper-high temperature, Na-Cl-SO_4^{2-}-HCO_3^--high

temperature, Na-Ca-SO_4^{2-}-medium temperature, Na-HCO_3^--Cl^--medium temperature, and Na-Ca-HCO_3^--SO_4^{2-}-low temperature. Waters with high temperature and acidic to neutral pHs generally contain more salts than water with lower temperature and acidic water (Karpov *et al.*, 2000; unpublished data).

The geothermal system in Kamchatka has considerable mineral and hydrocarbon resources. Volcanic ore formation prevails in the high thermal activity regions of Kamchatka. For instance, sulfur and Hg-Sb-As-FeS are two major ores observed in the Uzon Caldera. It is estimated that the total deposition of elements in the area is about 1000 tons of sulfur, 7000 tons of arsenic, 350 tons of antimony, and 200 tons of mercury (Karpov 1990; Karpov and Naboko, 1990). The formation of oil is also observed in the Uzon Caldera. Structural analyses indicate that oils are dominated by n-alkanes with C_{18} as the most abundant compound. Analyses of biomarker and carbon isotopic signatures suggest that oils are generated from multiple origins including recent plants and ancient biomass (Bazhenova *et al.*, 1998).

MICROBIOLOGY OF KAMCHATKA HOT SPRINGS

It has long been realized that microorganisms play essential roles in natural environments, particularly in extreme environments such as hot springs. Although Baas-Backing's formula of microbial biogeography, "everything is everywhere; the environment selects" is accepted by many microbiologists, it has been challenged by others including a recent study using hyperthermophilic archaeon *Sulfolobus* as model microorganism (Whitaker *et al.*, 2003) to show that the geographical distribution patterns exist in geothermal regions on a global scale. Therefore, investigation of microorganisms in isolated terrestrial hot springs would enhance our understanding of both thermophilic microbial diversity in nature and the evolutionary mechanisms that shape it.

Studies of microbial diversity in other terrestrial hydrothermal systems reveal that the microbial communities are usually highly diverse and contain representative ancient lineage of life forms. For example, *Aquificales* are thought to be one of the oldest bacterial lineages and have been isolated from a number of hot springs worldwide including those in the Yellowstone National Park (USA), Kamchatka (Russia), Iceland, and Lake Tanganyika (Africa) and Azores (Portugal; Aguiar *et al.*, 2004; Eder and Huber, 2002; Reysenbach and Shock, 2002; Yamamoto *et al.*, 1998). These studies imply that hot springs

may be modern analogs for studying the early evolution of microbial life in ancient geothermal systems that were predominant on Earth.

Recent approaches in microbiology combine culture-dependent and culture-independent technologies to understand the microbial diversity and ecological function in certain environments. The cultivation approach offers systematic studies on the physiology and phylogeny of individual species, thus their specific roles in a certain environment can be assessed. Currently, however, less than 1% of the assumed total amount of microbial species can be cultivated. Culture-independent approaches, such as phylogenetic analysis based on small subunit (SSU) ribosomal RNA genes sequences, overcome this deficiency and are essential for understanding microbial diversity in natural settings.

Unlike some well studied hot springs such as those in the Yellowstone National Park, hot springs in Kamchatka have not been explored in any detail in terms of microbial diversity. Therefore it is difficult to assess the microbial robustness of the region. However, microbiologists have isolated about 24 novel microorganisms from various regions of Kamchatka peninsula in the past twenty years. Many of them are anaerobic thermophiles. Half of them were collected from hot springs of Uzon Caldera-Geyser Valley systems. These microorganisms include not only autotrophic hydrogen-oxidizing bacteria, carbon monoxide-oxidizing bacteria and iron-oxidizing or reducing bacteria, but also heterotrophic fermentative or sulfur-reducing bacteria and archaea, and sulfur-oxidizing archaea as well (Table 1.2 and Table 1.3).

Although more heterotrophic species were obtained in isolation than autotrophs, this does not suggest Kamchatka hot springs are dominated by heterotrophic microorganisms as isolates alone do not represent the breadth of microbial diversity in every environment. For example, microorganisms are known to live across a wide range of pH in the hot springs of Kamchatka; however, most isolates are neutrophilic microorganisms (Table 1.2 and Table 1.3).

Recent studies based on quantitative measurements of phospholipid fatty acids showed that cyanobacteria, green-sulfur bacteria, and green non-sulfur bacteria may be dominant autotrophic species (Romanek *et al.*, 2004), which could contribute significant amounts of carbon to the total community in each hot spring. This may be particularly important in pools having significant outflow and negligible

terrestrial input from surface runoff.

Anaerobic chemolithoautotrophs appear to be important in Kamchatka hot springs. These include methanogens, autotrophic sulfate-reducing bacteria, carbon monoxide-oxidizing bacteria, sulfur-reducing bacteria and iron-reducing bacteria (Bonch-Osmolovskaya *et al.*, 1999). In situ radioisotope experiments with $H^{14}CO_3^-$ show that maximal rate of methanogenesis is about 0.2 μg C L^{-1} day^{-1} at pH 7.0 and 60°C (Bonch-Osmolovskaya *et al.*, 1999). No methanogenesis is observed in acidic pools. However, acetogenesis, a process that produces acetate from CO_2, was detected in pools over a wide range of pHs (3.5- 8.5) and varying temperatures (60-80°C; Bonch-Osmolovskaya *et al.*, 1999). Maximal acetogenesis occurred at pH 8.5 and 60°C with a rate of more than 20 μg C L^{-1} day^{-1} (Bonch-Osmolovskaya *et al.*, 1999).

Carboxydotrophs are organisms capable of oxidizing CO to CO_2 and assimilating part of oxidized CO_2. These microorganisms may contribute significantly to the carbon cycle as the first component of the food chain in Kamchatka hot springs because of the availability of CO in these environments. Anaerobic oxidization of CO is observed to couple with hydrogen production in hot spring water column at pH 8.5 (Bonch-Osmolovskaya *et al.*, 1999). Representative bacteria include *Carboxydothermus hydrogenoformans* with an optimal temperature of 70°C, and *Carboxydocella thermautotrophica* with an optimal temperature of 68°C (Gerhardt *et al.*, 1991; Svetlichny *et al.*, 1991; Sokolova *et al.*, 2002). The CO utilization rate of *C. hydrogenoformans* can reach up to 178 μmol (mL culture)$^{-1}$ day^{-1}(Svetlichny *et al.*, 1991).

Lithotrophic reduction of sulfur and sulfate is detected in acidic hot springs with temperature optima of 60°C and 80°C, which coincide with the rate maxima of sulfidogenesis at these temperatures. This indicates that lithotrophic metabolism of sulfur or sulfate can be performed by both thermophilic and hyperthermophilic microorganisms. Moderately thermophilic sulfur reducers are represented by the genus *Desulfurella,* which is a group of obligate anaerobic bacteria that can grow lithoautotrophically by using H_2, CO_2 and S^0 (Bonchosmolovskaya *et al.*, 1990; Miroshnichenko *et al.*, 1998).

Isolates of archaeal sulfur-reducers are mainly heterotrophic or fermentative species. For example,

Desulfurococcus amylolyticus and *Thermoproteus uzoniensis* belong to phylum Crenarchaeota and both have an optimal growth temperature of about 90°C. *D. amylolyticus* grows heterotrophically on peptides, amino acids, starch and glycogen using S^0 as electron acceptor (Bonchosmolovskaya *et al.*, 1988). *T. uzoniensis* is a facultative sulfur reducer and can ferment peptides (Bonchosmolovskaya *et al.*, 1990). *Thermococcus litoralis* and *Thermococcus stetteri*, belonging to Euryarchaeota, grow on peptides and have optimal growth temperatures of 88°C and 75°C, respectively (Miroshnichenko *et al.*, 1989; Svetlichnyi *et al.*, 1987).

Processes of sulfur cycling in the natural environment are examined using tracers and rate measurements. Rates of sulfate- and sulfur-reduction vary spatially. Temperature may play a major role in such variation. For instance, the rate of sulfate reduction increases from 0.16 to 6 μg S cm^{-2} h^{-1} when water temperature drops from 73°C to 40°C in some microbial mats (Bonchosmolovskaya *et al.*, 1987). Enumerations showed that thermophilic (60°C) sulfate-reducing bacteria are present in 10 to 10^5 cultivable cells per ml sediment in various hot springs of Uzon Caldera (personal communication with Elizabeth Burgess). Nevertheless, sulfur- and sulfate-reducing microorganisms are potentially important for biogeochemical cycling of sulfur species in hot springs and could be the major energy source for microorganisms in hot spring ecosystems. However, recent studies on bioenergetics in Yellowstone geothermal ecosystems based on 16S rRNA gene clone libraries reveal that H_2 should be the primary fuel for hot spring microbial communities (Spear *et al.*, 2005). It would be interesting to see if this holds true for Kamchatka hot springs. However, quantitative approaches, such as fluorescent in situ hybridization (FISH), should be used to complement the clone library approach.

In addition to sulfur-reducers, sulfur-oxidizers are another important group that influences the sulfur cycle. As an example, the archaeal species *Sulfurococcus mirabilis* represents a group of the hyperthermophilic, facultative lithotrophic sulfur oxidizers that oxidize sulfur to sulfate under acidic conditions (pH 1.0-5.8) and 50-86°C (Golovacheva *et al.*, 1987).

Lithotrophic Fe(III)-reducing bacteria occur under various pH and temperature conditions in hot springs of Kamchatka. *Thermoanaerobacter siderophilus* is a facultative Fe(III)-reducing bacterium

growing lithoautotrophically on H_2 and CO_2 with Fe(III) as the electron acceptor. *T. siderophilus* grows optimally at 69-71°C (Slobodkin *et al.*, 1999). Similar to sulfur, lithotrophic iron-oxidizing bacteria have also been isolated from Kamchatka hot springs. For example, *Leptospirillum thermoferroxidans* is an obligate chemoautotrophic bacterium that oxidizes Fe(II) to Fe(III) with optimal growth temperature of 56.2°C (Golovacheva *et al.*, 1992).

SUMMARY

Terrestrial hot springs are heterogeneous both biogeochemically and spatially. They occur in various environments and are distributed widely over the world. Microbial species are diverse in hot springs and their ecological functions are not completely known. Thus the role of hot springs in global biogeochemical cycling and the preservation of ancient metabolic forms are difficult to be precisely interpreted with current knowledge. Understanding the behavior of thermophilic microbial communities will broaden our view of the importance of hydrothermal systems in the evolution of life and global chemical cycling. Kamchatka is a unique location that allows us to explore novel microbial species and their biogeochemical functions in geothermal systems. Based on the achievements of microbiological and geochemical studies, more interdisciplinary studies such as microbial ecological studies can enhance our understanding of hot springs as microbial paradises.

ACKNOWLEDGEMENT

This work is supported by the NSF Microbial Observatory Program (JW, CRS) and by the Environmental Remediation Sciences Division of the Office of Biological and Environmental Research, U.S. Department of Energy through the Financial Assistant Award no. DE-FC09-96SR18546 to the University of Georgia Research Foundation (CSR, GM, and CLZ).

Table 1.1. Gas composition, surface water temperature and dominant minerals of hot springs in Kamchatka (Karpov, unpublished data)

Type of water	Number of observations	Maximum surface water temperature (°C)	Gas composition
Na-Cl	27	>90	H_2-N_2-CO_2
Na-Cl-Silicic acid and metaboric acid	59	50-90	N_2
Na-Cl-HCO_3	15	>20	CH_4

Table 1.2. Thermophilic bacteria isolated from Kamchatka hot springs[†]

Name of isolates	Gram type	G+C %	Optimum T(°C)	Optimum pH	electron acceptor	Reference
'Anaerocellum thermophilum' Z-1320^T	+	36.7	72-75	7.1-7.3		Svetlichnyi *et al.*, 1990
Anoxybacillus voinovskiensis TH13^T	+	43.9	54	7-8	NO_3^-, O_2	Yumoto *et al.*, 2004
Hydrogenobacter hydrogenophilus Z-829^T	–	39-41	72-76	6.0-7.0	O_2	Pitulle *et al.*, 1994; Kryukov *et al.*, 1983
Carboxydocella thermautotrophica 41^T	+	45-47	58	7.0	H_2O	Sokolova *et al.*, 2002
Carboxydothermus hydrogenoformans Z-2901^T	+	39.0	70-72	6.8-7.0	H_2O	Gerhardt *et al.*, 1991; Svetlichny *et al.*, 1991
'Clostridium Uzonii' 1501/60 and 1611^T	+	34	60-65	7.0	O_2	Krivenko *et al.*, 1990
Desulfurella acetivorans DSM 5264^T	–	31.4	52-55	6.4-6.8	S^0	Bonchosmolovskaya *et al.*, 1990
Desulfurella kamchatkensis K-119^T	–	31.6	54	6.9-7.2	S^0	Miroshnichenko *et al.*, 1998
Desulfurella propionica U-8^T	–	32.2	55	6.9-7.2	S^0, $S_2O_3^{2-}$	Miroshnichenko *et al.*, 1998
Dictyoglomus turgidum Z-1310^T	–	32.5	72	7.0-7.1		Svetlichnii and Svetlichnaya, 1988
Leptospirillum thermoferroxidans L-88^T	–	56.2	45-50	1.65-1.9	O_2	Golovacheva *et al.*, 1992
Meiothermus rubber 21^T	–	61	60	8.0	O_2	Loginova and Egorova, 1975
Thermoanaerobacter siderophilus SR4^T	+	32.0	69-71	6.3-6.5	Fe(III) Oxide, SO_3^{2-},$S_2O_3^{2-}$, S° MnO_2	Slobodkin *et al.*, 1999
Thermoanaerobacter sulfurophilus L64^T	+	30.3	55-60	6.8-7.2	S, $S_2O_3^{2-}$	BonchOsmolovskaya *et al.*, 1997
Thermanaerovibrio velox Z-9701^T	–	54.6	60-65	7.3	S^0	Zavarzina *et al.*, 2000
'Thermoanaerobacter lactoethylicum' ZE-1^T	+	34.6	65	7.0		Kondratieva *et al.*, 1989
Thermovenabulum ferriorganovorum Z-9801^T	+	36	63-65	6.7-6.9	Fe(III),Mn(IV), nitrate, fumarate, S^0,H_2S, $S_2O_3^{2-}$	Zavarzina *et al.*, 2002

[†] Updated till March 2005

Table 1.3. Archaea isolated from Kamchatka hot springs. Type: Cr = Crenarchaeota, Eu = Euryarchaeota.

Name of isolates	Type	G+C%	Optimum T (°C)	Optimum pH	Reference
Acidilobus aceticus 1904^T	Cr	53.8	85	3.8	Prokofeva *et al.*, 2000
Desulfurococcus amylolyticus Z-533^T	Cr	42.1	90-92	6.4	Bonchosmolovskaya *et al.*, 1988
Thermococcus litoralis Z-1301^T	Eu	41	88	6.4	Svetlichnyi *et al.*, 1987
Thermococcus stetteri K-3^T	Eu	50.2	73-77	6.5	Miroshnichenko *et al.*, 1989
Sulfurococcus mirabilis INMI AT-59^T	Cr	43-46	70-75	2.0-2.6	Golovacheva *et al.*, 1987
Thermoproteus uzoniensis Z-605^T	Cr	56.5	90	5.6	Bonchosmolovskaya *et al.*, 1990

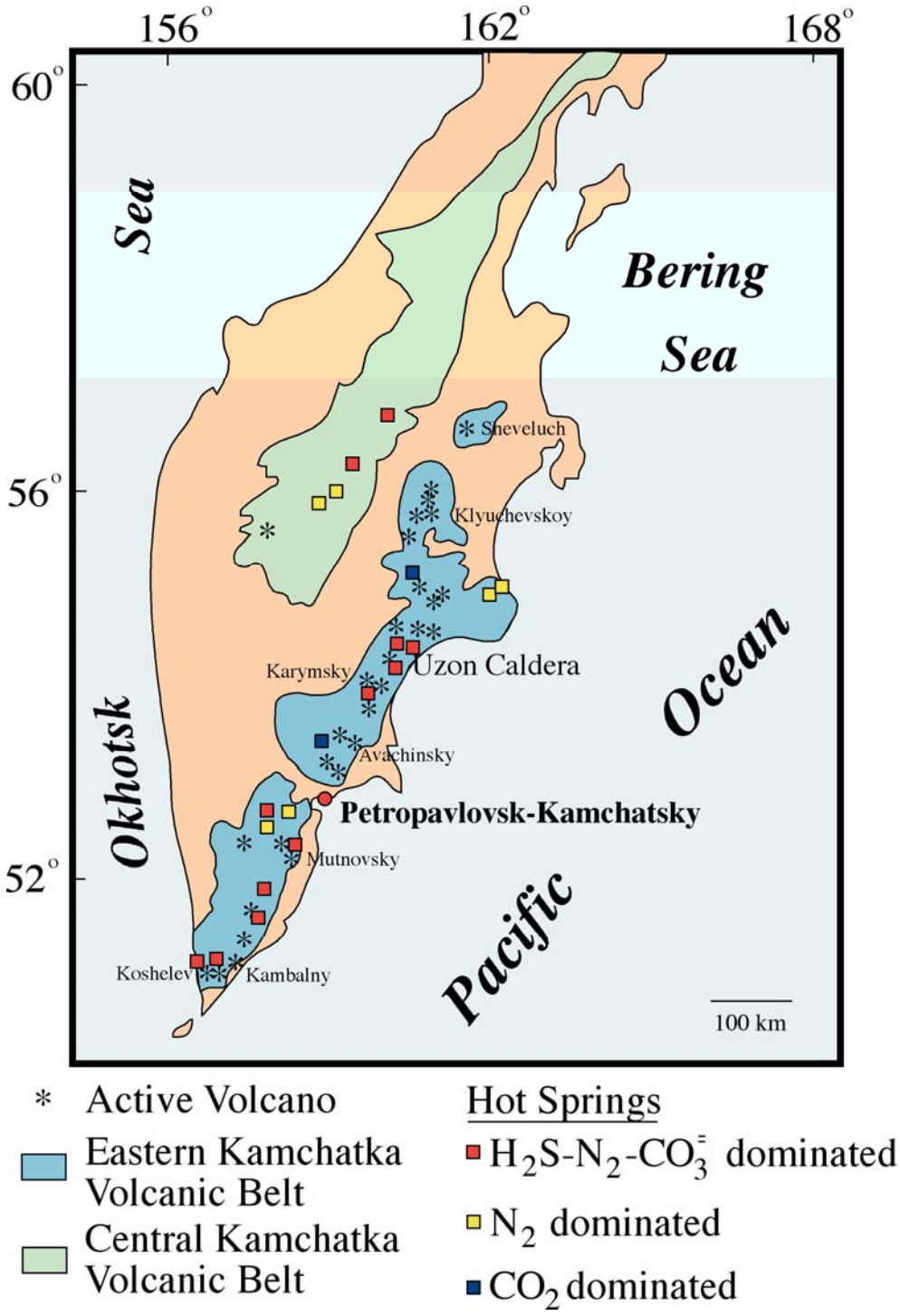

Fig 1.1. Map of Kamchatka peninsula, most volcanic activities were located in central and eastern Kamchatka volcanic belt. Hot spring waters defined by the gas emissions are shown (Crowe and Karpov, 2004).

REFERENCES

Aguiar, P., Beveridge, T.J. and Reysenbach, A.L., 2004. *Sulfurihydrogenibium azorense*, sp. nov., a thermophilic hydrogen-oxidizing microaerophile from terrestrial hot springs in the Azores. Int. J. Syst. Evol. Microbiol., 54: 33-39.

Bazhenova, O.K., Arefiev, O.A. and Frolov, E.B., 1998. Oil of the volcano Uzon Caldera, Kamchatka. Org. Geochem., 29(1-3): 421-428.

Bonch-Osmolovskaya, E.A., Miroshnichenko, M.L., Slobodkin, A.I. *et al.*, 1999. Biodiversity of anaerobic lithotrophic prokaryotes in terrestrial hot springs of Kamchatka. Microbiol., 68(3): 343-351.

Bonchosmolovskaya, E.A., Gorlenko, V.M., Karpov, G.A. and Starynin, D.A., 1987. Anaerobic destruction of the organic-matter in microbial mats of the Termofilnyi spring (Uzon Caldera, Kamchatka). Microbiol., 56(6): 812-818.

BonchOsmolovskaya, E.A., Miroshnichenko, M.L., Chernykh, N.A. *et al.*, 1997. Reduction of elemental sulfur by moderately thermophilic organotrophic bacteria and the description of *Thermoanaerobacter sulfurophilus* sp. nov. Microbiol., 66(5): 483-489.

Bonchosmolovskaya, E.A., Miroshnichenko, M.L., Kostrikina, N.A., Chernych, N.A. and Zavarzin, G.A., 1990. *Thermoproteus uzoniensis* sp. nov, a new extremely thermophilic archaebacterium from Kamchatka continental hot springs. Arch. Microbiol., 154(6): 556-559.

Bonchosmolovskaya, E.A., Slesarev, A.I., Miroshnichenko, M.L., Svetlichnaya, T.P. and Alekseev, V.A., 1988. Characteristics of *Desulfurococcus amylolyticus* sp. nov. A new extremely thermophilic arachaebacterium isolated from thermal springs of Kamchatka and Kunashir Island. Microbiol., 57(1): 78-85.

Bonchosmolovskaya, E.A., Sokolova, T.G., Kostrikina, N.A. and Zavarzin, G.A., 1990. *Desulfurella acetivorans* gen. nov. and sp. nov. A new thermophilic sulfur-reducing eubacterium. Arch. Microbiol., 153(2): 151-155.

Capaccioni, B., Martini, M., Mangani, F. *et al.*, 1993. Light hydrocarbons in gas-emissions from volcanic

areas and geothermal fields. Geochem. J., 27(1): 7-17.

Cheshko, A.L., 1994. The formation of main types of Kuril-Kamchatka region thermal waters based on the isotopic studies (D, O-18, He-3/He-4). Geokhimiya (7): 988-1001.

Clark, I.D. and Fritz, P., 1997. Environmental isotopes in hydrogeology. CRC Press, 328 pp.

Crowe D.E., Karpov G.A., 2004. Geologic setting of the Uzon Caldera, Kamchatka, Far East Russia. In: Geological Society of America Annual Meeting, Denver, CO, USA, Geological Society of America Abstracts with Programs, Vol. 36, No5: 432

Dymkin L.G., Solomonov V.A., Karpov G.A., 1988. Composition features of spontaneous gases in the Uzon Caldera; Geology and Geophysics J. NAUKA, Siberian Branch, Novosibirsk, n.5.

Eder, W. and Huber, R., 2002. New isolates and physiological properties of the aquificales and description of *Thermocrinis albus* sp. nov. Extremophiles, 6(4): 309-318.

Gerhardt, M., Svetlichny, V., Sokolova, T.G., Zavarzin, G.A. and Ringpfeil, M., 1991. Bacterial co utilization with H_2 production by the strictly anaerobic lithoautotrophic thermophilic bacterium *Carboxydothermus hydrogenus* DSM 6008 isolated from a hot swamp. FEMS Microbiol. Lett., 83(3): 267-272.

Golovacheva, R.S., Golyshina, O.V., Karavaiko, G.I. *et al.*, 1992. A new iron-oxidizing bacterium, *Leptospirillum thermoferrooxidans* sp. nov. Microbiol., 61(6): 744-750.

Golovacheva, R.S., Valekhoroman, K.M. and Troitskii, A.V., 1987. *Sulfurococcus mirabilis* gen. nov, sp. nov, a new thermophilic archaebacterium with the ability to oxidize sulfur. Microbiol., 56(1): 84-91.

Jones, C., Crowe, D.E. and Romanek, C., 2004. Geothermal fluid source determination in the Uzon Caldera, Kamchatka, Russia, Geological Society of America Annual Meeting, Denver, CO, USA, pp. 432.

Karpov, G., Esikov, A., Esikov, D., 2000. Isotopic geochemistry of acid lakes in the Uzon-Geyserny and Karymsky geothermal areas (Kamchatka). Proceedings World Geothermal Congress:2115-2119.

Karpov, G.A., Modern volcanism and hydrothermal systems in Kamchatka. Uniqueness of the Uzon-Geyser biogeochamical and hydrothermal system. Unpublished Data.

Karpov, G.A. and Naboko, S.I., 1990. Metal contents of recent thermal waters, mineral precipitates and hydrothermal alteration in active geothermal fields, Kamchatka. J. Geochem. Explor., 36(1-3): 57-71.

Kondratieva, E.N., Zacharova, E.V., Duda, V.I. and Krivenko, V.V., 1989. *Thermoanaerobium lactoethylicum* sp. nov. a new anaerobic bacterium from a hot-spring of Kamchatka. Arch. Microbiol., 151(2): 117-122.

Krivenko, V.V., Vadachloriya, R.M., Chermykh, N.A., Mityushina, L.L. and Krasilnikova, E.N., 1990. *Clostridium uzonii* sp. nov. An anaerobic thermophilic glycolytic bacterium isolated from hot-springs in the Kamchatka peninsula. Microbiol., 59(6): 741-748.

Kryukov, V.R., Saveleva, N.D. and Pusheva, M.A., 1983. *Calderobacterium hydrogenophilum* gen et sp. nov, an extremely thermophilic hydrogen bacterium and its hydrogenase activity. Microbiol., 52(5): 611-618.

Loginova, L.G. and Egorova, L.A., 1975. Obligately thermophilic bacterium *Thermus ruber* from hot springs in Kamchatka. Microbiol., 44(4): 593-597.

Miroshnichenko, M.L., Bonchosmolovskaya, E.A., Neuner, A. *et al.*, 1989. *Thermococcus stetteri* sp. nov, a new extremely thermophilic marine sulfur-metabolizing archaebacterium. Syst. Appl. Microbiol., 12(3): 257-262.

Miroshnichenko, M.L., Kostrikina, N.A., Hippe, H., Slobodkin, A.I. and Bonch-Osmolovskaya, E.A., 1998. Biodiversity of thermophilic sulfur-reducing bacteria: new substrates and new habitats. Microbiol., 67(5): 563-568.

Miroshnichenko, M.L., Rainey, F.A., Hippe, H. *et al.*, 1998. *Desulfurella kamchatkensis* sp. nov. and *Desulfurella propionica* sp. nov., new sulfur-respiring thermophilic bacteria from Kamchatka thermal environments. Int. J. Syst. Bacteriol., 48: 475-479.

Pitulle, C., Yang, Y., Marchiani, M. *et al.*, 1994. Phylogenetic position of the genus *Hydrogenobacter*. Int. J. Syst. Bacteriol., 44(4): 620-626.

Prokofeva, M.I., Miroshnichenko, M.L., Kostrikina, N.A. *et al.*, 2000. *Acidilobus aceticus* gen. nov., sp.

nov., a novel anaerobic thermoacidophilic archaeon from continental hot vents in Kamchatka. Int. J. Syst. Evol. Microbiol., 50: 2001-2008.

Reysenbach, A.L. and Shock, E., 2002. Merging genomes with geochemistry in hydrothermal ecosystems. Science, 296(5570): 1077-1082.

Romanek, C.S., Mills, G.L., Jones, M.E. *et al.*, 2004. Lipid biomarkers and stable isotope signatures of microbial mats in hot springs of Kamchatka, Russia, American Geophysical Union. Fall Meet. Suppl., Abstract, San Francisco, CA, USA.

Slobodkin, A.I., Tourova, T.P., Kuznetsov, B.B. *et al.*, 1999. *Thermoanaerobacter siderophilus* sp. nov., a novel dissimilatory fe(III)-reducing, anaerobic, thermophilic bacterium. Int. J. Syst. Bacteriol., 49: 1471-1478.

Sokolova, T.G., Kostrikina, N.A., Chernyh, N.A. *et al.*, 2002. *Carboxydocella thermautotrophica* gen. nov., sp. nov., a novel anaerobic, co-utilizing thermophile from a Kamchatkan hot spring. Int. J. Syst. Evol. Microbiol., 52: 1961-1967.

Spear, J.R., Walker, J.J., McCollom, T.M. and Pace, N.R., 2005. Hydrogen and bioenergetics in the yellowstone geothermal ecosystem. Proc Natl Acad Sci USA.: 0409574102.

Svetlichnii, V.A. and Svetlichnaya, T.P., 1988. *Dictyoglomus turgidus* sp. nov, a new extreme thermophilic eubacterium isolated from hot springs in the Uzon volcano crater. Microbiol., 57(3): 364-370.

Svetlichny, V.A., Sokolova, T.G., Gerhardt, M. *et al.*, 1991. *Carboxydothermus hydrogenoformans* gen. nov, sp. nov, a co-utilizing thermophilic anaerobic bacterium from hydrothermal environments of kunashir-island. Syst. Appl. Microbiol., 14(3): 254-260.

Svetlichnyi, V.A., Slesarev, A.I., Svetlichnaya, T.P. and Zavarzin, G.A., 1987. *Caldococcus litoralis* gen. nov.sp. nov. a new marine, extremely thermophilic, sulfur-reducing archaebacterium. Microbiol., 56(5): 658-664.

Svetlichnyi, V.A., Svetlichnaya, T.P., Chernykh, N.A. and Zavarzin, G.A., 1990. *Anaerocellum thermophilum* gen. nov. sp. nov. an extremely thermophilic cellulolytic eubacterium isolated from

hot-springs in the valley of Geysers. Microbiol., 59(5): 598-604.

Whitaker, R.J., Grogan, D.W. and Taylor, J.W., 2003. Geographic barriers isolate endemic populations of hyperthermophilic archaea. Science, 301(5635): 976-978.

Yamamoto, H., Hiraishi, A., Kato, K. *et al.*, 1998. Phylogenetic evidence for the existence of novel thermophilic bacteria in hot spring sulfur-turf microbial mats in Japan. Appl. Environ. Microbiol., 64(5): 1680-1687.

Yumoto, I., Hirota, K., Kawahara, T. *et al.*, 2004. *Anoxybacillus voinovskiensis* sp. nov., a moderately thermophilic bacterium from a hot spring in Kamchatka. Int. J. Syst. Evol. Microbiol., 54: 1239-1242.

Zavarzina, D.G., Tourova, T.P., Kuznetsov, B.B., Bonch-Osmolovskaya, E.A. and Slobodkin, A.I., 2002. *Thermovenabulum ferriorganovorum* gen. nov., sp. nov., a novel thermophilic, anaerobic, endospore-forming bacterium. Int. J. Syst. Evol. Microbiol., 52: 1737-1743.

Zavarzina, D.G., Zhilina, T.N., Tourova, T.P. *et al.*, 2000. *Thermanaerovibrio velox* sp. nov., a new anaerobic, thermophilic, organotrophic bacterium that reduces elemental sulfur, and emended description of the genus *Thermanaerovibrio*. Int. J. Syst. Evol. Microbiol., 50: 1287-1295.

CHAPTER 2

GEOCHEMISTRY OF REDUCED GASES AND CARBON DIOXIDE IN KAMCHATKA HOT SPRINGS

INTRODUCTION

A variety of thermogenic or biogenic gases (*e.g.*, CO_2, H_2, CH_4, H_2S, and CO) are often present in elevated concentrations in terrestrial hot springs such as those in Kamchatka. A thorough examination of the water and gas chemistry is essential for understanding *in-situ* biological processes such as carbon and energy metabolisms of hot spring microorganisms. In addition, both concentrations and isotope compositions of thermal vent gases have been widely used as geothermometers to estimate the temperature of the deep reservoir in geothermal environments where thermal gasses often originate (Giggenbach, 1980; 1997; Chiodini and Marini, 1998; Fiebig *et al.*, 2004). Moreover, stable isotopes provide a tool to determine the source of vent gases (Richet *et al.*, 1977; Clark and Fritz, 1997; Hoefs, 1997) and to trace pathways associated with biological or thermodynamic reactions (Whiticar *et al.*, 1986; Ragsdale, 1991; Romanek, 2005). Because hot spring gases often have primitive compositions, studies of the isotope geochemistry of hot spring gases chemistry may enhance our understanding for the origin of life on Earth and potentially elsewhere. In this study, biological exploited gases, such as CO_2, H_2, CH_4, H_2S and CO, were analyzed in hot springs of the Uzon Caldera for their individual gas content and stable isotope compositions (carbon-bearing gases only). These data are used to decipher the biogeochemical and isotopic reactions that occur in the hot springs of the Uzon Caldera, Kamchatka.

METHODS

Sample collection and preparation

Gas collection was conducted in the 2005 and 2006 field seasons from hot springs in the Uzon Caldera, Kamchatka. A set of gas samples was collected using a modified version of the Giggenbach technique where 2.5 to 5.0 liters of gas was passed sequentially through three traps: a liquid acid tap (1M

HCl), a liquid base trap (1M NaOH), and an evacuated container. All traps were prepared with 8-ml BD Vacutainers® blood collection tubes (BD Inc., Franklin Lakes, NJ, USA). Gaseous ammonia was collected as NH_4^+ in the acid trap while the base trap was used to collect H_2S (as S^{2-}) and CO_2 (as CO_3^{2-}). The blank BD Vacutainers were about 50% evacuated. The remaining gases in blank tubes were measured prior to every analysis as described below. A second set of bulk gas samples was also parallel collected by overpressure the tubes with 20 ml vent gases. Gaseous sulfide was only examined qualitatively for its presence and it was removed from the final gas container by the addition of 1ml 20-mM lead acetate prior to the analysis of other gases.

Gas analysis and calculation

Concentrations of H_2 and CO were determined using a SENTE methane gas analyzer (model GS-19S, Sente Inc., USA) under isothermal conditions at 54ºC using zero grade air as a carrier gas at a flow rate of 29.7ml min^{-1}. The reported peak area of H_2 on the chromatogram was used to calculate equivalence of pure H_2 volume based on a predetermined standard curve. The calculated volume was then divided by the injection volume to obtain percentage of H_2 gas in the sample. Variable volumes (5- 30 µl) were injected using Hamilton gastight syringes based on concentrations in each individual samples to ensure the optimal response.

The same approach was used to calculate concentrations of CO_2 and CH_4, which were measured with carbon isotope analysis using a Trace GC-C-IRMS (Finnigan MAT GmbH, Germany) equipped with a Carboxen 1010 plot column (Supelco, USA) under isothermal conditions at 100ºC using He as a carrier gas at a constant flow of 3 ml min^{-1}. Peak areas and stable carbon isotope compositions of CO_2 and CH_4 were determined on a ThermoQuest Delta Plus XL isotope ratio mass spectrometer (Finnigan MAT GmbH, Germany). CO concentrations were too low for the measurement of isotope compositions. The precision of the instrument was determined ±1% of measured values for gas composition measurements based on standard gas measurements. However, the actual error of multiple measurements were much higher, mainly due to errors introduced by subsampling from the Vacutainers because the measured values for the three gas species in a single sample always varied in the same way. A pure CO_2 gas as a

working standard was calibrated to the international PDB standard and has a $\delta^{13}C$ value of -45.0‰ versus PDB. Its amplitude 44 value was set to 4000 mV throughout the analysis. The linearity of isotope analysis was examined to be satisfactory from 700 mV to 8000 mV with a variation of 0.1‰ per volt. Variable gas volumes (30-500 µl) were injected using Hamilton gastight syringes to satisfy the working ranges.

For gas composition calculation, the standard curves were constructed specific to experimental range of each measured gas by injecting up to 20 µl of pure CH_4, pure CO_2 and 10 µl pure CO. The calculated mole percentage of each gas was not normalized to the total measured gas. Therefore, influence of water vapor was not considered. The isotope fractionation factor for CO_2-CH_4 system (as $\Delta^{13}C$ value) was calculated following the convention

$$\Delta^{13}C(CO_2\text{-}CH_4) = \delta^{13}C_{CO_2} - \delta^{13}C_{CH_4} \approx 10^3 \ln\alpha_{CO_2\text{-}CH_4} \quad (1)$$

Theoretical isotope equilibrium fractionation factor at various temperatures was calculated based on a modification of the equation provided by Richet (1977) as reported in Horita (2001):

$$10^3 \ln\alpha_{CO2\text{-}CH4} = 0.16 + 11.754 \times (10^6/T^2) - 2.3655 \times (10^9/T^3) + 0.2054 \times (10^{12}/T^4) \quad (2)$$

where T (in K) is valid from 273 to 1573K

RESULTS AND DISCUSSIONS

Gas composition

The analysis of remaining gases in blank Vacutainer tubes yielded no detectable H_2, CO, CH_4 and CO_2, therefore, measured values were regarded as true values from the gas samples. The 2006 samples collected with 3 trap systems were later determined in oversaturation for at least CO_2 and H_2S since all the third (final) traps were detected significant amounts of the CO_2 and many contained H_2S. Therefore, results of the second set with bulk gas samples (with -D suffix) were reported for the gas compositions (Table 2.1), but both the 3rd trap in the first set of samples (with -C suffix) and the bulk gas samples (with -D suffix) were reported for carbon isotope compositions (Table 2.2). A sample from Cascadnaya (CasA-C) was the only exception that was from the 3rd trap of the first sample set because the bulk sample (CasA-D) was damaged.

The percentages of H_2, CH_4, and CO_2 in the gas samples are reported in Figs 2.1 to 2.3, and CO compositions are reported in Fig 2.4. In general, stable gas compositions were observed for H_2 (<0.1% except ON1 and Arkashin pool), CH_4 (<2% except Arkashin, ON1 and Pool 13), and CO_2 (<30% except Pool 1 and Rubbermat pool) and between the two sampling years whereas CO varied considerably (0 to 174 ppm) from 2005 to 2006. CO_2 was the most abundant gas in all surveyed pools and constituted 30% to more than 90% of the total gas volume after removal of H_2S (Fig 2.3). CH_4 and H_2 were the next two abundant gases with concentrations up to 8.7 and 2.1%, respectively (Figs 2.1 and 2.2). Volume percentage of CO was the lowest among all gases analyzed but varied greatly from undetectable to 249 ppm. CO concentration in 2006 samples was generally lower than in 2005 (Fig 2.4), suggesting that production or consumption of CO is more variable than other gases. These gas compositions are in agreement with those in other geothermal sites where CO_2 is dominant followed by CH_4, H_2, H_2S, and CO (Giggenbach, 1997; Chiodini and Marini, 1998).

Methane and hydrogen gas concentration were positively correlated (r^2= 0.724; Fig 2.5), suggesting that both gases originated from a single source, possibly through the interaction between organic compound and more reduced rock surface to enhance the formation of H_2-containing and CH_4-rich gases (Giggenbach, 1997).

Isotope composition and origin of vent gases

The $\delta^{13}C$ values of CO_2 ($\delta^{13}CO_2$) ranged from -5.2 to -2.3‰ in 2005 (-3.7 ± 0.8‰, n = 26) and from -6.6 to -4.0‰ in 2006 samples (-5.3 ± 0.8‰, n = 35). The $\delta^{13}C$ values of CH_4 ($\delta^{13}CH_4$) ranged from -39.1 to -26.1‰ in 2005 (28.0 ± 2.8‰, n = 26) and from -29.9 to -24.3‰ in 2006 samples (-27.0 ± 1.3‰, n = 35; Table 2.2). Samples from 2005 were generally 1-2‰ enriched in both $^{13}CO_2$ and $^{13}CH_4$ compared with those from the same pool in 2006 with few exceptions. The cause for the small annual variation is not clear, but could attribute to the isotope exchange reaction between CO_2 and CH_4 over time (discussed later; Fig 2.7). However, changes in $\delta^{13}CH_4$ values in some pools, *e.g.*, Pool 1, Pool 13 and Thermophile, were more than 3‰ and as great as 10‰ between years (Table 2.2), indicating a temporal variation in the gas-generation activities in these sites, *e.g.*, mixing of CO_2 and CH_4 from different thermogenic or

biogenic sources, isotopic fractionation during transport. For majority samples collected in the two years, the coupled $\delta^{13}CO_2$ and $\delta^{13}CH_4$ values did not fall in the range of conventional biogenic gases but were consistent with values of thermogenic or juvenile gases (Fig 2.6a), including those of hydrothermal and volcanic origins (Clark and Fritz, 1997). This suggests that both CO_2 and CH_4 were primarily produced abiotically in the deep subsurface rather than by biological processes such as methanogenesis or respiratory pathways in the surficial geothermal environment. With a mean of -27.4‰ for $\delta^{13}CH_4$ and -4.6‰ for $\delta^{13}CO_2$, it is less likely that both gases were generated from a common source regardless of the attainment of chemical and isotopic equilibrium (Giggenbach, 1997). Instead, assuming a closed system, weighed average of $\delta^{13}C$ of the two gases calculated based on equation (3) showed a values from -2.8 to -8.3‰. The range would be a little smaller (-3.5 to -7.0‰) if the gases are derived solely from magmatic source (Fischer *et al.*, 1998). Therefore, mixing of different carbon sources with distinct $\delta^{13}C$ values may occur. Based on $\delta^{13}CO_2$ and $\delta^{13}CH_4$ values, it can be hypothesized that the end members of the vent gas may include those from thermo-decomposition of ^{13}C-depleted organic matters, *e.g.*, decarboxylation of kerogen that has a typical $\delta^{13}C$ value of -32‰ (Andresen *et al.*, 1994) and those from dissociation of ^{13}C-enriched marine limestone (0‰), but may probably have magmatic (-5‰) contributions as well (Giggenbach, 1997).

$$\delta^{13}C_{CO_2\text{-}CH_4} = (\delta^{13}CO_2 \times f_{CO_2} + \delta^{13}CH_4 \times f_{CH_4}) \qquad (3)$$

$$f_{CO_2} = X_{CO_2} / (X_{CO_2} + X_{CH_4})$$

$$f_{CH_4} = X_{CH_4} / (X_{CO_2} + X_{CH_4})$$

where X_{CO_2} and X_{CH_4} are mole percentages of CO_2 and CH_4 in the bulk gas, respectively.

$\delta^{13}CH_4$ values in a few 2005 samples was as depleted as -39.1‰ (Thermo-25A), it may still be due to the thermal cracking of the refractory kerogen (Clayton, 1991), but a biological production of CH_4 in shallow subsurface can not be totally ruled out.

Attainment of chemical and isotopic equilibria

While gas contents of the geothermal system can be affected by the chemical equilibria, their isotope

compositions can be affected by both kinetic and equilibria processes. In high temperature geothermal systems, chemical equilibrium between methane and carbon dioxide is usually assumed to be attained according to reaction 4 (Giggenbach, 1997; Chiodini and Marini, 1998; Fiebig *et al.*, 2004; Fiebig *et al.*, 2007) due to the long residence time of gas species in hydrothermal reservoirs with elevated temperature and relative short lapse of time in the up-flow channels (Chiodini and Marini, 1998)

$$CH_4 + 2H_2O \leftrightarrow CO_2 + 4H_2 \quad (4)$$

Horita (2001) showed that at intermediate temperatures, it is difficult to achieve chemical and isotope equilibria between CH_4 and CO_2 without catalysts; but in the presence of certain transition-metal catalysts, both chemical reaction and isotopic exchange can be greatly enhanced, although isotope equilibrium was still not attained after 1362 hrs at 350°C. This was in agreement with Giggenbach (1997) that the isotopic equilibrium was much slower than the chemical equilibrium. Water chemistry data in Kamchatka hot springs showed variable concentrations of transition-metal; *e.g.*, Fe, Ni and Co were measured with average concentrations of 18.7 ppm, 2.1 ppb and 4.1 ppb, respectively (Hollingsworth *et al.* in submission), indicating presence of solid phase transition-metal catalysts. Therefore, attainment of chemical equilibrium may be possible with presence of these catalysts in the hot springs surveyed.

The relative degree of attainment of chemical and isotopic equilibrium was examined in Fig 2.7 by comparing $\Delta^{13}C(CO_2\text{-}CH_4)$ and $\log(X_{CH_4}/X_{CO_2})$ pair with theoretical values calculated by equation 1 by Horita (2001) and equation 5 by Giggenbach (1997). Equation 5 is based on the $FeO/FeO_{1.5}$ buffer system, which is considered the most suitable parameter to govern hydrothermal systems (Giggenbach, 1997).

$$\log(X_{CH_4}/X_{CO_2}) = 5280/T\text{-}11.12 \quad (5)$$

where X_{CO_2} and X_{CH_4} are mole percentages of CO_2 and CH_4 in the bulk gas, respectively. The majority of the data fall below the theoretical lines, indicating a discrepancy of equilibrium temperature between isotope and gas content geothermometers (Fig 2.7). Measured isotope fractionation factors (Δ) between CO_2 and CH_4 was 18 to 26‰ in 2006 and 21 to 36‰ in 2005 (Table 2.2). The majority of data are consistent with computed theoretical values for Δ of 19.3 to 25.3‰ at temperature between 300ºC and

375ºC (Richet *et al.* 1977; Horita, 2001; Figs 2.6b and 2.7). However, $\log(X_{CH_4}/X_{CO_2})$ of measured values suggested lower equilibrium temperatures from 250 to 310°C based on equation 5 (Fig 2.7), which are common for deep aquifers in geothermal settings (Fiebig *et al.*, 2004) and may represent the true temperature of the deep reservoir under springs in the Uzon Caldera. Notably, values for the 2005 samples were closer to the theoretical equilibrium line of the two geothermometers than values for the 2006 sample, which indicates that isotope exchange between the CH_4 and CO_2 were more extensive in 2005 samples, probably due to the long storage time. Collectively, the above data suggested that the majority of gas samples attained chemical but not isotopic equilibrium; while on the other hand, partial attainment of isotope equilibrium or quenching at the high temperatures may have occurred (Fig 2.6b).

SUMMARY

Our data showed that hot spring gases in the Uzon Caldera, Kamchatka, were predominantly generated from abiotic processes and possessed characteristics of thermogenic gases. Isotopically depleted kerogen with a typical $\delta^{13}C$ value of -32‰, marine limestone with $\delta^{13}C$ value of 0‰ and perhaps the mantle (magmatic source) with $\delta^{13}C$ value of -5‰ seemed to be the end sources of the thermogenic gases. Gas contents and isotope signatures were generally consistent between 2005 and 2006. The discrepancy between equilibrium temperatures given by X_{CH_4}/X_{CO_2} and stable isotope geothermometers suggested that chemical but not isotope equilibrium was attained in most hot springs surveyed. However, partial attainment of isotope equilibrium or quenching at the high temperatures in selected hot springs can not totally be excluded.

Table 2.1. Gas composition in vent gas samples collected in 2005 and 2006.

	2006					2005				
Pool name	Sample ID	H_2 %	CH_4 %	CO_2 %	CO ppm	Sample ID	H_2 %	CH_4 %	CO_2 %	CO ppm
Arkashin	Ark-D	2.1	6.6	60.7	0	A-5A	1.8	4.2	75.8	0
Rubbermat	Rubbermat-D	0.2	1.9	82.8	0	Rubbermat-22A	0.2	0.7	42.7	52.31
Bright White*	BW-D	0.1	2.0	80.3	74.16					
Cascadnaya*	CasA-C	0.2	1.7	70.6	0					
Cascadnaya Bubbler*	CasBub-D	0.3	3.3	74.4	26.33					
CZ pool*	CZ1(old)-D	1.4	5.3	78.3	0					
Jenn's vent1	JV1-D	0.3	2.7	83.7	0	JV1-1A	0.4	2.4	84.2	74.63
Jenn's vent2*	JV2-D	0.6	4.5	64.6	0	JV2-2A	0.5	2.8	67.2	0
Jenn's vent3						JV3	0.6	3.9	93.3	0
Jenn's vent4						JV-04-4A	0.3	1.4	35.8	78.77
ON1 Orange field	ON1-D	2.0	8.0	90.0	0	ON1-21N	1.6	5.0	68.6	0
Pool 1*	Pool 1-D	0.1	0.6	80.2	0	CR05008-10A	0.0	0.2	30.7	82.04
Pool 2						CR05009-11A	0.2	1.7	69.3	248.75
Pool 3	Pool 3-D	0.5	2.7	64.5	0	CR05010-7A	0.5	1.9	69.1	54.06
Pool 4a*	Pool 4a-D	0.1	3.4	85.2	104.2	Pool 4a-15A	0.1	1.6	58.1	205.71
Pool 4*	Pool 4-D	0.4	2.8	75.8	0.56	CR05011-8A	0.4	2.9	79.2	84.78
Pool 5	Pool 5-D	0.5	2.9	74.8	0	Pool 5-16A	0.6	3.0	80.6	0
Pool 6						Pool 6#1-17A	0.6	2.5	64.6	141.78
Pool 7						Pool 7-18A	0.6	2.1	70.7	109.59
Pool 11	Pool 11-D	0.5	2.0	75.0	0					
Pool 12						Pool 12-19A	0.7	1.4	60.3	57.62
Pool 13	Pool 13-D	0.4	2.7	75.1	0	Pool 13-20A	0.3	0.7	52.3	40.94
RF14*	RF14-D	0.2	1.8	81.8	0					
RF7*	RF7-D	0.5	0.7	64.4	0					
RF9*	RF9-D	0.1	1.5	76.8	31.27					
Thermophile	Thermo A-D	0.2	0.6	36.4	39.44	Thermo-25A	0.2	0.5	51.0	52.99
Vent 1 North-a*						CR05025	0.2	1.8	84.9	85.21
Vent 1 North*	V1N-D	0.2	1.8	62.7	0	CR05026	0.1	1.5	55.1	173.53
Vent 2 North (New pool)	V2N (np)-D	0.5	3.1	72.8	0					
Vent 2 North						CR05023	1.1	5.4	68.2	0
Zavarzin II	Zavarzin-D	0.3	1.1	62.3	0	Zav-26A	0.2	1.0	48.2	26.42
Big Brother						Big Brother-9A	1.9	5.6	58.8	0
Pool JW05-18						CR05024-14A	1.1	3.7	67.1	0
Jess pool						Jess-6A	1.8	4.6	69.6	0
Burlyashi						CR05012-12A	0.1	1.8	58.8	139.46

Percentage was determined after removal of H_2S by the addition of lead acetate.

* H_2S in gas samples was detected.

The standard error of multiple measurements ($n \geq 2$) was determined to be ±5% for CO_2, ±1% for CH_4 using GC-C-IRMS; ±0.5% for H_2 and ±10 ppm for CO using SENTE gas analyzer..

Table 2.2. Carbon isotope values of gas samples collected in 2005 and 2006.

	2006				2005			
Pool name	Sample ID	$\delta^{13}CH_4$	$\delta^{13}CO_2$	$10^3\ln\alpha^*$	Sample ID	$\delta^{13}CH_4$	$\delta^{13}CO_2$	$10^3\ln\alpha^*$
Arkashin	Arkashin-C	-27.9	-5.3	22.6	A-5A	-27.6	-3.3	24.3
Arkashin	Arkashin-D	-28.5	-5.3	23.2				
Rubbermat	Rubbermat-D	-27.4	-4.9	22.5	Rubbermat-22A	-26.4	-3.6	22.8
Rubbermat	Rubbermat-C	-26.0	-5.0	21				
Bright White	Bright white-D	-27.3	-6.2	21.1				
Cascadnaya	CasA-C	-25.1	-4.0	21.1				
Cascadnaya bubbler	CasBub-C	-25.9	-5.5	20.4				
Cascadnaya bubbler	CasBub-D	-27.1	-5.4	21.7				
CZ' pool	CZ1(old)-D	-28.2	-6.1	22.1				
Jenn's vent1	JV1-D	-27.2	-6.6	20.6	JV1-1A	-26.5	-5.2	21.3
Jenn's vent2	JV2-C	-26.6	-6.5	20.1				
Jenn's vent2	JV2-D	-26.9	-6.4	20.5	JV2-2A	-26.1	-4.1	22
Jenn's vent3					JV3	-26.6	-4.5	22.1
Jenn's vent4					JV-04-4A	-27.4	-5.0	22.4
ON1 Orange field	ON1-D	-28.4	-5.3	23.1	ON1-21N	-26.6	-3.9	22.7
Pool 1	Pool 1-C	-24.3	-6.6	17.7				
Pool 1	Pool 1-D	-24.3	-6.2	18.1	CR05008-10A	-27.8	-4.9	22.9
Pool 2					CR05009-11A	-27.4	-3.7	23.7
Pool 3	Pool 3-C	-27.0	-5.6	21.4				
Pool 3	Pool 3-D	-27.0	-4.9	22.1	CR05010-7A	-26.8	-3.6	23.2
Pool 4a	Pool 4a-C	-26.4	-6.0	20.4				
Pool 4a	Pool 4a-D	-25.9	-5.7	20.2	Pool 4a-15A	-26.3	-3.8	22.5
Pool 4	Pool 4-C	-26.7	-5.3	21.4				
Pool 4	Pool 4-D	-26.9	-4.7	22.2	CR05011-8A	-26.9	-3.5	23.4
Pool 5	Pool 5-D	-26.6	-4.7	21.9	Pool 5-16A	-26.5	-2.8	23.7
Pool 6					Pool 6#1-17A	-26.6	-2.7	23.9
Pool 7					Pool 7-18A	-27.0	-3.0	24
Pool 11	Pool 11-C	-27.1	-4.7	22.4				
Pool 11	Pool 11-D	-25.4	-4.3	21.1				
Pool 12					Pool 12-19A	-27.1	-3.0	24.1
Pool 13	Pool 13-C	-28.4	-5.1	23.3				
Pool 13	Pool 13-D	-26.7	-4.2	22.5	Pool 13-20A	-29.6	-3.2	26.4
RF14	RF14-D	-26.3	-4.8	21.5				
RF7	RF7-C	-29.9	-4.2	25.7				
RF7	RF7-D	-25.5	-4.0	21.5				
RF9	RF9-C	-27.2	-5.8	21.4				
RF9	RF9-D	-26.2	-5.4	20.8				
Thermophile	Therm A-D	-29.4	-4.5	24.9	Thermo-25A	-39.1	-3.2	35.9
Vent 1 North-a				21.2	CR05025	-27.5	-4.6	22.9
Vent 1 North	V1N-D	-27.6	-6.4		CR05026	-28.4	-4.5	23.9
Vent 2 North (New pool)	V2N (np)-D	-27.7	-6.5	21.2				
Vent 2 North					CR05023	-27.7	-3.7	24
Zavarzin II	Zavarzin-D	-28.4	-4.2	24.2	Zav-26A	-28.1	-2.3	25.8
Big Brother					Big Brother-9A	-27.8	-3.5	24.3
Pool JW05-18					CR05024-14A	-27.8	-4.8	23
Jess pool					Jess-6A	-27.6	-3.3	24.3
Burlyashi					CR05012-12A	-34.5	-3.2	31.3

*, $10^3\ln\alpha$ is fractionation factor between CO_2 and CH_4 according to the equation $10^3\ln\alpha_{CO2\text{-}CH4} \approx \Delta^{13}C(CO_2\text{-}CH_4) = \delta^{13}CO_2\text{-}\delta^{13}CH_4$

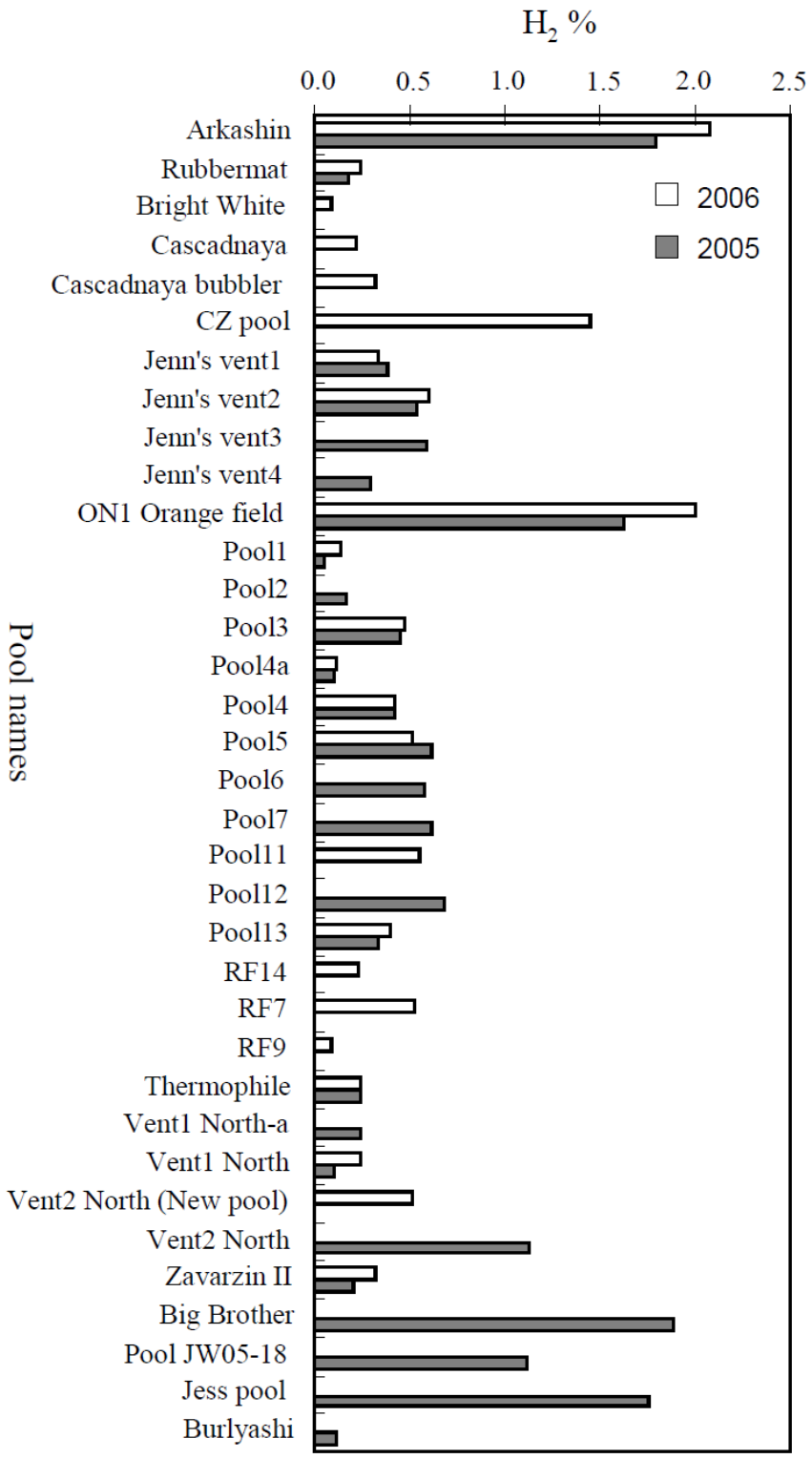

Fig 2.1. H_2 composition in vent gas samples.

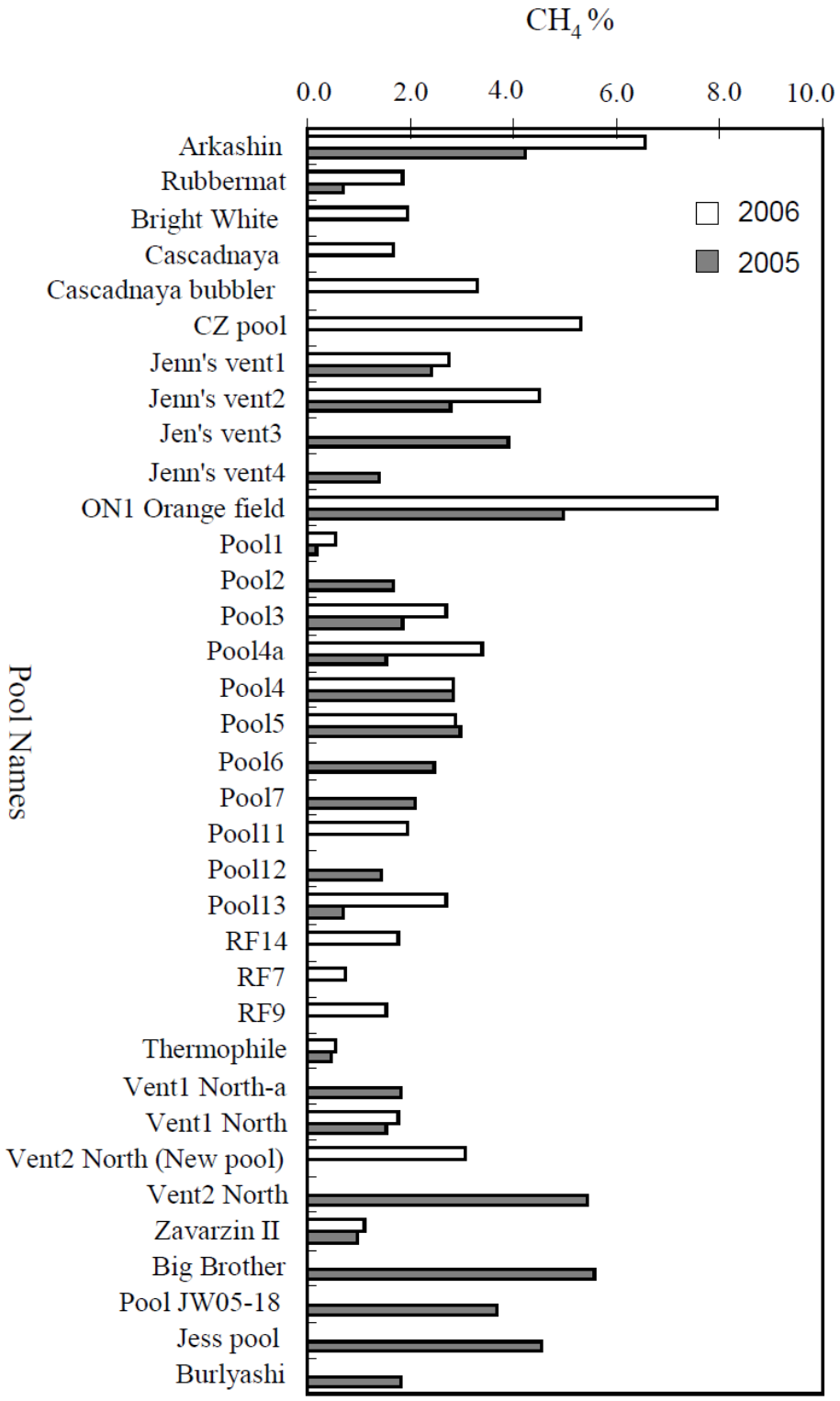

Fig 2.2. CH_4 composition in vent gas samples.

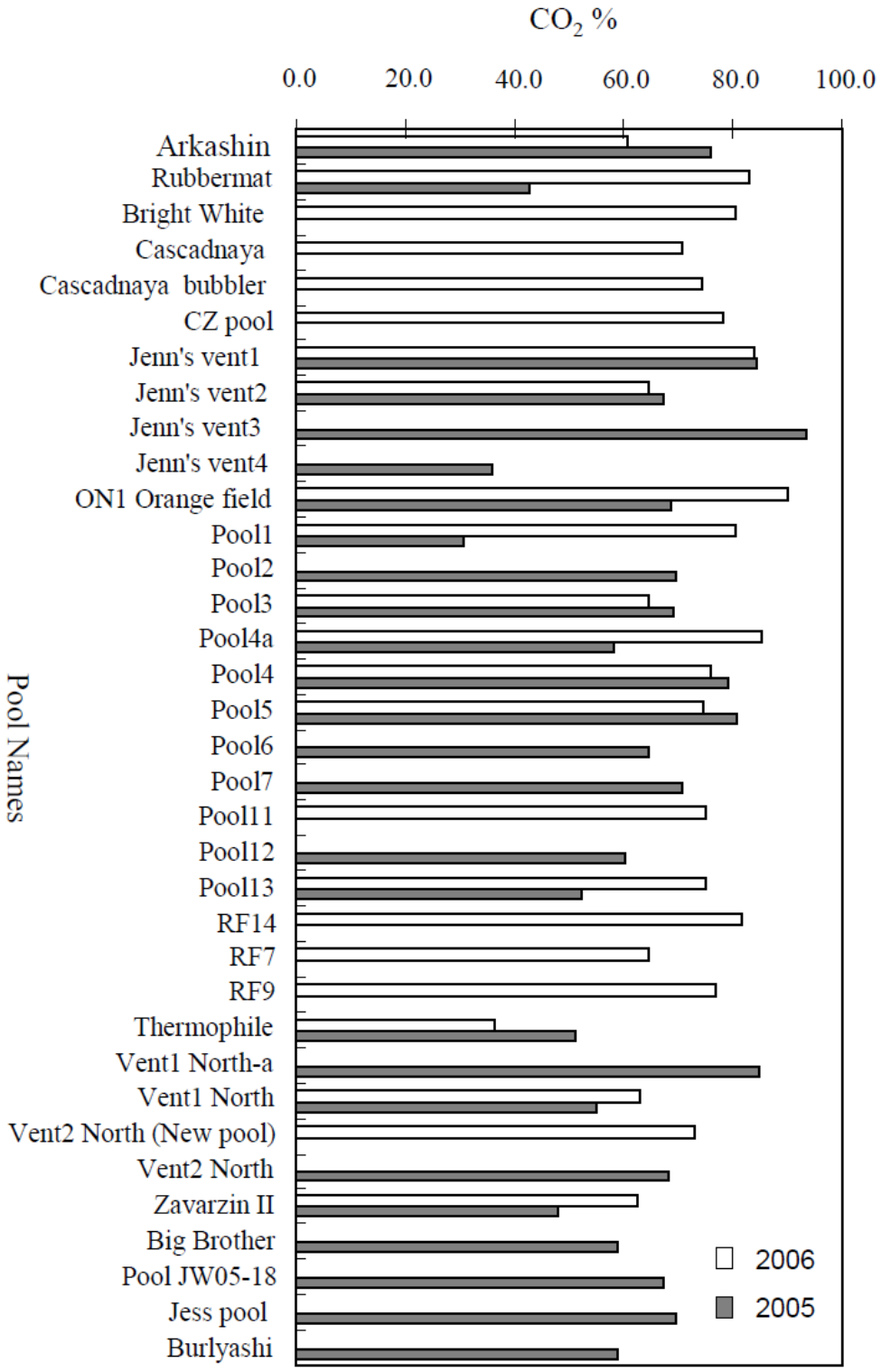

Fig 2.3. CO_2 composition in vent gas samples.

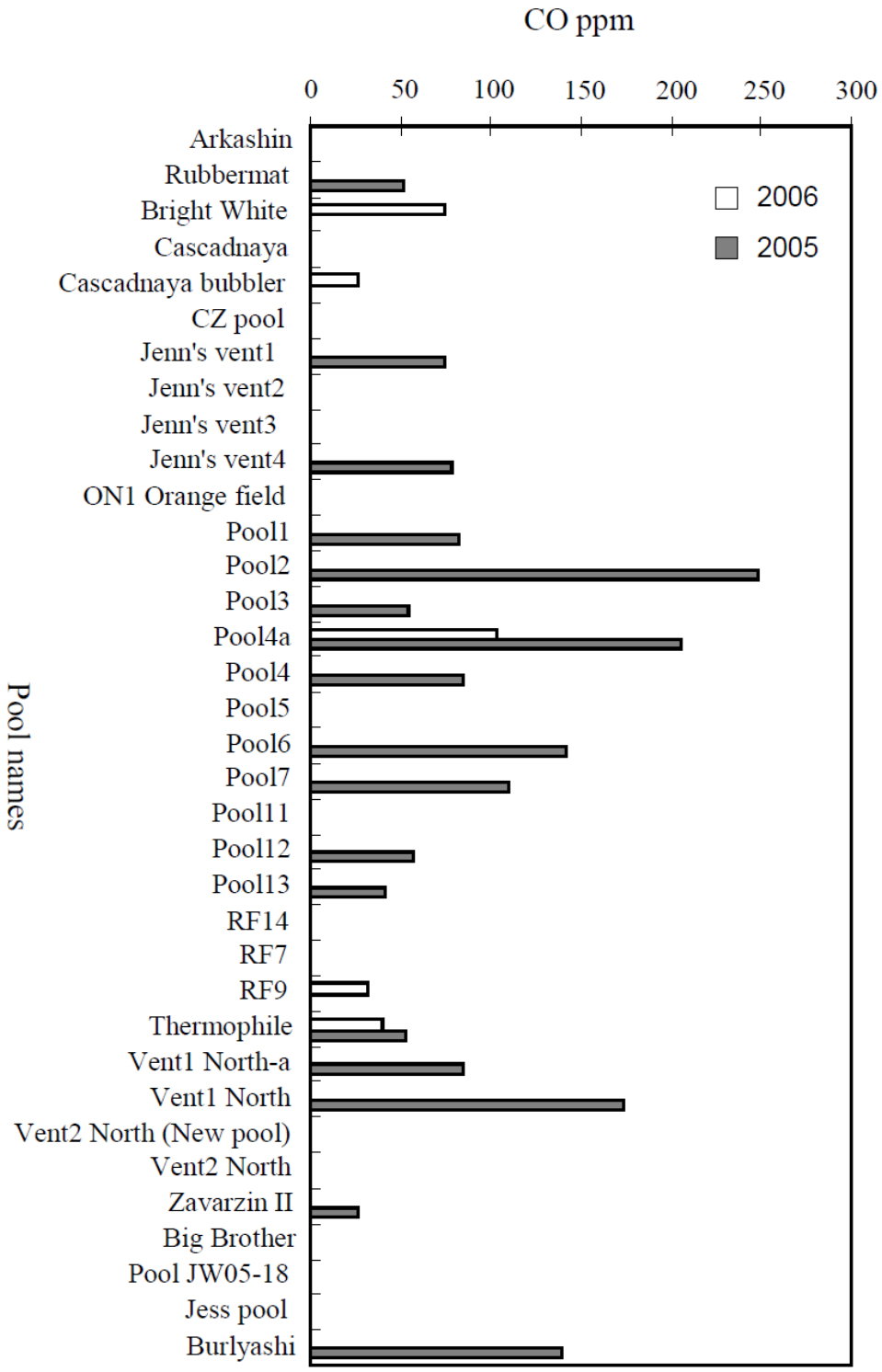

Fig 2.4. CO composition in vent gas samples.

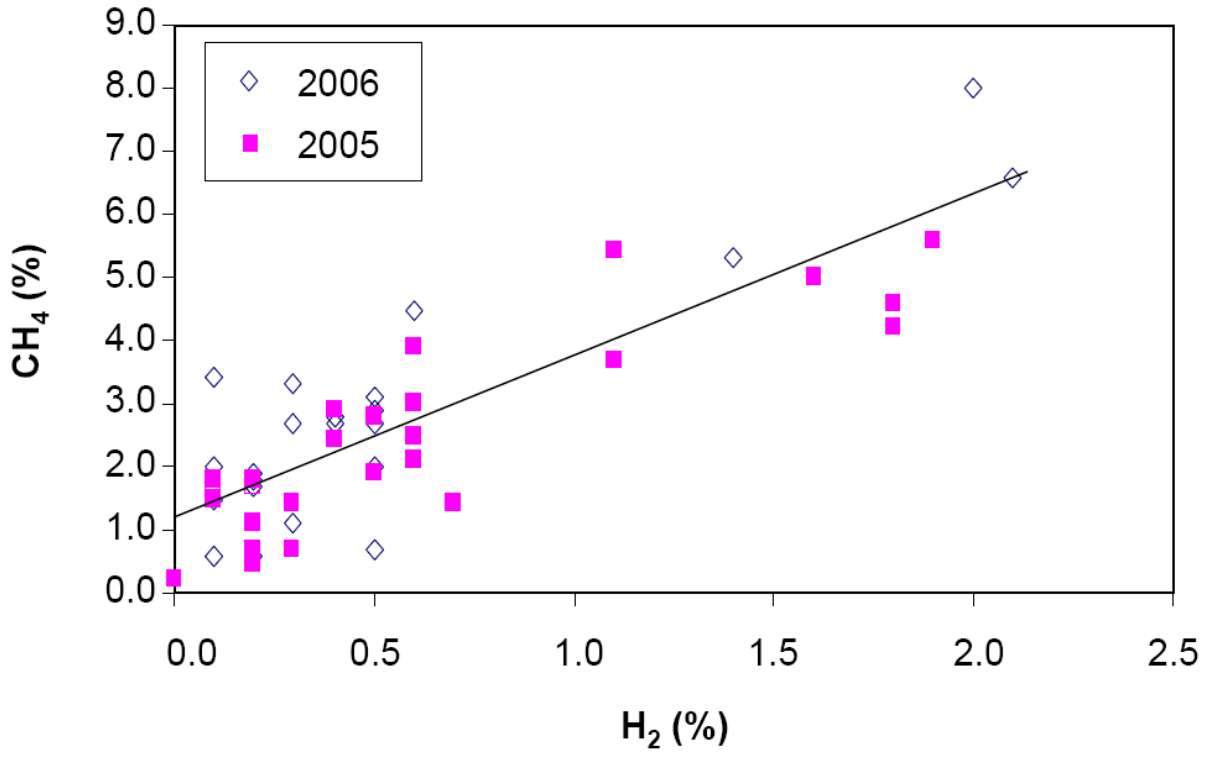

Fig 2.5. Correlation of CH_4 and H_2 gas contents in vent gas samples. Percentage was determined after removal of H_2S by the addition of lead acetate. The linear regression line (r^2= 0.724) used data from both years.

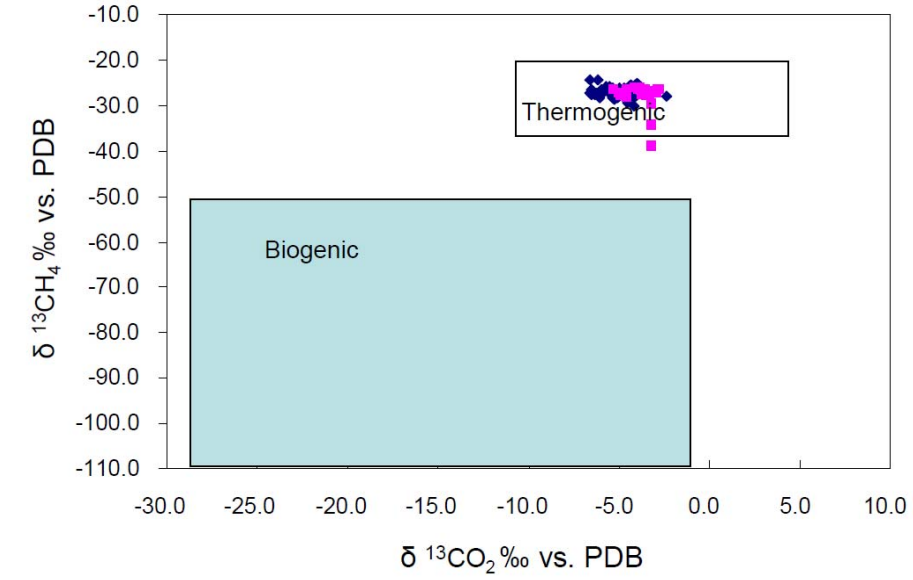

(a)

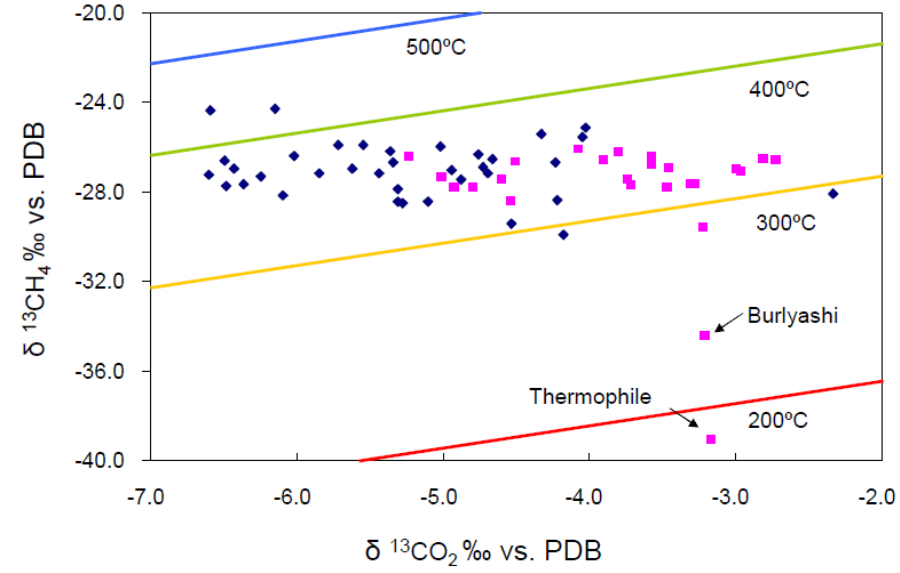

(b)

Fig 2.6. Upper panel, a) diagram showing typical range of $\delta^{13}C$ values of biogenic and thermogenic CH_4 and CO_2. Bottom panel, b) same plot at larger scale with computed carbon isotope equilibrium lines from 200 to 500°C. Each line represents compositions expected for two gases in the vapor phase at carbon isotope equilibrium as a function of temperature based on equation (2). Squares, 2005; diamonds, 2006.

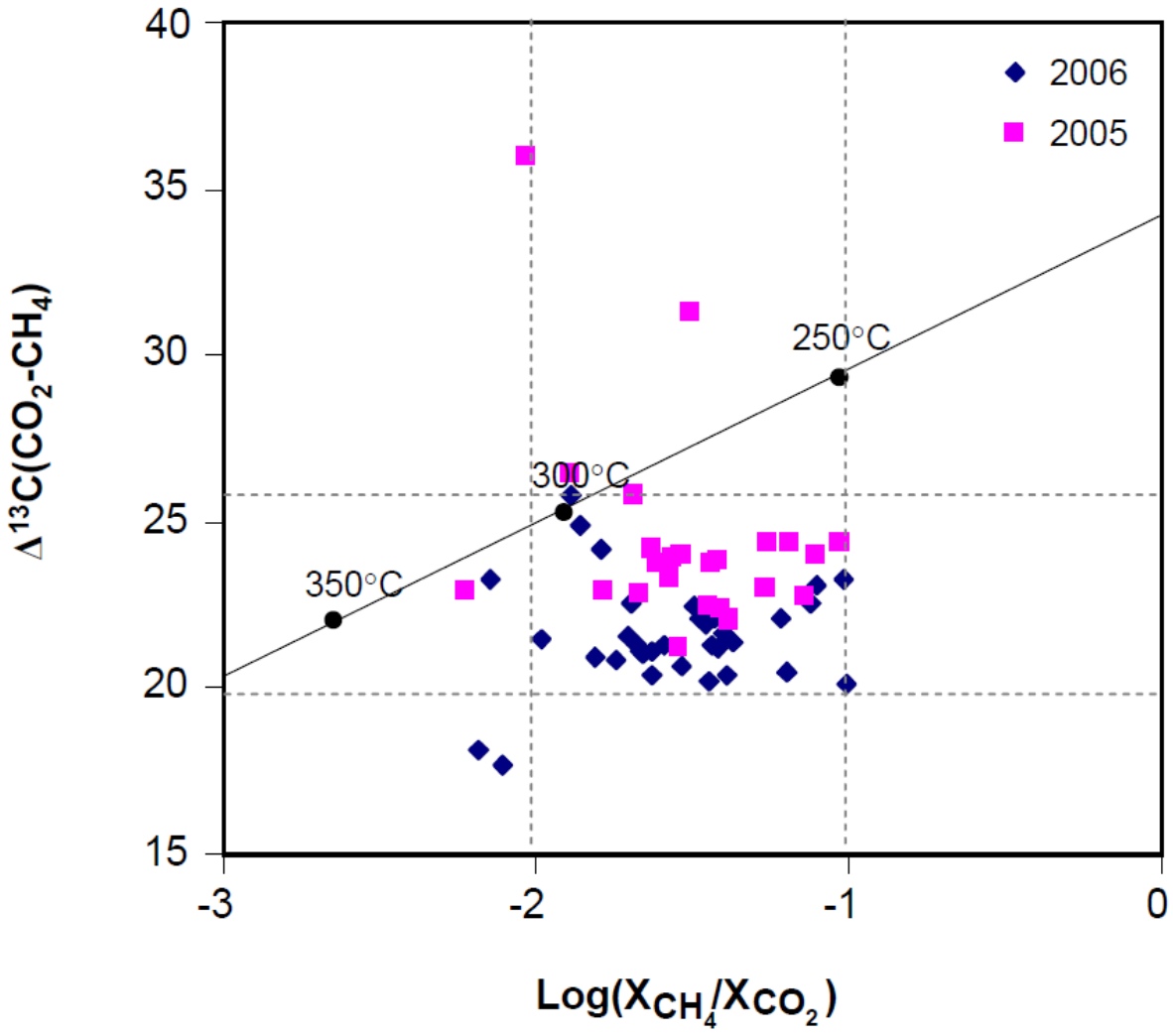

Fig 2.7. Comparison of measured values of $\Delta^{13}C$ for the CO_2-CH_4 system versus log (X_{CH_4}/X_{CO_2}) for gas samples collected from the Uzon Caldera in 2005 and 2006. The Solid line represents the theoretical values for gases in the vapor phase when both chemical and isotopic equilibria are attained; the dotted line defines the region that includes the majority of gas samples. The region indicates different equilibrium temperature ranges using the two geothermometers.

REFERENCES

Andresen, B., Throndsen, T., Barth, T., and Bolstad, J., 1994. Thermal generation of carbon-dioxide and organic-acids from different source rocks. *Org. Geochem.* **21**, 1229-1242.

Chiodini, G. and Marini, L., 1998. Hydrothermal gas equilibria: The H_2O-H_2-CO_2-CO-CH_4 system. *Geochim. Cosmochim. Acta* **62**, 2673-2687.

Clark, I. D. and Fritz, P., 1997. *Environmental isotopes in hydrogeology*. CRC Press.

Clayton, C., 1991. Carbon isotope fractionation during natural-gas generation from kerogen. *Mar. Petrol. Geol.* **8**, 232-240.

Fiebig, J., Chiodini, G., Caliro, S., Rizzo, A., Spangenberg, J., and Hunziker, J. C., 2004. Chemical and isotopic equilibrium between CO_2 and CH_4 in fumarolic gas discharges: Generation of CH_4 in arc magmatic-hydrothermal systems. *Geochim. Cosmochim. Acta* **68**, 2321-2334.

Fiebig, J., Woodland, A. B., Spangenberg, J., and Oschmann, W., 2007. Natural evidence for rapid abiogenic hydrothermal generation of CH_4. *Geochim. Cosmochim. Acta* **71**, 3028-3039.

Fischer, T. P., Giggenbach, W. F., Sano, Y., and Williams, S. N., 1998. Fluxes and sources of volatiles discharged from Kudryavy, a subduction zone volcano, Kurile Islands. *Earth Plane. Sci. Lett.* **160**, 81-96.

Giggenbach, W. F., 1980. Geothermal gas equilibria. *Geochim. Cosmochim. Acta* **44**, 2021-2032.

Giggenbach, W. F., 1997. Relative importance of thermodynamic and kinetic processes in governing the chemical and isotopic composition of carbon gases in high-heatflow sedimentary basins. *Geochim. Cosmochim. Acta* **61**, 3763-3785.

Hoefs, J., 1997. *Stable isotope geochemistry*. Berlin ; New York : Springer.

Hollingsworth, E.A, Crowe, D.E., Romanek, C.S., Schroeder, P.A., and Karpov, G.A., Sulfur speciation in the Uzon caldera geothermal system, Kamchatka, Far East Russia. In submission to Journal of Volcanology and Geothermal Research.

Horita, J., 2001. Carbon isotope exchange in the system CO_2-CH_4 at elevated temperatures. *Geochim. Cosmochim. Acta* **65**, 1907-1919.

Ragsdale, S. W., 1991. Enzymology of the acetyl-CoA pathway of CO_2 fixation. *Crit.Rev. Biochem. Mol. Biol.* **26**, 261-300.

Richet, P., Bottinga, Y., and Javoy, M., 1977. Review of hydrogen, carbon, nitrogen, oxygen, sulfur, and chlorine stable isotope fractionation among gaseous molecules. *Annu. Rev. Earth Planet. Sci.* **5**, 65-110.

Romanek, C., 2005. Stable isotopes as indicators of microbial processes in hot spring environments. *International Workshop "Biodiversity, Molecular Biology and Biogeochemistry of Thermophiles"*, Pratunka, Kamchatka Peninsula.

Whiticar, M. J., Faber, E., and Schoell, M., 1986. Biogenic methane formation in marine and fresh-water environments - CO_2 reduction vs acetate fermentation isotope evidence. *Geochim. Cosmochim. Acta* **50**, 693-709.

CHAPTER 3

LIPIDS AND STABLE CARBON ISOTOPES IN HOT SPRINGS OF THE UZON CALDERA, KAMCHATKA: IMPLICATIONS FOR MICROBIAL COMMUNITY DYNAMICS[‡]

[‡] Weidong Zhao, Randy Culp, Gary Mills, Noelle Garvin, Ann Pearson, Christopher S Romanek, Juergen Wiegel, and Chuanlun L Zhang, to be submitted

ABSTRACT

Phospholipid fatty acids (PLFAs) and glycerol dialkyl glycerol tetraethers (GDGTs) are core membrane lipids of bacteria and archaea, respectively. In this study, PLFAs and GDGTs were used as semi-quantitative proxies to understand the bacterial and archaeal communities in microbial assemblages of hot springs in the Uzon Caldera, Kamchatka (Russia). Cluster analysis grouped hot spring samples into four major bacterial groups (P1- P4) and six archaeal groups (G1- G6) based on the corresponding lipid profiles. Two of the bacterial community groups were dominated by *Aquificales* species and the other two were presumably dominated by *Cyanobacteria-Thermotogae* type or *Proteobacteria-Desulfurobacterium* type. Carbon isotope fractionations between PLFAs and CO_2 showed a pattern characteristic for CO_2 fixation via the Calvin cycle for most of groups P1, P2 samples and about half of group P3 samples; that of the other half group of P3 samples displayed carbon isotope system has characteristic for the rTCA cycle using *Aquificales* species. Due to the limited knowledge of GDGTs from pure isolates of archaea, taxonomy of archaea represented by the detected GDGTs was not determined. However, statistical analysis revealed that GDGTs -0, -1 and -4 may have distinct origins.

INTRODUCTION

Membrane lipids of microorganisms can carry specific taxonomic information. Phospholipid fatty acids (PLFAs) are characteristic of bacterial and eukaryotic organisms whereas isoprenoidal glycerol dialkyl glycerol tetraethers (GDGTs) are core lipids of archaea. Bacterial PLFA differ from those of eukaryotes in that the former mainly contain monounsaturated or terminally branched fatty acid (iso-fatty acid), whereas the later often contains high abundance of polyunsaturated fatty acids (Vestal and White 1989). It has been suggested that particular lineages of bacteria and archaea possess characteristic lipid components that can be used for taxonomic identification (Derosa *et al.* 1986; Gambacorta *et al.* 1994; Ringelberg *et al.* 1997; Zelles 1999). A pool of lipids from an environmental sample may reflect either the dominant or the weighed average of multiple lipids for microbial lineages in a community (Vestal and White 1989). Notably, the lipid composition often varies to some extent between phylogenetically related species as observed in *Bacillus* species (Kampfer 1994); further, it may change in response to the

environmental variations by changing stereo-configurations and/or the relative abundance of individual components (Vestal and White 1989). Therefore, comparison of lipid compositions between samples not only reveals the similarity of structures of microbial communities, but also insight into environmental constraints that dictate community structure.

Stable carbon isotope analysis reinforces the understanding of carbon metabolism of corresponding microorganisms because isotope fractionations between source CO_2, biomass, and individual lipid compound primarily reflects the different carbon fixation pathways of autotrophs (van der Meer *et al.* 1998; Zhang *et al.* 2002; House *et al.* 2003; van der Meer *et al.* 2003; Zhang *et al.* 2003). For examples, House *et al.* (2003) examined 21 thermophilic bacterial and archaeal isolates that use different carbon fixation pathways and summarized previously reported isotopic fractionations between bulk biomass and CO_2 ($\varepsilon_{Biomass\text{-}CO_2}$) to generate ranges for each carbon fixation pathway. The rTCA cycle and the 3-HP cycle were shown to have the smallest value for $\varepsilon_{Bio\text{-}CO_2}$ compared with the Calvin cycle and acetyl-CoA pathway. The latter has the largest possible $\varepsilon_{Biomass\text{-}CO_2}$ (House *et al.* 2003). Similarly, isotope fractionation between lipids or their derivatives and biomass ($\varepsilon_{Lipid\text{-}Bio}$) have also been determined for representative microorganisms that use distinct carbon fixation pathway (Summons *et al.* 1996; Sakata *et al.* 1997; van der Meer *et al.* 1998; van der Meer *et al.* 2001; Zhang *et al.* 2002). Taken together, the Calvin cycle and 3-HP cycle may generate $\varepsilon_{Lipid\text{-}CO_2}$ values of about -9‰ and -1‰, respectively (van der Meer *et al.* 1998; Jahnke *et al.* 2001; Zhang *et al.* 2002; van der Meer *et al.* 2003), whereas the acetyl-CoA pathway produce larger $\varepsilon_{Lipid\text{-}CO_2}$ values of more than -30‰ (Summons *et al.* 1998). By contrast, the rTCA cycle usually produces lipids that are enriched in ^{13}C relative to biomass and even CO_2 with $\varepsilon_{Lipid\text{-}CO_2}$ values as high as *ca.* 2 to 16‰ (van der Meer *et al.* 1998; Jahnke *et al.* 2001; Zhang *et al.* 2002; Zhang *et al.* 2004).

In terrestrial hot spring environments, island-like distribution of microorganisms may exist that are associated with dramatic spatial variations in physical and chemical environments (Papke *et al.* 2003). Because the temporal and spatial variation of physicochemical environments for hot springs is great, the

availability of carbon and energy sources for microorganisms may vary greatly. However, surveys of the microbial community using culture-independent molecular approaches are limited because these studies are labor intensive and costly. In contrast, with the aid of statistics and other techniques such as compound specific stable isotope analysis, analyses of bacterial phospholipids and archaeal GDGTs can be used as semi-quantitative tools to rapidly and efficiently examine the dynamics of microbial communities.

Lipid biomarkers of bacteria and archaea have been investigated in many major geothermal sites including Yellowstone National Park (Summons *et al.* 1996; Jahnke *et al.* 2001; Zhang *et al.* 2004; Schouten *et al.* 2007) and the Great Basin (Pearson *et al.* 2004; Zhang *et al.* 2006; Zhang *et al.* 2007; Pearson *et al.* 2008), Kamchatka, (Russia; Romanek *et al.* 2004), New Zealand (Pancost *et al.* 2005), and Iceland (Madureira *et al.* 1995). Coupling lipid analysis with stable isotope analysis can provide further insights into community structures, response to environmental variations and metabolic significance, such as the pathway of carbon fixation by autotrophs, because carbon isotope fractionation differs considerably in some instances (Jahnke *et al.* 2001; House *et al.* 2003; Papke *et al.* 2003; van der Meer *et al.* 2003; Pearson *et al.* 2004; Zhang *et al.* 2004; Zhang *et al.* 2007).

Hot springs in Kamchatka, Russia are one of the major terrestrial geothermal areas of the earth. Studies based on the cultivation approach (see review by Zhao *et al.* 2005) and selected 16S rRNA gene clone libraries (Burgess *et al.* 2006), together with field observations have shown that Kamchatka hot springs harbor microorganisms found in hot springs elsewhere (Hugenholtz *et al.* 1998; Ward *et al.* 1998; Kanokratana *et al.* 2004; Zhang *et al.* 2007) as well as unique microorganisms. These microorganisms appear to possess diverse metabolic strategies that utilize various volcanogenic or biogenic chemicals, such as hydrogen, sulfur, sulfide, iron, carbon monoxide, carbon dioxide, methane and organic compounds as energy or carbon sources. While previous culture-dependent and culture-independent studies have provided valuable information about the diversity and metabolic function of isolated communities, system-wide investigations are rare in hot springs. The primary objective of this study was to classify the prokaryotic community using bacterial PLFA and archaeal GDGT analysis and examine

the spatial and temporal variation in multiple microbial communities in hot springs of the Uzon Caldera, Kamchatka. Carbon isotope analysis and spring geochemistry are also examined for their relation to lipid distribution patterns using statistic analysis to build on our understanding of the community structure and the major metabolic pathways in these hot springs.

MATERIAL AND METHODS

Sampling location

The Uzon Caldera (54°26'-54°31'N, 159°55-160°07'E) is an area of 9×12 km and one of the major hydrothermal systems in Kamchatka Peninsula. Temperatures of hot springs within the caldera range from 30°C to near 100°, while the pH ranges from acidic to slightly alkaline but mainly in the range of 5-7 (reviewed in Zhao *et al*. 2005). In addition to these attributes, redox potentials, free phase gases, major ores, trace elements and other geochemical parameters have been characterized for many springs in the area (reviewed in Zhao *et al.* 2005).

Sample collection

From 2003 to 2006, microbial mats and sediment were collected from hot springs and associated outflow channels in the East Thermal Field (ETF; 54°29'57"N, 160°00'38"E), Orange Thermal Field (OTF; 54°30'25"N, 160°00'05"E), and North Thermal Field (NTF; 54°30'40", 160°00'19") of the Uzon Caldera; one sample was collected from the nearby Geyser Valley (GV; 54°28'41"N, 160°06'53"E) in 2006 (Figs. 3.1a, b). At each spring, temperature, pH and redox potential were measured *in situ* with portable probes prior to collection of samples. Standards of pH 4, 7, and 10 were used for pH calibration at ambient temperatures. Redox-sensitive species (*e.g.*, H_2S, SO_4^{2-}, NH_4^+) and alkalinity were measured using Hach kits in the field. Mat and sediment samples were collected and stored at 5°C in the field for up to 10 days before being transported to the University of Georgia. The samples were then stored at -80°C until analysis. Table 3.1 lists the samples analyzed in this study with *in situ* temperature and pH of the sampling sites.

Lipid extraction

Lyophilized mat material was used for lipid extraction according to the procedures based on White *et*

al. (1979). In brief, a single-phase organic solvent system comprised of chloroform, methanol, and aqueous 50-mM phosphate buffer (pH 7.4) in a ratio of 1:2:0.8 (vol/vol/vol) was used to extract the lipid fraction of mat samples. After overnight extraction, chloroform and nanopure water were added to the extract to achieve a final ratio of 1:1:0.9 (vol/vol/vol), which resulted in a two-phase system. The lower phase was collected and dried under pure N_2 gas to yield the total lipids. Half of the total lipids were separated on a silicic acid column (activated for more than 1 hr at 100°C) into neutral lipid, glycolipid, and polar lipid fractions (Guckert *et al.* 1985). The polar lipids were treated by mild alkaline methanolysis to produce fatty acid methyl esters (FAMEs). The other half of the total lipids was transesterified with 5% HCl in methanol, followed by solid phase extraction (SPE) using a C18 Bond-Elut® solid phase extraction (SPE) column (Varian Inc., Palo Alto, CA , USA) to obtain GDGT fractions (Pearson *et al.* 2008; Zhao *et al*. in review).

GC, GC-MS and LC-MS

GC analyses of FAME were performed on an Agilent 6890 GC with a flame ionization detector (FID). The GC equipped with a 30-m DB-5 column (5% phenyl). The oven temperature program for FAME analysis was initialized a 60°C, and ramped 10°C min^{-1} to 180°C, then 4°C min^{-1} to 320°C and held for additional 20 minutes. GC-MS analysis of FAME was performed on an Agilent 5890 Series II GC equipped with a 30-m, HP5-MSI column coupled to a HP5972 mass selective detector (Zhao *et al.* in review).

The GDGT fractions were dried under nitrogen and characterized using an Agilent 1100 series high performance liquid chromatograph (HPLC) interfaced with an atmospheric pressure chemical ionization-MS following methods described previously (Pearson *et al.* 2008). The HPLC was equipped with a Prevail Cyano column (2.1 × 150 mm, 3 μm; Alltech, Deerfield, IL, USA). Intact GDGTs were eluted isocratically in 1.3% isopropanol in hexane at 30°C. Spectra were scanned over the m/z range from 1,250 to 1,350. Relative abundances of GDGTs were determined by integration of *m/z* 1302, 1300, 1298, 1296, 1294, 1292, and 1290 single ion chromatograms (SIC) and compared to values from integrated total ion chromatograms (TIC). Crenarchaeol (4 cyclopentane + 1 cyclohexane; *m/z* 1292) and

GDGT-4 (4 cyclopentane; *m/z* 1294) co-elute under these conditions; their respective abundances were decoupled by mass spectral ion fragment balance as described previously (Zhang *et al.* 2006).

Stable Carbon Isotopes

Carbon-isotope compositions of the FAME derived from PLFA were determined on a ThermoQuest Delta Plus XL isotope ratio mass spectrometer (Finnigan MAT GmbH, Germany) interfaced with a Trace GC-combustion unit. The Trace GC was equipped with a 30-m DB-5 column (5% phenyl) and using the same temperature program as the GC-FID procedure described above. Measurements of FAME were corrected for the methyl moiety to obtain $\delta^{13}C$ value of PLFA ($\delta^{13}C_{PLFA}$) according to Abrajano *et al.* (1994) using the following equation:

$$\delta^{13}C_{PLFA} = [(C_n + 1) \times \delta^{13}C_{FAME} - \delta^{13}C_{MeOH}]/C_n$$

where C_n is the number of carbons in the fatty acid, $\delta^{13}C_{FAME}$ is the $\delta^{13}C$ of the methylated fatty acid, and $\delta^{13}C_{MeOH}$ is the $\delta^{13}C$ of the methanol (determined as -45‰) used for the methylation reaction.

The weighed average $\delta^{13}C$ value of PLFA ($\delta^{13}C_{\sum PLFA}$) in a single sample was determined using the following equation:

$$\delta^{13}C_{\sum PLFA} = \sum (f_n \times \delta^{13}C_{(PLFA)n})$$

where f_n and $\delta^{13}C_{(PLFA)n}$ are the percentage and $\delta^{13}C$ value of each detectable PLFA species.

The $\delta^{13}C$ value ratio of bulk sample was determined on a ThermoQuest Delta Plus XL isotope ratio mass spectrometer (Finnigan MAT GmbH, Germany) interfaced with an elemental analyzer. Dried bulk samples were pre-ground into fine particles. About 1-2 grams of each sample then was placed in a small beaker in a desiccator with fuming HCl underneath for an overnight digestion to remove carbonate. The residual material was rinsed with distilled H_2O, filtered and dried overnight at 50°C prior to analysis on the mass spectrometer.

A pure CO_2 gas with $\delta^{13}C$ value of -45.0‰ versus PDB was used as the working standard for isotope measurement of FAMEs. Its amplitude 44 value was set to 4000 mV throughout the analysis. The linearity of isotope analysis was examined to be satisfactory from 700 mV to 8000 mV with a variation of

0.1‰ per volt. The powdered dogfish muscle (DORM-1) was used as the working standard for bulk carbon isotope analysis. The precision of the analysis varied depending on the quantity of the material: samples with amplitude 44 values greater than 500 mV was determined to carry a ±0.11‰ standard deviation (SD) using DORM-1. Higher analytical error was estimated for samples with lower values of amplitude 44: ±1‰ for 100-500mV and ±2 for less than 100 mV (Appendix).

Statistical analysis

Primer V5 (PRIMER-E Ltd., Plymouth, UK) was used to perform statistical analysis. Data were transformed appropriately to meet the requirement for statistically valid matrix computations prior to analysis. For PLFA and GDGT compositional data, a log(X+1) transformation was generally applied and a Bray-Curtis similarity matrix was calculated. Geochemical and stable isotope data were transformed differently depending on the data and the normalized Euclidean distance was computed. A resulting similarity/distance matrix was then used for hierarchical cluster and non-metric multidimensional scaling (MDS) analysis. Analysis of similarity (ANOSIM) was performed to compare differences in individual parameters between groups. Similarity percentage analysis (SIMPER) was performed based on the hierarchical clustering analysis to identify the variables that primarily accounted for the observed assemblage differences. The BIOENV routine included in the software package was employed to examine the relationships between similarity matrices of biological data (*e.g.*, PLFAs or GDGTs) and different combinations of environmental variables (*e.g.*, temperature, pH and chemical concentrations). The correlations were ranked according the Spearman coefficient ρ_s (Clarke and Ainsworth 1993):

$$\rho_s = 1 - \frac{6}{N(N^2-1)} \sum_{i=1}^{N} (r_i - s_i)^2$$

Where r_i and s_i are the unraveled elements of the respective rank similarity matrices; N= n (n-1)/2 and n is the number of samples.

RESULTS

Phospholipid fatty acids

Up to thirty-one PLFAs were identified in each sample; most were saturated, monounsaturated and

branched fatty acids (Table 3.2). Polyunsaturated fatty acids (PUFA) were generally low in abundance except 18:2ω6, which was present in about one half of the samples analyzed with abundances of up to 14%. Samples containing this PUFA were mainly found in green microbial mats collected from pools of Zavarzin II, Rubbermat and Jenn's Vents (Table 3.2). Other components included mainly mid-branched and straight chain fatty acids that were generally less than 2% each, however, a methyl-branched fatty acid 10Me18:0 was observed at 10.2% and 8.3% in K4-E and K4-C samples, respectively.

Among the 31 PLFAs identified, 13 were predominant in most of the samples, covering 80 to 100% of total PLFA. These 13 major compounds were used for the cluster analysis (Table 3.2). Exclusion of PLFA components of rare occurrence or low abundance did not have a significant impact on the result of cluster analysis, suggesting that the patterns are reasonably robust indicators of the microbial community structure of a sample. Hierarchical cluster analysis revealed that the samples formed four major groups (P1-P4) with PLFAs having greater than 70% similarity within each group (Fig 3.2). Samples K4-E, Ark-03 and JV1A cannot be grouped at this similarity level mainly due to the low numbers of detected PLFA and the high abundance of a few particular biomarker, *i.e.,* 20:1ω9t in Ark-03, iso15:0 in JV1A and 20:1ω9c in K4-E. Groups P1 and P3 contained 34 out of total 43 samples whereas groups P2 and P4 contained 4 and 2 samples, respectively. The latter two groups therefore may represent rare community types in the surveyed area. Temporally, samples repetitively collected from the same spring but in different years generally showed low variations and clustered into the same group (*e.g.*, Rubbermat pool, Zavarzin II, Bright White pool or Vent 1 North), indicating temporally stable bacterial communities in those pools. However, the grouping did not seem to be geographically well defined since samples from the same spring system usually occurred in different PLFA groups, *e.g.* samples from the major pools of East Thermal Field and North Thermal field were present in multiple PLFA groups; On the other hand, samples from isolated fields were not limited to the same PLFA cluster pattern, *e.g.* sample ON1 from the Orange Thermal Field and samples from the North Thermal Field were shown to be closely related to samples from the ETF (Fig 3.2). This pattern suggested a highly patchy distribution of bacterial

community throughout the caldera. Both temporal and spatial PLFA distribution patterns were consistent with field observations. For example, Zavarzin II pool contained morphologically different bacterial mats, *e.g.* green mats around the edge of the pool and submersing grey mats/streamers. Different morphological types produced distinguishable PLFA profiles and were clustered in different groups or subgroups; whereas the same type of mats collected in different years contained highly similar PLFA (Fig 3.2).

SIMPER analysis was used to compare the similarity within groups and dissimilarity between groups. Table 3.3 show primary PLFA contributors that cumulatively explained 90% pattern of the grouping. Similarity within each group was mainly determined by the dominant species of PLFA. For example, groups P1 and P2 both were dominated and primarily explained by 16:0 and 18:1ω9c or 18:1ω7. Cumulative contribution of these fatty acids accounted for *ca.* 63 to 68% of the similarity for these two groups. In contrast, group P3 and P4 were dominated and primarily explained by 20:1ω9c and 18:1ω9c/t, which cumulatively accounted for 53% and 90% of the similarity in theses groups, respectively. 16:0 and 18:0 were also high in group P3 samples and cumulatively contributed another 22% to the similarity of this group (Table 3.3). An out-group sample JV-1A collected from Jenn's Vent 1 in 2006 had iso15:0 (76.2%) and iso17:0 (9.3%) as the most abundant PLFA components (Table 3.2).

Dissimilarities between groups were accounted for by both major and minor PLFAs (Table 3.4). In five out of six pair wise comparisons, differences in 20:1ω9c and 16:0 were the two primary contributors accounting for the dissimilarity between any two groups. For example, groups P1 and P2 had high abundance of 16:0 while groups P3 and P4 had high abundance of 20:1ω9c. Groups P1 and P2 were further differentiated by 18:1 and 16:1 fatty acids. Group P1 contained a higher abundance of 18:1ω9c while group P2 had a higher abundance of 18:1ω7 and 16:1ω7c. Between groups P3 and P4, P3 was relatively rich in 16:0 and terminally branched fatty acids (*e.g.* iso15:0 and anteiso17:0) and P4 was relatively rich in 18:1 and 18:0. From P1 to P4, the importance of 20:1ω9 increased whereas the importance of 16:0 decreased in defining the community structure patterns.

To better understand the relationship between environmental variables and the PLFA distribution, a subset of 15 PLFA samples, all derived from the 2006 season, were selected for comparison with six

measured environmental variables (Table 3.5). The comparison was made using the BIOENV routine procedure included in the PRIMER V5 package. The Bray-Curtis similarity of PLFA was compared pairwise with all possible combinations of normalized Euclidean distances among six environmental variables to determine the best correlation with the least variable combinations. The results show that temperature alone best explained the similarity pattern of PLFAs ($\rho_s = 0.44$). Combinations with other measured variables did not yield higher correlations between the two matrices (Table S3.1). Despite the result, each PLFA group appeared to have a wide range of temperatures. ANOSIM analysis showed that only group 2 was significantly different from other groups in the temperature ($p < 0.01$; Fig S3.2). Taken together, it suggested that other overlooked factors may play an important role in the PLFA distribution.

GDGT composition

Nine GDGTs were identified from multiple hot spring samples and six archaeal pure isolates (Table 3.6). The pure cultures were included as references in statistic analysis (*i.e.* cluster and MDS) to reveal potential phylogenetic and metabolic similarities with environmental samples analyzed. GDGTs with zero (GDGT-0, m/z 1302) to four (GDGT-4, m/z 1294) cyclopentane rings were predominant in most of the samples. Sample GV from Geyser Valley was the only sample from a moderately alkaline environment and it contained a significant amount of GDGT-cren (m/z 1292), *i.e.* crenarchaeol. Sample V2N, JV12 and three pure cultures contained relative higher abundance of GDGTs with more than four cyclopentane moieties (Table 3.6). Using the same statistical approach as for the PLFA analysis, seven primary GDGTs (*i.e.* GDGT-0 to GDGT-6) were selected for cluster analysis, which cumulatively accounted for over 96% of the total GDGTs detected. The samples were separated into seven groups at a similarity level of 86% (Fig 3.3). Only group G0 was formed solely by two pure cultures and no environmental sample was included. In contrast to PLFA distribution patterns, GDGTs were distributed in a consistent geographical pattern. Samples from the pools of Zavarzin II, Burlyashi, Cascadnaya, Thermophile and Jenn's Vent 2 grouped with their geographic neighbor samples with only a few exceptions. Samples repetitively collected from pools of Zavarzin II, Rubbermat and Jenn's Vents and 2006 showed greater than 90% average similarities (Fig 3.3), suggesting archaeal communities are temporally stable at these sites.

SIMPER analysis revealed that GDGT-4 primarily contributed to within-group similarity for groups G0, G1, G2, and G5 (25-35% contribution) and secondarily for groups G3, G4, and G6 (17-20% contribution). GDGT-0 primarily contributed to the within-group similarity for groups G3 and G6 and GDGT-3 primarily for group G4 (Table 3.7). Furthermore, a decoupling between GDGT-0 and GDGT-4 was observed as an increase in GDGT-0 was generally associated with a decrease in GDGT-4 (Fig 3.4). GDGTs -1 (m/z 1300), -2 (m/z 1298) and -3 (m/z 1296), on the other hand, largely co-varied in abundance (Fig 3.4). However, MDS analysis comparing the similarities between the five major GDGTs (-0 to -4) of all analyzed samples showed that that GDGT-1 also decoupled with GDGT-0 and GDGT-4 (Fig 3.5).

SIMPER analysis also revealed that dissimilarity between groups can be attributed to both major and minor GDGT components. For example, group G1 differed from other groups primarily by having high abundance of GDGT-6; G0 had a higher average of GDGT-4 and GDGT-5'; and group G6 had very high GDGT-0 and low abundance of GDGT-4. Comparisons with G2, G3 and G4 were not consistently determined by a certain GDGT. Notably, undetectable amount of GDGT-cren in groups G2, G5 and G6 contributed considerably to the dissimilarity computation, but may not be significant because the average amount of GDGT-cren (crenarchaeol) in each counterpart group was also low (< 0.05%) and the measurements for crenarchaeol potentially had higher error than for other GDGT species (see Material and Method).

GDGTs from a subset of 15 samples were analyzed using the BIOENV routine to compare with six measured environmental variables (Table 3.5) following a similar procedure to the analysis of PLFA. The results showed that combined temperature and pH was best related to the similarity pattern of GDGT with a Spearman correlation coefficient 0.46 (Table S3.2). Temperature or pH alone had a 0.25 or 0.39 Spearman coefficient ρ_s, respectively.

Carbon isotope composition and fractionations of PLFAs

Carbon isotope compositions were determined for 23 different PLFAs by GC-C-IRMS and bulk samples were analyzed for $\delta^{13}C$ values by EA-IRMS (Table 3.9). The range of $\delta^{13}C$ values of PLFA

($\delta^{13}C_{PLFA}$) for each sample was relatively consistent between the group P1 samples compared with other groups. Weighed average $\delta^{13}C_{PLFA}$ ($\delta^{13}C_{\sum PLFA}$) in group P1 ranged from -29.5 to -12.5‰, while individual PLFA species varied from -32.6 to -7.4‰. The standard deviation (SD) of $\delta^{13}C_{PLFA}$ in the group P1 samples ranged from 0.5 to 4.3‰. The two samples in group P2 had $\delta^{13}C_{\sum PLFA}$ values of -24.6‰ and -28.0‰ and standard deviation of 2.3‰ and 5.1‰, respectively. The group P3 samples had the largest $\delta^{13}C_{\sum PLFA}$ variations among all groups, ranging from -5.7 to -38.5‰ and the standard deviations of $\delta^{13}C_{PLFA}$ in individual sample ranged from 0.9 to 8.0‰. Individual $\delta^{13}C_{PLFA}$ values in this group ranged from as low as -51.2‰ to +0.9‰, although most of PLFA had values greater than -39‰ (Table 3.9). The samples K4-E, Ark-03, and JV1A had $\delta^{13}C_{\sum PLFA}$ values of -21.3, -30.0 and -23.5‰, respectively with standard deviations of 4.6, 1.0 and 5.7‰. The large SD of samples K4-E and JV1A indicate that PLFA may be derived from different microorganisms.

In the Uzon Caldera, the average $\delta^{13}C$ value for CO_2 was -4.6±1.1‰ based on analysis of vent gases in 2005 and 2006 (Chapter 2), therefore the variation in isotope fractionation between CO_2 and organic matter is largely determined by the isotope composition of individual organic matter. Using this value, isotope fractionation, represented by isotope fractionation factor ε, can be computed between CO_2 and PLFA: 1) -25 to -8‰ in group P1, 2) -25 to -19‰ in groups P2, and 3) -34 to -1‰ in group P3 (Table 3.9, Fig 3.6). The $\delta^{13}C$ value of bulk biomass ranged from -10 to -28‰ for these samples and seemed not to vary consistently relative to $\delta^{13}C_{\sum PLFA}$ as ε values for ∑PLFA-bulk biomass system ranged from -11.2 to +15.6‰ (Table 3.9). Notably, all samples with enriched $\delta^{13}C_{\sum PLFA}$ values relative to the individual bulk biomass were in group P3.

DISCUSSIONS

Major bacterial groups revealed by lipid profiles

Bacteria are dominant contributors to community PLFA in hot springs of the Uzon Caldera because polyunsaturated fatty acids (PUFAs) with more than 2 double bonds, which are considered as markers of eukaryotic cells, are either absent or in extremely low abundance. In addition, the only quantitatively significant PUFA 18:2ω6 may originate from *Cyanobacteria* (Vestal and White 1989). Three types of

bacterial PLFA groupings are predominant in Kamchatka hot springs: those dominated by 16:0 and 18:1 (groups P1 and P2, samples K4-E), those dominated by 20:1 and 18:0 dominances (groups P3 and P4, and sample Ark-03), and that dominated by iso- and anteiso-15:0 dominances (JV1A). The known PLFA compositions of commonly occurring bacteria in hot spring environments may help to explain and predict microbial assemblages (Hugenholtz *et al.* 1998; Ward *et al.* 1998; Kanokratana *et al.* 2004; Burgess *et al.* 2006; Zhang *et al.* 2007). Although 16:0 and 18:1 are dominant in groups P1 and P2, they are not diagnostic of specific taxonomic units; rather they are common in hot springs environments. Examples of the microorganisms include thermophiles such as *Desulfurobacterium* (L'Haridon *et al.* 1998), *Thermotogae* (Antoine *et al.* 1997; Zhang *et al.* 2002), *Thermodesulfobacteria* (Moussard *et al.* 2004), *Chloroflexi* (Hanada *et al.* 1995; Hanada *et al.* 2002), and α- (Maszenan *et al.* 2005), δ- (Nunoura *et al.* 2007) and ε- *Proteobacteria* (Nakagawa *et al.* 2005), as well as nonthermophilic members of *Cyanobacteria* (Ward *et al.* 1994). In contrast, the dominant fatty acids 20:1ω9c/t together with high abundances of 18:1 and 18:0 of the P3 and P4 groups are diagnostic of hydrogen-oxidizing bacteria in the order of *Aquificales* (Jahnke *et al.* 2001; Stohr *et al.* 2001; Takai *et al.* 2001; Gotz *et al.* 2002; Nakagawa *et al.* 2004) and account on average for 31 and 54% of total PLFA in these two groups, respectively. The high abundances of terminally branched saturated fatty acids as seen in sample JV1A are usually found in heterotrophic *Thermus* (Balkwill *et al.* 2004; Yang *et al.* 2004), *Firmicutes* (Zhao *et al.* 2006), and heterotrophic sulfate-reducing bacteria (Rutters *et al.* 2002; Goorissen *et al.* 2003).

Some more details about the variation of bacterial communities that are largely similar in PLFA compositions can be gained by comparing the quantitative differences of PLFA compositions. For example, group P1 has lower abundance of 16:1 and 18:1 but higher abundance of 16:0 and 18:0 than group P2; assuming the communities contain microorganisms mentioned above, *Thermotogae* and *Cyanobacteria* may be relatively more abundant in group P1 and *Proteobacteria* and sulfur-reducing bacteria more abundant in group P2 in these two groups because it has been found that *Thermotogae* and *Cyanobacteria* are richer in 16:0 and 18:0 (Ward *et al.* 1994; Antoine *et al.* 1997; Zhang *et al.* 2002); whereas *Proteobacteria* (Maszenan *et al.* 2005; Nunoura *et al.* 2007) and sulfur-reducing bacteria such as

Desulfurobacterium (L'Haridon *et al.* 1998) are richer in 18:1 and 16:1. Similarly, the increasing abundance of terminally branched saturated fatty acids, *i.e.* iso/anteiso 17:0 and 15:0, in the group P3 indicates higher contribution from heterotrophic *Thermus*, *Firmicutes* or heterotrophic sulfate-reducing bacteria. Therefore, from groups P1 to P4, a possible autotrophic community shift from *Cyanobacteria-Thermotogae* type to *Proteobacteria-Desulfurobacterium* type and to *Aquificales* type may be expected. From P2 to P4, a decrease in iso15:0 may indicate a decrease in the heterotrophic community contribution. Elevated amounts of 10Me18:0 in K4-C and K4-E samples indicate a potential contribution from *Actinomycetes* and sulfate-reducing bacteria (Frostegard *et al.* 1993; Rutters *et al.* 2002).

Stable carbon isotope fractionation between PLFA and carbon source

Because microorganisms that use different carbon metabolisms may cause different isotope fractionations between CO_2, biomass, or individual PLFAs (Hayes 2004), and carbon isotope compositions of individual fatty acids from the same microorganisms usually differ less than 5‰ (Zhang *et al.* 2002; Zhang *et al.* 2003), variation of $\delta^{13}C_{PLFA}$ within a single sample may reflect the diversity of the source of PLFAs. Therefore, standard deviation (SD) of $\delta^{13}C_{PLFA}$ values observed in the environmental sample may be regarded as a measure of carbon source diversity and provide some insight into community structure as well. For example, a small standard deviation among $\delta^{13}C_{PLFA}$ may suggest a homogenous or less diverse ecotype, such as in the samples ZV-03, ZV, ARK-03 and CZ1-03; large standard deviations on the other hand, may suggest diverse ecotypes that use multiple metabolic pathways, such as in the samples CAC-B, CAC-S and JV3 etc.

By comparing the measured range of both $\delta^{13}C_{PLFA}$ and $\delta^{13}C_{\sum PLFA}$ values with literature values, it is probable that autotrophs in the group P1 samples mainly use the Calvin Cycle for carbon fixation but may also have significant contributions from microorganisms using the rTCA cycle (Table 3.9); the group P2 samples and out-group samples K4-E and Ark-03 may also be dominated by microorganisms using the Calvin cycle, which appear to produce more depleted $\delta^{13}C$ values compared with those in group P1 samples, probably due to the use of different types of Rubisco as key enzymes (Robinson and Cavanaugh 1995); group P3 appears to have the greatest diversity in carbon fixation pathways. The rTCA cycle is

predominant in some of the samples due to the relative ^{13}C enriched PLFAs to biomass or source CO_2 (van der Meer *et al.* 1998; Zhang *et al.* 2002); importance of 3-HP pathway in this group can not be evaluated because of the overlapping range with the rTCA cycle. The Calvin cycle and/or reductive acetyl-CoA pathway may also function in samples V1N, V2N-03, ZV and TM-A.

While the groups P1 and P2 do not contain biomarkers having strong taxonomic specificity, group P3 contains *Aquificales* biomarker 20:1ω9 as the most abundant PLFA. However, the large variation in $\delta^{13}C$ values of 20:1ω9 (-34‰ to -24‰) in group P3 is not consistent with hypothesis that *Aquificales* is using the rTCA cycle for carbon fixation since the $\delta^{13}CO_2$ values in P3 sampling pools only vary by 4‰. It suggest that *Aquificales* may use alternative carbon acquisition metabolisms (*e.g.* the Calvin Cycle) like *Tiocapsa Roseopersicina*, which usually use the rTCA cycle for carbon fixation as well (van der Meer *et al.* 1998). In addition, the predominance of isotopically depleted values of fatty acids observed in sample TM-A in group P3 are consistent with the values of $\delta^{13}C$ of CH_4 (-24 to -30‰; Chapter 2), and therefore, can be attributed to the type II methanotrophs, which have relatively high iso17:0 PLFA (Bull *et al.* 2000; Knief *et al.* 2003; Crossman *et al.* 2005).

An important implication of stable isotope analysis of PLFA is that it provides insight into the patchy distribution of bacteria. For example, $\delta^{13}C_{\sum PLFA}$ values for ZV-03 and ZV, which were both taken from the Zavarzin II, differ by 7‰, indicating that the two samples represented distinct microbial assemblages within a single pool.

Major Archaeal group revealed by GDGT analysis

The non-metric multi-dimensional scaling (MDS) analysis among the five GDGT species (-0 to -4) show that GDGT-0, GDGT-1 and GDGT-4 are relatively independent from each other, suggesting they may be characteristic of different archaea (Fig 3.5). Many of these different archaea, however, may produce GDGT-2 and GDGT-3 as they occur together in the MDS plot. Pearson *et al.* (2008) observed a decoupling between GDGT-0 and GDGT-4, which was attributed to different sources of archaea; further, they speculated that GDGT-0 was derived from *Euryarchaeota* and GDGT-4 was from *Crenarchaeota* due to differences in relative occurrence rate of the two GDGTs in the two phyla of *Archaea*. GDGT-4 is

uncommon in samples from low temperature environments such as marine (Schouten *et al.* 2000; Wuchter *et al.* 2005; Weijers *et al.* 2007), lacustrine (Powers *et al.* 2004; Escala *et al.* 2007) and soil (Leininger *et al.* 2006; Weijers *et al.* 2006) environments, and it is low or undetected in the non-thermophilic Crenarchaeotal isolate "*Candidatus* Nitrosopumilus maritimus" (Schouten *et al.* 2008) and the uniarchaeon "*Candidatus* Cenarcheum symbiosum" (Damste *et al.* 2002; Schouten *et al.* 2008), where GDGT-0 to -3 predominant. The highest average GDGT-4 content occurred in groups G0 and G5 with the highest average temperatures (85 and 77°C, respectively) and the lowest average GDGT-4 content occurred in group G6 which had the second lowest average temperature (59°C; Table 3.7). Taken together, GDGT-4 may be particularly related to (hyper)thermophilic archaea. Decoupling between GDGT-0 and GDGT-1 is not frequently observed, but the presence of GDGT-1 and the absence of GDGT-0 in an enrichment culture from the North Sea suggest the decoupling does occur in some samples (Wuchter *et al.* 2004).

Limited GDGT information from cultivation studies constrains a better understanding of possible archaeal lineages from environmental samples. In addition, relationships between GDGT composition and environmental variables are often ambiguous (Pearson *et al.* 2004; Zhang *et al.* 2006; Schouten *et al.* 2007). Inclusion of several pure cultures in this study does not always show consistent grouping patterns with our current knowledge of archaeal taxonomy. For example, both *Thermoproteus uzoniensis* and *Vulcanisaeta sp.* are members of the family *Thermoproteaceae* and grouped together with an average similarity of 94.3%; on the other hand, two species in the genus *Desulfurococcus* are placed in different groups similar to *Sulfolobus solfataricus* and *Metallosphaera sedula* in the family *Sulfolobaceae*, which are also distant and only share an average GDGT similarity of 70%. The reason for the discrepancy between DNA divergence and GDGT dissimilarity awaits further investigation. However, assuming that GDGT-0, -1 and -4 are generated by different groups of archaea, group G2 samples (from Zavarzin II, Jenn's vent sites, Rubbermat pool in ETF and V1N-03 and V2N-03 in NTF) may contain archaea that contributed equal amounts of GDGT-0, -1, and -4; group G3 (Cascadnaya samples) appear to contain archaea containing similar amounts of GDGT-0 and GDGT-4 but also archaea having lower amount of

GDGT-1; group G4 (Burlyashi samples and K4-C) and group G5 (Ark-03) both may be dominated by archaea producing GDGT-4, but group G4 samples may have archaea that produce more GDGT-1; and group G6 (all samples from Thermophile and CAC-B and CAC-C from Cascadnaya) may be dominated by archaea mainly producing GDGT-0.

Spatial and temporal variations in microbial lipids in hot springs

In terrestrial hot spring systems, many geochemical properties of individual hot springs are often surprisingly stable over time as in the Uzon Caldera (reviewed in Zhao *et al.* 2005). This attribute may greatly affect PLFA distribution patterns that are spatially patchy but temporally stable (Fig 3.1). Patterns of GDGT distributions in these springs however, are different. Spatially, GDGT patterns appear to be largely defined based on their physical locations in the caldera's individual spring flow system in that samples within a spring system are more similar to each other, especially as seen in groups G2, G3, G4 and G6 (Fig 3.2). The inconsistency between the PLFA and GDGT distribution patterns may be explained by their different relationships with environmental variables. The BIOENV analysis revealed that temperature played a more important role in defining the distribution of bacteria than archaea in Uzon hot springs; the latter grouping was related to the combined effect of both pH and temperature, although pH seemed to be more important (Table S3.1). Therefore, archaeal communities may tend to be more stable than bacterial communities because pH varied much less than temperature from the source of the spring to the distal outflow channel. It has been previously reported that PLFA profiles vary according to the change in temperature (Hamamoto *et al.* 1994; Suutari and Laakso 1994; Konneke and Widdel 2003), which reflect different communities of bacteria living in different temperature provinces in the hot spring (Zhang *et al.* 2004). For archaea, lipid compositions have been observed to correlate to either temperature (Derosa *et al.* 1980; Gliozzi *et al.* 1986; Uda *et al.* 2001; Schouten *et al.* 2002; Wuchter *et al.* 2004) or pH (Macalady *et al.* 2004; Zhang *et al.* 2006; Schouten *et al.* 2007; Pearson *et al.* 2008). While our data are in agreement with those previous findings, the low coefficient ρ_s of the BIOENV analysis suggests other unknown variables may also contribute to the distribution patterns of both PLFA and GDGT in the natural environment. For example, autotrophic sulfate reducing bacteria can use alternative electron

acceptors such as nitrate and Fe (III) to extract energy from the environment (Dannenberg *et al*. 1992; Delgado and Back 1994; Henry *et al*. 1994; Richardson 2000); heterotrophs utilize a variety of organic compounds for carbon and energy sources. The alternative energy and carbon metabolisms may result in different fatty acid profiles for the same microorganism.

In summary, lipid profiles provided insight into microbial community in heterogeneous hot springs in the Uzon Caldera, Kamchatka. Both bacterial and archaeal community structures seem to be temporally stable. Spatial distributions are significantly different between bacterial and archaeal communities. Distributions of PLFA are mainly controlled by temperature, whereas distribution of GDGTs appears to be controlled by the coupling effect of pH and temperature. Spatially, geographical patterning is observed for archaeal lipids but not for bacteria. However, PLFA indicated a community shift from *Cyanobacteria-Thermotogae* type (group P1) to the *Proteobacteria-Desulfurobacterium* type (group P2) and to the *Aquificales* type (groups P3 and P4). Stable carbon isotope signatures generally agree with these predictions by showing that the carbon fixation pathways used by autotrophs are dominated by the Calvin Cycle in the groups P1 and P2, and by the rTCA cycle in groups P3. It also suggests that *Aquificales* in the group P3 hot springs may use the Calvin cycle as the alternative carbon fixation pathway. For archaeal community structure, limited GDGT data from pure archaeal isolates do not allow detailed taxonomic prediction for archaeal community structure as they do for some PLFAs. GDGT-4 and GDGT-0 were the most abundant GDGT compounds observed in the hot springs of the Kamchatka. GDGT-0, GDGT-1 and GDGT-4 appear to be characteristic of different archaeal lineages and vary differently between groups defined by the cluster analysis. GDGT-4, in particular, appears to be thermophile in origin. GDGT-2 and GDGT-3 seems to be commonly produced by archaea. A better understanding of the archaeal phylogeny in environments awaits novel isolates to be discovered, especially those with different temperature affiliations. Taken together, our results show the strength of using lipid and isotope analyses as an effective tool to semi-quantitatively examine the spatial and temporal variation of microbial assemblages in hot spring environments. Furthermore information from lipid and isotope studies can greatly improve the efficiency in conducting detailed genomic studies to gain insight into the microbial diversity and

ecological function in natural environments.

ACKNOWLEGEMENT

We thank Dr. Douglas E Crowe for providing the detailed map of the East Thermal Field, and Dr. Elizaveta Bonch-Osmolavskaya from the Microbiology Institute of the Russian Academy of Sciences for providing pure archaeal cultures for GDGT analysis. We thank Yundan Pi and Ann Pearson for assisting the GDGT analysis and Heather Brant for bulk carbon isotope analysis. The work was supported by the National Science Foundation through the Kamchatka Microbial Observatory project to JW, CSR.

Table 3.1. Sample identification and description. Temperature (T) and pH of sampling site were also listed.

Year	Original ID	Sample ID	Pool /Feature	Location[a]	T (ºC)	pH
	CR03004	ARK-03	Arkashin shaft, sediment	CETF	69	4.9
	CR03016	BW-03	Bright white pool, mat	ETF	55	5.5
	CR03018	CZ1-03	CZ pool, mat	NTF	40	5.8
	CR03007	JV12-03	Jenn's pool, between Vent 1 and Vent 2, green mat	CETF	76	5.8
2003	CR03008	JV2-03	Jenn's Vent 2, mat	CETF	80	5.5
	CR03012	JVB12-03	Jenn's pool, bubbler between Vent 1 and 2, mat	CETF	76	5.8
	CR03022	RM-03	Rubbermat pool, green mat	EETF	87	5.5
	CR03019	V1N-03	Vent 1, north of CZ1 pool, mat	NTF	70	5.0
	CR03026	V2N-03	Vent 2, blue pool, mat	NTF	78	5.0
	CR03021	ZV-03	Zavarzin II pool, mat and sediment	EETF	54	5.8
	JK04078	RM-04	Rubbermat pool, green mat	EETF	91	6.1
2004	JK04051	ZVGN-04	Zavarzin II pool, green mat	EETF	51	6.7
	JK04050	ZVGY-04	Zavarzin II pool, grey mat	EETF	57	6.3
	CZ05-013	BLS-05	Burlyashi outflow, sediment	CETF	51	6.9
	CZ05-015	JV2-05	Jenn's Vent 2, mat	CETF	41	5.7
	CZ05-26	TM-out-05	Thermophile spring outflow, mat (green/red)	EETF	32	9.7
2005	CZ05-025	V1N-05	Vent 1 north, mat/sediment	NTF	44	5.8
	CZ05-02	ZVGN-05	Zavarzin II green mat	EETF	71	7.0-8.5
	CZ05-03	ZVGR-05	Zavarzin II green-red mat	EETF	59	7.0-8.5
	CZ05-01	ZVGY-05	Zavarzin II grey mat	EETF	50	7.0-8.5
	CZ05-04	ZVM25-05	Zavarzin II brown mat	EETF	57	7.0-8.5
	CR06-012A	BLS-A	Burlyashi- A, water & black sand/mud	CETF	87	6.0
	CR06-012B	BLS-B	Burlyashi-B, black sand/mud	CETF	70	6.5
	CR06-012D	BLS-D	Burlyashi-D, black sand/mud	CETF	51	6.0
	CR06-012E	BLS-E	Burlyashi-E, black sand/mud	CETF	41	6.0
	CR06-012F	BLS-F	Burlyashi-F, black sand/mud	CETF	32	6.0
	CR06-073	BW	Bright White, water & sediment	ETF	44	5.0
	CZ06-012A	CAC-A	Cascadnaya-A, black mud	EETF	85	6.0
	CZ06-012B	CAC-B	Cascadnaya-B, streamer on hard surface	EETF	71	6.5
	CZ06-012C	CAC-C	Cascadnaya-C, dark/red mats on hard surface	EETF	59	6.0
	CZ06-012D	CAC-D	Cascadnaya-D, green mats next to streamers	EETF	50	5.5
	CZ06-012E	CAC-E	Cascadnaya-E, streamers	EETF	57	5.5
	CZ06-012S	CAC-S	Cascadnaya-Source, black mud at edge	EETF	74	6.0
2006	CZ06-019	JV1A	Jenn's Vent 1A, source, white streamer, gray sediment	CETF	75	5.5
	CZ06-020	JV1B	Jenn's Vent 1B, white/green mats	CETF	50	5.5
	CZ06-021	JV3	Jenn’s Vent 3, water & white streamers, gray sediments	CETF	73	4.8
	CR06-K4-C	K4-C	K4-well, yellow sand	CETF	68	6.8
	CR06-K4-E	K4-E	K4-well, water & green/flesh-red mats	CETF	50	7.0
	ON1	ON1	Orange Field, water & mud	OTF	72	5.5
	CR06-003-A	TM-A	Thermophile A black sand/gravel covered by streamers	EETF	70	6.0
	CR06-003-B	TM-B	Thermophile B dark green mats covered by streamers	EETF	64	6.5
	CR06-003-C	TM-C	Thermophile C dark green mats	EETF	53	6.5
	CR06-003-D	TM-D	Thermophile D dark green mats	EETF	42	7.0
	VIN-06	V1N	Vent 1 North, water & mud at edge (sampled)	NTF	68	5.5
	Vent 2 North	V2N	Vent 2 North, water & white streamers+ black mud	NTF	37	3.5
	CR06-002	ZV	Zavarzin II mat	EETF	55	5.5
	PS06096-98	GV	Mixture of lucky spring sediments	GV	na	8.0

a. Location code, EEFT, east sector of East Thermal Field; CETF, central sector of East Thermal Field; NTF, North Thermal Field; OTF, Orange Thermal Field; GV, the Geyser Valley.

Table 3.2. Mole% of 13 major phospholipid fatty acids from Kamchatka samples with the remaining fatty acids grouped as "others", which accounted for 0.00-20.44% of the total PLFA. See Table 3.1 for sample descriptions.

Sample ID	i15:0	a15:0	i16:0	16:1ω7c	16:0	i17:0	a17:0	18:2ω6	18:1ω9c	18:1ω7	18:0	20:1ω9c	20:1ω9t	Others	Total
ARK-03	0.00	0.00	0.00	0.00	13.85	0.00	0.00	0.00	5.28	7.72	14.18	22.20	19.63	17.13	100.00
BW-03	3.15	0.70	0.79	13.83	28.84	0.59	0.90	2.79	2.99	33.97	1.70	0.00	0.00	9.75	100.00
CZ1-03	2.31	1.17	0.67	11.34	39.41	0.80	1.09	5.79	13.03	14.38	3.86	1.28	0.51	4.36	100.00
JV12-03	1.74	1.39	0.26	3.10	45.59	0.60	0.34	5.51	20.05	2.15	9.60	0.00	0.00	9.67	100.00
JV2-03	3.47	5.12	2.03	8.12	30.83	2.00	1.63	3.19	10.49	6.10	10.33	0.74	0.00	15.96	100.00
JVB12-03	2.37	1.32	1.81	1.41	32.98	1.89	1.65	14.48	19.69	3.01	6.61	2.31	0.00	10.46	100.00
RM-03	3.94	2.40	2.02	3.18	35.04	3.13	1.86	5.02	15.72	4.58	8.37	0.72	0.16	13.89	100.00
V1N-03	0.89	0.73	1.59	0.83	4.78	2.88	8.56	0.65	11.02	13.04	6.66	32.95	9.99	5.43	100.00
V2N-03	0.00	0.00	3.05	2.01	9.30	6.09	11.43	0.00	7.36	11.04	12.84	23.01	7.56	6.30	100.00
ZV-03	3.06	1.39	2.46	4.63	41.18	1.91	1.96	3.39	12.10	9.55	7.43	2.65	0.85	7.45	100.00
RM-04	2.56	1.87	1.75	2.68	32.55	2.45	1.38	14.19	21.44	4.30	4.67	1.19	0.18	8.78	100.00
ZVGN-04	4.09	0.85	2.27	6.22	38.79	1.19	1.25	8.36	18.68	9.62	3.53	3.23	0.67	1.25	100.00
ZVGY-04	3.51	1.60	2.66	0.00	48.81	3.61	3.34	5.10	2.06	0.60	8.18	0.73	0.31	19.48	100.00
BLS-05	4.66	1.48	3.39	4.55	14.50	3.39	2.12	2.22	9.42	13.65	6.56	23.92	0.00	10.16	100.00
JV2-05	0.00	0.00	0.00	0.00	2.06	0.00	0.00	0.00	11.25	7.62	19.35	55.14	0.00	4.59	100.00
TM-out-05	7.03	2.62	3.34	4.05	35.52	3.22	0.00	1.55	7.39	4.41	8.34	5.36	0.00	17.16	100.00
V1N-05	1.42	0.00	1.18	0.83	3.07	1.54	0.00	0.00	17.85	16.31	5.67	52.13	0.00	0.00	100.00
ZVGN-05	2.28	1.35	1.45	6.64	37.55	0.83	0.00	8.40	17.32	11.41	4.25	0.73	0.00	7.78	100.00
ZVGR-05	1.82	1.02	0.45	15.34	28.64	0.34	0.00	4.32	5.45	37.39	0.00	0.00	0.00	5.23	100.00
ZVM25-05	5.21	2.92	3.65	1.46	36.29	5.42	2.92	4.28	3.23	3.65	8.03	2.50	0.00	20.44	100.00
ZVGY-05	7.14	6.12	4.42	2.15	31.07	9.18	0.00	2.95	6.35	0.00	15.19	3.40	0.00	12.02	100.00
BLS-D	10.58	0.00	9.33	0.00	15.14	7.72	0.00	0.00	13.74	8.05	9.98	25.47	0.00	0.00	100.00
BLS-E	6.78	2.22	3.77	7.05	19.50	2.61	1.97	3.03	7.95	12.99	6.43	16.09	3.39	6.21	100.00
BLS-F	7.18	3.53	2.12	12.61	24.28	2.39	1.38	1.88	5.02	13.94	4.23	1.60	0.00	19.84	100.00
BW	6.59	0.79	0.71	18.65	34.22	1.17	0.65	0.99	3.66	25.33	1.62	0.00	0.00	5.61	100.00
CAC-B	5.86	2.62	5.78	0.00	5.56	6.01	6.47	0.00	9.72	6.50	9.01	32.19	5.01	5.26	100.00
CAC-C	7.99	2.69	2.67	0.40	6.59	4.44	3.70	0.00	10.91	10.30	5.08	29.11	6.36	9.77	100.00
CAC-D	7.54	2.26	2.56	6.55	21.72	4.30	2.57	0.00	9.79	11.70	5.73	18.99	4.20	2.10	100.00
CAC-E	10.81	3.28	2.52	7.14	30.87	2.27	1.80	3.34	13.87	6.29	4.35	3.39	0.00	10.08	100.00
CAC-S	0.00	0.00	3.28	0.00	2.16	4.88	8.66	0.00	9.12	5.58	19.34	37.97	9.01	0.00	100.00
JV1A	76.19	6.46	0.00	1.39	1.55	9.31	1.41	0.00	1.25	0.00	0.89	0.00	0.00	1.54	100.00
JV1B	3.52	1.43	0.93	2.08	39.43	2.06	0.69	4.74	23.98	2.38	9.59	1.67	0.00	7.51	100.00
JV3	2.84	1.26	1.70	0.97	5.10	2.99	3.83	0.00	10.12	8.02	15.03	34.55	10.70	2.91	100.00
K4-C	11.01	4.50	9.72	1.74	5.86	9.50	4.72	1.38	4.07	1.46	9.15	18.85	2.09	15.93	100.00
K4-E	1.94	0.00	0.00	10.43	37.97	0.00	0.00	0.00	9.68	2.92	8.07	10.72	0.00	18.28	100.00
ON1	4.55	2.88	4.46	5.85	16.92	2.81	4.95	0.00	5.48	5.00	9.49	21.27	5.06	11.29	100.00
TM-A	0.00	0.00	0.00	0.00	5.46	10.25	6.34	0.00	10.71	8.04	13.87	34.16	11.16	0.00	100.00
TM-B	6.22	4.46	4.36	0.00	13.52	4.85	5.54	0.00	7.47	12.35	8.17	12.73	3.52	16.80	100.00
TM-C	4.14	1.15	2.14	6.71	37.18	2.07	0.58	6.35	18.92	5.56	3.31	0.25	0.00	11.64	100.00
TM-D	2.09	0.81	1.24	7.74	35.51	0.95	0.28	5.79	22.51	12.82	2.59	0.00	0.35	7.32	100.00
V1N	1.42	0.00	1.52	2.88	14.68	1.78	2.88	2.83	12.67	11.34	5.39	33.20	8.13	1.29	100.00
V2N	26.56	0.00	0.00	9.80	26.51	5.09	0.00	0.00	3.80	9.64	2.42	0.00	0.00	16.18	100.00
ZV	5.35	3.88	3.96	10.17	25.25	2.64	3.66	0.00	8.02	17.28	5.92	8.44	0.00	5.43	100.00

Table 3.3. Results of SIMPER analysis showing similarity of PLFA between samples in each group identified by the cluster analysis. Primary PLFAs that cumulatively explain more than 90% similarity are listed with their individual contribution percentage.

Group	Sample Avg. Sim.	# of samples	Avg. T (ºC)	Avg. pH	PLFA	Avg. Abd.	Avg. Sim.	Sim/SD	Ctrb.%	Cum.%
					16:0	36.27	37.29	8.26	48.78	48.78
					18:1ω9c	13.99	11.03	1.74	14.42	63.20
					18:0	6.80	5.67	2.31	7.42	70.62
P1	76.44	18	58.1±16.8	6.5±1.1	18:2ω6	5.80	4.35	2.21	5.69	76.31
					18:1ω7	6.38	4.21	1.29	5.51	81.82
					16:1ω7c	5.07	3.44	1.37	4.49	86.31
					i15:0	4.25	3.39	2.38	4.43	90.75
					16:0	29.55	30.40	48.53	40.79	40.79
					18:1ω7	26.58	20.61	1.84	27.65	68.45
P2	74.51	4	41.9±10.3	5.5±1.8	16:1ω7c	14.41	13.23	5.5	17.76	86.20
					18:1ω9c	3.98	3.69	8.23	4.95	91.16
					20:1ω9c	25.18	21.29	2.86	29.97	29.97
					18:1ω9c	9.22	8.27	4.07	11.64	41.61
					16:0	11.63	8.13	1.64	11.45	53.06
P3	71.05	16	62.7±11.9	5.8±0.6	18:1ω7	9.77	7.96	2.22	11.20	64.26
					18:0	9.29	7.51	3.44	10.57	74.83
					i17:0	4.82	3.65	2.46	5.13	79.96
					a17:0	4.84	3.39	1.68	4.77	84.73
					20:1ω9t	5.39	3.32	1.1	4.68	89.41
					i15:0	4.73	2.83	0.97	3.98	93.39
					20:1ω9c	53.64	53.35	na	66.21	66.21
P4	80.58	2	66.0±1.4	5.8±0.1	18:1ω9c	14.55	11.51	na	14.29	80.50
					18:1ω7	11.97	7.80	na	9.68	90.18

Abbreviations: Avg.= Average; Sim.= Similarity; Abd.=Abundance; SD=Standard deviation; Ctrb.= contributions; Cum.= cumulative contribution; na = not applicable.

Table 3.4. Results of SIMPER analysis showing primary contributors (cumulative contribution >90%) to dissimilarities between groups. Average PLFA abundance was shown in percentage

Group	P2				P3				P4			
	PLFA	Avg. Abd.		Ctrb.%	PLFA	Avg. Abd.		Ctrb.%	PLFA	Avg. Abd.		Ctrb.%
		P 2	P1			P3	P1			P4	P 1	
	18:1ω7	26.58	6.38	27.89	16:0	11.63	36.27	26.15	20:1ω9c	53.64	1.76	40.57
	18:1ω9c	3.98	13.99	13.92	20:1ω9c	25.18	1.76	24.73	16:0	2.57	36.27	26.33
	16:1ω7c	14.41	5.07	12.84	18:1ω9c	9.22	13.99	7.78	18:0	12.51	6.80	6.02
	16:0	29.55	36.27	10.50	18:1ω7	9.77	6.38	6.01	18:1ω7	11.97	6.38	5.49
P1	i15:0	9.53	4.25	10.31	20:1ω9t	5.39	0.17	5.57	18:1ω9c	14.55	13.99	4.93
	18:0	1.44	6.80	7.35	18:2ω6	0.63	5.80	5.48	18:2ω6	0.00	5.80	4.50
	18:2ω6	2.03	5.80	5.57	18:0	9.29	6.80	4.57	16:1ω7c	0.42	5.07	3.67
	i17:0	1.80	2.55	3.02	16:1ω7c	2.69	5.07	4.4				
					a17:0	4.84	1.23	4.03				
					i15:0	4.73	4.25	3.73				
						P3	P2			P4	P2	
					20:1ω9c	25.18	0.00	22.04	20:1ω9c	53.64	0.00	36.57
					16:0	11.63	29.55	15.72	16:0	2.57	29.55	18.37
					18:1ω7	9.77	26.58	15.39	18:1ω7	11.97	26.58	11.02
P2					16:1ω7c	2.69	14.41	10.26	16:1ω7c	0.42	14.41	9.49
					i15:0	4.73	9.53	7.21	18:0	12.51	1.44	7.59
					18:0	9.29	1.44	6.86	18:1ω9c	14.55	3.98	7.19
					20:1ω9t	5.39	0.00	4.70				
					18:1ω9c	9.22	3.98	4.62				
					a17:0	4.84	0.39	3.96				
										P4	P3	
									20:1ω9c	53.64	25.18	34.72
									16:0	2.57	11.63	11.08
P3									18:0	12.51	9.29	8.42
									18:1ω9c	14.55	9.22	6.77
									20:1ω9t	0.00	5.39	6.49
									18:1ω7	11.97	9.77	6.26
									a17:0	0.00	4.84	5.88
									i15:0	0.71	4.73	5.29
									i17:0	0.77	4.82	4.93
									i16:0	0.59	3.82	4.05

Abbreviation: Avg. Abd., Average Abundance; Ctrb, Contribution.

Table 3.5. A subset of samples used for BIOENV routine with 6 environmental variables.

Sample	T°C	pH	Alkalinity (ppm$CaCO_3$)	SO_4^{2-} (ppm)	H_2S (ppm S^{2-})	NH_4^+ (ppm N)
BLS-A[a]	87	6.0	118	220	1.4	15.0
BLS-B[a]	70	6.5	120	210	0.0	21.0
BLS-F	32	6.0	105	300	0.0	21.0
BW	44	5.0	135	30	11.0	3.8
CAC-A[a]	85	6.0	90	110	0.2	31.0
CAC-B	71	6.5	75	170	0.2	33.0
CAC-C	59	6.0	65	130	0.1	38.0
CAC-D	50	5.5	50	180	0.1	38.0
CAC-S	74	6.0	110	70	0.4	21.0
JV-1A	75	5.5	55	140	5.0	7.0
ON1[b]	72	5.5		60	0.5	19.5
TM-A	70	6.0	265	8	1.4	4.6
TM-B	64	6.5	330	13	0.0	4.3
TM-C[b]	53	6.5	320	29	0.0	4.0
TM-D	42	7.0	325	29	0.0	2.1
V1N	68	5.5	110	13	8.0	12.0
V2N	37	3.5		320	0.2	15.0
ZV[b]	55	5.5	178	20	0.2	18.0

a, sample not included in analysis with PLFA

b, sample not included in analysis with GDGT.

Table 3.6. GDGT compositions of hot spring samples from the Uzon Caldera. GDGT-7 was excluded from cluster analysis.

Sample ID	GDGT-0 m/z 1302	GDGT-1 m/z 1300	GDGT-2 m/z 1298	GDGT-3 m/z 1296	GDGT-4 m/z 1294	GDGT-Cren m/z 1292	GDGT-5' m/z 1292	GDGT-6 m/z 1290	GDGT-7 m/z 1288	Total
ARK-03	0.05	0.05	0.13	0.27	0.44	0.00	0.05	0.00	0.00	1.00
BLS-A	0.13	0.15	0.24	0.23	0.20	0.03	0.01	0.01	0.00	1.00
BLS-B	0.19	0.14	0.18	0.23	0.23	0.03	0.01	0.01	0.00	1.00
BLS-D	0.09	0.11	0.26	0.24	0.23	0.03	0.02	0.02	0.00	1.00
BLS-F	0.08	0.12	0.24	0.26	0.24	0.03	0.02	0.01	0.00	1.00
BW	0.23	0.07	0.24	0.15	0.31	0.00	0.00	0.00	0.00	1.00
CSC-A	0.20	0.12	0.10	0.16	0.35	0.02	0.03	0.02	0.00	1.00
CSC-B	0.46	0.14	0.14	0.10	0.13	0.00	0.01	0.01	0.00	1.00
CSC-C	0.48	0.10	0.06	0.07	0.23	0.00	0.00	0.06	0.00	1.00
CSC-D	0.27	0.08	0.15	0.08	0.30	0.01	0.04	0.05	0.02	1.00
CSC-E	0.19	0.05	0.09	0.08	0.41	0.01	0.06	0.07	0.04	1.00
CSC-S	0.35	0.11	0.14	0.10	0.21	0.01	0.04	0.04	0.00	1.00
GV	0.11	0.11	0.18	0.23	0.20	0.16	0.00	0.00	0.00	1.00
JV12-03	0.13	0.10	0.15	0.24	0.25	0.00	0.14	0.00	0.00	1.00
JV1A	0.24	0.18	0.16	0.15	0.18	0.03	0.04	0.02	0.00	1.00
JV2-03	0.22	0.11	0.15	0.17	0.32	0.00	0.03	0.00	0.00	1.00
JVB12-03	0.31	0.12	0.16	0.11	0.27	0.00	0.02	0.00	0.00	1.00
K4-C	0.11	0.11	0.17	0.40	0.20	0.01	0.00	0.00	0.00	1.00
K4-E	0.40	0.09	0.17	0.14	0.16	0.00	0.03	0.01	0.00	1.00
RM-03	0.18	0.11	0.18	0.22	0.28	0.00	0.04	0.00	0.00	1.00
RM-04	0.16	0.10	0.18	0.22	0.34	0.00	0.00	0.00	0.00	1.00
TM-A	0.48	0.13	0.14	0.11	0.13	0.00	0.00	0.02	0.00	1.00
TM-B	0.48	0.16	0.10	0.07	0.10	0.01	0.04	0.04	0.00	1.00
TM-D	0.55	0.11	0.11	0.07	0.13	0.00	0.03	0.00	0.00	1.00
V1N	0.26	0.15	0.14	0.15	0.23	0.01	0.04	0.02	0.00	1.00
V1N-03	0.27	0.11	0.17	0.18	0.23	0.00	0.04	0.00	0.00	1.00
V2N	0.08	0.05	0.11	0.10	0.33	0.01	0.13	0.18	0.01	1.00
V2N-03	0.27	0.10	0.14	0.18	0.27	0.00	0.04	0.00	0.00	1.00
ZV	0.26	0.10	0.16	0.20	0.26	0.01	0.01	0.00	0.00	1.00
ZV-03	0.21	0.09	0.19	0.19	0.31	0.00	0.01	0.00	0.00	1.00
ZVGY-04	0.21	0.09	0.16	0.21	0.33	0.00	0.00	0.00	0.00	1.00
*Desulfurococcus amylolyticus**	0.08	0.06	0.11	0.20	0.55	0.00	0.00	0.00	0.00	1.00
*Desulfurococcus fermentas**	0.09	0.10	0.19	0.30	0.33	0.00	0.00	0.00	0.00	1.00
*Metallosphaera sedula**	0.07	0.15	0.23	0.26	0.26	0.00	0.04	0.00	0.00	1.00
*Sulfolobus solfataricus**	0.00	0.01	0.04	0.15	0.34	0.00	0.29	0.16	0.00	1.00
*Thermoproteus uzoniensis**	0.05	0.02	0.06	0.08	0.62	0.00	0.15	0.02	0.00	1.00
*Vulcanisaeta sp.**	0.04	0.03	0.06	0.14	0.54	0.00	0.15	0.04	0.00	1.00

*reported (Pearson *et al.* 2008).

Table 3.7. Similarity of GDGT composition between samples in group G0 to G6.

Group	Avg. Sim.	# of samples	Avg. T(ºC)	Avg. pH	GDGT	Avg. Abd.	Avg. Sim.	Sim/SD	Ctrb. %	Cum. %
					GDGT-4	0.58	32.49	na	34.45	34.45
G0	94.3	2	85.0±0.0	5.0±0.7	GDGT-5'	0.15	17.12	na	18.16	52.61
					GDGT-3	0.11	12.51	na	13.26	65.88
					GDGT-2	0.06	10.83	na	11.48	77.36
					GDGT-4	0.37	22.50	na	25.27	25.27
					GDGT-2	0.10	11.75	na	13.20	38.47
G1	89.1	2	47.2±14.0	4.8±1.8	GDGT-0	0.14	11.08	na	12.44	50.91
					GDGT-3	0.09	11.08	na	12.44	63.35
					GDGT-6	0.13	10.36	na	11.64	74.99
					GDGT-5'	0.10	9.59	na	10.78	85.76
					GDGT-4	0.29	22.51	14.05	24.73	24.73
G2	91.0	13	66.3±11.1	5.8±0.5	GDGT-3	0.20	18.04	9.23	19.83	44.56
					GDGT-2	0.18	17.39	15.47	19.11	63.67
					GDGT-0	0.20	16.93	4.78	18.61	82.27
					GDGT-0	0.27	18.68	15.60	20.26	20.26
					GDGT-4	0.26	17.90	11.91	19.42	39.68
G3	92.2	5	70.6±12.9	5.7±0.3	GDGT-2	0.14	13.62	11.64	14.78	54.46
					GDGT-3	0.13	12.53	7.34	13.60	68.06
					GDGT-1	0.13	12.40	9.37	13.45	81.51
					GDGT-3	0.27	19.55	22.77	21.63	21.63
					GDGT-4	0.22	18.31	40.16	20.27	41.90
G4	90.4	6	62.6±18.9	6.6±0.8	GDGT-2	0.22	17.45	16.53	19.31	61.21
					GDGT-1	0.12	13.50	27.70	14.94	76.15
					GDGT-0	0.12	12.40	10.36	13.73	89.88
G5	88.8	2	77.0±11.3	5.5±0.8	GDGT-4	0.49	31.17	na	35.11	35.11
					GDGT-3	0.24	21.02	na	23.67	58.78
					GDGT-2	0.12	15.59	na	17.55	76.33
					GDGT-0	0.07	10.51	na	11.83	88.17
					GDGT-0	0.48	28.92	17.71	32.54	32.54
G6	88.9	6	59.3±11.2	6.5±0.4	GDGT-4	0.15	15.08	10.78	16.97	49.50
					GDGT-1	0.12	13.99	12.85	15.74	65.24
					GDGT-2	0.12	13.26	6.22	14.93	80.17

a. GDGTs that can cumulatively explain more than 80% similarity were listed with their individual contribution percentage.

b. Average abundance was shown in proportion of the total detectable GDGT. Abbreviations are the same as in table 3.3.

Table 3.8. Results of SIMPER analysis of archaeal GDGT showing primary contributors (cumulative contribution >90%) to dissimilarities between groups.

Group	G1				G2				G3				G4				G5				G6			
	GDGT	Avg. Abd		Ctrb %	GDGT	Avg. Abd		Ctrb %	GDGT	Avg. Abd		Ctrb %	GDGT	Avg. Abd		Ctrb %	GDGT	Av. Abd		Ctrb %	GDGT	Av. Abd		Ctrb %
		G1	G0			G2	G0			G3	G0			G4	G0			G5	G0			G6	G0	
G0	-6	0.13	0.03	20.53	-5'	0.03	0.15	19.21	-0	0.27	0.05	23.39	-5'	0.01	0.15	18.96	-5'	0.03	0.15	31.39	-0	0.48	0.05	30.36
	-4	0.37	0.58	18.23	-0	0.20	0.05	16.89	-4	0.26	0.58	20.03	-4	0.22	0.58	17.93	-6	0.00	0.03	19.26	-4	0.15	0.58	24.28
	-0	0.14	0.05	17.61	-4	0.29	0.58	16.61	-1	0.13	0.03	15.44	-2	0.22	0.06	13.39	-3	0.24	0.11	17.49	-5'	0.02	0.15	17.86
	-Cren	0.01	0.00	11.87	-2	0.18	0.06	12.94	-5'	0.04	0.15	14.93	-Cren	0.05	0.00	12.23	-2	0.12	0.06	11.40	-1	0.12	0.03	12.07
	-5'	0.10	0.15	10.12	-6	0.00	0.03	12.63	-2	0.14	0.06	9.71	-1	0.12	0.03	11.88	-1	0.06	0.03	8.75	-2	0.12	0.06	6.18
	-2	0.10	0.06	8.39	-1	0.10	0.03	12.13	-Cren	0.02	0.00	9.51	-3	0.27	0.11	11.69	-4	0.49	0.58	6.97				
	-1	0.05	0.03	7.89									-0	0.12	0.05	7.90								
G1						G2	G1			G3	G1			G4	G1	G1		G5	G1			G6	G1	
					-6	0.00	0.13	29.74	-6	0.03	0.13	21.24	-6	0.01	0.13	20.86	-6	0.00	0.13	32.44	-0	0.48	0.14	26.03
					-5'	0.03	0.10	15.99	-0	0.27	0.14	18.76	-5'	0.01	0.10	17.15	-5'	0.03	0.10	18.16	-4	0.15	0.37	18.05
					-3	0.20	0.09	12.76	-1	0.13	0.05	16.24	-3	0.27	0.09	16.82	-3	0.24	0.09	17.33	-6	0.02	0.13	16.87
					-0	0.20	0.14	9.91	-4	0.26	0.37	13.23	-2	0.22	0.10	11.31	-0	0.07	0.14	10.07	-5'	0.02	0.10	15.47
					-2	0.18	0.10	9.00	-5'	0.04	0.10	13.14	-4	0.22	0.37	10.60	-Cren	0.00	0.01	9.45	-1	0.12	0.05	9.76
					-1	0.10	0.05	8.42	-3	0.13	0.09	7.56	-1	0.12	0.05	9.74	-4	0.49	0.37	8.68	-Cren	0.00	0.01	6.65
					-Cren	0.00	0.01	8.01					-Cren	0.05	0.01	7.60								
G2										G3	G2			G4	G2			G5	G2			G6	G2	
									-6	0.03	0.00	22.87	-Cren	0.05	0.00	26.22	-0	0.07	0.20	26.80	-0	0.48	0.20	26.80
									-Cren	0.02	0.00	15.51	-0	0.12	0.20	16.59	-4	0.49	0.29	23.22	-4	0.15	0.29	16.93
									-3	0.13	0.20	13.22	-5'	0.01	0.03	14.13	-5'	0.03	0.03	17.60	-3	0.09	0.20	15.64
									-5'	0.04	0.03	13.02	-3	0.27	0.20	11.12	-1	0.06	0.10	12.35	-6	0.02	0.00	14.04
									-0	0.27	0.20	12.44	-6	0.01	0.00	9.91	-2	0.12	0.18	10.54	-5'	0.02	0.03	11.28
									-4	0.26	0.29	8.66	-4	0.22	0.29	9.34					-2	0.12	0.18	8.68
									-1	0.13	0.10	7.39	-2	0.22	0.18	7.73								
G3														G4	G3			G5	G3			G6	G3	
													-0	0.12	0.27	20.99	-0	0.07	0.27	22.62	-0	0.48	0.27	23.48
													-3	0.27	0.13	19.78	-4	0.49	0.26	17.12	-4	0.15	0.26	17.08
													-5'	0.01	0.04	13.98	-6	0.00	0.03	14.78	-Cren	0.00	0.02	14.30
													-6	0.01	0.03	11.79	-3	0.24	0.13	11.16	-5'	0.02	0.04	12.01
													-2	0.22	0.14	11.18	-Cren	0.00	0.02	10.68	-6	0.02	0.03	10.18
													-Cren	0.05	0.02	10.17	-1	0.06	0.13	10.61	-3	0.09	0.13	9.19
													-4	0.22	0.26	6.62	-5'	0.03	0.04	9.86	-1	0.12	0.13	6.93
G4																		G5	G4			G6	G4	
																	-4	0.49	0.22	23.28	-0	0.48	0.12	29.81
																	-Cren	0.00	0.05	20.14	-3	0.09	0.27	18.43
																	-2	0.12	0.22	11.82	-Cren	0.00	0.05	15.63
																	-1	0.06	0.12	11.72	-2	0.12	0.22	10.31
																	-5'	0.03	0.01	11.26	-4	0.15	0.22	8.12
																	-0	0.07	0.12	8.77	-6	0.02	0.01	7.47
																	-6	0.00	0.01	7.32	-5'	0.02	0.01	7.33
G5																						G6	G5	
																					-0	0.48	0.07	32.22
																					-4	0.15	0.49	23.68
																					-3	0.09	0.24	13.35
																					-6	0.02	0.00	9.66
																					-1	0.12	0.06	8.32
																					-5'	0.02	0.03	8.27

a. Average GDGT abundance was shown in proportion of the total detectable GDGT.

b, Abbreviations are the same as in table 3.4.

Table 3.9. $\delta^{13}C$ values of PLFAs, bulk organic matter and hot spring vent CO_2 analyzed in this study. Data were reported in ‰ vs. PDB.

Sample ID	Group #[a]	$\delta^{13}C_{org}$	$\delta^{13}CO_2$[b]	$\delta^{13}C_{PLFA}$ Summary				$\varepsilon\sum$PLFA-CO_2	$\varepsilon\sum$PLFA-Bio	$\delta^{13}C_{PLFA}$																		
				Max.	Min.	$\sum$PLFA	SD			14:0	i15:0	a15:0	15:0	i16:0	16:1ω7c	16:0	i17:0	a17:0	cy17:0	17:0	18:1ω9c	18:1ω7	18:0	br18:0	19:0cyc	19:1	20:1ω9c	20:1ω9t
BLS-F	P1	-20.0		-16.5	-26.9	-22.5	3.8	-18	-2.5		-20.1	-16.5			-26.9	-23.1			-26.5		-16.5	-19.9	-18.9			-22.7	-25.1	
CAC-E	P1	-9.8		-7.4	-21.2	-12.5	4.0	-8	-2.7	-12.6	-10.0	-7.4		-8.8	-13.0	-11.3	-8.4	-15.2	-19.3		-13.8	-15.4	-11.5			-21.2	-17.1	
CZ1-03	P1	-25.1	-5.1	-27.9	-31.1	-29.5	1.1	-25	-4.4		-29.8			-28.2	-27.9	-28.9					-29.8	-31.1	-29.6					
JV12-03	P1	-9.8	-5.1	-15.6	-25.2	-16.4	4.3	-12	-6.6						-25.2	-15.6					-16.3		-19.1					
JV1B	P1	-13.1		-13.5	-22.6	-21.3	4.2	-17	-8.2		-20.5	-13.5				-22.6	-13.7				-19.9		-22.5					
RM-03	P1	-11.4	-5.6	-13.7	-21.7	-17.4	2.9	-13	-6.0		-13.7				-18.6	-17.0					-17.0		-21.7					
TM-C	P1	-15.4		-18.0	-32.6	-24.3	3.8	-20	-8.8		-25.6	-18.0	-25.2	-21.5	-22.9	-21.8	-24.7	-22.6		-24.7	-27.8	-31.1	-24.1	-32.6		-25.2			
ZV-03	P1	-22.0	-5.1	-22.2	-23.1	-22.8	0.5	-18	-0.8							-23.1					-22.2	-22.2						
K4-E	OG	-11.5		-17.2	-30.7	-21.3	4.6	-17	-9.8		-17.8		-17.2		-18.3	-17.9					-21.1	-24.6	-21.0	-27.4	-24.7		-30.7	
BW	P2	-28.2	-6.2	-23.6	-33.4	-28.0	5.1	-23	0.1							-30.8						-23.6	-33.4					
V2N	P2	-19.2	-6.5	-20.6	-28.3	-24.6	2.3	-20	-5.4	-23.2	-24.9				-27.8	-23.3	-24.0		-24.5		-28.3	-25.9				-23.7		
JV3	P3	-16.8		-4.6	-27.3	-11.5	7.9	-7	5.3		-19.5	-13.8		-23.4		-21.8	-18.7	-27.3			-23.7	-4.7	-7.8				-4.6	-12.9
BLS-D	P3	-21.3	-3.2	-15.5	-31.1	-19.4	5.0	-15	1.9		-16.0			-19.1		-19.9	-20.0				-16.8	-15.5	-31.1				-18.5	
BLS-E	P3	-22.0		-4.6	-28.4	-15.4	6.9	-11	6.6		-19.6	-22.5		-18.4	-22.4	-22.4	-13.3		-28.4		-11.8	-12.7	-11.1				-4.6	-9.6
CAC-B	P3	-21.3	-4.0	1.8	-24.7	-5.7	8.0	-1	15.6		-16.3	-12.7		-13.8		-12.1	-11.7	-24.7		-15.0	1.8	-2.2	-3.7		-5.0		1.1	
CAC-C	P3	-10.6		0.9	-14.4	-6.6	5.6	-2	4.0		-12.2					-12.5					-14.4	-8.3					0.9	-12.4
CAC-D	P3	-20.1		-8.1	-22.5	-14.8	5.6	-10	5.3						-22.5	-21.5	-12.1					-11.3	-10.8				-8.1	-16.5
CAC-S	P3	-22.9	-5.4	-2.1	-27.3	-10.6	7.8	-6	12.3		-18.7	-18.3		-25.9		-20.6	-24.1	-27.3			-11.4	-9.1	-12.2				-2.1	-11.9
K4-C	P3	-13.3		-1.7	-23.3	-12.7	7.0	-8	0.6		-19.6	-14.9		-23.3		-21.4	-15.6	-14.4					-6.1	-12.0			-1.7	
ON1	P3	-27.0		-24.5	-26.2	-25.4	0.9	-21	1.6							-26.0							-26.2				-24.5	
TM-A	P3	-27.3	-4.5	-33.7	-51.2	-38.5	6.0	-34	-11.2							-37.1	-51.2	-43.6			-33.7	-38.8	-40.6				-34.6	
TM-B	P3	-24.6		-24.9	-38.3	-32.1	4.5	-28	-7.5		-33.7	-36.4	-24.9	-38.3		-27.6	-36.1	-37.3		-29.5	-25.1	-33.9	-33.5		-29.8		-34.7	-38.2
V1N	P3	-23.6	-6.4	-11.7	-36.2	-28.9	6.3	-24	-5.2		-25.6			-26.5	-11.7	-24.9	-33.2	-36.2			-26.1	-28.9	-28.3				-32.3	-30.0
V2N-03	P3	-24.0	-5.1	-24.4	-34.2	-29.5	3.4	-25	-5.5		-30.1			-32.5	-24.4	-25.4	-34.2				-25.6	-29.2	-31.2				-28.8	
ZV	P3	-23.8	-4.2	-29.2	-32.0	-31.2	1.0	-27	-7.4						-31.2	-31.4		-31.7				-31.4	-32.0				-29.2	
ARK-03	OG	-18.8	-4.3	-28.7	-31.1	-30.0	1.0	-25	-11.2							-31.1	-29.8				-28.7		-29.3					
JV1A	OG	-21.3	-6.6	-13.5	-30.0	-23.5	5.7	-19	-2.3		-24.2					-24.1	-17.9	-30.0					-15.4				-21.5	-13.5

a, Group number was based on the cluster analysis of PLFA. OG, out-group samples that did not group with other samples based on the current similarity cutoff.

b, $\delta^{13}CO_2$ was measured in 2005 and 2006 (Chapter 2 of this dissertation), $\delta^{13}CO_2$ data of 2003 samples were assumed the same as in 2005 and 2006 based on similarity in values from the latter two years. Average $\delta^{13}CO_2$ values of hot spring source gas in the Uzon Caldera was -4.6±1.1‰‰ (n = 61; Chapter 2 of this dissertation), which was used to compute ε value between ΣPLFA and CO_2.

Different shade represents different groups as defined by the cluster analysis.

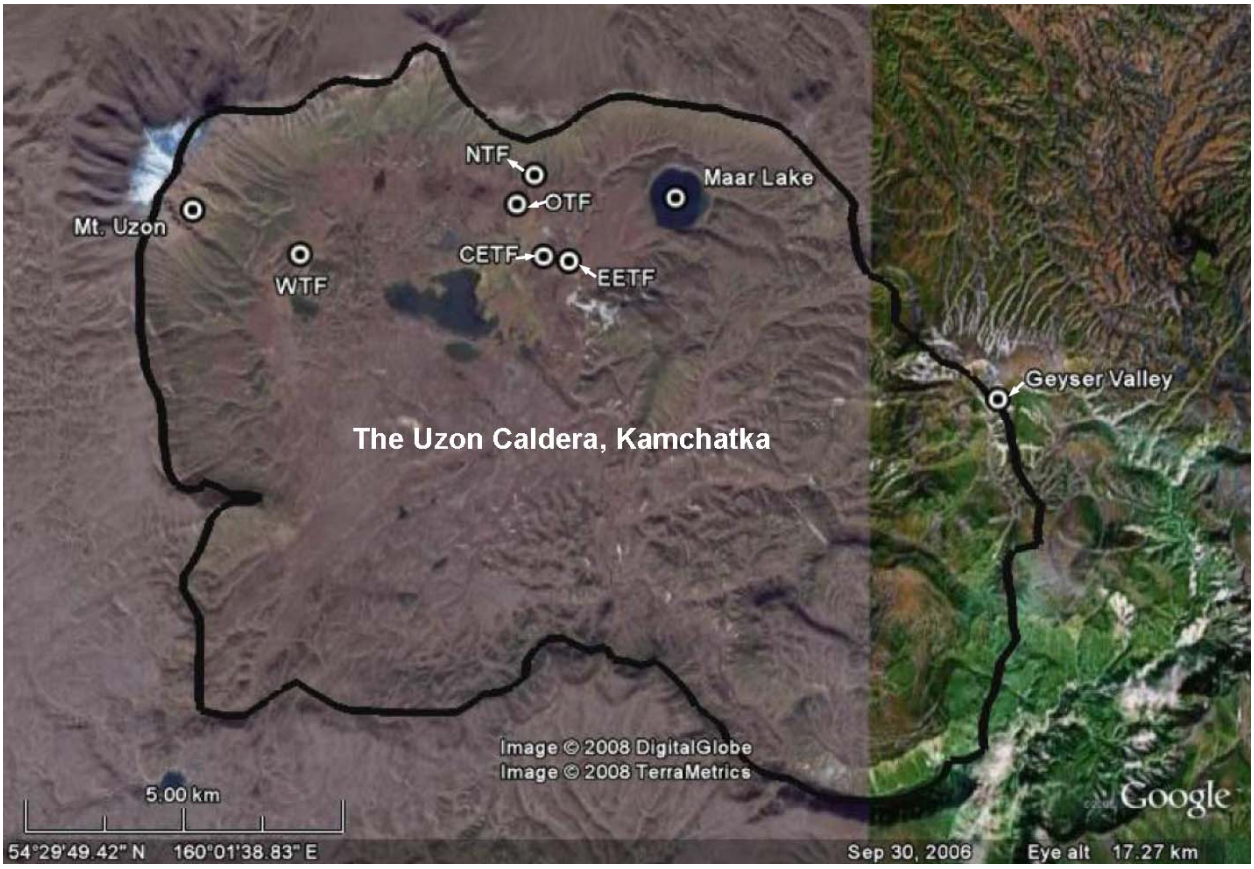

(a)

Fig 3.1. Map of sampling sites. (a) Satellite area map of the Uzon Caldera (Google Earth, Google Inc., CA, USA). Arrow indicates the sampling area. Area code: EETF, east Sector of East Thermal Field; CEFT, center sector of East Thermal Field; OTF, Orange Thermal Field; NTF, North Thermal Field; WTF, West Thermal Field. (b) Detailed map of sampling sites at the EETF and CETF. Modified from Hollingsworth *et al.* (in review)

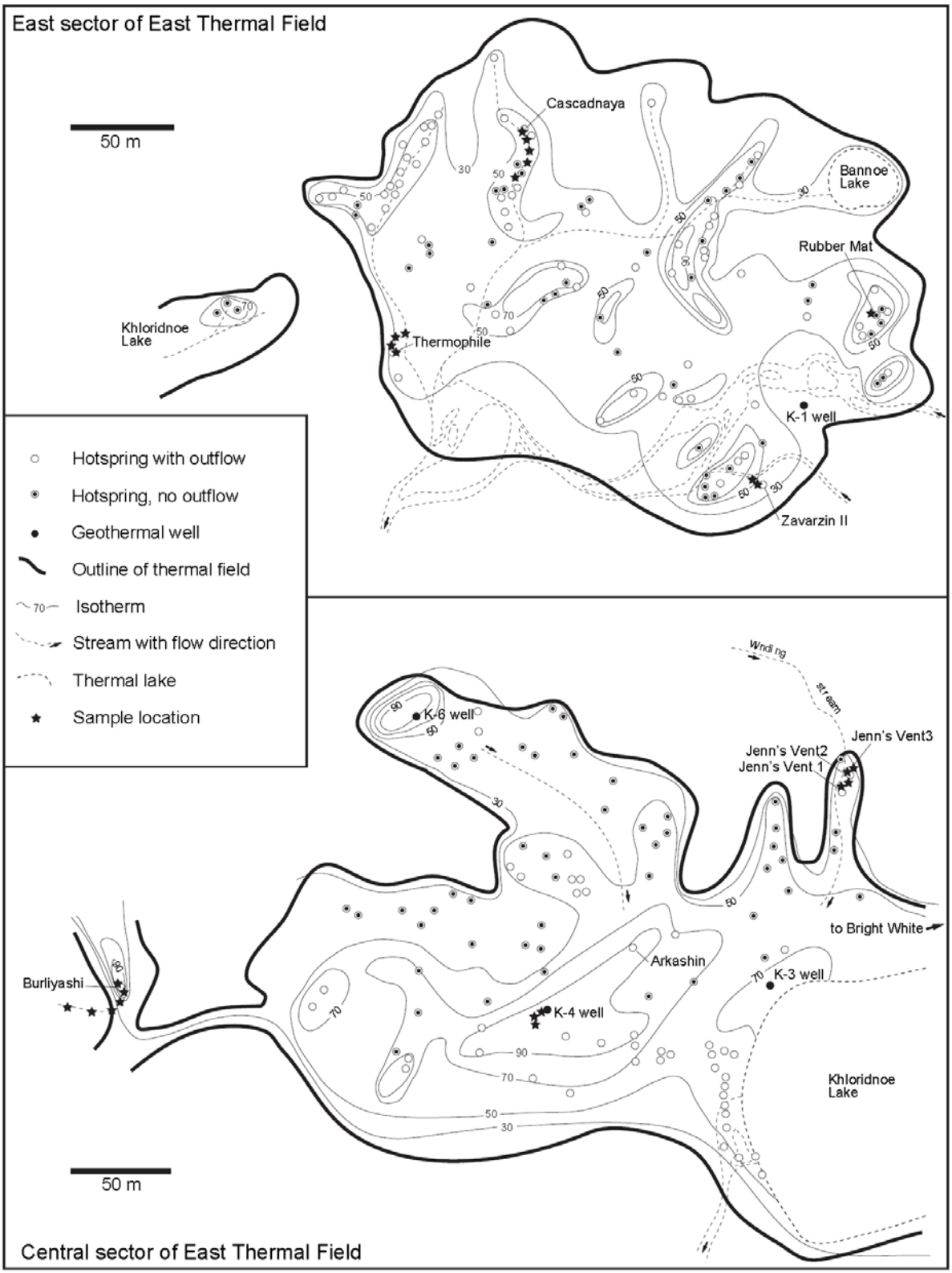
East sector of East Thermal Field
50 m
Cascadnaya
Bannoe Lake
Rubber Mat
Khloridnoe Lake
Thermophile
K-1 well
Zavarzin II
Hotspring with outflow
Hotspring, no outflow
Geothermal well
Outline of thermal field
Isotherm
Stream with flow direction
Thermal lake
Sample location
Winding stream
K-6 well
Jenn's Vent3
Jenn's Vent2
Jenn's Vent 1
to Bright White
Arkashin
K-3 well
K-4 well
Burliyashi
Khloridnoe Lake
50 m
Central sector of East Thermal Field

(b)

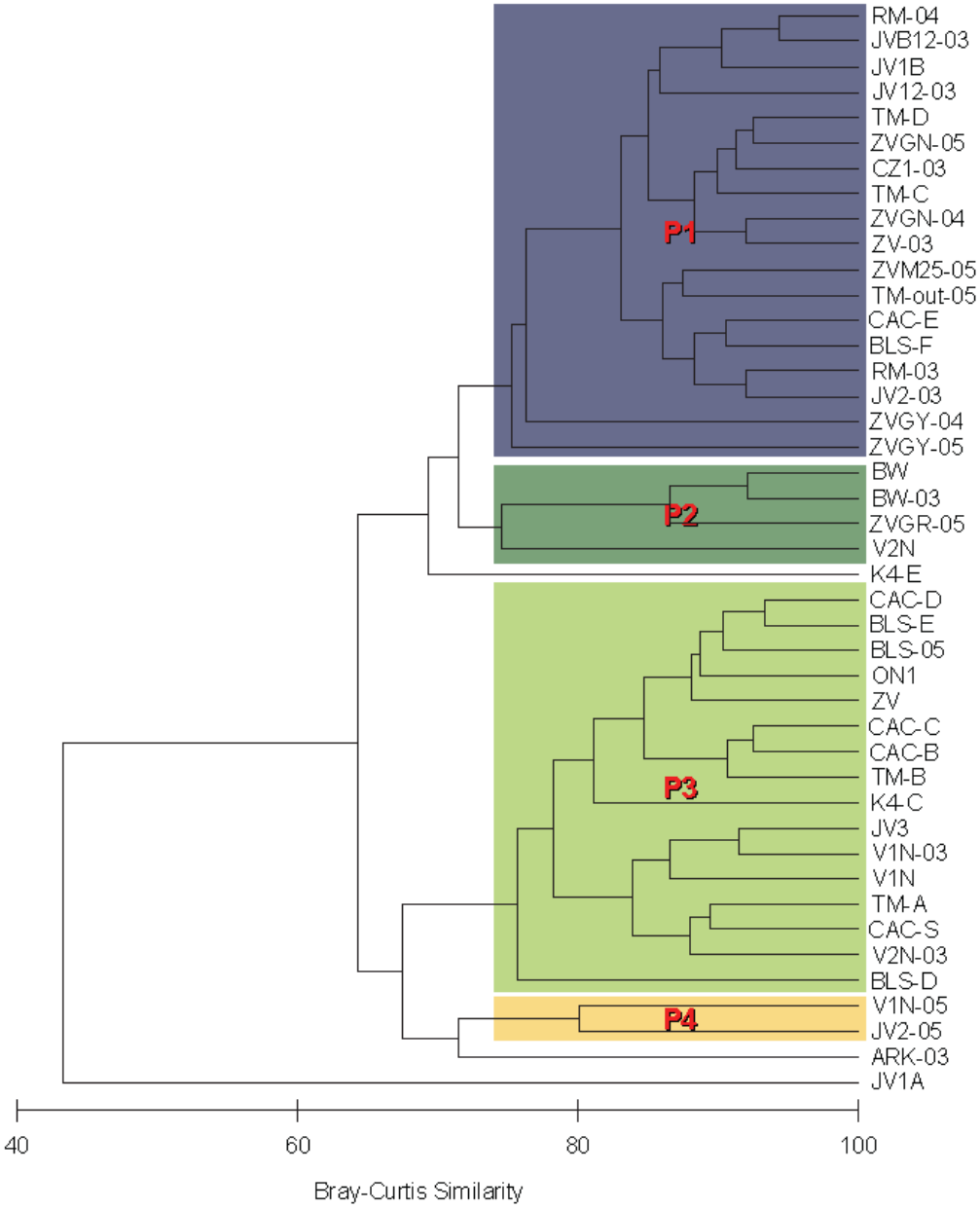

Fig 3.2. Hierarchical cluster tree of PLFAs. Percentage of each PLFA component was log(X+1) transformed prior to the calculation of the similarity matrix. Groups were defined by a 75% Bray-Curtis similarity cut-off and are shown in colored areas. The group average distances between samples were shown in the tree.

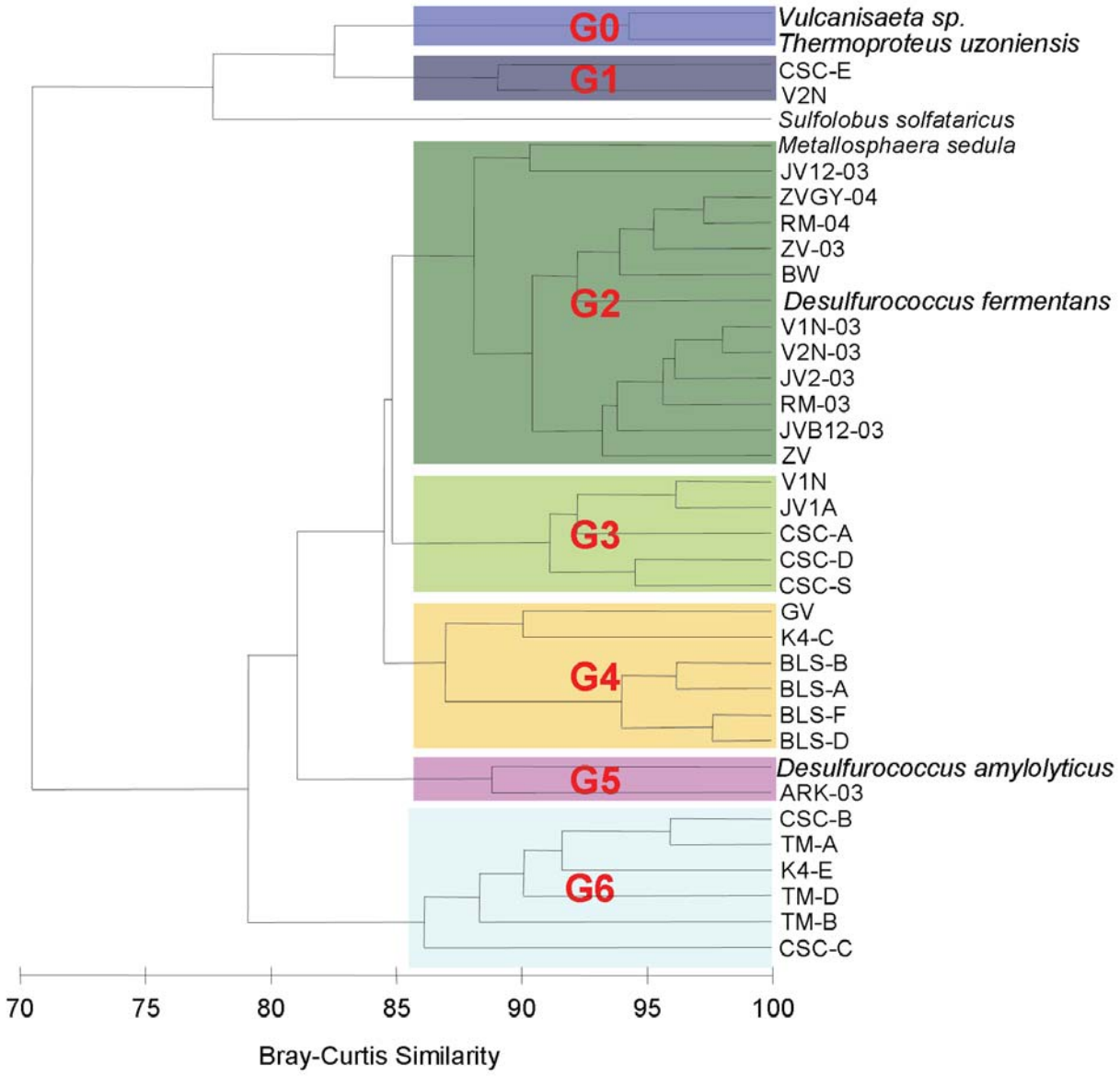

Fig 3.3. Hierarchical cluster tree of GDGTs. Percentage of each GDGT component was log(X+1) transformed prior to the calculation of the similarity matrix. Groups were defined by an 86% Bray-Curtis similarity cut-off and are shown in colored areas. The group average distances between samples were shown in the tree.

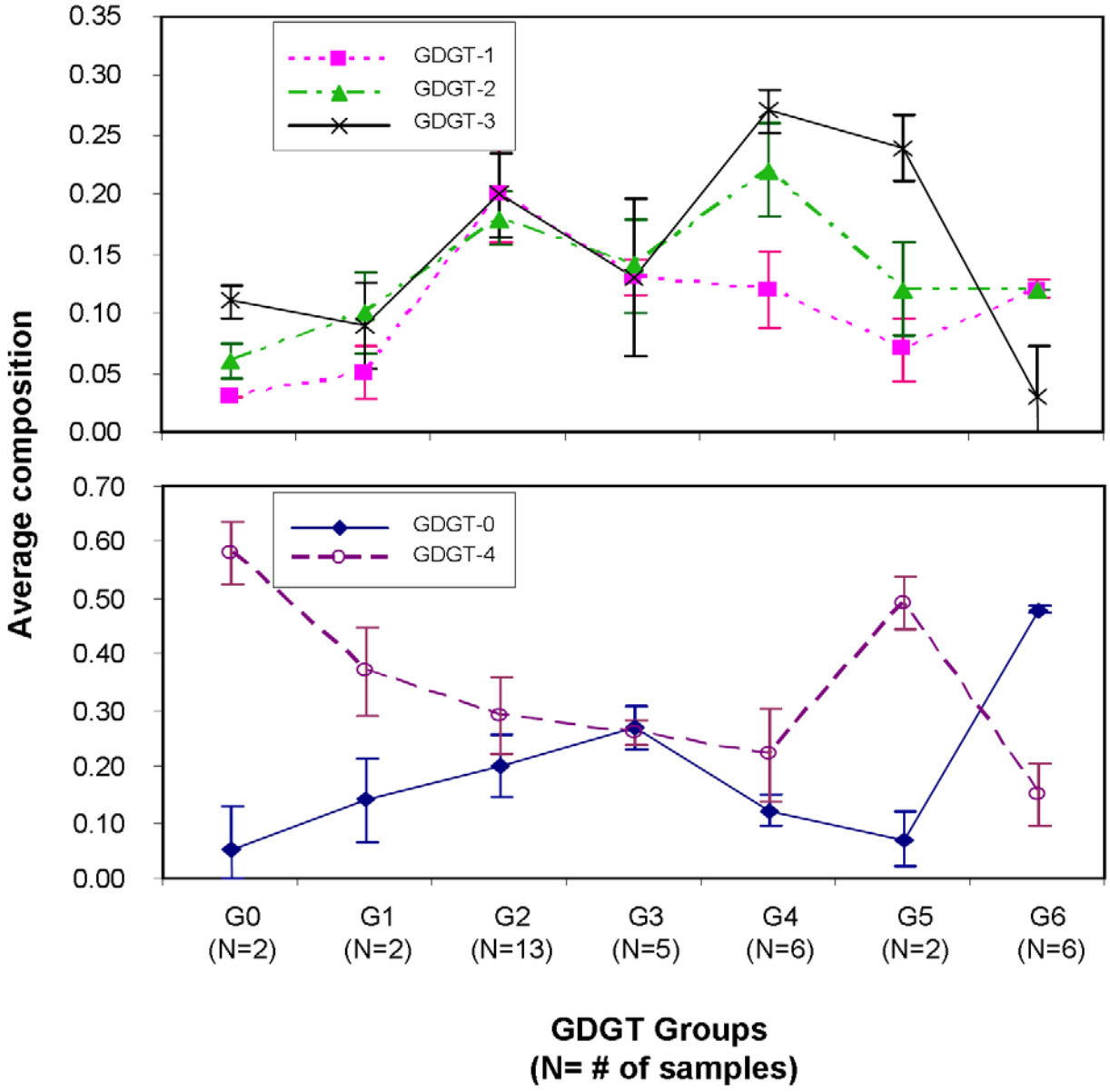

Fig 3.4. Variation of GDGT species between groups defined by the hierarchical cluster analysis. Average content of each GDGT species in the defined groups is shown. Upper panel, GDGT-1, -2 and -3; bottom panel, GDGT-0 and -4. Error bar represents one standard deviation. The number of samples (N) is shown in parentheses below each group.

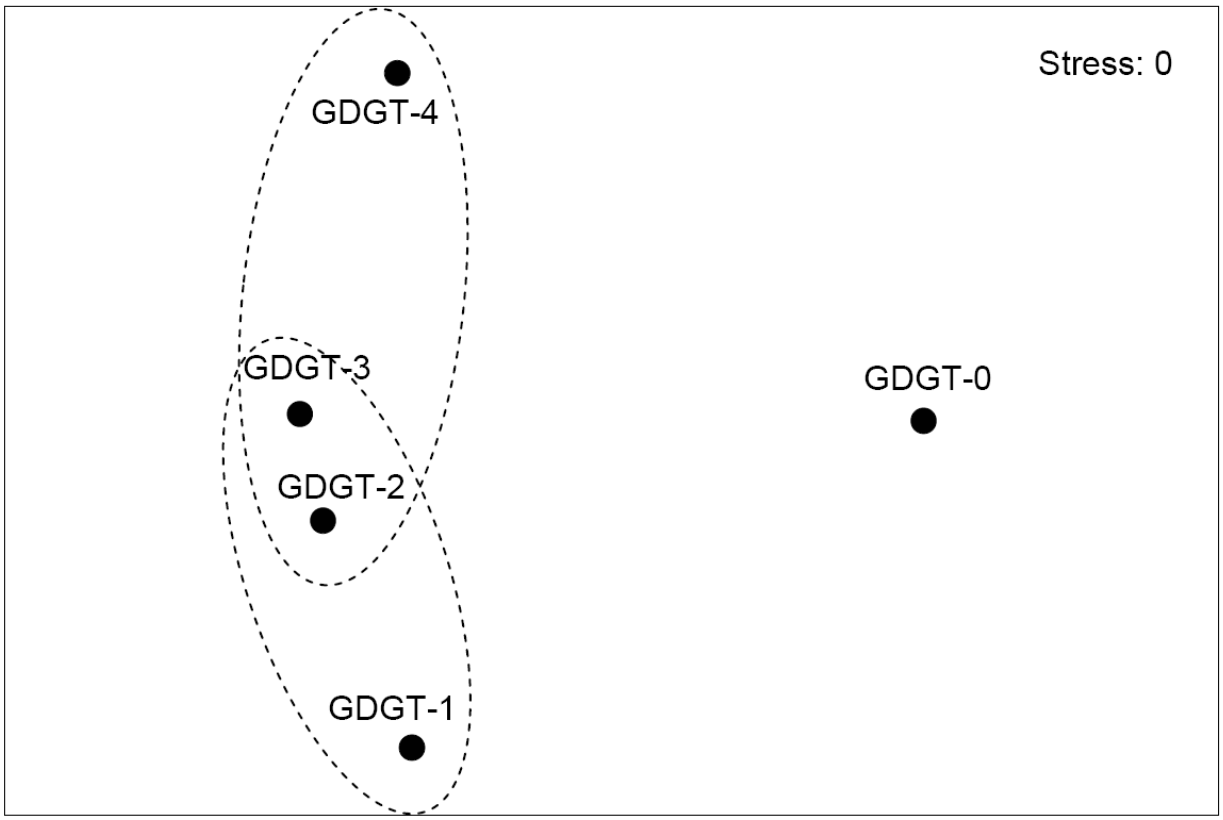

Fig 3.5. Non-metric multidimensional scaling (MDS) analysis of the five most abundant GDGTs. All samples listed in the Table 3.6 were used to compute the Bray-Curtis similarity between GDGT variables. Dashed ovals demonstrate relative closeness of GDGT-2 and GDGT-3 to either GDGT-1 or GDGT-4.

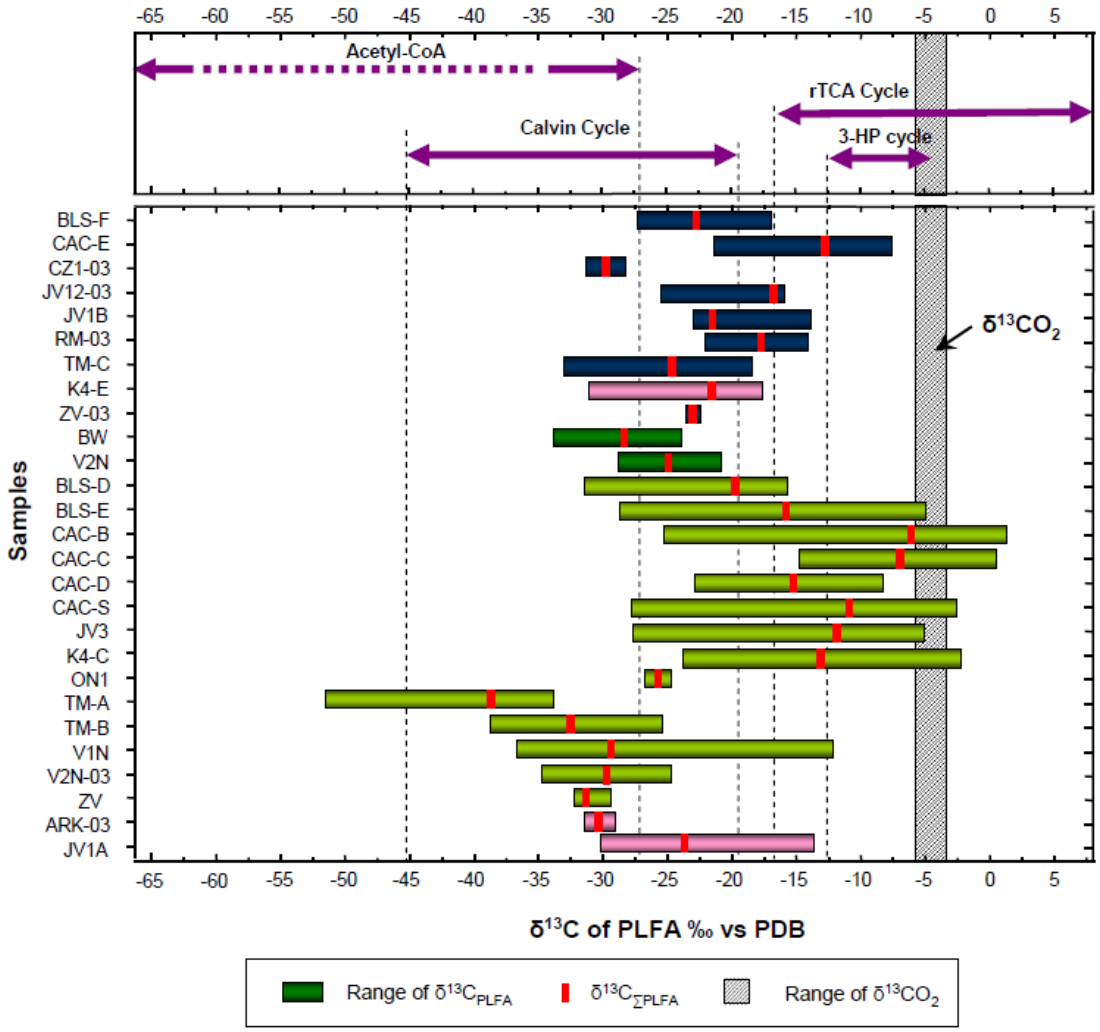

Fig 3.6. $\delta^{13}C$ values of PLFAs and their predicted ranges for different carbon fixation pathways relative to $\delta^{13}C$ values of CO_2. Isotope enrichment factors between PLFA and CO_2 ($\varepsilon_{PLFA\text{-}CO_2}$) are based on House *et al.* (2003), Summons *et al.* (1994; 1998); van der Meer *et al.* (1998; 2001) and Zhang *et al.* (2004). Bottom panel, ranges of $\delta^{13}C$ values for PLFA components (bars) and $\delta^{13}C_{\sum PLFA}$ of each sample (vertical line in bar). Colors represent different groups by PLFA cluster analysis. Blue = group P1; Dark green = group P2; Light green = group P3; Pink = out-group samples (see Fig 3.2 for details); upper panel, predicted ranges of $\delta^{13}C_{PLFA}$ values for different carbon fixation pathways relative to $\delta^{13}C$ values of CO_2 of the Uzon Caldera. The horizontal dotted region of $\delta^{13}C_{PLFA}$ values for the acetyl-CoA pathway is hypothetical and has not yet been experimentally supported.

SUPPLEMENTAL MATERIALS

Table S3.1. The best seven correlations between lipid distribution patterns and environmental variable combinations revealed by the BIOENV routine in Primer V5 program

PLFA		GDGT	
Environmental variable selections†	Correlation coefficient (ρ_s)	Environmental variable selections†	Correlation coefficient (ρ_s)
1	0.435	1, 2	0.457
1, 2	0.413	1, 2, 6	0.452
1, 2, 6	0.375	1, 2, 4	0.440
1, 2, 5	0.375	1, 2, 4, 6	0.439
1, 5	0.368	1, 3	0.437
1, 2, 5, 6	0.366	2, 6	0.435
1, 3	0.357	1, 2, 3, 6	0.433

† 1, Temperature; 2, pH; 3, Alkalinity; 4, SO_4^{2-}; 5, H_2S; 6, NH_4^+

Table S3.2. ANOSIM of PLFA sample groups using temperature data

groups	R Statistic[a, b]	Significance Level %
P1, P2	0.043	32
P1, P3	0.067	9
P1, P4	-0.021	45
P2, P3	0.442	1
P2, P4	0.679	13
P3, P4	-0.203	77
Global R[c]	0.069	11

a. R value close to 1 indicates statistical differences between the groups whereas R close to 0 indicates strong similarity.

b. Negative values indicate higher differences within a group than between groups.

c. Global R value indicates the level of similarity between all individual temperatures.

REFERENCES

Abrajano TA, Murphy DE, Fang J, Comet P, Brooks JM (1994) C-13 C-12 ratios in individual fatty-acids of marine mytilids with and without bacterial symbionts. Org. Geochem. 21:611-617

Antoine E, Cilia V, Meunier JR, Guezennec J, Lesongeur F, Barbier G (1997) *Thermosipho melanesiensis* sp. nov., a new thermophilic anaerobic bacterium belonging to the order *Thermotogales*, isolated from deep-sea hydrothermal vents in the Southwestern Pacific Ocean. Int. J. Syst. Bacteriol. 47:1118-1123

Balkwill DL *et al.* (2004) Identification of iron-reducing *Thermus* strains as *Thermus scotoductus*. Extremophiles 8:37-44

Bull ID, Parekh NR, Hall GH, Ineson P, Evershed RP (2000) Detection and classification of atmospheric methane oxidizing bacteria in soil. Nature 405:175-178

Burgess EA, Zhao W, Neal AL, Wiegel J (2006) Comparison of hot spring sediment communities using 16S rRNA gene sequences. In: American Society for Microbiology 107th Annual Meeting, Orlando, FL, USA

Clarke KR, Ainsworth M (1993) A method of linking multivariate community structure to environmental variables. Mar. Ecol.-Prog. Ser. 92:205-219

Crossman ZM, Ineson P, Evershed RP (2005) The use of C-13 labelling of bacterial lipids in the characterisation of ambient methane-oxidising bacteria in soils. Org. Geochem. 36:769-778

Dalsgaard T, Bak F (1994) Nitrate reduction in a sulfate-reducing bacterium, *Desulfovibrio desulfuricans*, isolated from rice paddy soil - sulfide inhibition, kinetics, and regulation. Appl Envion Microbiol 60:291-297

Damste JSS, Rijpstra WIC, Hopmans EC, Prahl FG, Wakeham SG, Schouten S (2002) Distribution of membrane lipids of planktonic crenarchaeota in the Arabian seat. Appl Envion Microbiol 68:2997-3002

Dannenberg S, Kroder M, Dilling W, Cypionka H (1992) Oxidation of H_2, organic-compounds and inorganic sulfur-compounds coupled to reduction of O_2 or nitrate by sulfate-reducing bacteria.

Archives of Microbiology 158:93-99

Derosa M, Esposito E, Gambacorta A, Nicolaus B, Bulock JD (1980) Effects of temperature on ether lipid-composition of *Caldariella acidophila*. Phytochemistry 19:827-831

Derosa M, Gambacorta A, Gliozzi A (1986) Structure, biosynthesis, and physicochemical properties of archaebacterial lipids. Microbiological Reviews 50:70-80

Escala M, Rosell-Mel A, Masqu P (2007) Rapid screening of glycerol dialkyl glycerol tetraethers in continental Eurasia samples using HPLC/APCI-ion trap mass spectrometry. Org. Geochem. 38:161-164

Frostegard A, Tunlid A, Baath E (1993) Phospholipid fatty-acid composition, biomass, and activity of microbial communities from 2 soil types experimentally exposed to different heavy-metals. Appl Envion Microbiol 59:3605-3617

Gambacorta A, Trincone A, Nicolaus B, Lama L, Derosa M (1994) Unique features of lipids of archaea. Systematic and Applied Microbiology 16:518-527

Gliozzi A, Bruno S, Basak TK, Derosa M, Gambacorta A (1986) Organization and dynamics of bipolar lipids from *sulfolobus solfataricus* in bulk phases and in monolayer membranes. Syst Appl Microbiol 7:266-271

Goorissen HP, Boschker HTS, Stams AJM, Hansen TA (2003) Isolation of thermophilic *Desulfotomaculum* strains with methanol and sulfite from solfataric mud pools, and characterization of *Desulfotomaculum solfataficum* sp nov. Int J Syst Evol Microbiol 53:1223-1229

Gotz D, Banta A, Beveridge TJ, Rushdi AI, Simoneit BRT, Reysenbach A (2002) *Persephonella marina* gen. nov., sp nov and *Persephonella guaymasensis* sp nov., two novel, thermophilic, hydrogen-oxidizing microaerophiles from deep-sea hydrothermal vents. Int J Syst Evol Microbiol 52:1349-1359

Guckert JB, Antworth CP, Nichols PD, White DC (1985) Phospholipid, ester-linked fatty-acid profiles as reproducible assays for changes in prokaryotic community structure of estuarine sediments.

FEMS Microbiology Ecology 31:147-158

Hamamoto T, Takata N, Kudo T, Horikoshi K (1994) Effect of temperature and growth-phase on fatty-acid composition of the *psychrophilic vibrio* sp strain no. 5710. FEMS Microbiology Letters 119:77-81

Hanada S, Hiraishi A, Shimada K, Matsuura K (1995) *Chloroflexus aggregans* sp. nov., a filamentous phototrophic bacterium which forms dense cell aggregates by active gliding movement. Int J Syst Bacteriol 45:676-681

Hanada S, Takaichi S, Matsuura K, Nakamura K (2002) *Roseiflexus castenholzii* gen. nov., sp. nov., a thermophilic, filamentous, photosynthetic bacterium that lacks chlorosomes. Int J Syst Evol Microbiol 52:187-193

Hayes JM (2004) Isotopic order, biogeochemical processes, and earth history - goldschmidt lecture, Davos, Switzerland, August 2002. Geochim. Cosmochim. Acta 68:1691-1700

Henry EA *et al.* (1994) Characterization of a new thermophilic sulfate-reducing bacterium - *Thermodesulfovibrio yellowstonii*, gen. nov. and sp. nov.- its phylogenetic relationship to *Thermodesulfobacterium* commune and their origins deep within the bacterial domain. Archives of Microbiology 161:62-69

Hollingsworth EA, Crowe DE, Romanek CS, Schroeder PA, Karpov GA (in review) Sulfur speciation in the Uzon caldera geothermal system, Kamchatka, Far East Russia. Journal of Volcanology and Geothermal Research

House CH, Schopf JW, Stetter KO (2003) Carbon isotopic fractionation by archaeans and other thermophilic prokaryotes. Org. Geochem. 34:345-356

Hugenholtz P, Pitulle C, Hershberger KL, Pace NR (1998) Novel division level bacterial diversity in a Yellowstone hot spring. J Bacteriol 180:366-376

Jahnke LL *et al.* (2001) Signature lipids and stable carbon isotope analyses of octopus spring hyperthermophilic communities compared with those of *Aquificales* representatives. Appl Envion Microbiol 67:5179-5189

Kampfer P (1994) Limits and possibilities of total fatty-acid analysis for classification and identification of bacillus species. Syst Appl Microbiol 17:86-98

Kanokratana P, Chanapan S, Pootanakit K, Eurwilaichitr L (2004) Diversity and abundance of bacteria and archaea in the Bor Khlueng hot spring in Thailand. Journal of Basic Microbiology 44:430-444

Knief C, Lipski A, Dunfield PF (2003) Diversity and activity of methanotrophic bacteria in different upland soils. Appl Envion Microbiol 69:6703-6714

Konneke M, Widdel F (2003) Effect of growth temperature on cellular fatty acids in sulphate-reducing bacteria. Environ Microbiol 5:1064-1070

L'Haridon S *et al.* (1998) *Desulfurobacterium thermolithotrophum* gen. nov., sp. nov., a novel autotrophic, sulphur-reducing bacterium isolated from a deep-sea hydrothermal vent. Int J Syst Bacteriol 48:701-711

Leininger S *et al.* (2006) Archaea predominate among ammonia-oxidizing prokaryotes in soils. Nature 442:806-809

Macalady JL, Vestling MM, Baumler D, Boekelheide N, Kaspar CW, Banfield JF (2004) Tetraether-linked membrane monolayers in *ferroplasma* spp: A key to survival in acid. Extremophiles 8:411-419

Madureira LAS, Conte MH, Eglinton G (1995) Early diagenesis of lipid biomarker compounds in north-Atlantic sediments. Paleoceanography 10:627-642

Maszenan AM, Seviour RJ, Patel BKC, Janssen PH, Wanner J (2005) *Defluvicoccus vanus* gen. nov., sp. nov., a novel gram-negative coccus/coccobacillus in the '*Alphaproteobacteria*' from activated sludge. Int J Syst Evol Microbiol 55:2105-2111

Moussard H *et al.* (2004) *Thermodesulfatator indicus* gen. nov., sp. nov., a novel thermophilic chemolithoautotrophic sulfate-reducing bacterium isolated from the Central Indian Ridge. Int J Syst Evol Microbiol 54:227-233

Nakagawa S, Nakamura S, Inagaki F, Takai K, Shirai N, Sako Y (2004) *Hydrogenivirga caldilitoris* gen.

nov., sp nov., a novel extremely thermophilic, hydrogen- and sulfur-oxidizing bacterium from a coastal hydrothermal field. Int J Syst Evol Microbiol 54:2079-2084

Nakagawa S, Takai K, Inagaki F, Horikoshi K, Sako Y (2005) Nitratiruptor tergarcus gen. nov., sp. nov. and Nitratifractor salsuginis gen. nov., sp. nov., nitrate-reducing chemolithoautotrophs of the epsilon-Proteobacteria isolated from a deep-sea hydrothermal system in the Mid-Okinawa Trough. Int J Syst Evol Microbiol 55:925-933

Nunoura T, Oida H, Miyazaki M, Suzuki Y, Takai K, Horikoshi K (2007) *Desulfothermus okinawensis* sp. nov., a thermophilic and heterotrophic sulfate-reducing bacterium isolated from a deep-sea hydrothermal field. Int J Syst Evol Microbiol 57:2360-2364

Pancost RD, Pressley S, Coleman JM, Benning LG, Mountain BW (2005) Lipid biomolecules in silica sinters: Indicators of microbial biodiversity. Environ Microbiol 7:66-77

Papke RT, Ramsing NB, Bateson MM, Ward DM (2003) Geographical isolation in hot spring cyanobacteria. Environ Microbiol 5:650-659

Pearson A *et al.* (2004) Nonmarine crenarchaeol in Nevada hot springs. Appl Envion Microbiol 70:5229-5237

Pearson A *et al.* (2008) Factors controlling the distribution of archaeal tetraethers in terrestrial hot springs. Appl Envion Microbiol 74:3523-3532

Powers LA, Werne JP, Johnson TC, Hopmans EC, Damste JSS, Schouten S (2004) Crenarchaeotal membrane lipids in lake sediments: A new paleotemperature proxy for continental paleoclimate reconstruction? Geology 32:613-616

Richardson DJ (2000) Bacterial respiration: A flexible process for a changing environment. Microbiology-SGM 146:551-571

Ringelberg DB, Sutton S, White DC (1997) Biomass, bioactivity and biodiversity: Microbial ecology of the deep subsurface: Analysis of ester-linked phospholipid fatty acids. FEMS Microbiology Reviews 20:371-377

Robinson JJ, Cavanaugh CM (1995) Expression of Form I and Form II Rubisco in chemoautotrophic

symbioses: Implications for the interpretation of stable carbon isotope values. Limnol. Oceanogr. 40:1496-1502

Romanek CS *et al.* (2004) Lipid biomarkers and stable isotope signatures of microbial mats in hot springs of Kamchatka, Russia. In: American Geophysical Union, San Francisco, CA, USA

Rutters H, Sass H, Cypionka H, Rullkotter J (2002) Phospholipid analysis as a tool to study complex microbial communities in marine sediments. Journal of Microbiological Methods 48:149-160

Sakata S, Hayes JM, McTaggart AR, Evans RA, Leckrone KJ, Togasaki RK (1997) Carbon isotopic fractionation associated with lipid biosynthesis by a cyanobacterium: Relevance for interpretation of biomarker records. Geochim. Cosmochim. Acta 61:5379-5389

Schouten S *et al.* (2008) Intact membrane lipids of "*Candidatus* Nitrosopumilus maritimus," A cultivated representative of the cosmopolitan mesophilic group I crenarchaeota. Appl Envion Microbiol 74:2433-2440

Schouten S, Hopmans EC, Pancost RD, Damste JSS (2000) Widespread occurrence of structurally diverse tetraether membrane lipids: Evidence for the ubiquitous presence of low-temperature relatives of hyperthermophiles. Proceedings of the National Academy of Sciences of the United States of America 97:14421-14426

Schouten S, Hopmans EC, Schefuss E, Damste JSS (2002) Distributional variations in marine crenarchaeotal membrane lipids: A new tool for reconstructing ancient sea water temperatures? Earth and Planetary Science Letters 204:265-274

Schouten S *et al.* (2007) Archaeal and bacterial glycerol dialkyl glycerol tetraether lipids in hot springs of Yellowstone national park. Appl Envion Microbiol 73:6181-6191

Stohr R, Waberski A, Volker H, Tindall BJ, Thomm M (2001) *Hydrogenothermus marinus* gen. nov., sp nov., a novel thermophilic hydrogen-oxidizing bacterium, recognition of *Calderobacterium hydrogenophilum* as a member of the genus *Hydrogenobacter* and proposal of the reclassification of *Hydrogenobacter acidophilus* as *Hydrogenobaculum acidophilum* gen. nov., comb. nov., in the phylum '*Hydrogenobacter/Aquifex*'. Int J Syst Evol Microbiol 51:1853-1862

Summons RE, Franzmann PD, Nichols PD (1998) Carbon isotopic fractionation associated with methylotrophic methanogenesis. Org. Geochem. 28:465-475

Summons RE, Jahnke LL, Simoneit BRT (1996) Lipid biomarkers for bacterial ecosystems: Studies of cultured organisms, hydrothermal environments and ancient sediments. In: Evolution of hydrothermal ecosystems on earth (and mars?), pp 174-194

Suutari M, Laakso S (1994) Microbial fatty-acids and thermal adaptation. Critical Reviews in Microbiology 20:285-328

Takai K, Komatsu T, Horikoshi K (2001) *Hydrogenobacter subterraneus* sp nov., an extremely thermophilic, heterotrophic bacterium unable to grow on hydrogen gas, from deep subsurface geothermal water. Int J Syst Evol Microbiol 51:1425-1435

Uda I, Sugai A, Itoh YH, Itoh T (2001) Variation in molecular species of polar lipids from *thermoplasma acidophilum* depends on growth temperature. Lipids 36:103-105

van der Meer MTJ, Schouten S, Damste JSS (1998) The effect of the reversed tricarboxylic acid cycle on the C-13 contents of bacterial lipids. Org. Geochem. 28:527-533

van der Meer MTJ, Schouten S, Damste JSS, de Leeuw JW, Ward DM (2003) Compound-specific isotopic fractionation patterns suggest different carbon metabolisms among *Chloroflexus*-like bacteria in hot spring microbial mats. Appl Envion Microbiol 69:6000-6006

van der Meer MTJ *et al.* (2001) Biosynthetic controls on the C-13 contents of organic components in the photoautotrophic bacterium *Chloroflexus aurantiacus* J Bioll Chem 276:10971-10976

Vestal JR, White DC (1989) Lipid analysis in microbial ecology. In. American Institute of Biological Sciences, pp 535-541

Ward DM, Ferris MJ, Nold SC, Bateson MM (1998) A natural view of microbial biodiversity within hot spring cyanobacterial mat communities. Microbiology and Molecular Biology Reviews 62:1353

Ward DM, Panke S, Kloppel KD, Christ R, Fredrickson H (1994) Complex polar lipids of a hot spring cyanobacterial mat and its cultivated inhabitants. Appl Envion Microbiol 60:3358-3367

Weijers JWH, Schouten S, Spaargaren OC, Damste JSS (2006) Occurrence and distribution of tetraether

membrane lipids in soils: Implications for the use of the TEX86 proxy and the BIT index. Org. Geochem. 37:1680-1693

Weijers JWH, Schouten S, van den Donker JC, Hopmans EC, Damste JSS (2007) Environmental controls on bacterial tetraether membrane lipid distribution in soils. Geochim. Cosmochim. Acta 71:703-713

White DC, Davis WM, Nickels JS, King JD, Bobbie RJ (1979) Determination of the sedimentary microbial biomass by extractible lipid phosphate. Oecologia 40 51-62

Wuchter C, Schouten S, Coolen MJL, Damste JSS (2004) Temperature-dependent variation in the distribution of tetraether membrane lipids of marine crenarchaeota: Implications for TEX86 paleothermometry. Paleoceanography 19:PA4028. doi: 4010.1029/2004PA001041.

Wuchter C, Schouten S, Wakeham SG, Damste JSS (2005) Temporal and spatial variation in tetraether membrane lipids of marine crenarchaeota in particulate organic matter: Implications for TEX86 paleothermometry. Paleoceanography 20

Yang F-L *et al.* (2004) Structural determination of the polar glycoglycerolipids from thermophilic bacteria Meiothermus taiwanensis. European Journal of Biochemistry 271:4545-4551

Zelles L (1999) Fatty acid patterns of phospholipids and lipopolysaccharides in the characterisation of microbial communities in soil: A review. Biology and Fertility of Soils 29:111-129

Zhang CL *et al.* (2004) Lipid biomarkers and carbon-isotopes of modern travertine deposits (Yellowstone national park, USA): Implications for biogeochemical dynamics in hot-spring systems. Geochim. Cosmochim. Acta 68:3157-3169

Zhang CL *et al.* (2007) Lipid biomarkers, carbon isotopes, and phylogenetic characterization of bacteria in California and Nevada hot springs. Geomicrobiology Journal 24:519-534

Zhang CL *et al.* (2003) Carbon isotope signatures of fatty acids in *Geobacter metallireducens* and *Shewanella algae*. Chemical Geology 195:17-28

Zhang CL, Pearson A, Li YL, Mills G, Wiegel J (2006) Thermophilic temperature optimum for crenarchaeol synthesis and its implication for archaeal evolution. Appl Envion Microbiol

72:4419-4422

Zhang CL *et al.* (2002) Carbon isotopic fractionations associated with thermophilic bacteria *Thermotoga maritima* and *Persephonella marina*. Environ Microbiol 4:58-64

Zhao W, Romanek CS, Mills G, Wiegel J, Zhang CL (2005) Geochemistry and microbiology of hot springs in Kamchatka, Russia. Geological Journal of China Universities 11:217-223

Zhao W, Romanek CS, Mou X, Wiegel J, Zhang CL (in review) Ammonia-oxidizing archaea in Kamchatka hot springs. Environ Microbiol

Zhao W *et al.* (2006) *Thermalkalibacillus uzonensis* gen. nov. sp. nov., a novel aerobic alkali-tolerant thermophilic bacterium isolated from a hot spring in Uzon Caldera, Kamchatka. Extremophiles 10:337-345

APPENDIX

Nitrogen and carbon elemental percentage and stable isotope compositions of bulk samples collected from 2004 to 2006 in the Uzon Caldera, Kamchatka. See the annual spreadsheet for sample descriptions.

Sample ID	Ampl. 28	$\delta^{15}N$	N %	Ampl. 44	$\delta^{13}C$	C %	Sample ID	Ampl. 28	$\delta^{15}N$	N %	Ampl. 44	$\delta^{13}C$	C %
040823.3	142	-9.99	0.06	464	-18.28	0.73	CR06012A		nd		136	-22.39	0.19
040823.3B	98	-13.91	0.03	201	-14.14	0.35	CR06012B	80	-4.52	0.02	324	-25.89	0.47
AN04003D	135	-9.24	0.05	377	-28.30	0.71	CR06012C		nd		112	-20.67	0.16
AN04004D	83	-6.50	0.02	300	-27.38	0.52	CR06012D	55	-0.92	0.01	188	-21.29	0.27
AN04005D	82	-5.69	0.02	180	-28.18	0.27	CR06012E	68	-3.04	0.01	250	-21.99	0.35
AN04006D	62	-5.44	0.01	247	-27.55	0.40	CR06012F	314	2.88	0.14	761	-19.99	1.16
AN04007D		nd		49	-27.68	0.07	CR06K4A		nd		227	-19.40	0.35
JK04050	575	-12.39	0.28	1696	-21.58	2.74	CR06K4B	109	2.18	0.03	321	-12.59	0.46
JK04051	384	-13.50	0.19	868	-18.22	1.79	CR06K4C	66	-0.29	0.01	215	-13.33	0.33
JK04078	1740	-21.15	0.90	3079	-13.42	5.69	CR06K4D	90	1.78	0.02	272	-13.39	0.39
JPRP072	1818	1.57	0.92	4192	-17.52	7.45	CR06K4E	351	4.00	0.16	688	-11.54	1.02
PS04010	86	-8.62	0.02	244	-28.36	0.47	CR06K4F	630	4.66	0.30	1313	-7.94	1.89
PS04014	76	-4.69	0.01	255	-27.40	0.38	CR06K4G	557	5.09	0.25	1154	-8.61	1.66
PS04015		nd		178	-27.48	0.27	CR06064	173	-5.26	0.08	533	-18.58	0.84
PS04016		nd		91	-26.31	0.13	CR06065	204	-1.52	0.07	305	-21.04	0.45
PS04039	1427	-5.86	0.73	3280	-15.42	5.46	CR06066	91	-3.34	0.03	223	-25.81	0.33
PS04040	235	-8.32	0.11	587	-21.71	1.09	CR06073	434	-17.58	0.18	1142	-28.16	1.64
PS04041	451	-7.25	0.26	905	-21.34	1.92	CZ06007	1393	-6.64	0.64	2437	-16.02	3.85
PS04042	71	-5.25	0.03	650	-27.82	1.38	CZ06007B	907	-4.62	0.43	1893	-11.22	2.79
PS04043		nd		117	-27.66	0.23	CZ06008	1002	-6.07	0.59	4928	-19.72	11.95
							CZ06009	732	-17.29	0.38	1118	-26.16	2.06
CZ05002	578	-13.77	0.29	1526	-23.87	2.77	CZ06010	129	-14.25	0.05	317	-24.24	0.47
CZ05003	5100	-10.75	2.59	9744	-14.80	21.16	CZ06011	122	-8.67	0.05	151	-23.65	0.23
CZ05004	499	-13.06	0.29	1677	-21.64	3.27	CZ06012S	138	-5.92	0.04	351	-22.95	0.49
CZ05006	98	-12.37	0.03	415	-27.78	0.71	CZ06012A		nd		190	-23.00	0.27
CZ05007	222	-12.16	0.10	448	-18.30	0.76	CZ06012B	283	-5.96	0.12	639	-21.31	0.96
CZ05012	54	-4.46	0.01	230	-21.77	0.32	CZ06012C	327	-3.66	0.14	620	-10.61	0.89
CZ05013	856	-1.56	0.44	1628	-18.25	2.75	CZ06012D	105	-4.05	0.03	228	-20.09	0.32
CZ05015	282	-18.55	0.10	728	-15.89	0.97	CZ06012E	670	-6.03	0.30	1096	-9.84	1.58
CZ05016	373	-19.28	0.15	1086	-14.28	1.47	CZ06013	1199	-7.72	0.57	2039	-13.58	3.22
CZ05017	72	-17.50	0.02	373	-22.49	0.64	CZ06014	359	-11.02	0.16	739	-15.55	1.10
CZ05018	2725	-0.57	1.37	573	-28.58	1.02	CZ06015	119	-6.97	0.04	964	-27.54	1.54
CZ05019	134	-8.09	0.04	280	-21.90	0.47	CZ06016	60	-13.87	0.01	423	-26.02	0.54
CZ05021		nd		142	-24.44	0.20	CZ06017		nd		260	-25.53	0.37
CZ05024	95	-14.27	0.03	258	-21.66	0.40	CZ06018	186	-10.14	0.09	610	-19.87	1.08
CZ05025	92	-14.49	0.03	306	-22.94	0.42	CZ06019	167	-17.89	0.07	528	-21.27	0.79
CZ05026	7914	-2.46	3.46	11731	-19.82	22.99	CZ06020	282	-15.91	0.12	526	-13.06	0.76
CZ05029	81	-2.72	0.02	328	-22.08	0.50	CZ06021	319	-18.20	0.14	802	-16.81	1.22
							IGN	61	-6.67	0.01	91	-22.52	0.12
CR06002	338	-12.41	0.14	672	-23.82	0.94	ON1	272	-9.11	0.12	1134	-27.02	1.81
CR06003A		nd		120	-27.33	0.17	SOIL1	1112	-5.03	0.52	4837	-26.67	8.04
CR06003B	1014	-6.29	0.47	2260	-24.64	3.33	SOIL 1_1	861	-5.02	0.44	3708	-26.66	6.78
CR06003C	3705	-0.57	1.55	10934	-15.42	19.88	SOIL2	454	-6.63	0.20	4193	-25.48	7.26
CR06003D	3408	0.39	1.51	7634	-14.70	12.40	SOIL2_1	223	-5.89	0.09	2163	-25.51	3.65
							V1N	84	-11.33	0.02	201	-23.65	0.28
							V2N	117	-7.13	0.04	265	-19.19	0.38
							YOUNGER BROTHER	69	-8.17	0.02	258	-21.84	0.40

a. Samples were grounded into fine powder and digested by fuming HCl for overnight. Solid residuals were collected on 0.45 µm polycarbonate filters tried overnight in 50°C oven. A portion of dry mass was quantitatively transferred into tin cup for isotope and content analysis using EA-IRMS.

b. Experimental errors, 2‰ if Ampl 44 and Ampl 28 values were lower than 100 mV; 1‰ if Ampl 44 and Ampl 28 values were between 100 and 500 mV; 0.11 and 0.15 for $\delta^{13}C$ and $\delta^{15}N$ respectively if both Ampl 44 and Ampl 28 are greater than 500 mV.

CHAPTER 4

THERMALKALIBACILLUS UZONENSIS GEN. NOV. SP. NOV., A NOVEL AEROBIC ALKALITOLERANT THERMOPHILIC BACTERIUM ISOLATED FROM A HOT SPRING IN THE UZON CALDERA, KAMCHATKA[§]

[§] Zhao, W. D., Weber, C., Zhang, C. L., Romanek, C. S., King, G. M., Mills, G., Sokolova, T. & Wiegel, J. 2006. Extremophiles 10, 337-345.
Reprinted here with permission of publisher.

ABSTRACT

A novel thermophilic, alkalitolerant, and CO-tolerant strain JW/WZ-YB58^T was isolated from green mat samples obtained from the Zarvarzin II hot spring in the Uzon Caldera, Kamchatka (Far East Russia). Cells were Gram-type and Gram-positive, strictly aerobic, 0.7-0.8 μm in width and 5.5-12 μm in length and produced terminal spherical spores of 1.2-1.6μm in diameter with the mother cell swelling around 2 μm in diameter (drumstick type morphology). Cells grew optimally at pH$^{25°C}$ 8.2-8.4 and temperature 50-52°C and tolerated maximally 6% (w/v) NaCl. They were strict heterotrophs and could not use either CO or CO_2 (both with and without H_2) as sole carbon source, but tolerate up to 90% (v/v) CO in the headspace. The isolate grew on various complex substrates such as yeast extract, on carbohydrates, and organic acids, which included starch, D-galactose, D-mannose, glutamate, fumarate and acetate. Catalase reaction was negative. The membrane polar lipids were dominated by branched saturated fatty acids, which included iso-15:0 (24.5%), anteiso-15:0 (18.3%), iso-16:0 (9.9%), iso-17:0 (17.5%) and anteiso-17:0 (9.7%) as major constituents. The DNA G + C content of the strain is 45 mol%. Phylogenetic analyses based on 16S rRNA gene sequences revealed that strain JW/WZ-YB58^T is distantly (<93% similarity) related to members of *Bacillaceae*. On the basis of 16S rRNA gene sequence, physiological and phenotypic characteristics, the isolate JW/WZ-YB58^T (= ATCC BAA-1258 = DSM 17740) is proposed to be the type strain for the type species of the new taxa within the family *Bacillaceae, Thermalkalibacillus uzonensis* gen. nov. sp. nov. The 16S rRNA gene sequence Genbank accession number is DQ221694.

INTRODUCTION

Alkalitolerant bacteria and alkaliphiles have been investigated for decades for their potential in industrial applications and biotechnology (Horikoshi 1999, 2004). Many of these organisms are mesophilic and halophilic (Nielsen *et al.* 1995; Horikoshi 2004). Thermophilic representatives, however, are less well known. Many previously described aerobic alkaliphiles and alkalitolerant bacteria belong to the *Firmicutes*, and are represented by species within the *Bacillaceae* (Nielsen *et al.* 1995; Blum *et al.*

1998; Yumoto *et al.* 1998, 2003), although many thermophiles are not validly published taxa (Kevbrin *et al.* 2004).

The family *Bacillaceae* is presently one of the taxonomically and phylogenetically diverse taxa undergoing revaluation. Based on the 16S rRNA gene sequences and G+C contents, many members of *Bacillaceae* have been re-classified from the genus *Bacillus* to novel genera, or even novel families, for example, *Alicyclobacillaceae* (Garrity *et al.*, 2004). Currently (January, 2006), the family *Bacillaceae* contains 23 genera. (http://www.ncbi.nlm.nih.gov/Taxonomy/Browser/wwwtax.cgi). Most bacteria within these genera share the features of being aerobic or microaerophilic, Gram-type and Gram-stain positive and spore-forming rods. However, diversity within *Bacillaceae* members may result in more novel genera created and more separations from the genus *Bacillus*.

During the course of enrichments for carboxydotrophic bacteria from CO-oxidizing hot spring microbial mats in the Uzon Caldera, Kamchatka, we isolated a novel member of the *Bacillaceae* (strain JW/WZ-YB58) that tolerates high CO concentrations (up to 90% in the head space), but appears unable to utilize CO as a carbon or energy source. CO tolerance has been reported previously for several members of the *Proteobacteria* (Cypionka and Meyer, 1982), but has not been documented for *Firmicutes*. King (2003) has shown that some CO-oxidizing bacteria only consume CO at low (< 1%) concentrations. To verify the potential for CO-utilization, King (2003) used a polymerase chain reaction (PCR) assay to amplify the large sub-unit gene (*coxL*) of carbon monoxide dehydrogenase. Primers for this assay (King, 2003) have been used to successfully amplify *coxL* from another member of the *Bacillaceae*, the carboxydotroph, *Bacillus schlegelii* (Dunfield and King, 2004).

METHODS

Sampling and Enrichment

Enrichments were carried out using a suspended mat sample obtained from the Zarvarzin II hot spring in the Uzon Caldera, Kamchatka, Russia. The sample previously oxidized CO when incubated with concentrations from 3 to 5% (Wiegel and Weber, unpubl. data). The mat was greenish in color, located at the edges of the pool and frequently submerged by the splashing pool water but intermittently exposed to

air. Water temperature varied from 55 to 72°C at the sampling location; the temperature below the mat surface (0.5-2 cm thick) was 55 to 65ºC. The pH of the spring varied from 6.0 to 7.5 within the mats and at the location where mats were collected.

Mineral media supplemented with 0.05% (w/v) yeast extracts and 20-27 mM pyruvate were used for enrichment and subsequent isolations. The mineral media contained (L^{-1} distilled water): 1 g NH_4Cl, 3.6 g NaCl, 1 g KCl, 0.5 g Na_2SO_4, 0.04 g $CaCl_2$, 0.04 g $MgCl_2 \cdot 6H_2O$, 0.5 g NaH_2PO_4, and 1 g K_2HPO_4, 1 mL vitamin solution, 1 mL trace-element solution and 1 mL Na_2SeO_3-Na_2WO_3 solution (Widdel and Bak 1992). The pH of the media was adjusted to 8.5 by titration with 2 M NaOH. Serum bottles (125 mL) for tenfold-dilution series contained 15 mL media and 2-4% (v/v) CO in air as the headspace. Cultures were incubated at 60°C for up to 4 weeks. Positive-growth cultures from the highest dilution were used as inocula for three successive transfers on agar (2%, w/v) plates. Agar plates were incubated in anaerobic containers (Difco) having approximately 4% (v/v) of CO in the air headspace. Colonies from the third batch of plates were transferred to liquid media. Cells in the culture were checked for uniformity by phase-contrast light microscopy (Olympus VANOX) and later by 16S rDNA sequence analysis.

Utilization of electron donors and acceptors

The ability of the bacterium to utilize different substrates was studied in mineral media containing 0.02% (w/v) yeast extract (Difco) supplemented with filter-sterilized substrate stock solutions (final substrate concentrations 20 mM). Autotrophic growth of the bacterium was checked using mineral media containing 0.02% (w/v) yeast extracts under a head space gas of 5% (v/v) CO, and 5% CO_2 with or without 20% H_2 (v/v) and balanced by air.

The CO utilization of enrichments and pure cultures was assessed by the gas chromatography (Carle Analytical Gas Chromatograph Series 400 by Chandler Engineering LLC) equipped with a thermal conductivity detector (TCD) and using helium as the carrier gas at isothermal 70°C oven temperature. The CO-tolerant range for the isolate was determined in mineral media supplemented with 0.05% (w/v) yeast extracts, 30 mM lactate and 10 to 90% (v/v) CO in air as the head space gas. To assess the CO-oxidation at low concentration (100ppm), *T. uzonensis* was grown at 50 °C in stoppered 60 mL serum

bottles containing 5ml enrichment. CO was added to the head space at a final concentration of 100 ppm. Using a needle and syringe, headspace samples were obtained at intervals over a 57 hour period. Samples were analyzed using a Trace Analytical reduced gas detector (model RGA3; Hardy and King, 2001).

The use of electron acceptors was determined in anaerobic nutrient-broth media under a N_2 atmosphere and supplemented with autoclaved stock solutions of 15 mM electron acceptors, *i.e.* fumarate, nitrate, nitrite, sulfate, thiosulfate, Fe (III) hydroxide and Fe (III) citrate. Freshly grown cultures to be used as inocula were pre-flushed with pure nitrogen gas. The medium was supplemented with $Na_2S{\cdot}9H_2O$ (0.5 g l^{-1}) to remove trace amounts of oxygen. The cultures were incubated for up to 2 weeks at 52ºC. Utilization of a particular substrate or an electron acceptor by the culture was determined by both direct cell-counts using a phase-contrast microscope and by measuring the increase in the optical density at 600 nm (OD_{600}; Spectronic 21; Baush and Lomb). Controls containing mineral medium with 0.02% (w/v) yeast extracts were performed in triplicates. Positive growth was identified if OD_{600} was at least two-fold higher than that of the controls.

Temperature, pH and NaCl concentration

The ranges and optima of temperature, pH and NaCl concentration for growth were determined using mineral media supplemented with 0.05% (w/v) yeast extract and 20 mM fumarate. Temperature optimum was determined using media with a $pH^{25ºC}$ 8.0 in a temperature-gradient shaking incubator (Scientific Industries) set between 30 and 80ºC with a 2°C interval. Increase in cell numbers was followed for up to 2 weeks. The pH range for growth was determined at 52°C using the basal media with 0.05 % (v/w) yeast extract and supplemented with a mixture of 10 mM each of MES, HEPES, CAPS and TAPS as buffers for the different pH values. The pH^{25C} values were adjusted by titration with HCl (5 M) and NaOH (5 M) before autoclaving and measured at room temperature again after 30 min incubation. Salt requirement and tolerance were determined at pH^{25C} 8.2 and 55°C over a range from 0-15% NaCl (w/v) by measuring increase of optical density (600 nm) over time and calculating the doubling time of each individual culture.

Microscopy

Light Microscopy. Routine examinations and cell counts were performed with an Olympus microscope (VANOX). Phase-contrast micrographs of bacteria were taken using agar-coated slides.

Scanning Electron Microscopy. Cells were fixed in 2% glutaraldehyde / 0.1 M cacodylate, post fixed in osmium tetroxide / 0.1 M cacodylate, dehydrated through graded ethanol washes, critical point dried, and coated with gold by a SPI-Module Sputter Coater. SEM images were gathered on LEO 982 SEM/FEG using an accelerating voltage of 5 kV.

Transmission Electron Microscopy. Cultured cells were fixed in 2% glutaraldehyde / 0.1 M cacodylate buffer for 1 hour (RT), rinsed, and post fixed in 1% osmium tetroxide (OsO_4) for 1 hour (4ºC). Samples were then washed in deionized water, dehydrated with ethanol graded washes and embedded in Epon 812 resin. Cells were infiltrated in fresh resin and polymerized for 24-48 hours at 60°C. 50 nm-thick sections were cut using a diamond knife and post stained with 4% uranyl acetate for 30 minutes followed by staining in 1% lead citrate for 5 minutes. TEM images were captured on a JEOL 100CX with an accelerating voltage of 80 kV.

Lipid analysis

Bacterial cell-membrane lipids were extracted from lyophilized cells grown in 30 mM nutrient broth (Difco) under optimal conditions ((pH 8.3, temperature 55ºC) and collected at the late exponential growth phase by centrifugation. Cells were kept under oxygen-free nitrogen gas at -80°C until analysis. The total lipids were extracted, fractionated and transformed to obtain fatty acid methyl esters (FAME) of phospholipid as described previously (Guckert *et al.* 1985). FAMEs were analyzed by gas chromatography equipped with a flame ionization detector (Hewlett-Packard 6890; Guckert *et al.* 1985). The commercial bacterial acid methyl ester (BAME) standard and GC-MS system were used for peak-identification.

Biochemical characterization

Sensitivity to antibiotics was determined using Sensititre COMEQ2F plates (Trek Diagnostic

Systems Ltd., UK). Biochemical characterization was performed following Claus and Berkeley (1986) API 20E strips (BioMerieux Inc.) and the BBL Crystal GP ID system (Becton Dickinson and Company, USA). Incubation temperature was 50ºC.

DNA isolation and base composition

DNA was extracted using Qiagen DNeasy Tissue kit (Qiagen Inc.) according to the manufacture's instruction. The DNA G+C content was determined by high performance liquid chromatography as described previously (Mesbah *et al.* 1989).

16S rRNA gene sequence

16S rRNA genes were amplified using the universal primer pairs 27f and 1492r (*Escherichia coli* numbering). PCR was conducted with 30 cycles of amplification at 94°C (1 min), 58°C (30 s), and 72°C (30 s), and a final extension at 72 °C for 7 min. PCR products were purified using Qiaquick PCR purification Kit (Qiagen Inc.), and sequenced by Macrogen Inc. (Seoul, Korea). The assembled 16S rRNA gene sequence was aligned with a representative set of 16S rRNA sequences obtained from the Genbank database using ClustalX software (Higgins and Sharp 1988). Pairwise evolutionary distances were calculated by using the correction of Jukes and Cantor (1969). Phylogenetic trees were constructed with both neighbor-joining method (Saitou and Nei 1987) and maximum-parsimony method, with bootstrap analysis of 1,000 replications using the Mega 3.1 software (Kumar *et al.* 2004).

PCR amplification of *cox*L gene fragments

PCR amplification of fragments of *cox*L, which codes for the large subunit of carbon monoxide dehydrogenase, was carried out using 50 µl reactions in 200 µl tubes. Reactions contained standard final concentrations of deoxynucleoside triphosphates and buffer and 0.5U of MasterTaq DNA Polymerase (Brinkmann Inc.); primers were present at 0.1µM each and Magnesium ion was present at 1.5 mM. The final DNA template concentration in the reaction was 3-4 ng. Two separate reactions were carried out using primer sets that target authentic (OMP) and putative (BMS) *cox*L fragments. The forward primers for OMP and BMS fragments have the following nucleic acid sequences: OMPf (5'-GGCGGCTT[C/T]GG[C/G]AA[C/G] AAGGT-3' and BMSf (5'-

GGCGGCTT[C/T]GG[C/G]TC[C/G]AAGAT-3'. The same reverse primer was used in both reactions: O/Br (5'-[C/T]TCGA[T/C]GATCATCGG[A/G]TTGA-3'). A DNA extract from *Stappia aggregata* (King, 2003), a known CO-oxidizer was used for a positive control in both reactions. Amplification was completed using an Eppendorf Mastercycler thermocycler (Brinkmann Inc.). First, the templates were denatured for 3 minutes at 94 °C, then thirty cycles of the following steps were completed: denaturation for 45 s at 94 °C, annealing for 60 s at 58 °C, and extension for 90 s at 72 °C. The thirty cycles were followed by a final 10 min extension at 72 °C. PCR products were viewed under UV light after standard ethidium bromide gel electrophoresis.

RESULTS

Colony and cell morphology

Four to 10-day-old colonies of strain JW/WZ-YB58^T, growing aerobically on solidified (agar, 2% w/v) basal media containing 0.05 % (w/v) yeast extract, were circular with entire edges, 2-3 mm in diameter and transparent in color. After an additional week, swarming was observed leading to irregular spreading of the colonies. Cells of strain JW/WZ-YB58^T were motile rods of 0.7-0.8 μm in width and 5.5-12 μm in length with rounded ends (Fig 4.1) and two to five peritrichously inserted flagella (Fig 4.2a). Cells from early stationary phase tended to form chains of 3-12 cells. Spherical spores (1.2-1.6 μm in diameter) were located terminally with swelling (around 2 μm in diameter) of the mother cell (drumstick morphology; Fig 4.1). Transmission electron microscopy revealed the cells contain two types of unusual cytoplasmic inclusions of unknown nature and function and thus need further studies in the future (Fig 4.2b).

Physiology

Stain JW/WZ-YB58^T was unable to use CO (1-5%, v/v) or CO_2 (5%, v/v) as the sole carbon source in the presence or absence of 10-20% (v/v) H_2 within a 4-week incubation with or without shaking. No CO-oxidation was observed at 100 ppm CO, neither. By using a PCR assay, could a presence of either the authentic or the putative *cox*L fragments of a gene for *cox*L be demonstrated, suggesting that the

bacterium does not contain the ability of CO-utilization. However, while growing on 0.05% (w/v) yeast extract alone or with 10 mM pyruvate, the cultures were not inhibited by 0-70% (v/v) CO in the air head space, and still grew under 90% (v/v) CO-containing air but the cell morphology became irregular. In the presence of 0.02% (w/v) yeast extract, strain JW/WZ-YB58^T grew on complex organic compounds as carbon and energy sources such as beef extract, casamino acid, peptone, starch and tryptone. The following compounds served as carbon and energy source: dextrin, raffinose, lactose, sucrose, arabinose, fructose, D-galactose, D-glucose, D-mannose, and trehalose, gluconate, glutamate, fumarate, lactate, pyruvate, and acetate. Cells did not grow on alcohols and sugar alcohols. Cells were strict aerobes and unable to use nitrate, nitrite, fumarate, thiosulfate, Fe (III) hydroxide, and Fe (III) citrate as electron acceptors for anaerobic growth while using 20 mM pyruvate as the carbon source. The substrate and electron acceptor spectrum of strain JW/WZ-YB58^T indicated an aerobic, organoheterotrophic, and CO-tolerant physiology.

The temperature range for growth was between 42 and 64ºC, with an optimum at 50-52ºC at pH^{25ºC} 8.0. No growth occurred at 40 or 66ºC. At 52ºC, the strain grew at pH^{25ºC} between 6.4 and 9.7, with an optimum of 8.2-8.4. However, the growth of the strain at or below pH^{25ºC} 7 was very poor with doubling times longer than 14 hours. The observed minimal doubling time under optimal growth conditions (pH^{25C} 8.3, 52ºC) was 2.5 h.

Biochemical characterization

Cultures were positive for Gram-staining reaction, oxidase reactions, ONPG hydrolysis and gelatin hydrolysis. Results were negative for catalase reaction, Voges-Proskauer reaction, indole production, urea hydrolysis and starch hydrolysis.

Membrane polar lipids of strain JW/WZ-YB58^T were dominated by branched saturated fatty acids including iso-14:0 (1%), iso-15:0 (24.5%), anteiso-15:0 (18.3%), iso-16:0 (9.9%), iso-17:0 (17.5%) and anteiso-17:0 (9.7%) accounting for about 81% of the total fatty acids (area %). Other important fatty acids were 14:0 (1.2%), 15:0 (5.1%), 16:1 (2.1%), 16:0 (7.6%), 17:0 (1.1%), 18:1 (0.9%) and an unknown fatty acid (1.1%).

The strain JW/WZ-YB58^T was sensitive to the following antibiotics (microgram per milliliter): Amikacin, 4; Amoxicillin/clavulanic acid, 4/2; Ampicillin, 0.25; Cefazolin, 0.25; Cefoxitin, 2; Cefpodoxime, 2; Ceftiofur, 0.25; Cephalothin, 2; Chloramphenicol, 4; Clindamycin, 0.25; Enrofloxacin, 0.5; Erythromycin, 0.5; Imipenem, 1; Gentamicin, 1; Marbofloxacin, 0.25; Orbifloxacin, 1; Oxacillin, 2; Penicillin, 0.06; Rifampin, 1; Tetracycline, 1; Ticarcillin, 8; Ticarcillin/clavulanic acid, 8/2, Trimethoprim/sulphamethoxazole, 0.5/9.5.

DNA composition and 16S rDNA sequences

The G+C content of genomic DNA of strain JW/WZ-YB58T was 45 mol% (chromatographic method). The obtained 16S rRNA gene sequence (accession number DQ221694 in Genbank) contained 1,436 nucleotides corresponding to positions 33-1470 of the E. coli 16S rRNA gene sequence. Using BLAST to compare with the currently available sequences in Genbank, no closely related sequence was found. The sequence suggests a distant relationship to the alkaliphilic isolate Bacillus sp. TA2.A1 (AF113512; 96.6% similarity; Cook *et al.* 2003; Olsson *et al.* 2003; Peddie *et al.* 2000). A phylogenetic tree, based on neighbor-joining method, revealed that strain JW/WZ-YB58^T was phylogenetically related to the members of *Bacillaceae*. The closest neighbor was *Bacillus horti* DSM 12751 (93.1% similarity), a mesophilic and alkaliphilic bacterium isolated from soils in Japan (Fig 4.3). Similarities to other previously described *Bacillaceae* members were low (around 90.0%), and nearly equally distant to other major groups; for example, *B. clarkii* DSM8720^T 91.0% (X76444), *B. halodurans* DSM497^T 90.3% (AJ302709), *B. subtilis* W168/PY79 89.4% (K00637), *B. thermocloacae* DSM5250^T 89.6% (Z26939), *Geobacillus subterraneus* DSM13552^T 90.6% (AF276306), *G. stearothermophilus* DSM6285^T 90.3% (AY608989), *Aneurinibacillus thermoaerophilus* DSM10154^T 90% (X94186) and *Brevibacillus thermoruber* DSM7064^T 89.2% (Z16921).

DISCUSSION

The pH and temperature profiles indicate that the strain JW/WZ-YB58^T is an alkalitolerant, moderately thermophilic Gram-staining and Gram-type positive (Wiegel 1981) rod-shaped bacterium, which differs from the closest phylogenetic neighbor *B. horti* in many aspects. The most distinguishable

characteristics are the growth range of temperature and NaCl concentration, spore morphology, O_2 requirement, Gram-staining and catalase reactions (Table 4.1). The 16S rRNA gene sequence analysis reveals that the other phylogenetic neighbors are alkaliphilic or thermophilic members of the *Bacillaceae* family. However, the growth of strain JW/WZ-YB58^T occurs at higher temperature and lower pH than other strictly alkaliphilic *Bacillus* species. In addition, strain JW/WZ-YB58^T is lower in tolerance to salt (0-6%, w/v, NaCl) and higher in the DNA G+C content than major alkaliphilic *Bacillus* species (Nielsen *et al.* 1995; Table 4.1). Thermophilic members of the Order *Bacillales* such as species belonging to the genera *Geobacillus, Aneurinibacillus* and *Brevibacillus*, on the other hand, usually grow optimally at neutral or slightly acidic pH (Nazina *et al.* 2001). The absence of a positive catalase reaction in strain JW/WZ-YB58^T distinguishes it from the majority of *Bacillus* species as well, which commonly show positive catalase reactions (Claus and Berkeley 1986). Terminally located spherical spores produced by strain JW/WZ-YB58^T rarely occur in its phylogenetic neighbors, which usually form centrally or sub-terminally located ellipsoidal spores (Table 4.1). The DNA G+C content for strain JW/WZ-YB58^T is 45 mol% and thus greater than that of most mesophilic-alkaliphilic *Bacillus* species but lower than that of neutral-thermophilic ones (Nazina *et al.* 2001; Manachini *et al.* 1985; Table 4.1). Presently, it is unclear how far the insensitivity toward CO is a taxonomically useful property because CO-utilization and/or inhibition by CO are not a common test for characterizing novel microorganisms, especially thermophiles. Gee and Brown (1980) and Cypionka and Mayer (1982) showed that different bacteria including *E. coli* are not inhibited by concentrations of up to 30% (v/v) CO, although at a slower growth rate. Further more, the question whether an organism can utilize CO needs to be carefully examined since CO-utilization can be inhibited by elevated CO concentrations (King 2003; King *et al.* unpubl. data; Moran *et al.* 2004). Examples include CO-oxidizing members of the marine genus *Stappia*, which do not oxidize CO when CO concentration is above 1000 ppm (King, unpublished data). However, the failure to demonstrate the presence of the *cox*L gene, which codes for the large subunit of carbon monoxide dehydrogenase, suggests that this bacterium is not a CO-utilizer. Also at this time it is not clear how important the observed CO-insensitivity is for the isolate to function within the microbial mat from the hot spring pool

Zarvarzin II and possibly similar mat in the caldera. King and Weber (unpublished results) have measured *in situ* CO formation and CO-utilization in those mats. The role of CO-utilization and CO insensitivity of bacteria in the hot spring mats needs further investigations.

Cell membranes of *Bacillus species* are characterized by branched saturated fatty acids (Kaneda 1967; Claus and Berkeley 1986; Kampfer 1994; Nazina *et al.* 2001). The majority of alkaliphilic *Bacillus* species are dominated by anteiso-fatty acids with the ratio of total anteiso-/total iso- greater than 1, whereas strain JW/WZ-YB58^T has a total anteiso-/total iso- ratio of only 0.53 with the iso-15:0 as the most abundant component (Table 4.2). Thermophilic *Geobacillus* species and *Aneurinibacillus* species have similar membrane fatty-acid compositions to strain JW/WZ-YB58^T with iso-15:0 being the most abundant fatty acid (Nazina *et al.* 2001; Heyndrickx *et al.* 1997; Meier-Stauffer *et al.* 1996). However, the total anteiso-/total iso- ratio is usually lower than 0.4 for *Geobacillus* species and even lower in *Aneurinibacillus* species (Nazina *et al.* 2001; Meier-Stauffer *et al.* 1996), which may be due to the lower growth pH of species in these genera than that of strain JW/WZ-YB58^T.

On the basis of physiological characteristics, phenotypic and phylogenetic properties, the isolate is placed within the Phylum BXIII *Firmicutes,* the class *"Bacilli"*, Order I *Bacillales*, and tentatively the Family I *Bacillaceae* according to the recent electronic Bergey' s Outline (Garrity *et al.*, 2004) as a novel taxa, *Thermalkalibacillus uzonensis* gen. nov. sp. nov. with strain JW/WZ-YB58^T (=ATCC BAA-1258 = DSM 17740) as the type strain for the type species *T. uzonensis*. Besides the type genus *Bacillus* with *B. subtilis* as type species, the Family I *Bacillaceae* also contains the genus *Geobacillus* (Fig 4.3), which contains several thermophilic and alkalitolerant/alkaliphilic species previously belonging to the genus *Bacillus*. However, the genus *Anaeurobacillus* (Fig 4.3) is assigned to the Family V *'Paenibacillaceae'* (Garrison *et al.*, 2004). Constructing several trees using the type species of the different genera and various algorithms (figures not shown) reveals that the phylogeny of the order *Bacillales* is not clear at this time, as is evident from low (below 50%) boot strap values. Furthermore, defining the boundary for the novel genus has to wait for further isolations of species and strains belonging to this group, *i.e.,* to decide whether the closest neighbor in the phylogenetic trees, *B. horti* (Fig 4.3), belongs to the novel

genus or not.

Description of *Thermalkalibacillus* gen. nov.

Thermalkalibacillus, (therm.al.ka.li.ba.cil.lus. Gr. n. thermê, heat; Arabic word alkali (al-qaliy), the ashes of saltwort; L. masc. n. bacillus, a small staff, a wand; N.L. masc. n. *Thermalkalibacillus*, rod loving combined growth conditions of elevated temperature and alkaline pH).

Cells are aerobic, spore-forming rods. Thermophilic and facultative alkaliphilic. Strict heterotroph. Utilizing carbohydrate and organic acids for growth. DNA G+C mol% is about 45%.

Description of Thermalkalibacillus uzonensis sp. nov

Thermalkalibacillus uzonensis (u.zo.nen'sis. N.L. masc. adj. uzonensis pertaining to the isolation habitat Uzon Caldera, east of Mt Uzon in Kamchatka (Far East Russia).

Cells are Gram-type and Gram-staining positive, straight to slightly curved rods with 0.7-0.8 μm×5.5-12 μm in dimension. Terminally located spherical spores (1.2–1.6 μm in diameter) causing swelling of the mother cells. Cells are motile with two to five peritrichous flagella. Growth only under aerobic conditions observed. Colonies on nutrient broth agar are circular with entire edges and transparent. Swarming occurs when colony ages. Oxidase reactions, ONPG hydrolysis and gelatin hydrolysis are positive. Catalase reaction, Voges-Proskauer reaction, indole production, urea hydrolysis and starch hydrolysis are negative. At $pH^{25ºC}$ 8.0, the temperature range is 42-64ºC with optimum at 50-52ºC. The $pH^{25ºC}$ range is 6.4-9.7 (pH optimum 8.2-8.4) when grown at 52ºC. Tolerated NaCl concentration range is 0-6% (w/v). Cells grow on complex substrates (such as yeast extract), carbohydrates and acids but not on alcohols and sugar alcohols. Acid production occurs from trehalose, lactose, sucrose, arabinose and fructose. Major membrane fatty acids are iso-15:0 (24.5%), anteiso-15:0 (18.3%), iso-16:0 (9.9%), iso-17:0 (17.5%), anteiso-17:0 (9.7%) and 16:0 (7.6%). The G+C content of genomic DNA is 45 mol% (chromatographic method). Cells do not grow chemolithoautotrophically on 1-5% v/v CO or 5% CO_2 with or without H_2 and do not oxidize CO at low concentrations (100 ppm). Grown under shaking, CO is tolerated up to 90% (v/v) in the air-containing gas headspace. The type strain is JW/WZ-YB58^T (=ATCC BAA-1258 = DSM 17740), which was isolated from a microbial mat sample collected from the edges of

the hot spring Zarvarzin II in the Uzon Caldera, Kamchatka (Far East Russia). The Genbank accession number for the 16S rRNA gene sequence of the type strain is DQ221694.

ACKNOWLEDGEMENTS

We thank Rich Davis for performing the electron microscopy, Jean P. Euzeby for help with the correct naming of *T. uzonensis*. We are indebted to Elizaveta Bonch-Osmolovskaya (RAS-Moscow) and Gennadii Karpov (Petropavlovsk-kamchatkii) for logistic help for our Field Season and obtaining sampling permits. This research was supported by a grant through National Science Foundation Microbial Observatory Program NSF-MCB 0238407 (JW, CSR) and partially supported by the Environmental Remediation Sciences Division of the Office of Biologic and Environmental Research, U.S. Department of Energy through the Financial Assistant Award to the University of Georgia Research Foundation (CLZ, CSR).

Table 4.1. Differentiating characteristics of strain JW/WZ-YB58^T and other related *Firmicutes* species.

Characteristics	1	2	3	4	5	6	7	8	9	10
Sporangia										
Shape[a]	S	E	ND	E	E	E	E	E	E	E
Position[b]	T	S	ND	S	S	ST	ST	T	C	ST
Sporangia swollen	+	ND	ND	-	+	E	-	v	+	+
Catalase	-	+	ND	+	ND	+	+	+	-	-
Growth at pH 7	+	+	-	-	v	-	+	+	+	+
Growth at										
10°C	-	-	-	+	-	-	-	-	-	-
40°C	-	+	+	+	+	+	-	+	+	+
50°C	+	-	-	-	+	+	+	+	+	+
Growth in 10% (w/v) NaCl	-	+	+	-	v	-	-	-	-	-
Hydrolysis of starch	-	+	-	+	+	-	+	+	-	+
Reduction of nitrate	-	+	+	-	-	-	+	-	-	-
mol% G+C content	45	40-41	42-43	36-38	42-44	42	50-52	52	47	56-58

+, positive; -, negative; v, variable; ND, not determined. a, S, spherical; E, ellipsoidal. b, T, terminal; S, subterminal; C, central. Species, 1, JW/WZ-YB58^T; 2, *B. horti* (Yumoto *et al.* 1998); 3, *B. clarkii*; 4, *B. alcolophilus*; 5, *B. halodurans*; (Nielsen *et al.* 1995) 6, *B. thermocloacae* (Demharter, 1989); 7, *Gb. subterraneus* (Nazina *et al.* 2001); 8, *Gb. stearothermophilus* (Kampfer 1994); 9, *Anb. thermoaerophilus* (Meier-Stauffer *et al.* 1996); 10, *Bb. thermoruber* (Manachini *et al.* 1985)

Table 4.2. Membrane fatty-acid composition of strain JW/WZ-YB58^T and other related species (shown in percentage of total fatty acid).

Fatty acid	1	2	3	4	5	6	7
a-13:0	-	-	-	-	5.1	-	-
i-14:0	1.0	-	0.6	1.8	0.1	2.9	0.2
14:0	1.2	2.4	0.5	0.3	1.5	-	0.2
i-15:0	24.5	38	32	29.1	40	37.8	54.3
a-15:0	18.3	30	43	37.9	6.4	2.3	0.6
15:0	5.1	-	0.3	-	0.5	1.4	0.6
i-16:0	9.9	4.4	1	4.9	6.2	29.2	2.3
16:1	2.1	5.3	1.5	0.2	-	1.7	3.5
16:0	7.6	1.1	2.1	3.2	9.2	-	-
i-17:0	17.5	1.4	4.3	11.2	17	18.5	32.8
a-17:0	9.7	7.9	11	9.6	13	5.8	0.8
i-17:1	-	-	1.7	0.3	-	-	-
a-17:1	-	-	0.9	0.2	-	-	-
C17:0	1.1	1.9	-	-	-	0.4	0.2
i-16:1	-	-	-	0.1	-	-	-
Other	2	8	0.6	1.3	0.8	-	4.5
Branched saturated	80.9	89	92	94.5	88	93.6	90.8
Total iso-	52.9	44	38	47	63	85.5	89.4
Total anteiso-	28	45	54	47.5	25	8.1	1.4
anteiso/iso	0.53	1.02	1.44	1.01	0.39	0.09	0.02
Total	100	101	99	100	100	100	100

1, JW/WZ-YB58^T; 2, *B. horti* DSM12751^T (Yumoto *et al.* 1998); 3 *B. alcalophilus* DSM485^T ; 4. *B. subtilus* (Yumoto *et al.* 2003); 5, *G. stearothermophilus* DSM6285^T (Kampfer 1994); 6, *G.subterraneus* DSM13552^T (Nazina *et al.* 2001); 7, *Aneurinibacillus thermoaerophilus* DSM10154^T (Meier-Stauffer *et al.* 1996).

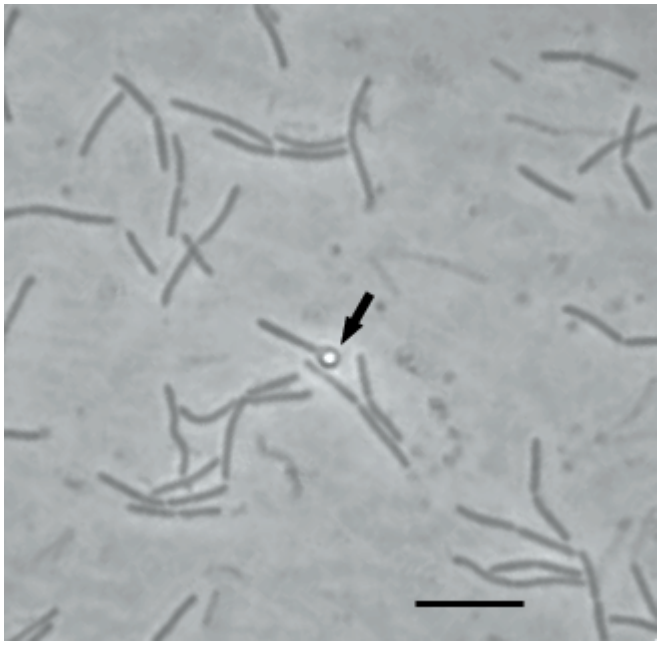

Fig 4.1. Phase-contrast microphotograph of strain JW/WZ-YB58^{T}. Cells from the late exponential growth phase. Arrow indicates a sporulated cell. *Bar* 10 μm.

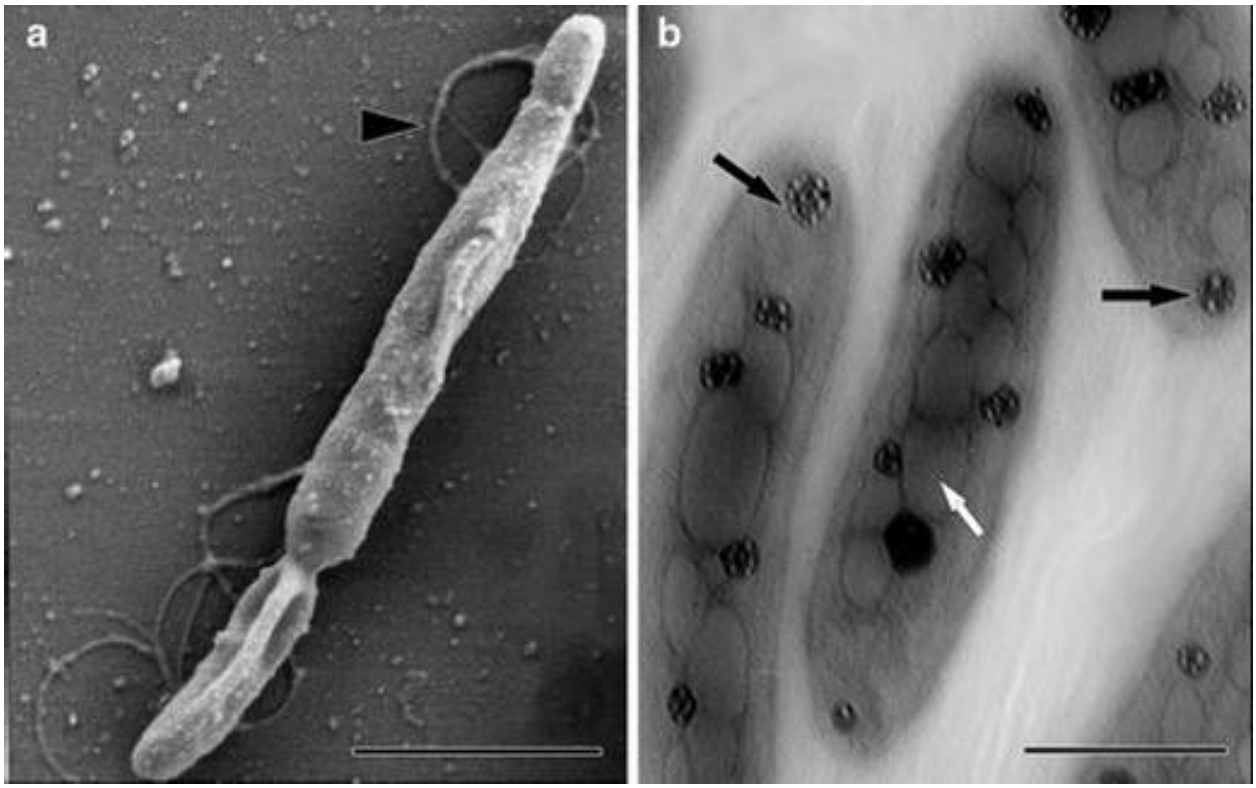

Fig 4.2. Electron micrographs. a, scanning electron microscopy revealing retarded peritrichous flagellation (arrow head) and an uneven cell surface. *Bar*, 1 μm. b, transmission electron microscopy revealing organized internal features (white arrow) as well as several circular electron dense bodies (black arrow) of unknown function and nature in each cell. *Bar*, 250 nm (courtesy of Rich Davis, UGA)

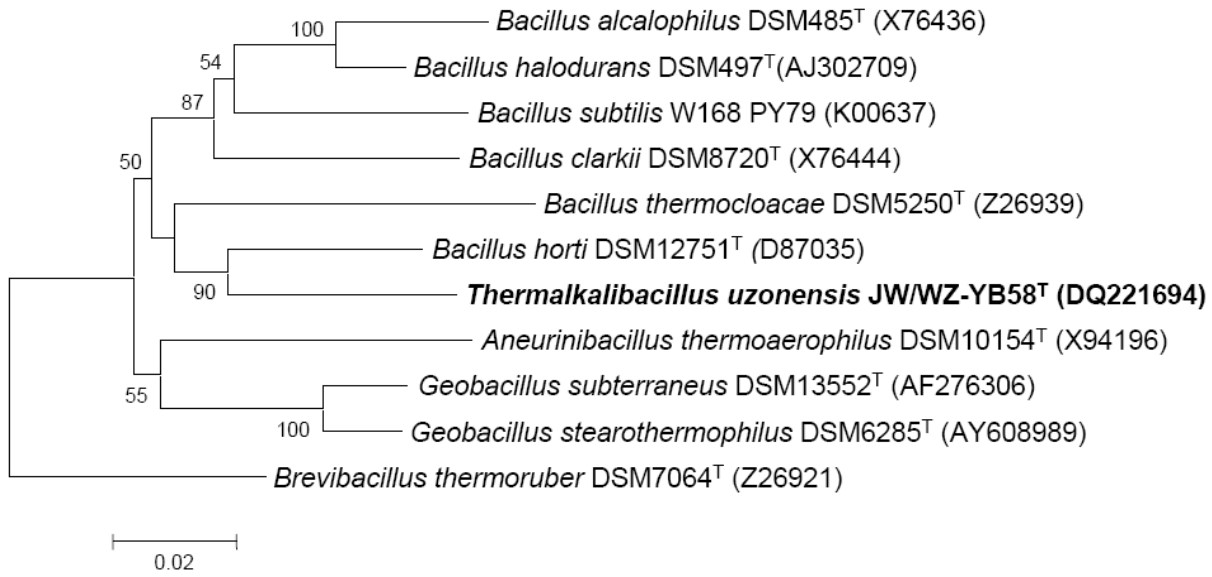

Fig 4.3. Phylogenetic tree based on 16S rRNA gene sequences. Comparison between strain JW/WZ-YB58^T and other related, mainly alkaliphilic and thermophilic species was based on neighbor-joining method with bootstrap analysis of 1,000 replicates. Bootstrap values greater than 50% are shown. *Bar*, 0.02 *Knuc*.

REFERENCES

Blum JS, Bindi AB, Buzzelli J, Stolz JF, Oremland RS (1998) *Bacillus arsenicoselenatis*, sp. nov., and *Bacillus selenitireducens*, sp. nov: Two haloalkaliphiles from Mono lake, California that respire oxyanions of selenium and arsenic. Arch. Microbiol. 171:19-30

Claus D, Berkeley RCW (1986) Genus *Bacillus* cohn 1872. In: Sneath. PHA, Mair NS, Sharpe ME, Holt JG (eds) Bergey's manual of systematic bacteriology. Williams & Winkins, Baltimore, pp 1105-1139

Cook GM, Keis S, Morgan HW, van Ballmoos C, Matthey U, Kaim G, Dimroth P (2003) Purification and biochemical characterization of the F1FO-ATP synthase from thermoalkaliphilic *Bacillus* sp. strain TA2.A1. J. Bacteriol. 185:4442-4449

Cypionka H, Meyer O (1982) Influence of carbon monoxide on growth and respiration of carboxydotrophic and other aerobic organisms. FEMS Microbiol. Lett. 15:209-214

Demharter W, Hensel R (1989) *Bacillus thermocloaceae* sp. nov, a new thermophilic species from sewage-sludge. Syst. Appl. Microbiol. 11:272-276

Dunfield KE, King GM (2004) Molecular analysis of carbon monoxide-oxidizing bacteria colonizing recent Hawaiian volcanic deposits. Appl. Environ. Microbiol. 70: 4242-4248

Gee DL, Brown WD (1980) The effect of carbon monoxide on bacterial growth. Meat Science 5:215-222

Garrity MG, Bell JA, Lilburn TG (2004) Taxonomic Outline of the Prokaryotes. Bergey's Manual of Systematic Bacteriology, second edition, release 5.0 May 2004. http://141.150.157.80/bergeysoutline/outline/bergeysoutline_5_2004.pdf

Guckert JB, Antworth CP, Nichols PD, White DC (1985) Phospholipid, ester-linked fatty-acid profiles as reproducible assays for changes in prokaryotic community structure of estuarine sediments. FEMS Microbiol. Ecol. 31:147-158

Hardy K, King GM (2001) Enrichment of a high affinity CO-oxidizer in Maine forest soil. Appl. Environ. Microbiol. 67: 3671-3676.

Heyndrickx M *et al.* (1997) A polyphasic reassessment of the genus *Aneurinibacillus*, reclassification of

Bacillus thermoaerophilus (Meier-stauffer *et al.* 1996) as *Aneurinibacillus thermoaerophilus* comb. nov., and emended descriptions of *A. aneurinilyticus* corrig, *A. migulanus,* and *A. thermoaerophilus*. Int. J. Syst. Bacteriol. 47:808-817

Higgins DG, Sharp PM (1988) Clustal: A package for performing multiple sequence alignments on a microcomputer. Gene 73:237-244

Horikoshi K (1999) Alkaliphiles: Some applications of their products for biotechnology. Microbiol. Mol. Biol. Rev. 63:735-750

Horikoshi K (2004) Alkaliphiles. Proc. Jpn. Acad. Ser. B. Phys. Biol. Sci. 80:166-178

Jukes TH, Cantor CR (1969) Evolution of protein molecules. In: Munro HN (ed) Mammalian protein metabolism. Academic Press, New York, pp 21–123

Kampfer P (1994) Limits and possibilities of total fatty-acid analysis for classification and identification of bacillus species. Syst. Appl. Microbiol. 17:86-98

Kaneda T (1967) Fatty acids in genus *Bacillus*. I. iso- and anteiso-fatty acids as characteristic constituents of lipids in 10 species. J. Bacteriol. 93:894-903

Kevbrin VV, Romanek CS, Wiegel J (2004) Alkalithermophiles: A double challenge from extreme environments. In: Seckbach J (ed) Cellular origins: Life in extreme habitats and astrobiology. Kluwer, Dordrecht

King GA (2003) Molecular and culture-based analyses of aerobic carbon monoxide oxidizer diversity. Appl. Environ. Microbiol. 69:7257-7265

Kruger B, Meyer O (1984) Thermophilic *Bacilli* growing with carbon-monoxide. Arch. Microbiol. 139:402-408

Kumar S, Tamura K, Nei M (2004) MEGA3: Integrated software for molecular evolutionary genetics analysis and sequence alignment. Brief Bioinform. 5:150-163

Manachini PL, Fortina MG, Parini C, Craveri R (1985) *Bacillus thermoruber* sp. nov., nom. rev., a red-pigmented thermophilic bacterium. Int. J. Syst. Bacteriol. 35:493-496

Meier-Stauffer K *et al.* (1996) Description of *Bacillus thermoaerophilus* sp. nov., to include sugar beet

isolates and *Bacillus brevis* ATCC 12990. Int. J. Syst. Bacteriol. 46:532-541

Mesbah M, Premachandran U, Whitman W (1989) Precise measurement of the G+C content of deoxyribonucleic acid by high-performance liquid chromatography. Int. J. Syst. Bacteriol. 39: 159-167

Meyer O, Frunzke K, Gadkari D, Jacobitz S, Hugendieck I, Kraut M (1990) Utilization of carbon-monoxide by aerobes-recent advances. FEMS Microbiol. Rev. 87:253-260

Moran MA *et al.* (2004) Genome sequence of *Silicibacter pomeroyi* reveals adaptations to the marine environment. Nature. 432:910-913

Nazina TN *et al.* (2001) Taxonomic study of aerobic thermophilic *Bacilli*: Descriptions of *Geobacillus subterraneus* gen. nov., sp. nov. and *Geobacillus uzenensis* sp. nov. from petroleum reservoirs and transfer of *Bacillus stearothermophilus Bacillus thermocatenulatus*, *Bacillus thermoleovorans*, *Bacillus kaustophilus*, *Bacillus thermoglucosidasius* and *bacillus thermodenitrificans* to *Geobacillus* as the new combinations *G. stearothermophilus*, *G. thermocatenulatus, G. thermoleovorans*, *G. kaustophilus*, *G. thermoglucosidasius* and *G. thermodenitrificans*. Int. J. Syst. Evol. Microbiol. 51:433-446

Nielsen P, Fritze D, Priest FG (1995) Phenetic diversity of alkaliphilic *Bacillus* strains-proposal for 9 new species. Microbiol. UK 141:1745-1761

Olsson K, Keis S, Morgan HW, Dimroth P, Cook GM (2003) Bioenergetic properties of the thermoalkaliphilic *Bacillus* sp. strain TA2.A1. J. Bacteriol. 185:461-465

Peddie CJ, Cook GM, Morgan HW (2000) Sucrose transport by the alkaliphilic, thermophilic *Bacillu*s sp. strain TA2.A1 is dependent on a sodium gradient. Extremophiles 4:291-296

Saitou N, Nei M (1987) The neighbor-joining method: A new method for reconstructing phylogenetic trees. Mol. Biol. Evol. 4:406-425

Widdel F, Bak F (1992) Gram-negative mesophilic sulfate-reducing bacteria. In: Balows A, Trüper HG, Dworkin M, Harder W, Schleifer H (eds) The Prokaryotes, 2nd edn. Springer, New York, pp 3352-3378

Wiegel, J. (1981) Distinction between the Gram reaction and the Gram type of bacteria. Int. J. Syst. Bacteriol. 31:88.

Yumoto I *et al.* (1998) *Bacillus horti* sp. nov., a new gram-negative alkaliphilic *Bacillus*. Int. J. Syst. Bacteriol. 48:565-571

Yumoto I *et al.* (2003) *Bacillus krulwichiae* sp. nov., a halotolerant obligate alkaliphile that utilizes benzoate and m-hydroxybenzoate. Int. J. Syst. Evol. Microbiol. 53:1531-1536

CHAPTER 5

CALDALKALIBACILLUS UZONENSIS SP. NOV., AND EMENDED DESCRIPTION OF THE GENUS *CALDALKALIBACILLUS*[**]

[**] Zhao, W. D., Zhang, C. L., Romanek, C. S., and Wiegel, J. *Int J Syst Evol Microbiol* 58: 1106-1108
Reprinted here with permission of publisher.

ABSTRACT

Strain JW/WZ-YB58^T, a thermophilic (42-64^{o}C), aerobic, alkali-tolerant (pH^{25C} 6.4-9.7), heterotrophic, sporulating, retarded-peritrichously flagellated, and slightly curved rod-shaped bacterium, was isolated from the hot spring Zarvarzin II in the East Thermal Field of the Uzon Caldera, Kamchatka (Far East Russia). The isolate tolerated high concentrations of CO. The major membrane phospholipid fatty acids of JW/WZ-YB58^T included iso15:0 (24.5%), anteiso15:0 (18.3%) and iso17:0 (17.5%). The mol % G+C of the genomic DNA is 45 (HPLC method). Based on 16S rRNA sequence analysis and physiological properties the isolate JW/WZ-YB58^T is proposed as the type strain of *Caldalkalibacillus uzonensis* sp. nov. (ATCC BAA-1258; DSM 17740). In contrast to the type species *C. thermarum,* a catalase reaction positive aerobe, *C. uzonensis* was catalase reaction negative, thus the description of the genus *Caldalkalibacillus* is emended to include a catalase reaction negative species.

INTRODUCTION

An aerobic heterotrophic, flagellated and slightly curved rod-shaped bacterium, strain JW/WZ-YB58^T, which tolerated high concentrations of carbon monoxide (up to 90%) in the head space was isolated from a hot spring located in the Uzon Caldera (Kamchatka, Far East Russia) and previously invalidly published as '*Thermalkalibacillus uzonensis'* (Zhao *et al.*, 2006). Analysis of 16S rRNA gene sequences suggested JW/WZ-YB58^T is a novel species of the genus *Caldalkalibacillus* (Xue *et al.*, 2006), which previously contained only the type strain of the type species, *Caldalkalibacillus thermarum* HA6^T, an aerobic heterotrophic thermophilic bacterium (Xue *et al.*, 2006). The 16S rRNA gene sequence of HA6^T was 96.5% similar to that of strain JW/WZ-YB58^T (GenBank accession no. DQ221694; Zhao *et al.*, 2006) and 99% similar to that of *Bacillus* sp. TA2.A1 (Peddie *et al.*, 2000), suggesting that the strain JW/WZ-YB58^T represented a separate species of the genus *Caldalkalibacillus*, and thus is proposed as the type strain of *Caldalkalibacillus uzonensis* sp. nov. (ATCC BAA-1258; DSM 17740). The next closest neighbor *Bacillus horti* was 92-93% similar in 16S rDNA to the *Caldalkalibacillus* (Fig 5.4).

Physiological and biochemical properties of the strain JW/WZ-YB58^T were described in detail by Zhao *et al.*, (2006). Major phospholipid fatty acids of strain JW/WZ-YB58^T included iso15:0 (24.5%),

anteiso15:0 (18.3%), iso16:0 (9.9%), iso17:0 (17.5%), anteiso17:0 (9.7%), and 16:0 (7.6%). Strain JW/WZ-YB58^T and *C. thermarum* HA6^T shared many similar properties. For example, both were strictly aerobic thermophilic, alkali-tolerant, Gram-staining positive, sporulating rods, and able to grow on a variety of organic substrates including yeast extract, carbohydrates, and organic acids. Both species contained iso15:0 (24.5-33.8%) and iso17:0 (17.5-35.5%) as major phospholipid fatty acids, and the G+C contents of genomic DNA of both strains were about 45 mol% (although one was determined using HPCL and the other by T_m).

However the two species differed significantly in several properties (Table 5.3). For example, in contrast to the type species of the genus *C. thermarum*, *C. uzonensis* JW/WZ-YB58^T was motile, contained 2-5 peritrichously inserted flagella, and was unable to utilize alcohol and sugar alcohol (*e.g.*, D-sorbitol, D-mannitol, glycerol) as carbon and energy sources. *C. uzonensis* also contained anteiso15:0 as the second most abundant fatty acid and was catalase reaction negative (Table 5.3). The latter difference led to the emendation of the genus description.

EMENDATION OF THE GENUS *CALDALKALIBACILLUS* DESCRIPTION (XUE *ET AL.*, 2006):

The genus *Caldalkalibacillus* contains catalase reaction positive and catalase reaction negative species. Predominant cellular phospholipid fatty acids include iso15:0, anteiso15:0 and iso17:0.

DESCRIPTION OF *CALDALKALIBACILLUS* UZONENSIS SP. NOV.

Caldalkalibacillus uzonensis u.zo.nen'sis. N.L. masc. adj. *uzonensis* pertaining to the isolation habitat Uzon Caldera, east of Mt Uzon in Kamchatka (Far East Russia).

The description is based on the detailed publication as *'Thermalkalibacillus uzonensis'* JW/WZ-YB58^T (Zhao *et al.*, 2006). Cells are Gram-type (Wiegel, 1981) and Gram-staining positive, straight to slightly curved rods with 0.7-0.8 μm×5.5-12 μm in dimension. Terminally located spherical spores (1.2-1.6 μm in diameter) causing swelling of the mother cells. Cells are motile with two to five peritrichously inserted flagella. Growth is only observed under aerobic conditions. Colonies on nutrient broth agar are circular with entire edges and transparent. Swarming occurs when colony ages. Oxidase reactions, ONPG

hydrolysis and gelatin hydrolysis are positive. Catalase reaction, Voges-Proskauer reaction, indole production, urea hydrolysis and starch hydrolysis are negative. At $pH^{25ºC}$ 8.0, the growth temperature range is 42-64ºC with optimum at 50-52ºC. The $pH^{25ºC}$ range is 6.4-9.7 with optima 8.2-8.4 when grown at 52ºC. NaCl concentrations are between 0- 6% (w/v). Cells grow on complex substrates (such as yeast extract), carbohydrates and acids but not on alcohols and sugar alcohols. Acid production occurs from trehalose, lactose, sucrose, arabinose and fructose. Major phospholipid fatty acids are iso15:0 (24.5%), anteiso15:0 (18.3%), iso16:0 (9.9%), iso17:0 (17.5%), anteiso17:0 (9.7%), and 16:0 (7.6%). The G+C content of genomic DNA is 45 mol% (HPLC; Mesbah *et al.*, 1989). Cells do not grow chemolithoautotrophically on 1-5% v/v CO or 5% CO_2 with or without H_2 and do not oxidize CO at low concentrations (100 ppm). Cells growing under shaking tolerate up to 90% (v/v) CO in the air-balanced head space. The type strain is JW/WZ-YB58^T (=ATCC BAA-1258 = DSM 17740), which was isolated from a microbial mat sample collected from the edges of the hot spring Zarvarzin II in the East Thermal Field of the Uzon Caldera, Kamchatka (Far East Russia). The Genbank accession number for the 16S rRNA gene sequence of the type strain is DQ221694.

ACKNOWLEDGEMENTS

This research was supported by a grant through National Science Foundation Microbial Observatory Program NSF-MCB 0238407 (JW, CSR) and partially supported by the Environmental Remediation Sciences Division of the Office of Biologic and Environmental Research, U.S. Department of Energy through the Financial Assistant Award to the University of Georgia Research Foundation (CSR, CLZ).

Table 5.1. Differentiating characteristics of strain JW/WZ-YB58^T and other related *Firmicutes* species.

Characteristics		1	2	3
Spores:				
	Shape	S	S	E
	Position	T	T	ST
Catalase		-	+	+
Growth at:				
	10°C	-	-	-
	40°C	-	-	+
	50°C	+	+	-
	pH 7	+	-	+
	pH 9	+	+	+
Growth in 10% NaCl (w/v)		-	-	+
Hydrolysis of starch		-	w	+
Reduction of nitrate		-	-	+
Major phospholipid fatty acids		iso15:0 anteiso15:0 iso17:0	iso15:0 iso17:0	iso15:0, anteiso15:0
G+C content (mol%)		45	45.2	40 -41

Abbreviation, +, positive; -, negative; v, variable; w, weak; S, spherical; E, ellipsoidal; T, terminal; ST, subterminal.

Species, 1, JW/WZ-YB58^T; 2, *Caldalkalibacillus thermarum* (Xue *et al.*, 2006); 3, *B. horti* (Yumoto *et al.*, 1998)

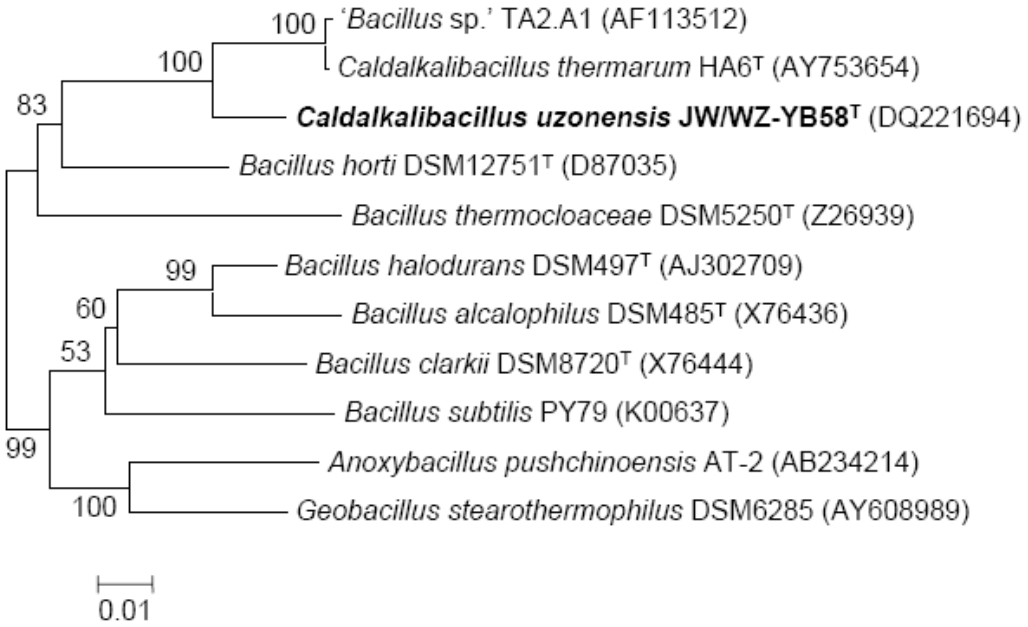

Fig 5.1. Phylogenetic tree based on 1,448bp of 16S rDNA sequences. Sequences of *Caldalkalibacillus uzonensis* JW/WZ-YB58^T (DQ221694) and other related, mainly alkaliphilic and thermophilic species were calculated using neighbor-joining method with MEGA 3.1 software. Bootstrap analysis of 1000 replicates was performed and values greater than 50% were shown at nodes. Bar equals 0.01 changes per nucleotide.

REFERENCES

Kampfer, P. (1994). Limits and possibilities of total fatty-acid analysis for classification and identification of bacillus species. *Syst Appl Microbiol* 17, 86-98.

Mesbah, M., Premachandran, U. & Whitman, W. B. (1989). Precise measurement of the G+C content of deoxyribonucleic acid by high-performance liquid chromatography. *Int J Syst Bacteriol*, 159-167.

Peddie, C. J., Cook, G. M. & Morgan, H. W. (2000). Sucrose transport by the alkaliphilic, thermophilic *Bacillus* sp. strain TA2.A1 is dependent on a sodium gradient. *Extremophiles* 4, 291-296.

Xue, Y. F., Zhang, X. Q., Zhou, C., Zhao, Y., Cowan, D. A., Heaphy. S., Grant, W. D., Jones, B. E., Ventosa, V. **&** Ma, Y. (2006). *Caldalkalibacillus thermarum* gen. nov., sp. nov., a novel alkalithermophilic bacterium from a hot spring in China. *Int J Syst Evol Microbiol* 56, 1217-1221.

Yumoto, I., Yamazaki, K., Sawabe, T., Nakano, K., Kawasaki, K., Ezura, Y. & Shinano, H. (1998). *Bacillus horti* sp. nov., a new gram-negative alkaliphilic bacillus. *Int J Syst Bacteriol* 48, 565-571.

Wiegel, J. (1981). Distinction between the Gram reaction and the Gram type of bacteria. *Int J Syst Bacteriol* 31:88.

Zhao, W. D., Weber, C., Zhang, C. L., Romanek, C. S., King, G. M., Mills, G., Sokolova, T. & Wiegel, J. (2006). *Thermalkalibacillus uzonensis* gen. nov. sp. nov., a novel aerobic alkali-tolerant thermophilic bacterium isolated from a hot spring in Uzon Caldera, Kamchatka. *Extremophiles* 10, 337-345.

CHAPTER 6

STABLE CARBON ISOTOPE FRACTIONATION ASSOCIATED WITH CARBON FIXATION BY CHEMOLITHOAUTOTROPHIC ANAEROBIC CO-OXIDIZING BACTERIUM *CARBOXYDOTHERMUS HYDROGENOFORMANS*[††]

[††] Zhao W., Zhang, C. L., Brant H, Sokolova, T., Wiegel, J., Robb, F. T., Romanek, C. S., to be submitted.

INTRODUCTION

Carbon monoxide (CO) is the third most common carbon-bearing trace gas in the atmosphere (Wahlen 1994). The annual global emissions of CO into the atmosphere is estimated to be up to 2600 million tons, of which about 60% originates from human activities and about 40% is derived from natural processes (EPA 1991; Ragsdale 2004). However, CO concentration is low (about 60 to 300 ppb in suburban environments) due to its rapid turnover time of about 100 days (Crutzen and Gidel 1983; King 2003). Despite the relatively low concentration, CO participates in a number of chemical reactions that control the atmospheric chemistry of greenhouse gases including methane and ozone (Crutzen and Gidel 1983; King 2003). Surprisingly, as much as 15% of the annual CO flux to the atmosphere is removed by microorganisms such as fungi, actinomycetes, and bacteria (Bartholomew and Alexander 1982; Conrad 1996).

It has been shown that CO-oxidizing bacteria are phylogenetically and taxonomically diverse, (Zavarzin and Nozhevnikova 1977; Meyer *et al.* 1990; King 2003; Ragsdale 2004). Members include aerobic carboxydotrophs and the anaerobic acetogens, sulfate reducers, methanogens and phototrophs (Meyer and Schlegel 1983; Svetlichny *et al.* 1991; Svetlitchnyi *et al.* 2001; Ragsdale 2004). Carbon-fixation pathways used by different CO-oxidizing bacteria are shown to be different between aerobes and anaerobes; aerobic CO-oxidizers use the Calvin cycle whereas anaerobic species use the reductive acetyl-CoA pathway (also called Wood-Ljungdahl pathway; Meyer and Schlegel 1983; Ragsdale 2004). Unlike aerobic CO-oxidizing microorganisms containing Mo-binding enzymes (Meyer 1982; Ferry 1995; Evans 2005), anaerobic CO-oxidizers contain the Ni-binding key enzyme carbon monoxide dehydrogenases, which may be monofunctional (CODH type I) or bifunctional as CODH type II (Svetlitchnyi *et al.* 2001). The latter enzyme class is associated with acetyl-CoA synthetase (ACS) to form a complex CODH/ACS that have been referred to as CODH type III in the genome of *Carboxydothermus hydrogenoformans* (Wu *et al.* 2005). This enzyme is used to convert CO_2 molecules or CO molecules into acetyl-CoA (Wood 1991). This pathway is the most direct biological reaction to covert inorganic carbon to organic matter (Fig 6.1), therefore, it has been proposed as the first biochemical pathway for carbon fixation (Russell and

Martin 2004). The pathway is also known for having variable steps.

A number of anaerobic CO-oxidizers, particularly thermophilic species, have been isolated and described (Gerhardt *et al.* 1991; Svetlichny *et al.* 1991; Sokolova *et al.* 2002), which display diverse energy metabolisms. For instance, many acetogens and methanogens are able to showed ability to utilize H_2 and CO_2 for autotrophic growth, while others use CO as sole energy and carbon source to produce CO_2 and H_2 with the consumption of H_2O according to the reaction $CO+H_2O \rightarrow CO_2+H_2$ (Ragsdale 2004 and references therein). The latter group is usually referred to as the CO-oxidizing hydrogenogens, which include *Carboxydothermus, Carboxydocella* and other non-acetogenic anaerobic CO-oxidizing bacteria and archaea (Gerhardt *et al.* 1991; Svetlichny *et al.* 1991; Sokolova *et al.* 2004). Unlike other carbon fixation pathways such as the Calvin Cycle and the reductive tricarboxylic acid cycle, the reductive acetyl CoA pathway may lead to diverse carbon isotope fractionations between carbon substrate and cell biomass due to these variations in carbon and energy metabolism. Carbon isotope tracer studies have been used to understand the source and flow of carbon in this pathway (Svetlitchnyi *et al.* 2001; Henstra *et al.* 2007); however, understanding the intrinsic stable carbon isotope fractionation between source carbon and biomass remains a challenge for microorganisms using this pathway due to the involvement of CO and CO_2 during carbon fixation. This research is important, however, for a better understanding of the carbon cycle in nature and the role that microorganisms play in biological processes that shape hot spring environments.

C. hydrogenoformans is a model thermophilic, anaerobic CO-oxidizing hydrogenogen and a biofuel candidate for the generation of H_2 (Seth-Smith 2007). The genome of *C. hydrogenoformans* strain Z-2901 showed it contains five difference CODH complexes, which is in contrast to one or two types of the enzyme in other CO-oxidizing hydrogenogen (Wu *et al.* 2005). In this study, CO and CO_2 gases with different stable carbon isotope compositions were used in time series culture experiments using *C. hydrogenoformans* DSM 6008 to determine how different growth phases and isotope composition of substrate CO and CO_2 may affect the isotope fractionation between carbon sources and bacterial biomass.

MATERIAL AND METHOD

Medium composition and cultivation

Carboxydothermus hydrogenoformans strain DSM 6008 was obtained from the Dr. Frank Robb at the University of Maryland. It was cultivated under strictly anaerobic conditions in a basal phosphate-carbonate-buffered medium, which contained (l^{-1} of distilled water): 1.4 g NH_4Cl, 2.0 g NaCl, 0.5 g KCl, 0.5 g Na_2SO_4, 0.04 g $CaCl_2$, 0.04 g $MgCl_2 \cdot 6H_2O$, 0.7 g $NaH_2PO_4 \cdot 7H_2O$, and 0.35 g K_2HPO_4, 0.02 g yeast extract (Fluka, Biochemika, Buchs, Switzerland), 1 ml vitamin solution, and 1 ml trace-element solution (Widdel and Bak 1992). The medium was degassed using a stream of pure nitrogen gas at boiling temperature. $KHCO_3$ (0.5 g) and $Na_2S \cdot 9H_2O$ 9 (1 g) were then added to the medium after it was cooled down. The pH of the medium was adjusted to 6.8 by titration with 2 M NaOH. Two hundred milliliters of medium were transferred each to 1 liter serum bottles under pure nitrogen atmosphere and then thoroughly flushed with pure CO for 7 min at a flow rate of 800 ml min^{-1} before the bottles were sealed with butyl rubber stoppers and crimped with aluminum caps. The bottles were autoclaved for 40 min at 121°C. Inocula were prepared using the same media in 125 ml serum bottles with the same medium:headspace volume ratio and incubated overnight before inoculation. All the cultures were incubated at 60°C in a shaking incubator in this study.

Sampling

Two experiments were designed. Experiment 1 was set up using CO and CO_2 of different isotope composition pairs to examine the effect of initial gas isotope fraction to the evolution of $\delta^{13}C$ values over the incubation. Variable amount of pure (>99.9%) ^{13}CO and $^{12}CO_2$ were add into bottle C and D containing regular cylinder-gas of CO (-44.0 ‰) and dissolved bicarbonate ($\delta^{13}C$ value of equilibrium CO_2 gas = -27.0 ‰) to yield isotopically different headspace gases. The uninoculated bottles were incubated at 60°C for two hours before being sampled for a set of time zero headspace gases, which were then analyzed for $\delta^{13}C$ values of CO and CO_2: CO (-45.0 ‰) and CO_2 (-27.4 ‰; bottles A and B as replicates), CO (-22.4‰) and CO_2 (-36.9‰; bottle C), and CO (-36.4‰) and CO_2 (-40.3 ‰; bottle D).

The experiment 2 was set up to use a single isotope composition pair to examine both gases and

biomass for their $\delta^{13}C$ values changes over time. Four experimental bottles and two negative control bottles contained CO (-45.0 ‰) and bicarbonate ($\delta^{13}C$ value of equilibrium CO_2 gas = -27.0 ‰). Duplicate samples of CO, CO_2 and biomass were collected at both the early and late exponential growth phases. Gas composition and $\delta^{13}C$ values for CO and CO_2 were analyzed every 24 hrs for 72 hrs..

In both experiments, time series samples from were collected in a course of up to 80 hrs (Table 6.1). At each sampling point, pressure of the head space was measured by a digital pressure gauge at 40ºC; liquid samples were withdrawn using sterile syringes to measure the cell optical density at 600nm (OD600; 23°C; 1 ml each) using a Beckman DU-64 spectrometer (Beckman instruments Inc. Fullerton, CA), and the pH (23°C; 1ml, the same liquid sample for OD600 measurements) using Fisher Accument pH meter (Fisher Scientific Inc., Pittsburgh, PA); additional duplicate of 1.5 ml culture liquid using sterile syringes and 4-ml headspace gas using Hamilton gas tight syringes were collected and transferred to 6-ml Vacuette® serum blood collection tubes (Greiner Bio-One, Monroe, NC, USA). The Vacuette tubes were then stored upside-down at the room temperature until gas content and carbon isotope analysis. The Vacuette tubes only evacuated for ~50% atm and the gas residuals are air (personal communication with technical representative). Incubation and time series sampling were terminated at the early stationary phase and cell biomass was collected for bulk carbon isotope analysis for the experiment 1; for the experiment 2, two of the four experimental bottles were stopped for incubation each at early and late exponential growth phase to collect biomass for carbon isotope analysis.

Gas composition and isotope analysis

Concentrations of H_2 were determined using a SENTE methane gas analyzer (model GS-19S, Sente Inc., USA) under isothermal conditions at 54ºC using zero grade air as a carrier gas at a flow rate of 29.7ml min^{-1}. The reported peak area of H_2 on the chromatogram was used to calculate equivalence of pure H_2 volume based on a predetermined standard curve. The calculated volume was then divided by the injection volume to obtain percentage of H_2 gas in the sample. Variable volumes (5- 30 µl) were injected using Hamilton gastight syringes based on concentrations in each individual samples to ensure the optimal response.

The same approach was used to calculate concentrations of CO, and CO_2, which were measured together with carbon isotope analysis using a Trace GC-C-IRMS (Finnigan MAT GmbH, Germany) equipped with a Carboxen 1010 plot column (Supelco, USA) under isothermal conditions at 100ºC using pure helium as a carrier gas at a constant flow of 3 ml min^{-1}. Peak areas and stable carbon isotope compositions of CO and CO_2 were determined on a ThermoQuest Delta Plus XL isotope ratio mass spectrometer (Finnigan MAT GmbH, Germany). The precision of the instrument was determined ±1% of measured values for gas composition measurements based on standard gas measurements. However, the actual error of multiple measurements were much higher, mainly due to errors introduced by subsampling from the Vacuette tubes because the measured values for the three gas species in a single sample always varied in the same way. A pure CO_2 gas as a working standard was calibrated to the international PDB standard and has a $\delta^{13}C$ value of -45.0‰ versus PDB. Its amplitude 44 value was set to 4000 mV throughout the analysis. The linearity of isotope analysis was examined to be satisfactory from 700 mV to 8000 mV with a variation of 0.1‰ per volt. Variable gas volumes (10-200 µl) were injected using Hamilton gastight syringes to satisfy the working ranges. For gas composition calculation, the standard curves were constructed specific to experimental range of each measured gas by injecting up to 20 µl of pure CO_2 and 25 µl pure CO. The total CO_2 in the bottle was calculated with the program CO_2 sys-marco (Lewis and Wallace 1998) by input the pH and free CO_2 concentrations.

Liquid culture samples were acidified to extract CO_2 prior to analysis by IRMS. Bulk biomass was filtered using pre-combusted and pre-weighed GF/F glass fiber filter and thoroughly washed with 2N HCl and DI water. After drying at 50°C overnight, the filter was weighed, and loaded into tin cups for analysis by EA-IRMS. The bulk carbon isotope composition of yeast extract used in the growth medium was determined by EA-IRMS analysis similarly. Carbon isotope compositions are reported in delta notation:

$$\delta^{13}C = 10^3 \times (R_{sample}/R_{standard}-1)$$

where $R={}^{13}C/{}^{12}C$

Enrichment factor ε was calculated as following:

$$\varepsilon_{A-B} = \delta^{13}C_A - \delta^{13}C_B$$

RESULTS

Preliminary experiments demonstrated that CO_2 and trace amount of yeast extract were required for the growth of the *C. hydrogenoformans*, thus 0.5 g l^{-1} bicarbonate and 0.02 g yeast extract were included in the medium for both experiments. The yeast extract had isotope composition of -24.2±0.05‰ (n = 4), and the carbon content was 30.7±0.4% (n =4). The dissolved CO_2 equilibrated with bicarbonate had an isotope composition of -27.4±0.5‰ (n = 4).

In all bottles, CO was consumed while CO_2 and H_2 were produced (Tables 6.1 and 6.2). The total pressure accumulated in each bottle to up to 1.46 atm at the end of the experiment, while the pH decrease for as many as 1 unit (Tables 6.1 and 6.2). Stoichiometric relationship between CO, total CO_2 and H_2 was not obtained (*e.g.* H_2 and calculated total CO_2 for both experiment; Tables 6.1 and 6.2) mainly due to the experimental errors, which may be partially caused by the potential gas leakage of tight syringes, which do not have push buttons to seal the withdrawn volume. The trends in gas evolution are consistent with previous studies (Svetlichny *et al.* 1991). At the end of each experiment, the remaining CO_2 may have originated from CO oxidation and exchange with bicarbonate and account for 25 to 70% of total inorganic carbon ($CO + HCO_3^-$) additions at the beginning. The loss of inorganic carbon from the total CO and CO_2/ HCO_3^- pool was calculated to be approximately 10-40 mmole carbon at the end of each experiment (Table 6.1). The biomass remaining in each bottle at the end of the experiment was 1 mg for dry biomass in average, and determined to contain 60% carbon EA-IRMS analysis.

In Experiment 1, the $\delta^{13}C$ values for CO varied considerably compared with the $\delta^{13}C$ value for CO_2 (Fig 6.2). In bottle A and B that used isotopically depleted CO (-45.0‰) and enriched CO_2 (-27.4‰; panel A and B in Fig 6.2), $\delta^{13}C$ values for CO and CO_2 changed less than 1‰ when *ca.* 30% CO had been consumed. The $\delta^{13}C$ values for CO then varied dramatically in bottle A while depleted steadily (by 7‰) in bottle B until the late exponential growth phase (panel A and B in Fig 6.2). In the two cultures, $\delta^{13}C$ values for CO dropped by 25 to 47‰ from ~-50‰ at the late exponential growth phase, but returned to more positive values in the stationary growth phase. In contrast, $\delta^{13}C$ value for CO_2 remain constant until about the late exponential growth phase, followed by a decrease of about 16‰ to the end of the

experiment. Carbon isotope composition of bulk biomass ($\delta^{13}C_{Bio}$) was -26.2 and -27.1‰ in bottles A and B, respectively, close to the initial $\delta^{13}C$ value for CO_2 and greater than the $\delta^{13}C$ value for CO_2 at the end of the experiment (Table 6.3).

In bottle C that used ^{13}C-enriched CO (-22.4‰) and ^{13}C-depleted CO_2 (-36.9‰; panel C in Fig 6.3), $\delta^{13}C$ values decrease steadily for CO and increase for CO_2 until the late exponential growth phase, when both CO and CO_2 showed increases in their $\delta^{13}C$ values; after this point, the $\delta^{13}C$ value decreased again at the beginning of the stationary growth phase. The $\delta^{13}C$ value for biomass was -26.2‰, which was greater than the $\delta^{13}C$ value for CO_2 at both the beginning and end of the experiment (Tables 6.1 and 6.3). In bottle D, where CO and CO_2 had similar initial isotope compositions (-36.4‰ and -40.3‰, respectively), $\delta^{13}C$ values for CO changed dramatically over the course of incubation with an initial increase to +21‰ during the first 24 hrs, which was followed by a sharp decrease to -57 ‰ by the end of the experiment; The $\delta^{13}C$ value for CO_2 varied similarly but values only ranged from -18‰ at the 24 hr time point to a value of -31‰ at the end of the experiment (panel D in Fig 6.2). The $\delta^{13}C$ value for biomass was -32.3‰ (Table 6.3), similar to the $\delta^{13}C$ value for CO_2 at the end of the experiment but enriched relative to the initial $\delta^{13}C$ value for CO_2 (-40.3‰) (Table 6.1).

In the experiment two, all bottles contained ^{13}C-depleted CO (-45.0‰) and ^{13}C-enriched CO_2 (-27.4‰). The two negative control bottles, which were not inoculated with bacteria, remained unchanged for both gas compositions and isotope compositions for CO and CO_2, as well as the pH and headspace pressure, over the course of 72 hrs. Similar to the experiment 1, the four inoculated bottles were observed that the optical density, gas pressure, and H_2 contents in the headspace increased, while the pH and CO contents in the headspace decreased. $\delta^{13}C$ values for CO decreased gradually from initial -45.0‰ (all four bottles) to -54.9‰ at the early exponential phase (2 bottles, E1 and E2), and to -80.6‰ at the late exponential phase (2 bottles, L1 and L2; Table 6.2). On the other hand, average $\delta^{13}C$ value for CO_2 varied within 5‰ from -27.4‰ to -30.8‰ over the same period for the four bottles (Table 6.2). The average instantaneous enrichment factors for the CO-CO_2 system ($\varepsilon_{CO\text{-}CO_2}$) at the early and late exponential

growth phase were -29.6‰ and -49.8%, respectively. These $\varepsilon_{CO\text{-}CO_2}$values were similar to values of bottle A (at 41 and 53 hr time points) and B (at 57 and 69 hr time points) in the experiment 1 (Table 6.1). The biomass collected from the bottles weighed all 1.0 mg except biomass from the L1 bottle being 0.8 g. The $\delta^{13}C$ values for biomass from the four bottles varied little and insignificant difference were observed between the two sampling points ($n = 4$, $p < 0.01$). The average of $\delta^{13}C$ values for biomass was 25.5 ± 0.3‰ ($n = 4$) (Table 6.3)

DISCUSSIONS

Direct incorporation of CO into biomass is documented for anaerobic hydrogenogens such as *C. hydrogenoformans* (Ragsdale 2004 and references therein). However, it is unclear whether or not CO_2 can be directly incorporated into the cell by hydrogenogens because they cannot utilize CO_2 and H_2 to produce acetyl-CoA as many autotrophic methanogen and acetogens can (Gerhardt *et al.* 1991; Svetlichny *et al.* 1991; Sokolova *et al.* 2004). Enzymatic experiments on *Clostridium thermoaceticum* (Wood 1991) and NMR analysis of *Archaeoglobus fulgidus* culture (Henstra *et al.* 2007) with ^{14}C- or ^{13}C-labeled CO and CO_2 as substrates demonstrate that CO is the primary source of the carbonyl moiety whereas CO_2 is the source of the methyl moiety of the acetyl-CoA. The similar process that directly fixes CO_2 may occur for *C. hydrogenoformans*. In the experiment one, $\delta^{13}C$ values for CO_2 appear to follow the trend observed for CO in most circumstances but the magnitude of variation was lower (Table 6.1), which may be caused by the decrease in CO and increase in CO_2 abundances over time; in addition, $\delta^{13}C$ values for terminal CO_2 were lower or close to the initial $\delta^{13}C$ values of CO_2 in bottles of A, B and C (Table 6.1; Fig 6.2); the trends indicate that oxidized CO has contributed to the CO_2 pool. On the other hand, there are a few exceptions, especially in the bottle C, where decrease in the $\delta^{13}C$ value for CO is coupled with increase in $\delta^{13}C$ value for CO_2 during the first three time points (Table 6.1; Fig 6.2). It is less likely due to the experimental error because of the consistent trend and magnitude of $\delta^{13}C$ value changes for both CO and CO_2; instead, it may suggest that an independent CO_2 sink exist, which is most likely the direct incorporation of CO_2 into the cell biomass. The $\delta^{13}C$ values for the biomass of bottles C and D (Table 6.3) may also indirectly support the hypothesis because the increase of $\delta^{13}C$ values of initial CO did not

yielded higher $\delta^{13}C$ values for biomass, suggesting CO is not the only carbon source.

Because the cells preferentially takes up ^{12}CO due to the kinetic and equilibrium isotope effect, the $\delta^{13}C$ values of biomass should be lower than the $\delta^{13}C$ values of source CO and CO_2. However, $\delta^{13}C$ values for biomass were higher than $\delta^{13}C$ values for terminal CO_2 in bottles A, B and C and initial CO and CO_2 in bottles of A, B and D (Table 6.3); in addition, residual CO should become isotopically heavier over time; however, decrease in $\delta^{13}C$ values for CO in all bottles occurred, in particular at the early growth phase of bottle C (Table 6.1). These suggest that a sink of ^{12}C-enriched carbon for biomass and a source of ^{12}C-enriched carbon for CO may exist. Studies have shown that CO oxidation to formyl derivative [HCOOH] (a formate oxidation level intermediate on CODH) is a reversible reaction (Hu *et al.* 1982), and carbon atom exchange between CO and ^{14}C-labeled acetyl-CoA molecules occurs without expense of the acetyl-CoA (Ragsdale and Wood 1985; Wood 1991). Therefore, the exchange reaction between CO and intermediate may be the sink of ^{12}C-enriched carbon for biomass and a source of ^{12}C-enriched carbon for CO according to the Rayleigh distillation effect. Since the CO content in the headspace was greatly reduced to the end of the experiments, a small input of ^{12}C-enriched carbon may drive the $\delta^{13}C$ values for CO significantly lower as occurring in all these bottles. Therefore the apparent carbon isotope fractionation for the system of CO-biomass ($\varepsilon_{CO\text{-}Bio}$) may be the sum of isotope fractionations of two processes: CO fixation (ε_{COF}) and carbon exchange (ε_{EXCH}). On the other hand, methyl group of acetyl-CoA uses carbon derived from the methylated corrinoid enzyme through CO_2 reduction and transfers the formed methyl group to the CODH site. This carbon is not exchange reversibly with CO_2 (Ragsdale 1991). Therefore the apparent carbon isotope fractionation for the system of CO_2-biomass ($\varepsilon_{CO_2\text{-}Bio}$) may be solely the isotope fractionation of CO_2 fixation (ε_{CO_2F}). Besides, since there is no sign that $\delta^{13}C$ values of CO and CO_2 move to an equilibrium in these bottles, the isotope exchange of the two molecules can be neglected; therefore the CO oxidation should account for the apparent isotope fractionation for the CO-CO_2 system ($\varepsilon_{CO\text{-}CO_2F} = \varepsilon_{OX}$).

A potential complication of the isotope fractionations for the CO-CO_2-Biomass system is the yeast

extract contained in the medium (0.02%) because *C. hydrogenoformans* appears to require the yeast extract as a growth factor and probably takes up some carbon from this small amount of carbon source. The yeast extract had a average $\delta^{13}C$ value of *ca*. -24‰, based on above discussion, it will not be the source of ^{13}C enriched carbon for biomass, unless a carbon component with a higher than -25‰ $\delta^{13}C$ value enters the biomass assuming a -1‰ isotope fractionation between the carbon and biomass, but then the same carbon cannot be the contribute directly to the CO pool for ^{12}C-enriched carbon. Further, the yeast extract contribution may not be a dominant source, because otherwise the terminal $\delta^{13}C$ values for biomass should not change -6‰ in bottle D compared with other bottles and more importantly, the total amount of yeast extract added in each 200 ml culture was calculated about 12 mg, far less than total consumed CO and CO_2 (assuming a consumption rate of 25% for about 444 mg total initial carbon from CO and bicarbonate in each bottle).

In the experiment two where biomass were collected at both the early and late exponential growth phases, insignificant difference of $\delta^{13}C$ values for biomass (Table 6.3) between the two sampling points also suggests the existence of sinks of ^{12}C-enriched carbon for the biomass to balance the gain of ^{12}C-enriched carbon through CO and CO_2 fixation processes. Furthermore, because $\delta^{13}C$ values for biomass did not change significantly over time, it is unlikely that an additional ^{12}C-enriched carbon in the medium (such as from yeast extract) greatly contributes to the overall carbon pool and affects the isotope composition of CO.

An intriguing phenomenon is that in the experiment one, despite the differences in initial gas isotope composition in the four bottles, $\delta^{13}C$ values for CO was always lower than CO_2 after the mid-exponential growth phase, and instantaneous ε value for the CO and CO_2 system ($\varepsilon_{CO\text{-}CO_2}$) were always negative (-16 to -26‰) at the end of the experiment (Table 6.1). There appears to exist a point where $\delta^{13}C$ values for CO (-45‰), CO_2 (-27‰), and biomass (-25‰; arrow points in Figs 6.2 and 6.3) are independent of initial isotope composition of CO and CO_2. While the $\delta^{13}C$ values for biomass do not change over time (based on the data from the experiment two), isotope compositions for both CO and CO_2 deviating far from these

values tend to change towards this point; once this point is achieved, carbon isotope compositions of CO, CO_2 and biomass tend to remain constant unless one of the carbon pools is significantly consumed, such as $\delta^{13}C$ values for CO at the late exponential growth phases in all bottles of the experiment one. Therefore, this point can be hypothesized as a steady state point of $\delta^{13}C$ values for CO, CO_2, and biomass. Based on above discussions, the steady state is probably achieved through a feedback system as shown in Fig 6.4. A steady state allows computing the isotope fractionation factor between any of the three pools. Based on our data, it is hypothesized that carbon isotope fractionations are 18‰ between CO_2 and CO ($\varepsilon_{CO_2\text{-}CO} = \varepsilon_{OX}$), 2‰ between biomass and CO_2 ($\varepsilon_{Bio\text{-}CO_2} = \varepsilon_{CO_2F}$), and -20‰ between CO and biomass ($\varepsilon_{CO\text{-}Bio} = \varepsilon_{EXCH}\text{-}\varepsilon_{COF}$). The $\varepsilon_{CO_2\text{-}CO}$ is greater than $\varepsilon_{Bio\text{-}CO_2}$ and suggests the slower reaction rate, which explains $\delta^{13}C$ values for CO_2 follow the trend for CO in most circumstances but the magnitude of variation was lower. The CO_2 fixation on the other hand, may be a fast reaction, which is agreed by the close $\delta^{13}C$ values between terminal CO_2 and biomass in most cases.

SUMMARY

Time series isotope data from a series of batch cultures suggest that both CO_2 in addition to CO provide the carbon source for growth of *C. hydrogenoformans*. Our data indicate that a feedback system based on the reductive acetyl-CoA pathway (also called Wood-Ljungdahl pathway) may exist. Processes in the system include both CO and CO_2 fixation to biomass, CO-oxidation and exchange of CO between CO_2. CO oxidation appears to be a slow process, while CO_2 fixation seems fast. The data also suggests the existence of a point where $\delta^{13}C$ values of CO, CO_2 and biomass (*ca.* -45, -27, and -25‰, respectively) tend to remain constant. The point is hypothesized a steady state of carbon isotope compositions for CO, CO_2 and biomass through the feedback system. It is further hypothesized that carbon isotope fractionations at the steady state reflect the isotope fractionations for the CO, CO_2 and biomass system, which are 18‰ between CO_2 and CO ($\varepsilon_{CO_2\text{-}CO} = \varepsilon_{OX}$), 2‰ between biomass and CO_2 ($\varepsilon_{Bio\text{-}CO_2} = \varepsilon_{CO_2F}$), and -20‰ between CO and biomass ($\varepsilon_{CO\text{-}Bio} = \varepsilon_{EXCH}\text{-}\varepsilon_{COF}$).

Table 6.1. The head space gas compositions and $\delta^{13}C$ values for CO and CO_2 over the course of incubation for the experiment one. Also shown are optical density at 600 nm, pH of the culture, and pressure of the head space at 40ºC at each sampling point.

Bottle[a]	Time	OD_{600}	pH	P	H_2	CO	SD_{CO}	$\delta^{13}C_{CO}$‰[d]		CO_2	SD_{CO2}	TCO_2[e]	$\delta^{13}C_{CO_2}$‰		εCO-CO_2[d]
	hr			atm	mmole[b]	mmole	mmole	Avg[c].	SD[c]	mmole	mmole	mmole	Avg.	SD	
	0.0	0.000	6.9	0.99	0.00	46.63		-43.8							
	12.0	0.011	6.9	1.01	0.54	41.27		-44.4							
	16.0	0.015	6.9	1.00	0.70	37.65		-44.7		0.49		3.31	-26.9		-17.8
A	18.0	0.024	6.9	1.00		30.08	19.14	-45.2	0.4	0.94		6.28	-27.8		-17.4
	29.0	0.029	6.7	1.05	0.70	25.00	0.29	-29.1	0.2	0.80	0.04	3.57	-24.7	0.4	-4.5
	41.0	0.041	6.5	1.14	0.63	17.23	0.05	-49.4	0.2	3.42	0.02	10.28	-27.0	0.1	-22.4
	53.3	0.051	6.5	1.32	7.13	4.50	1.00	-75.2	3.8	4.94	1.39	14.83	-35.0	4.7	-40.2
	64.3	0.052	6.5	1.46		0.09		-62.6	1.9	12.85	0.04	38.59	-42.9	0.1	-19.8
	0.0	0.000	6.8	0.99	0.57	61.51		-44.0							
	27.5	0.015	6.8	1.01	0.78	48.19				0.50		2.71	-27.7		
	31.5	0.019	6.8	1.00	0.98	47.00		-43.7		0.58	0.02	3.18	-26.8	0.4	-16.9
B	33.5	0.032	6.6	1.03		44.78	0.42	-45.0	0.5	0.90	0.01	3.28	-27.8	1.3	-17.1
	44.5	0.038	6.4	1.05	1.08	32.90	0.33	-47.7	0.2	2.63	0.03	6.57	-27.5	0.3	-20.3
	56.5	0.045	6.4	1.20	0.55	11.43	0.15	-51.2	0.2	4.46	0.07	11.16	-26.7	0.1	-24.5
	68.8	0.045	6.3	1.43	8.93	0.98		-96.9	0.2	7.55	0.08	15.88	-40.1	0.0	-56.8
	79.8	0.030	6.2	1.44		0.14	0.01	-61.9	0.8	7.89	0.40	16.58	-42.7	0.1	-19.2
	0.0	0.000	6.9	0.99	0.01	57.00		-22.4	0.0				-36.9	3.5	14.5
	24.0	0.020	6.9	1.03	0.80	41.98	5.03	-38.6	0.2	1.16	0.16	7.82	-24.7	1.0	-13.8
	36.0	0.020	6.6	1.08	1.25	30.62	0.30	-40.9	0.2	3.46	0.02	12.60	-21.1	0.1	-19.8
C	48.7	0.023	6.2	1.24	5.52	17.32	0.04	-46.4	0.4	6.42	0.05	11.46	-22.1	0.4	-24.3
	51.0	0.027	6.2	1.25	5.05	15.00	0.18	-24.6	0.6	8.00	0.12	14.28	-18.3	0.0	-6.3
	60.0	0.031	6.1	1.37	8.09	6.18	0.11	-68.6	0.2	9.84	0.12	15.09	-24.7	0.2	-43.9
	71.7			1.43		0.17		-62.1	0.6	12.18	0.01	18.68	-35.6	0.3	-26.5
	0.0	0.000	6.8	0.99	0.00	57.03		-36.4					-40.3		3.9
	24.0	0.033	6.8	1.02	0.84	35.00		21.3	0.4	0.22		1.18	-18.3	0.2	39.6
D	36.7	0.043	6.2	1.29	6.82	11.21	1.74	-41.5	0.1	6.87	0.85	14.44	-31.2	0.2	-10.2
	39.0	0.061	6.2	1.36	32.08	7.74	0.02	-53.5	0.2	9.14	0.03	16.32	-27.9	0.1	-25.6
	48.0	0.060	6.0	1.39		3.46	0.06	-56.6	0.1	10.48	0.14	18.71	-31.6	0.1	-25.0

a. See Material and Method for bottle ID information.

b. Gas contents for H_2, CO and CO_2 in mmole are calculated based on the partial volume of each gas, pH and temperature in each bottle, which has a headspace volume of about 800 ml.

c. Avg = average; SD = standard deviation; all Avg and SD values reported in this and following tables are based on multiple gas measurements from the same gas sample and not replicate samples. The SD values reflect the precision and consistency of the manual injections.

d. $\delta^{13}C$ and ε values in ‰ vs. PDB. $\varepsilon_{CO\text{-}CO_2}$ is instantaneous enrichment factor between CO and CO_2 in the head space.

e. Total CO_2 (TCO_2) was calculated using the program CO_2sys-macro (Lewis and Wallace 1998) using T, pH and CO_2 partial volume data.

Table 6.2. The head space gas compositions and $\delta^{13}C$ values for CO and CO_2 at the beginning and terminal time points of the incubation for the experiment two. Also shown are optical density at 600 nm, pH of the culture, and pressure of the head space at 40ºC at each sampling point.

Bottle[a]	Time	OD_{600}	pH	P	H_2	CO	SD_{CO}	$\delta^{13}C_{CO}$ ‰[d]		CO_2	SD_{CO2}	TCO_2[e]	$\delta^{13}C_{CO_2}$ ‰		εCO-CO_2[d]
	hr			atm	mmole[b]	mmole	mmole	Avg.[c]	SD[c]	mmole	mmole	mmole	Avg.	SD	
E1	0	0.000	6.8	0.99	0.00	28.24	4.31	-45.0	0.3	0.24	0.01	1.18	-26.3	0.6	-18.7
	16.5	0.020	6.8	1.32	0.35	13.18	4.14	-54.9	0.4	4.25	1.06	29.04	-26.3	0.7	-28.6
E2	0	0.000	6.8	0.99	0.00	25.93	6.08	-44.9	0.4	0.19		1.28	-27.5	0.8	-17.3
	16.5	0.017	6.8	1.21	3.40	4.59	1.80	-54.9	3.8	2.99	0.45	20.87	-24.2	0.8	-30.7
L1	0	0.000	6.8	0.99	0.00	27.70		-45.0	0.2	0.22		1.01	-24.6	1.0	-20.4
	33.0	0.050	6.7	1.23	0.20	6.35	0.15	-78.8	0.1	9.67	0.16	14.68	-30.4	0.1	-48.5
L2	0	0.000	6.8	0.99	0.00	19.31	3.24	-45.1	0.2	0.16		0.89	-26.8		-18.3
	33.0	0.050	6.7	1.41	1.88	3.64	0.18	-82.4	0.3	5.83	0.26	21.19	-31.1	0.06	-51.3

a. Bottle ID, E1 and E2 represent two replicate bottles that were terminated for incubation at the early exponential growth phase; L1 and L2 were two replicate bottles that were terminated for incubation at the late exponential growth phase .

b-e. Table 6.1, see Table 6.1 table notes.

.

Table 6.3. $\delta^{13}C$ values of bulk biomass, CO, and CO_2 for the experiments one and two, and instantaneous enrichment between CO and CO_2 ($\varepsilon_{CO\text{-}CO_2}$) at the end of the experiments.

		T_0		T_{End}						
	Bottle	$\delta^{13}C_{CO}$	$\delta^{13}C_{CO_2}$	hr	$\delta^{13}C_{Bio}$	Avg. $\delta^{13}C_{CO}$	SD $\delta^{13}C_{CO}$	Avg. $\delta^{13}C_{CO_2}$	SD $\delta^{13}C_{CO_2}$	$\varepsilon_{CO\text{-}CO_2}$
	A	-45.0	-27.4	64.3	-26.2	-62.6	1.9	-42.9	0.1	-19.8
Exp. 1	B	-45.0	-27.4	79.8	-27.1	-61.9	0.8	-42.7	0.1	-19.2
	C	-22.4	-36.9	71.7	-26.2	-62.1	0.6	-35.6	0.3	-26.5
	D	-36.4	-40.3	48.0	-32.3	-56.6	0.1	-31.6	0.1	-25.0
	E1	-45.0	-27.4	16.5	-25.2	-54.9	0.4	-26.3	0.7	-28.6
Exp. 2	E2	-45.0	-27.4	16.5	-25.5	-54.9	3.8	-24.2	0.8	-30.7
	L1	-45.0	-27.4	33.0	-25.8	-78.8	0.1	-30.4	0.1	-48.5
	L2	-45.0	-27.4	33.0	-25.4	-82.4	0.3	-31.1	0.1	-51.3

The $\delta^{13}C$ values for CO and CO_2 at the beginning of the experiments are reported

T_0 and T_{End} represent the initial and terminal time points.

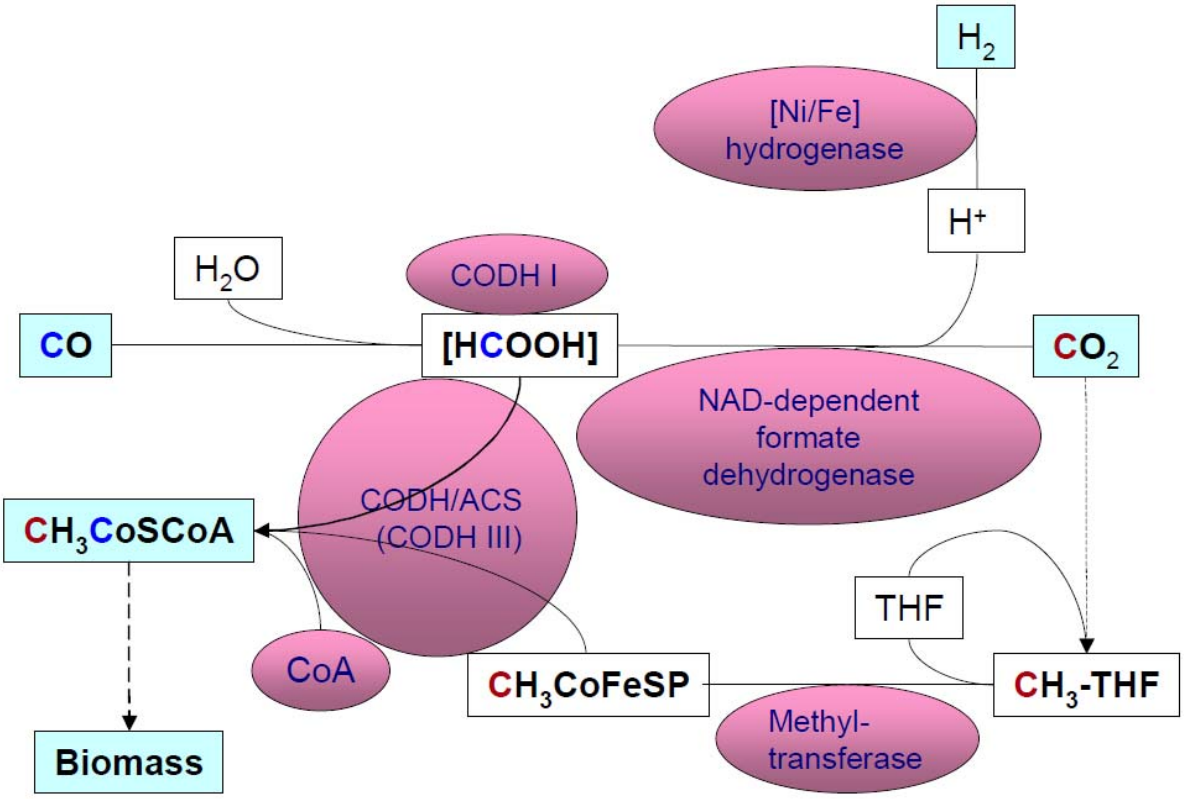

Fig 6.1. Proposed acetyl-CoA pathway for the CO-oxidizing hydrogenogenic bacterium *Carboxydothermus hydrogenoformans* based on the genome sequence of *C. hydrogenoformans* Z2901 (Wu *et al.* 2005) and KEGG pathway database. The dashed and dotted lines represent multiple biochemical steps. Key enzymes are shown in circles and ovals. THF = tetrahydrofolate; CoFeSP = Corrinoid iron-sulfur protein; CoA = corrinoid protein (Modified from Wood 1991; Ragsdale 2004).

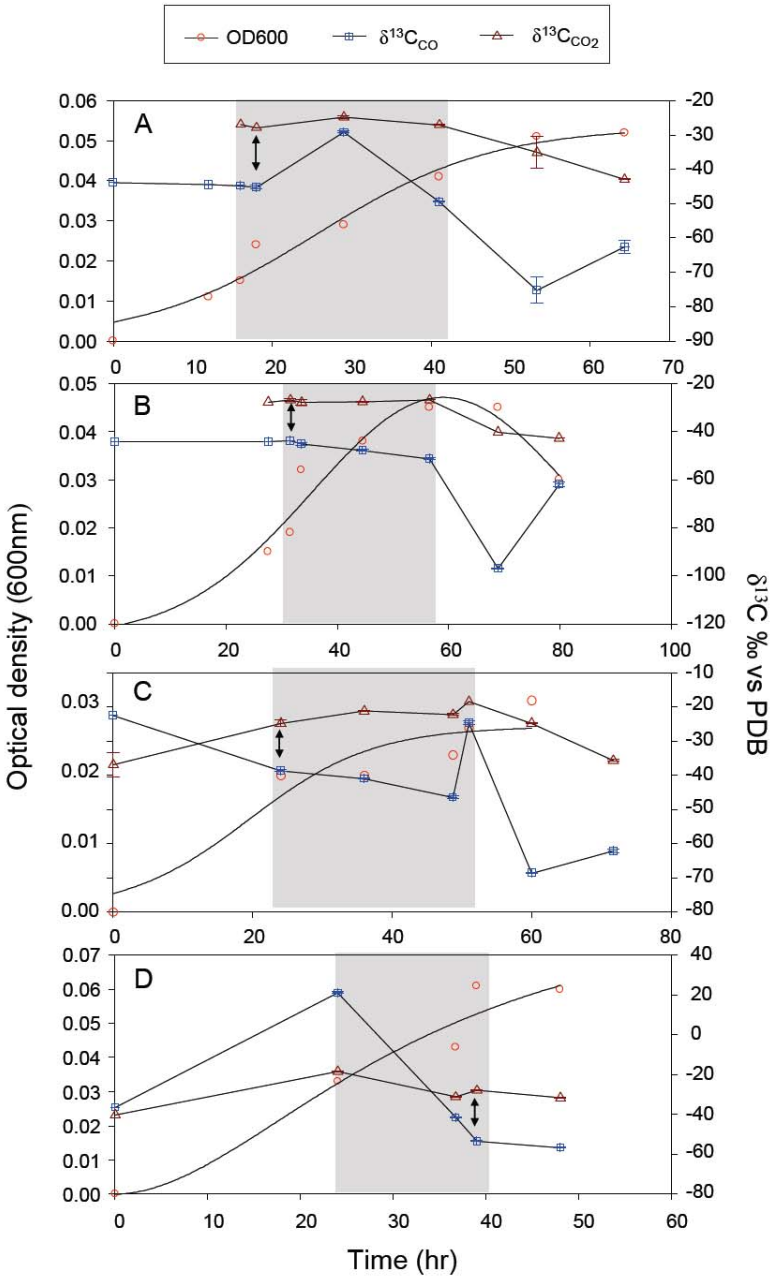

Fig 6.2. Optical density of *C. hydrogenoformans* cultures and changes in carbon isotope compositions of head space CO and CO_2 in Experiment 1. See text for bottle descriptions. Arrows indicates the hypothetical steady state point for carbon isotope compositions between CO, CO_2 and biomass. The gray regions represent the most reliable measurements where both $\delta^{13}C$ values of CO and CO_2 were obtained from the detection linearity range of the IRMS.

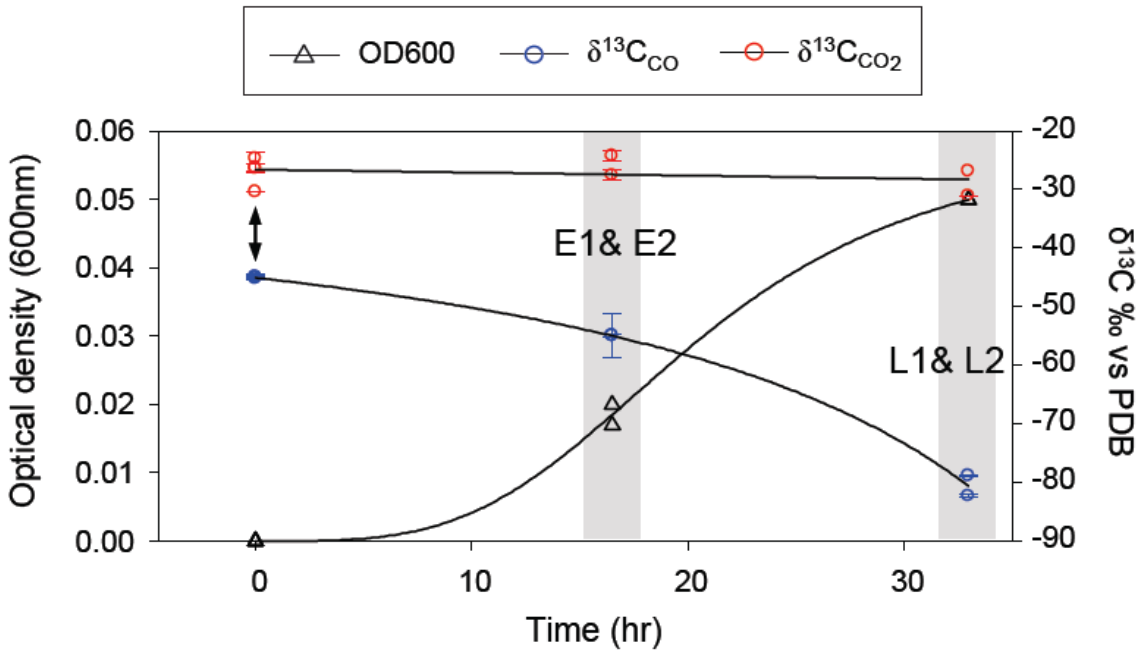

Fig 6.3. Optical density of *C. hydrogenoformans* cultures and changes in the carbon isotope compositions of head space CO and CO_2 for experiment 2. All data for the four bottles, E1, E2, L1 and L2 are plotted as replicates at each sampling point in the graph. Arrows indicate the hypothetical steady state point for carbon isotope compositions of CO, CO_2 and biomass, see text for detail.

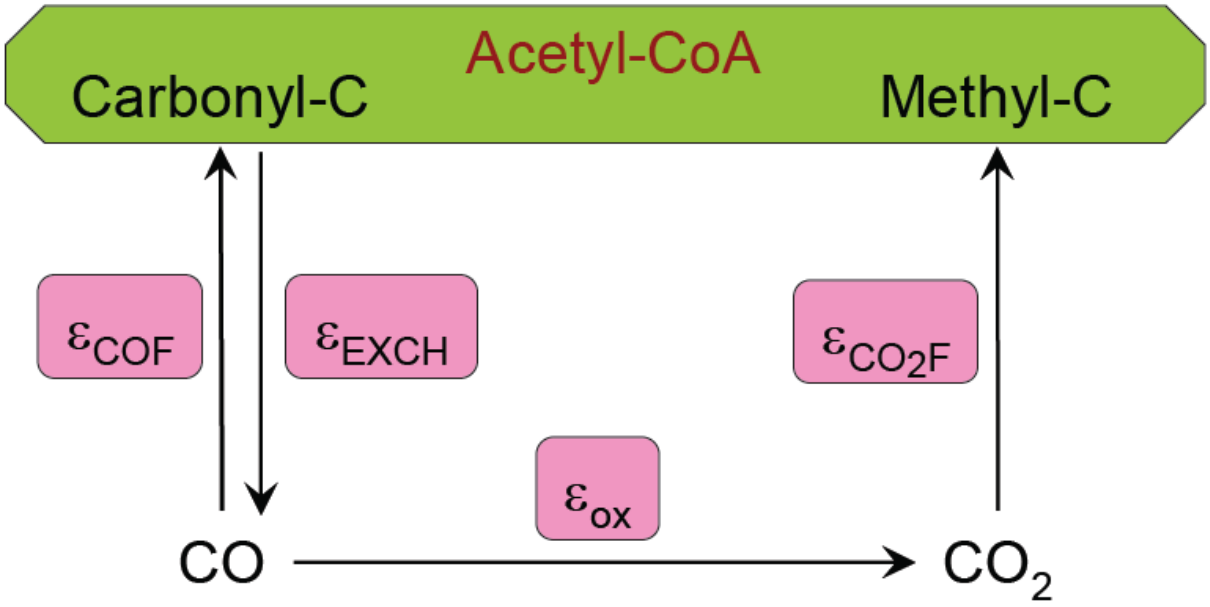

Fig 6.4. A hypothetical feedback system for the CO and CO_2 fixation by *C. hydrogenoformans*. Isotope enrichment factor (ε) associated with each process is labeled in the pink square. Processes: COF, CO fixation; EXCH, exchange; OX, oxidation; CO_2F, CO_2 fixation.

REFERENCES

Bartholomew G, Alexander M (1982) Microorganisms responsible for the oxidation of carbon monoxide in soil. . Environ. Sci. Technol. 16:300-301.

Conrad R (1996) Soil microorganisms as controllers of atmospheric trace gases (H_2, CO, CH_4, OCS, N_2O, and NO). Microbiol. Rev. 60:609-640

Crutzen P, Gidel L (1983) A two-dimensional photochemical model of the atmosphere. 2: The tropospheric budgets of the anthropogenic chlorocarbons, CO, CH_4, CH_3Cl and the effect of various nox sources on tropospheric ozone J. Geophys. Res. 88:6641-6661

Evans DJ (2005) Chemistry relating to the nickel enzymes CODH and ACS. Coordination Chemistry Reviews 249:1582-1595

Ferry JG (1995) CO dehydrogenase. Annual Review of Microbiology 49:305-333

Gerhardt M, Svetlichny V, Sokolova TG, Zavarzin GA, Ringpfeil M (1991) Bacterial CO utilization with H_2 production by the strictly anaerobic lithoautotrophic thermophilic bacterium *carboxydothermus hydrogenus* DSM 6008 isolated from a hot swamp. FEMS Microbiology Letters 83:267-272

Henstra AM, Dijkema C, Stams AJM (2007) *Archaeoglobus fulgidus* couples CO oxidation to sulfate reduction and acetogenesis with transient formate accumulation. Environmental Microbiology 9:1836-1841

Hu SI, Drake HL, Wood HG (1982) Synthesis of acetyl coenzyme a from carbon monoxide, methyltetrahydrofolate, and coenzyme a by enzymes from *clostridium thermoaceticum*. Journal of Bacteriology 149:440-448

King GA (2003) Molecular and culture-based analyses of aerobic carbon monoxide oxidizer diversity. Appl. Environ. Microbiol. 69:7257-7265

Lewis E, Wallace DWR (1998) Program developed for CO_2 system calculations In: ORNL/CDIAC-105. Carbon Dioxide Information Analysis Center, Oak Ridge National Laboratory, U.S. Department of Energy, Oak Ridge, Tennessee

Meyer O (1982) Chemical and spectral properties of carbon-monoxide - methylene-blue oxidoreductase - the molybdenum-containing iron-sulfur flavoprotein from pseudomonas-carboxydovorans. Journal of Biological Chemistry 257:1333-1341

Meyer O, Frunzke K, Gadkari D, Jacobitz S, Hugendieck I, Kraut M (1990) Utilization of carbon-monoxide by aerobes - recent advances. FEMS Microbiology Reviews 87:253-260

Meyer O, Schlegel HG (1983) Biology of aerobic carbon-monoxide oxidizing bacteria. Annual Review of Microbiology 37:277-310

Ragsdale SW (1991) Enzymology of the acetyl-CoA pathway of CO_2 fixation. Critical Reviews in Biochemistry and Molecular Biology 26:261-300

Ragsdale SW (2004) Life with carbon monoxide. Critical Reviews in Biochemistry and Molecular Biology 39:165-195

Ragsdale SW, Wood HG (1985) Acetate biosynthesis by acetogenic bacteria - evidence that carbon-monoxide dehydrogenase is the condensing enzyme that catalyzes the final steps of the synthesis. Journal of Biological Chemistry 260:3970-3977

Richet P, Bottinga Y, Javoy M (1977) Review of hydrogen, carbon, nitrogen, oxygen, sulfur, and chlorine stable isotope fractionation among gaseous molecules. Annu. Rev. Earth Planet. Sci. 5:65-110

Russell MJ, Martin W (2004) The rocky roots of the acetyl-CoA pathway. Trends in Biochemical Sciences 29:358-363

Seth-Smith H (2007) A more convenient truth. Nature Reviews Microbiology 5:248-250

Sokolova TG *et al.* (2004) The first evidence of anaerobic CO oxidation coupled with H_2 production by a hyperthermophilic archaeon isolated from a deep-sea hydrothermal vent. Extremophiles 8:317-323

Sokolova TG, Kostrikina NA, Chernyh NA, Tourova TP, Kolganova TV, Bonch-Osmolovskaya EA (2002) *Carboxydocella thermautotrophica* gen. nov., sp nov., a novel anaerobic, CO-utilizing thermophile from a Kamchatkan hot spring. International Journal of Systematic and Evolutionary Microbiology 52:1961-1967

Svetlichny VA, Sokolova TG, Gerhardt M, Ringpfeil M, Kostrikina NA, Zavarzin GA (1991) *Carboxydothermus hydrogenoformans* gen. nov, sp. nov, a CO-utilizing thermophilic anaerobic bacterium from hydrothermal environments of Kunashir Island Systematic and Applied Microbiology 14:254-260

Svetlitchnyi V, Peschel C, Acker G, Meyer O (2001) Two membrane-associated NiFeS-carbon monoxide dehydrogenases from the anaerobic carbon-monoxide-utilizing eubacterium *carboxydothermus hydrogenoformans*. Journal of Bacteriology 183:5134-5144

Wahlen M (1994) Carbon dioxide, carbon monoxide and methane in the atmosphere: Abundance and isotopic composition. In: RH LKaM (ed) Stable isotopes in ecology and environmental science. Blackwell Scientific Publication Cambridge MA

Widdel F, Bak F (1992) Gram-negative mesophilic sulfate-reducing bacteria. In: Balows A, Trüper HG, Dworkin M, Harder W, Schleifer H (eds) The prokaryotes, 2nd edn. Springer, New York, pp 3352-3378

Wood HG (1991) Life with CO or CO_2 and H_2 as a source of carbon and energy. Faseb Journal 5:156-163

Wu M *et al.* (2005) Life in hot carbon monoxide: The complete genome sequence of *carboxydothermus hydrogenoformans* Z-2901. Plos Genetics 1:563-574

Zavarzin GA, Nozhevnikova AN (1977) Aerobic carboxydo-bacteria. Microbial Ecology 3:305-326

CHAPTER 7

AMMONIA-OXIDIZING ARCHAEA IN KAMCHATKA HOT SPRINGS[‡‡]

[‡‡] Weidong Zhao, Christopher S. Romanek, Xiaozhen Mou, Juergen Wiegel and Chuanlun L. Zhang, to be submitted to the Environmental Microbiology

SUMMARY

Culture-independent molecular studies have suggested that ammonia-oxidizing archaea (AOA) are ubiquitous and perhaps even more abundant than their bacterial counterparts (AOB) in soil or marine environments. Recent findings in high temperature settings have shed light on the importance of AOA in geothermal environments. However, the diversity, distribution and ecological significance of thermophilic AOA in terrestrial hot springs remain largely unexplored. In this study, AOA and AOB were screened by PCR amplification for a number of microbial mats and sediments in three hot springs (42°C to 87°C and pH 5.5-7.0) in the Uzon Caldera, Kamchatka (Far East Russia). No AOB were detected and thus our efforts focused on AOA using multiple approaches including archaeal *amo*A gene clone libraries, archaeal core membrane lipids analysis, and quantitative PCR of the 16S rRNA gene. The *amo*A genes of AOA formed three distinct phylogenetic clusters with cluster 3 representing the majority (59%) of OTUs. This cluster groups with sequences from an acidic soil, suggesting that the majority of hot spring sequences are indigenous to the acidic geothermal environment in Kamchatka. Species richness (estimated by Chao1) was more frequently higher at temperatures below 75°C than above it, indicating that AOA may be favored in the moderately high temperature environments. The archaeal lipids (glycerol dialkyl glycerol tetraethers) were well separated among the three springs, suggesting a spatial patterning of archaea controlled by unknown mechanisms. Quantitative PCR of 16S rRNA genes showed that crenarchaeota counted for up to 80% of total archaea. Finally, S-LIBSHUFF separated all samples into two phylogenetic groups, which may be controlled by the total community structure intertwined by water chemistry.

INTRODUCTION

Ammonia oxidizing bacteria (AOB) and archaea (AOA) oxidize ammonia to nitrite through hydroxylamine (Kowalchuk and Stephen, 2001), which is the first step of nitrification and a key component of the global nitrogen cycle. These organisms are ubiquitously distributed in natural environments (Kowalchuk and Stephen, 2001; Nicol and Schleper, 2006). AOB are exclusive members of β- and γ- subgroups of *Proteobacteria*, and were previously considered as the most important contributors

to the ammonia oxidation process (Purkhold *et al.*, 2000; Prosser and Embley, 2002). Increasing evidence from genomic and molecular studies, however, indicates that non-thermophilic archaea in the crenarchaeota lineage may play a more important role in aerobic oxidation of ammonia (*e.g.*, Nicol and Schleper, 2006; Francis *et al.*, 2007). Genes encoding putative homologues of ammonia monoxygenase subunits A (*amo*A) and B (*amo*B) have been identified in association with the 16S rRNA gene of crenarchaeota through metagenomic studies of marine and soil samples (Venter *et al.*, 2004; Schleper *et al.*, 2005), and subsequently confirmed by whole genome studies of "*Candidatus* Nitrosopumilus maritimus" (Konneke *et al.*, 2005) and a sponge symbiont *Cenarchaeum symbiosum* (Hallam *et al.*, 2006). PCR-based surveys using primers specific to putative archaeal *amo*A-like genes have indicated widespread occurrence of ammonia-oxidizing archaea (AOA) in soils (Leininger *et al.* 2006), marine (Francis *et al.*, 2005; Leininger *et al.*, 2006; Wuchter *et al.*, 2006) and more recently, high temperature environments (Spear *et al.*, 2007; Weidler *et al.*, 2007; Reigstad, *et al.*, 2008; Zhang *et al.*, in review). The latter finding is in accordance with the successful enrichment of thermophilic AOA, "*Candidatus* Nitrosocaldus yellowstonii" (T_{opt} = 65-72°C) from a hot spring in Yellowstone National Park (de la Torre *et al.*, 2008) and moderately thermophilic "*Candidatus* Nitrososphaera gargensis", (T_{opt} = 46°C) from the Sibrian Garga hot spring (Hatzenpichler *et al.*, 2008).

Advances in molecular studies of crenarchaeota are paralleled by discoveries of novel lipids of these organisms using high performance liquid chromatography-mass spectrometry (Hopmans *et al.*, 2000; Schouten *et al.*, 2000). Glycerol dialkyl glycerol tetraethers (GDGTs) are core membrane lipids of archaea, which mainly contain zero to four cyclopentyl rings (Koga *et al.*, 1993; Koga and Morii, 2005) but can also contain up to eight rings in some hyperthermophilic archaea (Derosa and Gambacorta, 1988). One unique crenarchaeota-specific GDGT is crenarchaeol, containing one cyclohexyl-ring and four cyclopentyl rings. It was originally observed to be specifically associated with marine nonthermophilic crenarchaeota (DeLong *et al.*, 1998; Schouten *et al.*, 2000; Schouten *et al.*, 2002) but has been later found in lakes, soils, hot spring environments and a thermophilic AOA culture (Pearson *et al.*, 2004; Weijers *et al.*, 2006; Zhang *et al.*, 2006; Schouten *et al.*, 2007; de la Torre *et al.*, 2008). The function of ring

structures of GDGT is to adjust the flexibility of the cell membrane in response to changes in growth conditions such as temperature and pH (Schouten *et al.*, 2002; Turich *et al.*, 2007; Pearson *et al.*, 2008). Positive correlation between the number of rings in GDGT and temperature has been demonstrated (Derosa *et al.*, 1980; Gliozzi *et al.*, 1983; Uda *et al.*, 2001; Schouten *et al.*, 2002; Powers *et al.*, 2004; Wuchter *et al.*, 2004), but not always found in environmental samples. Instead, pH was increasingly observed to control GDGT compositions (Macalady *et al.*, 2004; Zhang *et al.*, 2006; Schouten *et al.*, 2007; Pearson *et al.*, 2008). Therefore, GDGT can be used as a quantification tool (Leininger *et al.*, 2006) as well as a proxy to reveal the chemical environments where archaea may be found (Zhang *et al.*, 2006; Schouten *et al.*, 2007; Pearson *et al.*, 2008).

So far, most AOA studies have focused on marine (*e.g.*, Venter *et al.*, 2004; Francis *et al.*, 2005; Konneke *et al.*, 2005; Lam *et al.*, 2007), and soil (*e.g.*, Schleper *et al.*, 2005; Leininger *et al.*, 2006) systems and only a few on geothermal springs. It remains unclear to what extent thermophilic ammonia-oxidizing microorganisms are involved in nitrification in geothermal systems. Many of the hot springs in the Uzon Caldera of Kamchatka (Far East Russia) have neutral to slightly acidic pH with high concentrations of ammonium. They provide an ideal setting to investigate the occurrence, distribution and diversity of AOA in high temperature and lower pH environments. Here, we report AOA from three hot springs in the Uzon Caldera, Kamchatka using molecular and chemical approaches. Occurrence, diversity and distribution of AOA were examined using the putative archaeal *amo*A gene. Abundance of AOA was estimated using qPCR of archaeal and crenarchaeotal 16S rRNA genes. Relationship between biological features of AOA and environmental variables including pH and temperature was evaluated and discussed.

RESULTS

Physicochemical characteristics of the hot springs

The geochemical conditions varied considerably among the three hot springs. The Thermophile spring had temperatures from 70°C at the source to 42°C in the distal outflow channel while the pH on the other hand increased from 6.0 to 7.0. This spring had low total dissolved solids (TDS), high alkalinity (2.6-3.3 mmol L^{-1} $CaCO_3$), and low sulfate (0.1-0.3 mmol L^{-1}), nitrite (0.3-0.6 µmol L^{-1} N) and ammonium (0.2-0.3 mmol L^{-1} N). Sulfide concentration was extremely high (43.1 µmol L^{-1}) at the source but dropped sharply to below 1.3 µmol L^{-1} in the outflow channel. The Cascadnaya spring had decreasing pH from 6.5 at the source (85°C) to 5.5 in the distal outflow channel (50°C). TDS (>904 mg L^{-1}), sulfate (0.7-1.9 mmol L^{-1}), sulfide (1.6-12.5 µmol L^{-1}), nitrite (0.4-1.4 µmol L^{-1} N) and ammonium (1.5-2.7 mmol L^{-1} N) were higher than those at the Thermophile except for sulfide at the source. Alkalinities were lower than those at Thermophile (Table 7.1). The Burlyashi spring had temperature and pH profiles similar to those at Cascadnaya, and had moderate values of water-chemistry in terms of TDS, alkalinity and ammonium concentrations comparing with the other two pools. Sulfide concentration was high at the source of Burlyashi (43.8 µmol L^{-1}), dropped to 6.3 µmol L^{-1} at BLS-C, and was below detection limit at BLS-B and BLS-D (Table 7.1). The oxidation-reduction potentials (ORP) varied between -365 mV and -62 mV with an average value of -240 mV for all site. The ORP tended to increase from the source to the distal outflow channel in Cascadnaya and Burlyashi, perhaps caused by increasing diffusion of atmospheric oxygen into the spring water as temperature decreased. However, this was not the case for Thermophile, where ORP was overall stable and slightly elevated at the source and the distal outflow channel (Table 7.1).

Gas compositions differed considerably among the three pools. Among measured gases, CO_2 was predominant in all sources (36-71%); CH_4 was the next highest component but less than 2.5%. H_2 was 0.1 to 0.2% and CO ranged from 140 ppm to below detection limit (Table 7.1).

These results showed that variations in gas and water chemistry were generally greater between springs than within the same spring.

Diversity and distribution of the archaeal *amo*A gene

Archaeal *amo*A gene was PCR amplified from 8 out of the 13 samples. At Burlyashi, the only sample that contained archaeal *amo*A gene was BLS-D at 51°C and pH 6 (Table 7.2). On the other hand, none of the samples yielded positive results for PCR amplification of the bacterial *amo*A gene while the positive control DNA from *Nitrosomonas Europaea* was always amplified successfully.

A total of 323 sequences of archaeal *amo*A gene fragments were obtained (Table 7.2). The deduced amino acid sequences yielded 34 operational taxonomic units (OTUs) using a 5% cutoff, which were grouped into three distinct phylogenetic clusters (Figs 7.1 and 7.2). Cluster 1 contained 160 sequences in 9 OTUs and counted for 49.5% of the total sequences. It also contained characteristic crenarchaeotal group 1.1a sequences, including "*Candidatus* Nitrosopumilus maritimus"*, Cenarchaeum symbiosum* and Sargasso Sea whole-genome shotgun sequences. One of the OTUs, CAC-A03 representing 37% of the cluster sequence, was closely related to the sequence from Nevada hot springs (94% homologous; Zhang *et al.*, in review; Fig 7.1). Cluster 2 contained 21 sequences in 5 OTUs and counted for 6.5% of total sequences. The hot spring sequences were mixed with some non-thermophilic soil and sediment sequences at similarity of 95-98% and were distantly related to a fosmid clone 54d9 (88-92% homologous) representing crenarchaeotal group 1.1b from soil. Cluster 2 also included the sequence from thermophilic "*Candidatus* Nitrosocaldus yellowstonii", which had less than 80% homologous with Kamchatka sequences (Fig 7.1). Cluster 3 contained 142 sequences in 20 OTUs and counted for 44% of total sequences. This cluster had two major clades that were overall 91% similar. One contained a single OTU CAC-AF-A07 that represented sequences closely related to a fertilized soil sequence (He *et al.*, 2007). The other clade included 124 sequences in 19 OTUs, some of which were closely related to fertilized soil sequence (He *et al.*, 2007) and others were closely related to an estuary sediment sequence (Francis *et al.*, 2005).

Good's sampling coverage estimator (Kemp and Aller, 2004), nonparametric Chao1 estimator of species (OTUs) richness and Shannon's diversity index H' were estimated using the numbers of sequences and OTUs in each clone library (Table 7.2). Good's sampling coverage estimator showed 90 to

97% coverage, indicating that the majority of each library was sampled. However, due to having only a limited numbers of sequences for each sample, the Chao 1 estimator and Shannon's index were mainly used to present the trend of diversity variation between samples rather than a quantitative estimation. In Thermophile, AOA phylotype richness and diversity increased with decreasing temperature from source to the outflow channel (Table 7.2). However, in Cascadnaya, AOA Shannon's index was comparable (1.8-2.0) in three of the four locations (-S, -A and -D); the Chao1 richness estimator was high at both source locations (-S and –A) but was highest at the most distal outflow channel (-D). Sample CAC-B had the lowest values of both Chao1 estimator and Shannon's index and was similar to those of TM-A and BLS-D. Nevertheless, most samples in the three hot springs appeared to positively co-vary between Chao1 richness estimator and the Shannon's index, suggesting that increase in diversity corresponded to increase in richness of AOA.

S-LIBSHUFF was used to compare the AOA community structures between samples (clone libraries). In general, the eight samples were separated into two groups: group A comprising BLS-D, CAC-B and TM-A and group B containing the rest samples (Table 7.3). This grouping did not coincide with the geographic separation of hot springs. In addition, group A did not contain any OTUs from cluster 3, whereas group B contained sequences from all three clusters (Fig 7.2). All group A samples, BLS-D, TM-A and CAC-B, are dominated by cluster 1 sequences (Fig 7.2). They had lower values for both Chao1 estimator and Shannon's diversity index H' than group B samples, indicating that group A samples had lower AOA-phylotype richness and diversity than group B.

Quantitative PCR

The relative abundance of 16S rRNA genes varied by three orders of magnitude (10^2 to 10^5 copies per ng template DNA) among the eight samples (Fig 7.3). The highest abundances ($>10^4$ copies/ng DNA) of both archaeal and crenarchaeotal 16S rRNA genes were all found in group A samples (BLS-D, TM-A and CAC-B). Group B samples (TM-B and -D, and CAC-S, -A and -D) contained much less abundant gene copies ($<1.3\times10^4$ copies/ng DNA; Fig 7.3). The percentage of crenarchaeota in total archaea varied dramatically from 4% to 80% and did not correlate to the variation of total archaea (Fig 7.3). However,

there was an inverse correlation between the *amo*A Shannon's index and the abundance of archaeal (r^2 = 0.81) and crenarchaeotal (r^2 = 0.88) 16S rRNA gene copies (Fig 7.4), indicating that the diversity of AOA decreased with increasing abundances of total archaea or crenarchaeota.

GDGTs

Eight different GDGTs were identified in the samples from the three pools (Fig 7.5a). GDGT-0 (acyclic caldarchaeol) was predominant (48-55%) in all Thermophile samples. GDGTs 1-4 had similar relative abundances in these samples, with each contributing 7-16% to the total GDGTs. Cascadnaya samples contained variable GDGT-0 (15-45%) and elevated GDGT-4 up to 35% (CAC-A). In Burlyashi, GDGT 2-4 had similar abundances and accounted for 76% of total GDGTs; whereas GDGT-0 and GDGT-1 had lower abundances and together counted for 20% of total GDGTs. Other GDGT components including GDGT-5, -6, -7 and crenarchaeol were all less than 5% in each sample (Fig 7.5a).

Cluster analysis of the GDGT compositions indicated spatial separation of archaeal populations among these springs (Fig 7.5b). One exception is CAC-B, which was closely grouped with TM-A at Thermophile spring. The high similarity in GDGT profile between CAC-B and TM-A corroborates the similarity in their AOA community structure (Table 7.3) and the similarly high abundance of total archaea in these samples (Fig 7.3). BLS-D in group A showed the most diverse GDGT composition and formed a separate branch that significantly differed from CAC and TM samples (Fig 7.5b).

To examine if any relationships exist between temperature/pH and membrane lipid function of archaea, the ring index (RI) was calculated for each group using the equation

$$\mathrm{RI} = \sum_{i=1} (n_i \times C_i) / \sum_{i=1} C_i$$

Where n_i is the ring numbers in the GDGT structure and C_i is the percentage of each peak area over the total area. Average ring indices were 1.4 ± 0.1 (n = 4), 2.4 ± 0.3 (n = 3) and 2.4± 0.2 (n = 3) for Thermophile (including CAC-B), Cascadnaya and Burlyashi groups, respectively (Fig 7.5b). No correlations were found between RI and pH or temperature, indicating that other chemical or genetic variables may control ring structures of the archaeal lipids.

DISCUSSIONS

Occurrence of AOA in Kamchatka hot springs

Hot springs are extreme environment representing ecological islands and contain microbial communities significantly different from lower temperature soil and marine sediments. For example, in soil and marine sediments, ammonia-oxidizing bacteria (AOB) usually co-occur with AOA although evidences show that AOA are predominant (Francis *et al.*, 2005; Leininger *et al.*, 2006; Wuchter *et al.*, 2006; Lam *et al.*, 2007). However, screening using the bacterial *amo*A gene primers (*amo*A_1F and *amo*A_2R; Rotthauwe *et al.*, 1997) for the eight samples used in this study and additional 27 samples (data not shown) from hot springs in the Uzon Caldera showed all negative PCR results whereas positive results were always obtained from the DNA of ammonia-oxidizing bacterium *Nitrosomonas Europea*, suggesting that AOB is absence or present in a very low abundance in the Kamchatka hot spring systems. This result is consistent with a recent environmental study for high temperature hot springs in Iceland and Kamchatka (Reigstad *et al.*, 2008), and the finding from a moderately thermophilic enrichment culture (46°C) of microbial mats collected from the Sibrian Garga hot spring, in which no AOB but a monophylotype of AOA "*Candidatus* Nitrososphaera gargensis" was observed (Hatzenpichler *et al.*, 2008) even though the same enrichment culture Ga9.2a originally contained *Nitrosospira*-like bacteria (AOB) species at the same temperature (Lebedeva *et al.*, 2005). There appears to be a patterning that elevated temperatures (>40°C) does not favor AOB and hot spring AOB enrichments at 40-55°C were usually difficult to maintain (Golovacheva, 1976; Lebedeva *et al.*, 2005).

AOA on the other hand, are apparently more stable and occur in a wide temperature range (Nicol and Schleper, 2006; Francis *et al.*, 2007; de la Torre *et al.*, 2008; Hatzenpichler *et al.*, 2008; Zhang *et al.*, in review), which is consistent with our results that the major OTUs occur in multiple locations with temperature varying from 42°C (*e.g.*, TM-D) up to 85°C (*e.g.*, CAC-A; Fig 7.1). These organisms also are found in varying pH environments such as acidic or alkaline soils (Leininger *et al.*, 2006; He *et al.*, 2007; Shen *et al.*, 2008) and geothermal springs (Weidler *et al.*, 2007; Reigstad *et al.*, 2008; Zhang *et al.*, in review). This study corroborates with Reigstad *et al.* (2008) to show that AOA are widespread in neutral

to acidic hot springs with elevated temperatures. Ammonia ionization due to lower pH can be compensated by higher temperature so that equilibrium constant between ammonia and ammonium favors free ammonia gas. At the sampling locations in the Uzon Caldera, estimated equilibrium NH_3 with the *in situ* temperature, pH and NH_4^+ concentration ranges from 2.5 nmol L^{-1} to 70 nmol L^{-1} (online free-ammonia calculator http://cobweb.ecn.purdue.edu/~piwc/w3- research/free-ammonia/nh3.html). It is also observed that lower pH site may need to have either higher ammonium concentration (*e.g.*, CAC-D) or high temperature (*e.g.*, TM-A) to support AOA (Table 7.1). Surprisingly, diversity of the AOA phylotype in the neutral to slightly acidic hot springs in the Uzon Caldera is estimated to be even higher than many natural alkaline environments where NH_3 availability are more advantageous (Francis *et al.*, 2005; Beman and Francis, 2006). This enhanced diversity of AOA may be due to the dynamic physicochemical gradients caused by the chemical and physical heterogeneity of the hot spring environment.

Recent evidence shows that the presence of AOA is not constrained by temperature and that thermophilic AOA may fall in a previously designated non-thermophilic phylogenetic clade (de la Torre *et al.*, 2008; Hatzenpichler *et al.*, 2008). Although the exact origin is unknown for AOA phylotypes in Kamchatka hot springs, some of the sequences from cluster 2 may have a thermophilic origin as they are grouped with "*Candidatus* N. yellowstonii" and "*Candidatus* N. gargensis". Sequences in the cluster 3 are unique as they are separated from all known isolates and other hot spring sequences that are distributed in Clusters 1 and 2 (Fig 7.1). On the other hand, these sequences are closely related to those from an acid soil (He *et al.*, 2007), which occurred only within cluster 3 (Fig 7.1). This suggests that the majority of the hot spring AOA (59% of total OTUs) may be acidotolerant thermophiles.

Distribution and diversity of AOA

The separation of major OTUs in Kamchatka hot springs (cluster 1 and cluster 3) from those retrieved elsewhere may suggest a biogeographic patterning at the global scale as evidenced in our recent study that included a limited number of samples from Kamchatka (Zhang *et al.*, in review). Physicochemical factors including pH, salinity (or TDS), and ammonium usually show weak and inconsistent relationships to AOA diversity and distribution (Francis *et al.*, 2005; Wuchter *et al.*, 2006;

He *et al.*, 2007; Urakawa *et al.*, 2008). In Kamchatka samples examined, inconsistent correlations exist amongst nine physicochemical variables and AOA distribution (Table 7.1). Major OTUs of AOA are usually present in temperature- and chemistry-distinct sites of different springs. However, AOA distribution clearly shows two groups, A and B, as identified by the clone library comparison. A similar scenario was observed for AOB in a continuous-flow reactor of activated sludge, in which *Nitrosomonas oligotropha* and *Nitrosomonas europaea* showed selective affiliation with different ammonium and nitrite load treatments (Limpiyakorn *et al.*, 2007). But this is clearly not the case for Kamchatka samples as no correlation exists between species distribution and concentrations of ammonium or nitrite.

Similar to the distribution of AOA, diversity index and phylotype richness estimator of AOA do not show a consistent variation with temperature and water chemistry. However, Chao1 richness estimator is an exception, which is consistently the highest at the lowest temperature sites (42 and 50°C, respectively) in both Thermophile and Cascadnaya springs. The possible trend of Chao1 estimator could suggest that AOA in hot springs may be most favorably adapted to the moderately high temperature environment. It also has been demonstrated that lower temperature decreases the phylogenetic diversity of AOA in <19°C aquarium systems (Urakawa *et al.*, 2008).

On the other hand, the overall AOA diversity and richness pattern are clearly different between the two sample groups. Group A samples containing BLS-D, TM-A and CAC-B is characteristic of lower AOA species diversity and Chao1 phylotype richness than group B samples (Table 7.2). The grouping is supported by other lines of evidence. For example, Q-PCR shows that abundances of total archaea and crenarchaeota are one order of magnitude higher in group A samples than those in the group B, respectively (Fig 7.3), and inversely correlate to the AOA Shannon's diversity indices (Fig 7.4). Morphologically, TM-A and CAC-B in the group A are dominated by white streamers whereas group B samples are mostly dark green mats at lower temperature locations and black mud at higher temperature locations. Moreover, the GDGT patterns showed that the two streamer samples, CAC-B and TM-A, have the highest similarity in lipid structures (Fig 7.5). Taken together, this strong association among the AOA distribution and diversity, abundance of archaea and crenarchaeota, archaeal diversity (by GDGT), and

the total morphological property of the studied samples suggest that the overall community structure and interactions among coexisting microorganisms may have a greater influence on AOA distribution and diversity than water temperature and chemistry in Kamchatka hot springs. Although the mechanism is unclear, it is temping to speculate that this association may represent a biological synergy for distinct AOA communities to exist in different environment. For example, low diverse AOA community in group A samples may tend to live with high crenarchaeotal abundance community and streamers.

Abundance of AOA

Genomics study of *C. symbiosum* and molecular quantification of environmental samples demonstrate that AOA can possess one (Hallam *et al.*, 2006, Mincer, 2007) to three *amo*A gene copies (Wuchter *et al.*, 2006). Our attempt to amplify *amo*A gene using the protocol of Wuchter *et al.* (2006) resulted even higher ratio of *amo*A to crenarchaeotal gene copies (data not shown). Although the ratio may suggest that higher relative abundance of AOA in crenarchaeota, the cause of absolute *amo*A gene copies are not yet determined whether by multiple *amo*A gene copies in an AOA genome or experimental error such as unspecific amplification (Wuchter *et al.* 2006). In this study, the abundance of AOA were estimated using qPCR of 16S rRNA genes of crenarchaeotal and total archaea and the analysis of GDGTs. Assuming the same amount of environmental DNA contains the same amount of prokaryotic 16S rRNA genes, archaea are more abundant in group A samples than those of group B. The abundance of crenarchaeota within archaea varies substantially among both sample groups. However, except CAC-B, normalized crenarchaeotal abundances to the maximal archaeal 16S rRNA gene copies (3×10^5 copies/ng DNA of CAC-B) is less than 10%. Because all known AOA sequences are classified as crenarchaeotal origin, the data suggest that AOA abundance (if represented by crenarchaeota) vary extensively from sample to sample although being low in most samples (Fig 7.3).

Archaeal core membrane lipid GDGT has been used to quantitatively estimate the AOA contribution in total archaea. Leininger *et al.* (Leininger *et al.*, 2006) showed that both total isoprenoidal GDGT and crenarchaeol correlated with *amo*A gene copies in soils and therefore suggested that AOA constituted a major proportion of crenarchaeota and that the retrieved crenarchaeol had a common origin from AOA.

de la Torre *et al.* (de la Torre *et al.*, 2008) further proposed that crenarchaeol may be characteristics of AOA because crenarchaeol was abundant in the ammonia-oxidizing archaea *Nitrosopumilus maritimus* and "*Candidatus* Nitrosocaldus yellowstonii" (Konneke *et al.*, 2005; de la Torre *et al.*, 2008). Our data are in agreement with the proposal in that both crenarchaeol abundance and estimated AOA abundance by qPCR approach are low in all our samples. It is also consistent with estimates of AOA abundance in hot springs of Iceland and Kamchatka (Reigstad *et al.*, 2008). However, lower pH (5-7) of the sampling locations may also negatively affect the crenarchaeol abundance as suggested by several culture and environment based studies that the synthesis of crenarchaeol may be constrained by pH of the habitats (Macalady *et al.*, 2004; Pearson *et al.*, 2004; Zhang *et al.*, 2006; Schouten *et al.*, 2007). Since environments having high abundances of crenarchaeol usually have alkaline pH with a great range of temperature, such as marine environment, culture media and alkaline hot springs (DeLong *et al.*, 1998; Schouten *et al.*, 2000; Pearson *et al.*, 2004; Konneke *et al.*, 2005; Weidler *et al.*, 2007; de la Torre *et al.*, 2008; Pearson *et al.*, 2008). Lower pH (≤7 at 25ºC) environments may inhibit the synthesis of crenarchaeol. Therefore, significant abundance of AOA can occur in lower pH environments and may not necessarily correlate with the abundance of crenarchaeol due to the pH effect. This may explain the low or below detectable crenarchaeol in AOA-containing samples, *e.g.*, TM-A and TM-D. On the other hand, the lack of correlation between archaeal ring index and water temperature or pH suggests that other chemical variables may also affect the lipid ring structures of archaea in these samples.

In summary, this study shows that AOA are present in high temperature terrestrial hot springs in Kamchatka. Diverse AOA potentially including thermophilic members are widespread. Phylotypes of AOA in hot springs comprise three major clusters representing 1) crenarchaeotal group 1.1a (cluster 1), 2) crenarchaeotal group 1.1b (cluster 2), and 3) an acid hot spring/soil clade (He *et al.*, 2007), which is unique to and predominant in the Kamchatka hot springs. The distribution and diversity of the AOA phylotypes in Kamchatka hot springs appear to be dictated by the overall microbial structure and the abundance of archaea or crenarchaeota. Two AOA groups with distinct biological features can be outlined: group A mainly contains less diverse *amo*A sequences and are associated with streamers containing high

abundance of archaea; whereas group B samples comprise highly diverse *amo*A sequences that are present in all three clusters and are associated with bacteria-dominant communities as indicated by low abundance of archaeal 16S rRNA gene copies. Phylotypes of AOA have the highest richness at low temperature end of Thermophile and Cascadnaya where samples were collected along a temperature gradient, which indicates that moderately high temperature conditions are more favorable for AOA than hyperthermal (>75°C) locations. Although the AOA abundance is low in most sites, the wide occurrence of these organisms in contrast to the absence of AOB still suggest that AOA may be playing an important role in nitrogen cycle in Kamchatka hot springs.

MATERIAL AND METHOD

Site descriptions, sample collection, and physicochemical measurements

The three hot springs are Thermophile (54°29'55.18"N, 160°00'42.42"E), Cascadnaya (54°29'59.68"N, 160°00'46.00"E), and Burlyashi (54°29'58.79"N, 160°00'08.09"E) in the East Thermal Field of the Uzon Caldera, Kamchatka (Far East Russia). At each spring, water samples were collected along a temperature gradient in the outflow channel. Temperature, pH, and oxidation-reduction-potential (ORP) were measured *in situ* with a portable pH meter prior to sample collection. The pH meter was calibrated at 25°C and pH values were measured at *in situ* temperature. Microbial mats and underneath sediments were collected at each location. Water chemistry was measured using Hach kits in the field. Solid samples were saved in plastic bags and stored in freezing water in the field for up to 10 days before transported to the University of Georgia on ice. The samples were then stored -80°C until analysis. Vent gases were collected using a gas sampler and stored immediately in Vacutainers (BD Inc., Franklin Lakes, NJ, USA). Gaseous H_2S was removed by addition of up to 1 ml of 0.25 mol L^{-1} lead acetate prior to GC analysis. Concentrations of H_2, CH_4 and CO were determined using the SENTE methane gas analyzer (model GS-19S, Sente Inc., USA) under an isothermal condition of 54°C. CO_2 concentration was determined using a Trace GC (Finnigan MAT GmbH, Bremen, Germany) equipped with a Carboxen 1010 plot column (Supelco, Bellefonte, PA, USA) under an isothermal condition of 100°C.

DNA extraction, *amo*A gene amplification and cloning libraries

DNAs were extracted from sediment and mat materials using MoBio PowerSoil™ DNA extraction kit. The putative archaeal *amo*A gene was PCR amplified with the primer set Arch-*amo*AF (5‘-STAATGGTCTGGCTTAGACG) and Arch-*amo*AR (5‘-GCGGCCATC CATCTGTATGT; Francis *et al.*, 2005). Presence of the bacterial *amo*A gene was also tested using the primer set *amo*A_1F and *amo*A_2R (Rotthauwe *et al.*, 1997). Triplicate archaeal *amo*A gene PCR products were pooled and purified using QIAquick® gel extraction kit (QIAGEN, Valencia, CA, USA) followed by cloning reaction and transformation using the TOPO TA Cloning® kit (Invitrogen Inc., Carlsbad, CA, USA) with kanamycin as the selection agent. Clones with positive inserts were re-grown in the secondary agar plates and were subsequently transferred to freezing LB broth containing 50 µg/ml kanamycin in 96-well-plates, grown overnight at 37°C, and frozen at -80°C until sequencing.

Sequencing, phylogenetic and statistical analyses

From each clone library, 40 to 60 randomly selected clones were sequenced using either Arch-*amo*AF or Arch-*amo*AR primers on an ABI3730xl capillary sequencer in the Laboratory for Genomics and Bioinformatics at the University of Georgia. Chimeric sequences were excluded by manual BLAST examination of putative chimeras following the Bellerophon screening (http://foo.maths.uq.edu.au/~huber/bellerophon.pl). Deduced amino acid sequences were aligned using ClustalX. A total of 323 archaeal *amo*A deduced amino acid sequences containing 176 aligned positions were chosen for phylogenetic analysis using MEGA3.1 (Kumar *et al.*, 2004). DOTUR software was used for calculating rarefaction, Chao1 phylotype richness estimators and Shannon’s diversity index (Schloss and Handelsman, 2005). A threshold of 5%, representing *ca.* 9 amino acid differences was used to define the operational taxonomic unit (OUT) due to the high diversity of AOA. S-LIBSHUFF was used to compare the similarity between archaeal *amo*A clone libraries (Schloss *et al.*, 2004). The Jones, Taylor and Thornton (JTT) substitution method was used for calculating distance matrices in these applications.

Quantitative PCR

For each sample, 5 to 10 ng of DNA templates were added in triplicates with iQ™ SYBR® Green

Supermix (Bio-Rad, Hercules, CA, USA). Universal primers A364aF (5"-CGGGGYGCASCAGGCGCGAA) /A934b (5'-GTGCTCCCCCGCCAATTCCT), (Kemnitz *et al.*, 2005) and Cren-28F (5'- AATCCGGTTGATCCTGCCGGACC) / Cren-457R (5'-TTGCCCCCCGCTTATTCSC CCG; Schleper *et al.*, 1997) were used to quantify the copy numbers of 16S rRNA genes of total archaea and crenarchaeota respectively. Quantitative PCR was performed using an iCycler system (Bio-Rad, Hercules, CA, USA) as following program: initial denaturation at 95°C for 30 s, followed by 40 cycles of denaturation at 95°C for 30 s, annealing at 57°C for 30 s, and extension at 72°C for 50 s. Calibration of samples was performed using known copies of *Sulfolobus acidocaldarius* (ATCC 33909) 16S rRNA gene (10^2 and 10^7 copies), amplified with the universal primer set 7F (5'-TTCCGGTTGATCCYGCCGGA) and 1492R (5'-TACGGYTACCTTGTTACGACTT). Data were reported using gene copies per nanogram of DNA. Q-PCR of *amo*A gene was performed as previously described (Wutcher *et al.* 2006).

Lipid extraction and LC-MS analysis

Freeze-dried samples (~5 g) were extracted using the modified Bligh and Dyer method (White *et al.*, 1979) for total lipid extracts (TLE). TLE were evaporated under high-purity nitrogen gas and subsequently hydrolyzed in 5% HCl in methanol (transesterification) for 2 h at 70°C to cleave polar head-groups. The transesterified products were extracted using CH_2Cl_2, dried under nitrogen gas, and loaded on to a C18 Bond-Elut® solid phase extraction (SPE) column (Varian Inc., Palo Alto, CA , USA), which separated TLE into 3 fractions. The polar fraction was eluted by using 1:1 acetonitrile: ethyl acetate, the GDGT fraction by using 1:3 ethyl acetate: hexane, and the nonpolar fraction by using 1:10 ethyl acetate: hexane. The GDGT fractions were dried under nitrogen and dissolved in 1.3% isopropanol in hexane for analysis by HPLC-MS (Pearson *et al.*, 2004). Intact GDGTs were identified with an Agilent 1100 series high performance liquid chromatograph (HPLC)/atmospheric pressure chemical ionization-MS using a Zorbax NH_2 (4.6 by 250 mm, 5 μm) column. GDGTs were eluted isocratically in 1.3% isopropanol in hexane at 30°C. Spectra were scanned over the m/z range from 1,000 to 1,350.

Nucleotide sequence accession numbers

Sequence data have been deposited in GenBank (accession numbers EF654133-EF654511).

ACKNOWLEDGEMENTS

This work was supported by the National Science Foundation Microbial Observatory Program (to J.W. and C.S.R.). We thank Dr. Ann Pearson and Yundan Pi (Harvard University) for their assistance in performing HPLC analysis of GDGT, and Qi Ye for her technical assistance throughout the work.

.

Table 7.1. Physicochemistry of sampling sites

		BLS-A	BLS-B	BLS-C	BLS-D	TM-A	TM-B	TM-C	TM-D	CAC-S	CAC-A	CAC-B	CAC-C	CAC-D
Sample description		S/Md	S/Md	S/Md	Md	S, St	Mt, St	Mt	Mt	Md	Md	St	Mt	Mt
T°C		86.8	70	58	51	70	64	52.7	42	74	85	71	59.1	50
$pH^{25°C}$		6	6.5	6.5	6	6	6.5	6.5	7	6	6	6.5	6	5.5
TDS (mg L^{-1})		730	461	586	733	493	499	499	497	NA	1471	1332	1242	904
ORP (mV)		-305	-153	-163	-170	-301	-365	-336	-288	NA	-323	-141	-62	-271
Alk (mmol L^{-1} $CaCO_4$)		1.18	1.20	1.23	1.2	2.65	3.3	3.2	3.25	1.1	0.9	0.75	0.65	0.5
SO_4^{2-} (mmol L^{-1})		2.3	2.2	2.2	2.2	0.1	0.1	0.3	0.3	0.7	1.1	1.8	1.4	1.9
S^{2-} (µmol L^{-1})		43.8	BD	6.3	BD	43.1	1.3	0.6	0.6	12.5	5.6	5.0	4.1	1.6
NO_2^- (µmol L^{-1} N)		0.1	0.1	0.1	0.3	0.6	0.3	0.2	0.4	0.4	1.4	1.1	0.3	0.4
NH_4^+ (mmol L^{-1} N)		1.1	1.5	1.5	1.5	0.3	0.3	4.0	0.2	1.5	2.2	2.4	2.7	2.7
Vent Gases[a]	H_2 %	0.1				0.2					0.2			
	CH_4 %	2.2				0.4					1.4			
	CO_2 %	59				36					71			
	CO ppm	140				39					BD			

a. Gas samples were only available at the source of each spring

b. Sampling sites: BLS, Burlyashi spring; TM, Thermophile spring; CAC, Cascadnaya spring; suffix of pool name represents the different sampling locations in the pool

c. Abbreviations: TDS, total dissolved solids; ORP, oxidation-reduction potential; Alk, alkalinity; NA, not available; BD, below detection limit. In sample description, S = sand, Md = mud, Mt = Mat, and St = streamer

Table 7.2. Statistics of *amo*A gene clone libraries.

		BLS-D	TM-A	TM-B	TM-D	CAC-S	CAC-A	CAC-B	CAC-D
Temperature (ºC)		51	70	64	42	74	85	71	50
pH		6	6	6.5	7	6	6	6.5	5.5
No. of clones		40	37	43	40	44	44	35	40
No. of singletons		3	1	3	4	2	1	1	1
No. of total OTUs (N_{OTU})		7	4	11	15	12	10	6	10
N_{OTU} (N_{clone})	Cluster1	6(35)	3(34)	1(17)	1(7)	1(11)	1(14)	4(31)	1(11)
	Cluster2	1(5)	1(3)	2(2)	2(2)	1(2)	1(1)	2(4)	2(2)
	Cluster3	0	0	8(24)	12(31)	10(31)	8(29)	0	7(27)
Chao1 estimator		7.5	4.0	14.0	24.0	15.0	15.0	5.5	25.0
Shannon‘s index		0.91	0.90	1.93	2.25	2.01	1.79	0.76	1.84

a. Chao1 phylotype richness estimator and Shannon’s diversity index are calculated using individual numbers of clones and OTUs in each sample.

b. OTU coverage is greater than 90% for all samples (see Fig 7.2).

Table 7.3. S-LIBSHUFF comparison of *amo*A gene clone libraries. Values in the table represent P values for ΔC_{XY} of homologous library X and heterologous library Y (below the diagonal) and ΔC_{YX} of homologous library Y and heterologous library X (above the diagonal). Minimum P-value is 0.0009 and 0.0000 for family-wise and Monte Carlo Error at 95% margin of error. Significant P values for 56 comparisons are shaded. Two libraries are distinct if both ΔC_{XY} and ΔC_{YX} are statistically significant.

		Y							
	-	BLS-D†	TM-A†	TM-B‡	TM-D‡	CAC-S‡	CAC-A‡	CAC-B†	CAC-D
	BLS-D	-	0.3011	0.0000	0.0000	0.0000	0.0000	0.5575	0.0000
	TM-A	0.9919	-	0.0000	0.0000	0.0000	0.0000	0.4229	0.0000
	TM-B	0.0000	0.0000	-	0.0685	0.0011	0.0021	0.0000	0.0103
X	TM-D	0.0000	0.0000	0.0540	-	0.2852	0.8383	0.0000	0.7860
	CAC-S	0.0000	0.0000	0.0610	0.4449	-	0.3464	0.0000	0.2854
	CAC-A	0.0000	0.0000	0.1713	0.7617	0.5593	-	0.0000	0.6880
	CAC-B	0.4175	0.4133	0.0000	0.0000	0.0000	0.0000	-	0.0000
	CAC-D	0.0000	0.0000	0.0567	0.5354	0.1030	0.6665	0.0000	-

† Group A samples (see text for explanation).

‡ Group B samples (see text for explanation).

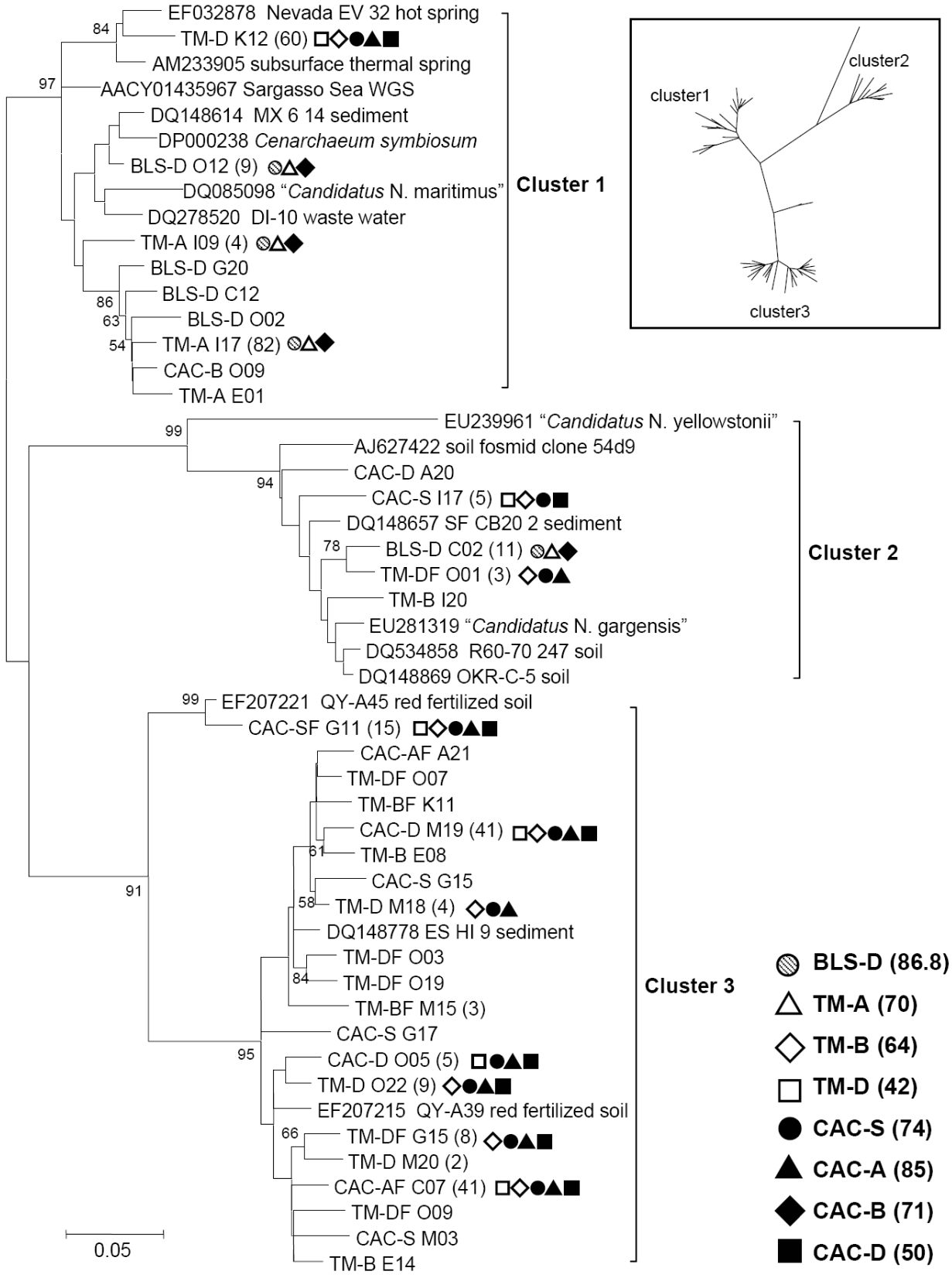
EF032878 Nevada EV 32 hot spring
TM-D K12 (60)
AM233905 subsurface thermal spring
AACY01435967 Sargasso Sea WGS
DQ148614 MX 6 14 sediment
DP000238 Cenarchaeum symbiosum
BLS-D O12 (9)
DQ085098 "Candidatus N. maritimus"
DQ278520 DI-10 waste water
TM-A I09 (4)
BLS-D G20
BLS-D C12
BLS-D O02
TM-A I17 (82)
CAC-B O09
TM-A E01
Cluster 1
cluster1
cluster2
cluster3
EU239961 "Candidatus N. yellowstonii"
AJ627422 soil fosmid clone 54d9
CAC-D A20
CAC-S I17 (5)
DQ148657 SF CB20 2 sediment
BLS-D C02 (11)
TM-DF O01 (3)
TM-B I20
EU281319 "Candidatus N. gargensis"
DQ534858 R60-70 247 soil
DQ148869 OKR-C-5 soil
Cluster 2
EF207221 QY-A45 red fertilized soil
CAC-SF G11 (15)
CAC-AF A21
TM-DF O07
TM-BF K11
CAC-D M19 (41)
TM-B E08
CAC-S G15
TM-D M18 (4)
DQ148778 ES HI 9 sediment
TM-DF O03
TM-DF O19
TM-BF M15 (3)
CAC-S G17
CAC-D O05 (5)
TM-D O22 (9)
EF207215 QY-A39 red fertilized soil
TM-DF G15 (8)
TM-D M20 (2)
CAC-AF C07 (41)
TM-DF O09
CAC-S M03
TM-B E14
Cluster 3
0.05
BLS-D (86.8)
TM-A (70)
TM-B (64)
TM-D (42)
CAC-S (74)
CAC-A (85)
CAC-B (71)
CAC-D (50)

Fig 7.1. Deduced amino acid trees of archaeal *amo*A gene obtained from hot springs in the Uzon Caldera. Only representative OTUs (<95% sequence identity) are shown. Neighbor-joining distance was calculated using the Jones, Taylor and Thornton (JTT) substitution method, and greater than 50% support in bootstrapping values from 1000 replicates are shown at the major nodes. A radiation tree illustrating the three clusters is also shown on the top right. Maximum Parsimony (1000 replicates) and Minimum Evolution (JTT, 1000 replicates) were also computed and showed nearly identical tree reconstructions. Numbers of clones greater than 1 within each OTU are shown in parentheses. Symbols indicate sample sources (Table 7.1). *In situ* temperatures in °C were shown in parenthesis.

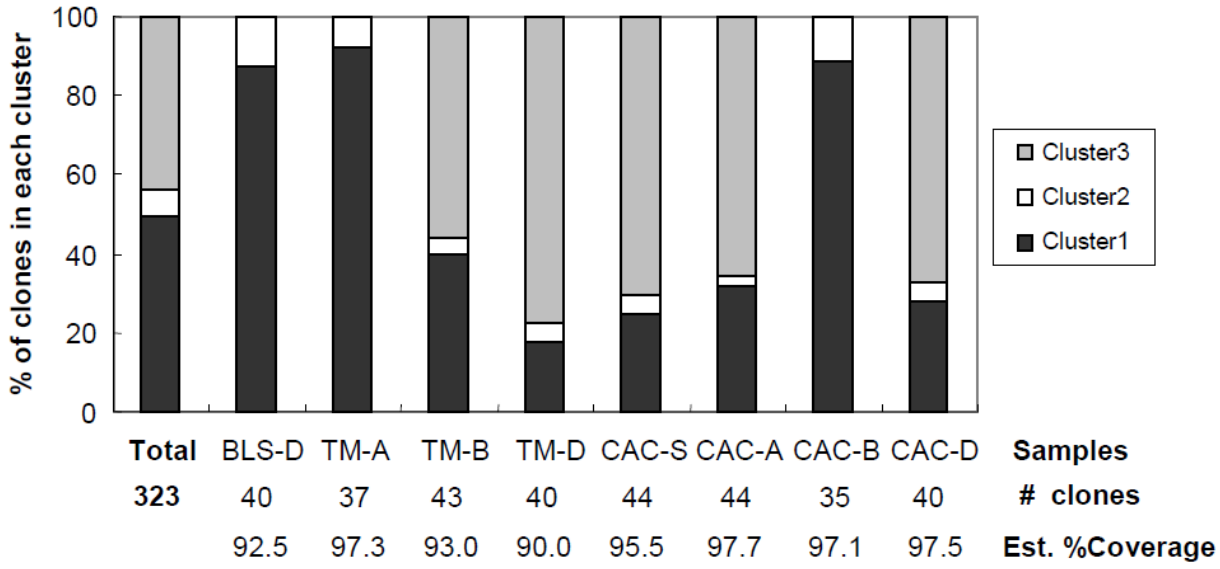

Fig 7.2. Relative distribution of *amo*A gene clones in the three phylogenetic clusters. Numbers of clones sequenced and Good's estimator of coverage for each sample are shown at the bottom panel. Good's coverage was calculated based on formula (1-n/N)*100, where n is the number of singletons and N is the total number of clones in that sample.

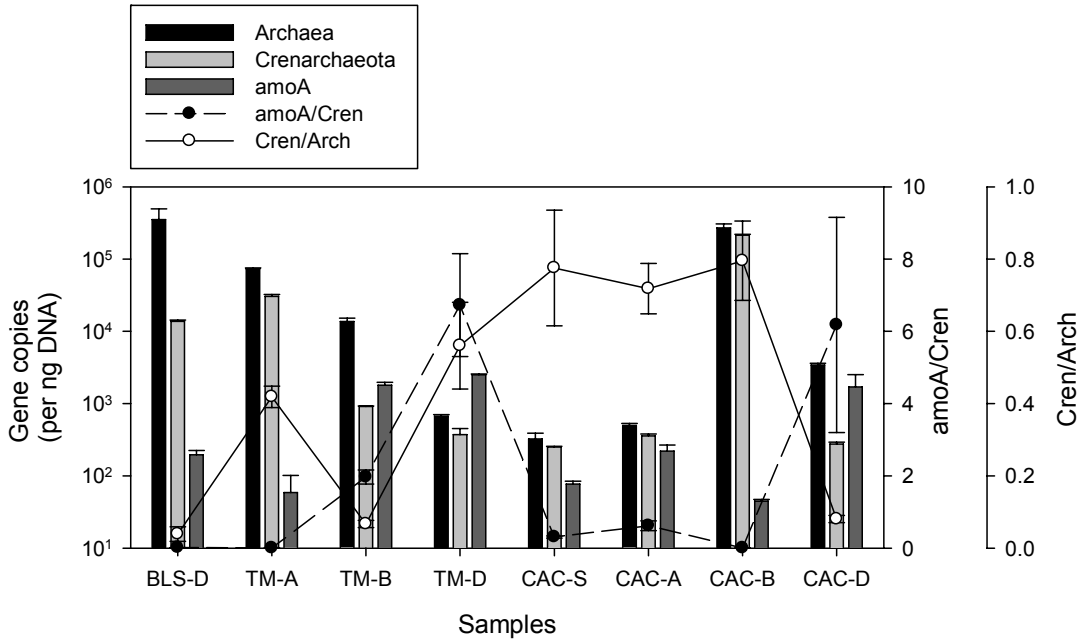

Fig 7.3. Abundances of total archaea and crenarchaeota in each sample determined by quantitative PCR. Data shown are based on the 16S rRNA gene copies per nanogram template DNA. Scatters connected by the solid or dashed lines illustrate the abundance ratio of 16S rRNA genes of crenarchaeota and archaea and ratio of *amo*A gene and crenarchaeotal 16S rRNA gene.

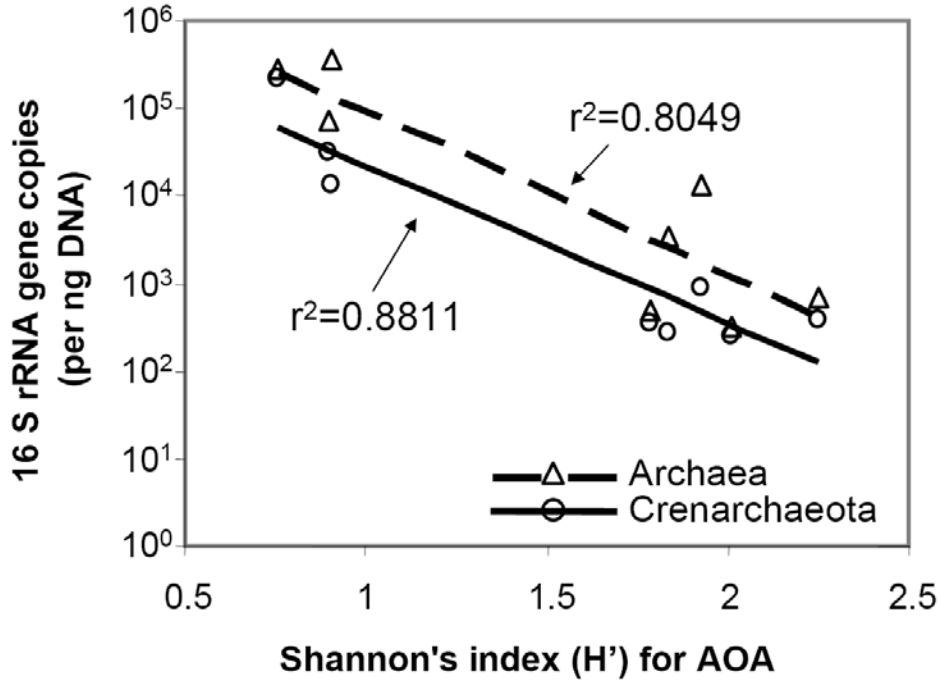

Fig 7.4. Inverse linear correlation between the Shannon's diversity index of AOA phylotypes and 16S rRNA gene copies of total archaea and crenarchaeota.

5a)

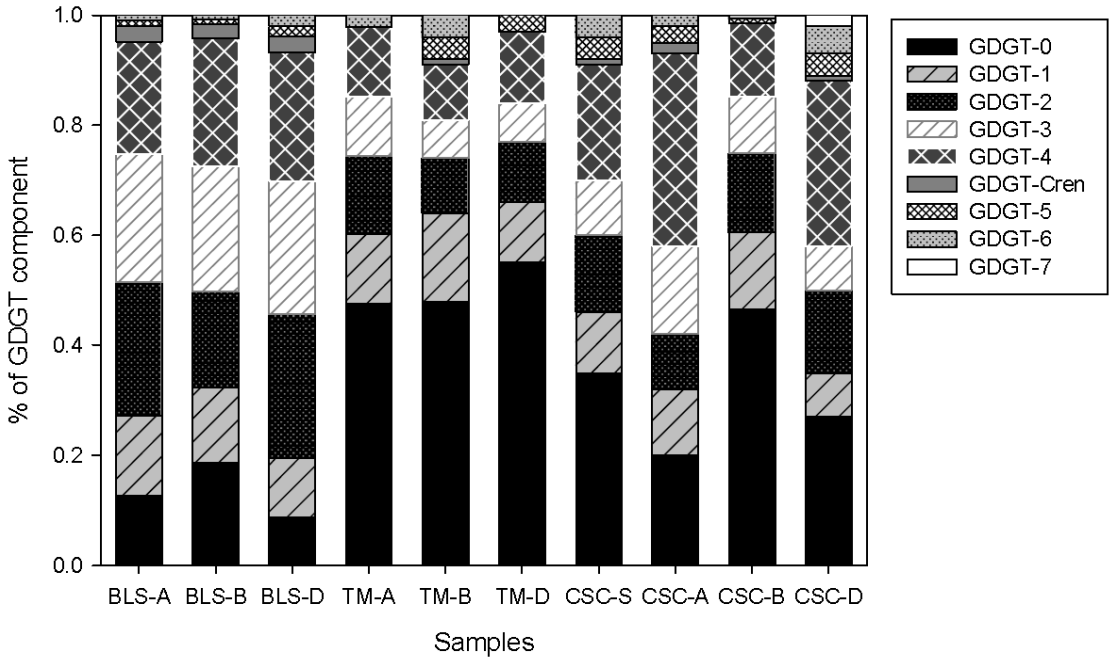
1.0
0.8
0.6
0.4
0.2
0.0
% of GDGT component
BLS-A
BLS-B
BLS-D
TM-A
TM-B
TM-D
CSC-S
CSC-A
CSC-B
CSC-D
Samples
GDGT-0
GDGT-1
GDGT-2
GDGT-3
GDGT-4
GDGT-Cren
GDGT-5
GDGT-6
GDGT-7

5b)

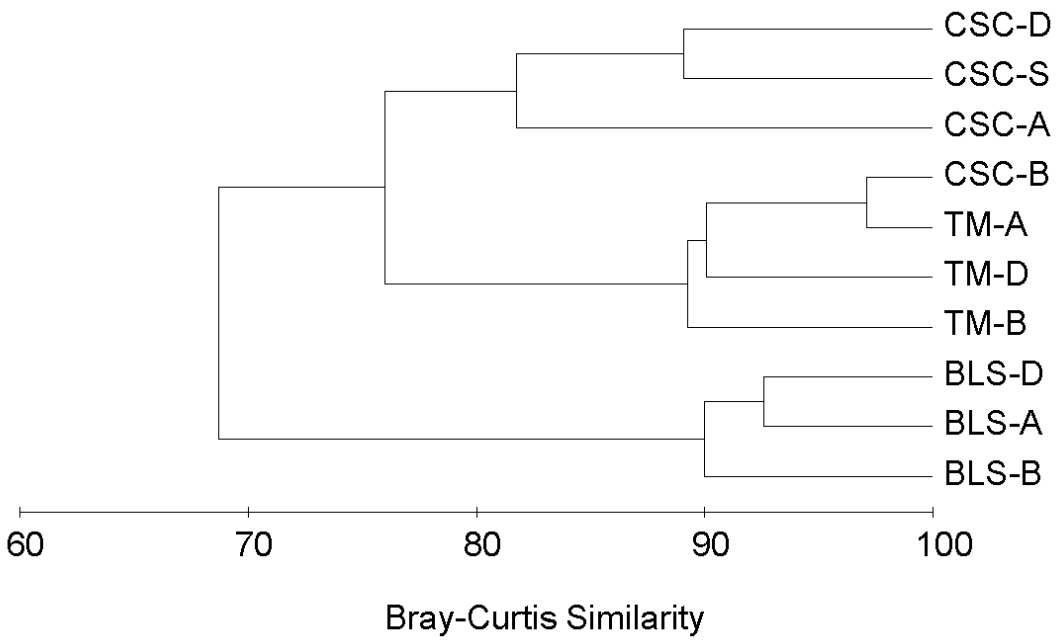
CSC-D
CSC-S
CSC-A
CSC-B
TM-A
TM-D
TM-B
BLS-D
BLS-A
BLS-B
60
70
80
90
100
Bray-Curtis Similarity

Fig 7.5. a) Normalized GDGT compositions of the bulk environmental samples. GDGT compounds are identified as (Schouten *et al.*, 2002): GDGT-0, *m/z* 1,302, zero ring; GDGT-1, *m/z* 1,300, one cyclopentyl ring; GDGT-2, *m/z* 1,298, two cyclopentyl rings; GDGT-3, *m/z* 1,296, three cyclopentyl rings; GDGT-4, *m/z* 1,294, four cyclopentyl rings; GDGT-Cren, crenarchaeol, *m/z* 1,292, four cyclopentyl rings, one cyclohexyl ring; GDGT-5, *m/z* 1,292, crenarchaeol regioisomer, five cyclopentyl rings; GDGT-6, *m/z* 1,290, six cyclopentyl ring; GDGT-7, m/z 1288, seven cyclopentyl ring. b) Cluster analysis of the GDGT composition. Percentage of GDGT components was log(x+1) transformed before Bury-Curtis similarity was computed between samples with nine GDGT components using PRIMER5 (Clarke, 1993).

REFERENCES

Beman, J.M., and Francis, C.A. (2006) Diversity of ammonia-oxidizing archaea and bacteria in the sediments of a hypernutrified subtropical estuary: Bahia del Tobari, Mexico. *Appl Environ Microbiol* **72**: 7767-7777.

Clarke, K.R. (1993) Nonparametric multivariate analyses of changes in community structure. *Australian Journal of Ecology* **18**: 117-143.

de la Torre, J.R., Walker, C.B., Ingalls, A.E., Konneke, M., and Stahl, D.A. (2008) Cultivation of a thermophilic ammonia oxidizing archaeon synthesizing crenarchaeol. *Environmental Microbiology* **10**: 810-818.

DeLong, E.F., King, L.L., Massana, R., Cittone, H., Murray, A., Schleper, C., and Wakeham, S.G. (1998) Dibiphytanyl ether lipids in nonthermophilic crenarchaeotes. *Appl Environ Microbiol* **64**: 1133-1138.

Derosa, M., and Gambacorta, A. (1988) The lipids of Archaebacteria. *Prog Lipid Res* **27**: 153-175.

Derosa, M., Esposito, E., Gambacorta, A., Nicolaus, B., and Bulock, J.D. (1980) Effects of temperature on ether lipid-composition of *Caldariella Acidophila*. *Phytochemistry* **19**: 827-831.

Francis, C.A., Beman, J.M., and Kuypers, M.M.M. (2007) New processes and players in the nitrogen cycle: the microbial ecology of anaerobic and archaeal ammonia oxidation. *ISME Journal* **1**: 19-27.

Francis, C.A., Roberts, K.J., Beman, J.M., Santoro, A.E., and Oakley, B.B. (2005) Ubiquity and diversity of ammonia-oxidizing archaea in water columns and sediments of the ocean. *Proc Natl Acad Sci U S A* **102**: 14683-14688.

Gliozzi, A., Paoli, G., Derosa, M., and Gambacorta, A. (1983) Effect of isoprenoid cyclization on the transition-temperature of lipids in thermophilic Archaebacteria. *Biochim Biophys Acta* **735**: 234-242.

Golovacheva, R.S. (1976) Thermophilic nitrifying bacteria from hot springs. *Microbiology (English translation of Mikrobiologiya)* **45**: 329-331.

Hallam, S.J., Mincer, T.J., Schleper, C., Preston, C.M., Roberts, K., Richardson, P.M., and DeLong, E.F.

(2006) Pathways of carbon assimilation and ammonia oxidation suggested by environmental genomic analyses of marine crenarchaeota. *PLoS Biology* **4**: 0520-0536.

Hatzenpichler, R., Lebedeva, E.V., Spieck, E., Stoecker, K., Richter, A., Daims, H., and Wagner, M. (2008) A moderately thermophilic ammonia-oxidizing crenarchaeote from a hot spring. *Proc Natl Acad Sci U S A* **105**: 2134-2139.

He, J., Shen, J., Zhang, L., Zhu, Y., Zheng, Y., Xu, M., and Di, H.J. (2007) Quantitative analyses of the abundance and composition of ammonia-oxidizing bacteria and ammonia-oxidizing archaea of a Chinese upland red soil under long-term fertilization practices. *Environmental Microbiology* **9**: 2364-2374.

Hopmans, E.C., Schouten, S., Pancost, R.D., van der Meer, M.T.J., and Damste, J.S.S. (2000) Analysis of intact tetraether lipids in archaeal cell material and sediments by high performance liquid chromatography/atmospheric pressure chemical ionization mass spectrometry. *Rapid Commun Mass Spectrom* **14**: 585-589.

Kemnitz, D., Kolb, S., and Conrad, R. (2005) Phenotypic characterization of Rice Cluster III archaea without prior isolation by applying quantitative polymerase chain reaction to an enrichment culture. *Environmental Microbiology* **7**: 553-565.

Kemp, P.F., and Aller, J.Y. (2004) Bacterial diversity in aquatic and other environments: what 16S rDNA libraries can tell us. *FEMS Microbiology Ecology* **47**: 161-177.

Koga, Y., and Morii, H. (2005) Recent advances in structural research on ether lipids from archaea including comparative and physiological aspects. *Bioscience Biotechnology and Biochemistry* **69**: 2019-2034.

Koga, Y., Akagawamatsushita, M., Ohga, M., and Nishihara, M. (1993) Taxonomic significance of the distribution of component parts of polar ether lipids in methanogens. *Syst Appl Microbiol* **16**: 342-351.

Konneke, M., Bernhard, A.E., de la Torre, J.R., Walker, C.B., Waterbury, J.B., and Stahl, D.A. (2005) Isolation of an autotrophic ammonia-oxidizing marine archaeon. *Nature* **437**: 543-546.

Kowalchuk, G.A., and Stephen, J.R. (2001) Ammonia-oxidizing bacteria: A model for molecular microbial ecology. *Annu Rev Microbiol* **55**: 485-529.

Kumar, S., Tamura, K., and Nei, M. (2004) MEGA3: Integrated software for molecular evolutionary genetics analysis and sequence alignment. *Briefings in Bioinformatics* **5**: 150-163.

Kvist, T., Ahring, B.K., and Westermann, P. (2007) Archaeal diversity in Icelandic hot springs. *FEMS Microbiology Ecology* **59**: 71-80.

Kvist, T., Mengewein, A., Manzei, S., Ahring, B.K., and Westermann, P. (2005) Diversity of thermophilic and non-thermophilic crenarchaeota at 80°C. *FEMS Microbiol Lett* **244**: 61-68.

Lam, P., Jensen, M.M., Lavik, G., McGinnis, D.F., Muller, B., Schubert, C.J. *et al.* (2007) Linking crenarchaeal and bacterial nitrification to anammox in the Black Sea. *Proc Natl Acad Sci U S A* **104**: 7104-7109.

Lebedeva, E.V., Alawi, M., Fiencke, C., Namsaraev, B., Bock, E., and Spieck, E. (2005) Moderately thermophilic nitrifying bacteria from a hot spring of the Baikal rift zone. *FEMS Microbiology Ecology* **54**: 297-306.

Leininger, S., Urich, T., Schloter, M., Schwark, L., Qi, J., Nicol, G.W. *et al.* (2006) Archaea predominate among ammonia-oxidizing prokaryotes in soils. *Nature* **442**: 806-809.

Limpiyakorn, T., Kurisu, F., Sakamoto, Y., and Yagi, O. (2007) Effects of ammonium and nitrite on communities and populations of ammonia-oxidizing bacteria in laboratory-scale continuous-flow reactors. *FEMS Microbiology Ecology* **60**: 501-512.

Macalady, J.L., Vestling, M.M., Baumler, D., Boekelheide, N., Kaspar, C.W., and Banfield, J.F. (2004) Tetraether-linked membrane monolayers in *Ferroplasma* spp: a key to survival in acid. *Extremophiles* **8**: 411-419.

Nicol, G.W., and Schleper, C. (2006) Ammonia-oxidising Crenarchaeota: important players in the nitrogen cycle? *Trends Microbiol* **14**: 207-212.

Pearson, A., Huang, Z., Ingalls, A.E., Romanek, C.S., Wiegel, J., Freeman, K.H. *et al.* (2004) Nonmarine crenarchaeol in Nevada hot springs. *Appl Environ Microbiol* **70**: 5229-5237.

Pearson, A., Pi, Y., Zhao, W., Li, W., Li, Y., Inskeep, W. *et al.* (2008) Factors controlling the distribution of archaeal tetraethers in terrestrial hot springs. *Appl Environ Microbiol*. in press.

Powers, L.A., Werne, J.P., Johnson, T.C., Hopmans, E.C., Damste, J.S.S., and Schouten, S. (2004) Crenarchaeotal membrane lipids in lake sediments: a new paleotemperature proxy for continental paleoclimate reconstruction? *Geology* **32**: 613-616.

Prosser, J.I., and Embley, T.M. (2002) Cultivation-based and molecular approaches to characterisation of terrestrial and aquatic nitrifiers. *Antonie Van Leeuwenhoek International Journal of General and Molecular Microbiology* **81**: 165-179.

Purkhold, U., Pommerening-Roser, A., Juretschko, S., Schmid, M.C., Koops, H.P., and Wagner, M. (2000) Phylogeny of all recognized species of ammonia oxidizers based on comparative 16S rRNA and *amo*A sequence analysis: Implications for molecular diversity surveys. *Appl Environ Microbiol* **66**: 5368-5382.

Reigstad, L.J., Richter, A., Daims, H., Urich, T., Schwark, L., and Schleper, C. (2008) Nitrification in terrestrial hot springs of Iceland and Kamchatka. *FEMS Microbiol Ecol* **64**: 167-174.

Rotthauwe, J.H., Witzel, K.P., and Liesack, W. (1997) The ammonia monooxygenase structural gene *amo*A as a functional marker: molecular fine-scale analysis of natural ammonia-oxidizing populations. *Appl Environ Microbiol* **63**: 4704-4712.

Schleper, C., Holben, W., and Klenk, H.P. (1997) Recovery of Crenarchaeotal ribosomal DNA sequences from freshwater-lake sediments. *Appl Environ Microbiol* **63**: 321-323.

Schleper, C., Jurgens, G., and Jonuscheit, M. (2005) Genomic studies of uncultivated archaea. *Nature Reviews Microbiology* **3**: 479-488.

Schloss, P.D., and Handelsman, J. (2005) Introducing DOTUR, a computer program for defining operational taxonomic units and estimating species richness. *Appl Environ Microbiol* **71**: 1501-1506.

Schloss, P.D., Larget, B.R., and Handelsman, J. (2004) Integration of microbial ecology and statistics: a test to compare gene libraries. *Appl Environ Microbiol* **70**: 5485-5492.

Schouten, S., Hopmans, E.C., Pancost, R.D., and Damste, J.S.S. (2000) Widespread occurrence of structurally diverse tetraether membrane lipids: Evidence for the ubiquitous presence of low-temperature relatives of hyperthermophiles. *Proc Natl Acad Sci U S A* **97**: 14421-14426.

Schouten, S., Hopmans, E.C., Schefuss, E., and Damste, J.S.S. (2002) Distributional variations in marine crenarchaeotal membrane lipids: a new tool for reconstructing ancient sea water temperatures? *Earth Planet Sci Lett* **204**: 265-274.

Schouten, S., van der Meer, M.T.J., Hopmans, E.C., Rijpstra, W.I.C., Reysenbach, A.-L., Ward, D.M., and Sinninghe Damste, J.S. (2007) Archaeal and bacterial glycerol dialkyl glycerol tetraether lipids in hot springs of Yellowstone National Park (USA). In, pp. AEM.00630-00607.

Turich, C., Freeman, K.H., Bruns, M.A., Conte, M., Jones, A.D., and Wakeham, S.G. (2007) Lipids of marine Archaea: Patterns and provenance in the water-column and sediments. *Geochim Cosmochim Acta* **71**: 3272-3291.

Shen, J., Zhang, L., Zhu, Y., Zhang J., and He, J. (2008) Abundance and composition of ammonia-oxidizing bacteria and ammonia-oxidizing archaea communities of an alkaline sandy loam. *Environ Microbiol* **10**: 1601–1611.

Spear, J. R., Barton, H. A., Robertson, C. E., Francis, C. A., and Pace, N. R. (2007) Microbial community biofabrics in a geothermal mine adit. *Appl Environ Microbiol* **73:** 6172-6180.

Uda, I., Sugai, A., Itoh, Y.H., and Itoh, T. (2001) Variation in molecular species of polar lipids from *Thermoplasma acidophilum* depends on growth temperature. *Lipids* **36**: 103-105.

Urakawa, H., Tajima, Y., Numata, Y., and Tsuneda, S. (2008) Low temperature decreases the phylogenetic diversity of ammonia-oxidizing archaea and bacteria in aquarium biofiltration systems. *Appl Environ Microbiol* **74**: 894-900.

Venter, J.C., Remington, K., Heidelberg, J.F., Halpern, A.L., Rusch, D., Eisen, J.A. *et al.* (2004) Environmental genome shotgun sequencing of the Sargasso Sea. *Science* **304**: 66-74.

Weidler, G.W., Dornmayr-Pfaffenhuemer, M., Gerbl, F.W., Heinen, W., and Stan-Lotter, H. (2007) Communities of archaea and bacteria in a subsurface radioactive thermal spring in the Austrian

Central Alps, and evidence of ammonia-oxidizing Crenarchaeota. *Appl Environ Microbiol* **73**: 259-270.

Weijers, J.W.H., Schouten, S., Spaargaren, O.C., and Damste, J.S.S. (2006) Occurrence and distribution of tetraether membrane lipids in soils: Implications for the use of the TEX86 proxy and the BIT index. *Org Geochem* **37**: 1680-1693.

White, D.C., Davis, W.M., Nickels, J.S., King, J.D., and Bobbie, R.J. (1979) Determination of the sedimentary microbial biomass by extractible lipid phosphate. *Oecologia* **40** 51-62.

Wuchter, C., Schouten, S., Coolen, M.J.L., and Damste, J.S.S. (2004) Temperature-dependent variation in the distribution of tetraether membrane lipids of marine Crenarchaeota: Implications for TEX86 paleothermometry. *Paleoceanography* **19**: PA4028. doi: 4010.1029/2004PA001041.

Wuchter, C., Abbas, B., Coolen, M.J.L., Herfort, L., van Bleijswijk, J., Timmers, P. ***et al.*** (2006) Archaeal nitrification in the ocean. *Proc Natl Acad Sci U S A* **103**: 12317-12322.

Zhang, C., Ye, Q., Huang, Z., Li, W., Chen, J., Song, Z. ***et al.*** (in review) Global occurrence and biogeographic patterning of putative archaeal *amo*A genes in terrestrial hot springs. *Envrionmental Microbiology*.

Zhang, C.L., Pearson, A., Li, Y.L., Mills, G., and Wiegel, J. (2006) Thermophilic temperature optimum for crenarchaeol synthesis and its implication for archaeal evolution. *Appl Environ Microbiol* **72**: 4419-4422.

CONCLUSIONS

This dissertation explores the geochemistry and microbiology of hot springs in three major thermal fields (Table 3.1) of the Uzon Caldera, Kamchatka. Spatial studies at field scale and pool scale were conducted which included the analysis of lipids (Chapter 3), cultivation methods (Chapters 4 and 5) and molecular DNA techniques (Chapter 7) to gain insights into the biogeochemical processes of hot springs. Chapter 6 extended the study of CO-oxidizing bacteria by examining potential biochemical mechanisms of carbon fixation for *C. hydrogenoformans* using stable carbon isotope spike. These studies provide new insights into the diversity and distribution of microorganisms and their geochemical functions from multiple perspectives. The main findings of this research are the following:

In Chapter 2, it was determined that the gas discharges from the hot spring vents originated mainly from thermogenic sources in the deep subsurface (Fig 2.7) and they were relatively stable in both composition and carbon isotope signature (Tables 2.1 and 2.2). Weighed average $\delta^{13}C$ values for CO_2 and CH_4 suggested that isotopically depleted kerogen, marine limestone and/or perhaps even the mantle carbon (magmatic source) may be the source of the thermogenic gases. Using both gas content and stable isotope geothermometers, it was determined that chemical equilibrium and partial isotope exchange may be attained between CO_2 and CH_4 in the deep reservoir (Fig 2.7). The $\delta^{13}C$ values for these carbon sources permitted major carbon fixation pathways used by dominant autotrophic bacteria to be predicted using compound specific isotope analysis of PLFA in Chapter 3, where the Calvin cycle and the rTCA cycles were determined to be predominant (Fig 3.6). Statistical analyses of PLFA and GDGT compositions in Chapter 3 grouped bacterial and archaeal communities based on their similarities in lipid profiles. Similarity percentage (SIMPER) analysis further revealed the most important lipid compounds that contribute to the within group similarity, which allowed predictions related to the most common microorganisms in different bacterial community groups including *Cyanobacteria-Thermotogae* type, *Proteobacteria-Desulfurobacterium* type or *Aquificales* type. Similarly, GDGT profiles suggested

presence of three types of archaea that produced each of GDGT-0, GDGT-1 and GDGT-4 as the main membrane lipid, respectively (Fig 3.5). Temperature was the most important environmental factor associating to PLFA distributions whereas combined temperature and pH were the most important factor associating to GDGT distributions. On the other hand, low correlation coefficients in both analyses suggest that other unknown variables may play important roles (Table S3.1).

In Chapter 4 and 5, a novel aerobic, alkalitolerant, thermophilic bacterium *Caldalkalibacillus uzoniensis* stain JW/WZ-YB58^T (= ATCC BAA-1258 = DSM 17740) was described (pH^{25^oC} optimum 8.2-8.4; temperature optimum 50-52°C). The isolate was obtained in an effort to isolate aerobic, thermophilic CO-oxidizing bacteria because few aerobic and thermophilic carboxydotrophs or carboxydovores (terms to differentiate CO-oxidizing microorganisms growing with elevated and low concentrations of CO, respectively) have been described (Gadkari *et al.* 1990; King and Weber 2007). The strain was a member of the family *Bacillaceae*. Although the isolate could tolerate more than 90% CO in the headspace without significant growth inhibition, it could not utilize CO as a carbon or energy source. One of the features that differentiated the strain from its phylogenetic neighbors was the negative catalase reaction (Tables 4.1 and 5.1). Transmission electron microscopy revealed the cells of strain JW/WZ-YB58^T contained two types of unusual cytoplasmic inclusions of unknown nature and function (Fig 4.2b). Failure to isolate aerobic CO-oxidizing thermophiles suggests this metabolism type is uncommon in thermophiles of the Uzon to relative to their anaerobic counterparts. In Chapter 6, efforts were made to elucidate the carbon fixation mechanism and associated carbon isotope fractionations between different carbon pools for the model anaerobic CO-oxidizing hydrogenogen *Carboxydothermus hydrogenoformans*, which was originally isolated from a Kamchatka hot spring. Time series isotope data from a series of batch cultures suggested that both CO and CO_2 provide carbon sources for bacterial growth. Surprisingly, both $\delta^{13}C$ values for CO and CO_2 were depleted over time relative to the initial values in multiple cultures (Figs 6.2 and 6.3). A feedback system therefore was proposed based on the reductive acetyl-CoA pathway (also called Wood-Ljungdahl pathway; Figs 6.1 and 6.4). Further, a steady state was hypothesized for carbon isotope compositions of CO, CO_2 and biomass with $\delta^{13}C$ values of *ca.* -

45, -27, and -25‰, respectively, as being observed in multiple bottles (Fig 6.2). Based on this steady state, it is further hypothesized that the isotope fractionations for the CO, CO_2 and biomass system are 18‰ between CO_2 and CO ($\varepsilon_{CO_2\text{-}CO} = \varepsilon_{OX}$), 2‰ between biomass and CO_2 ($\varepsilon_{Bio\text{-}CO_2} = \varepsilon_{CO_2F}$), and -20‰ between CO and biomass ($\varepsilon_{CO\text{-}Bio} = \varepsilon_{EXCH} - \varepsilon_{COF}$).

Chapter 7 focused on diversity and distribution of ammonia oxidizing archaea (AOA) in slightly acidic hot springs of the Uzon Caldera, an environment that has few reports about the occurrence of AOA. Surprisingly, AOA were present in high temperature and slightly acidic hot springs. Three major phylogenetic clusters were identified. Two of them were grouped within two widespread crenarchaeotal groups 1.1a (cluster 1) and 1.1b (cluster 2). An acid hot spring/soil clade unique to and predominant in the Kamchatka hot springs stood out as a third cluster (Fig 7.1). The distribution and diversity of the AOA phylotypes appeared to be dictated by the overall microbial structure and the abundance of archaea or crenarchaeota (Fig 7.4). Two AOA groups with distinct biological features were determined (Table 7.3): group A, which mainly contained less diverse *amo*A sequences, were associated with streamers containing high abundance of archaea; and group B, which contained samples comprised highly diverse *amo*A sequences, were present in all three clusters and associated with bacteria-dominant communities as indicated by low abundance of archaeal 16S rRNA gene copies (Fig 7.3). Phylotypes of AOA had the highest richness at low temperature end of Thermophile and Cascadnaya hot springs, which indicate that moderately high temperature conditions were more favorable for AOA than hyperthermal (>75°C) environments (Table 7.2). The archaeal lipid GDGTs showed the three springs were well separated despite the cross-spring patterning of AOA phylogeny, which indicated low abundance of AOA in the total archaea (Fig 7.5b). However, the wide occurrence of these organisms in contrast to the absence of AOB still suggests that AOA may be playing an important role in nitrogen cycle in Kamchatka hot springs.

The studies contribute to our knowledge of microorganisms and their metabolisms in hot springs of the Uzon Caldera from an ecological perspective. They complement advances in studies of conventional

microbiology and geochemistry and may enhance our understanding of terrestrial hot springs on a global scale.

REFERENCES

Gadkari D, Schricker K, Acker G, Kroppenstedt RM, Meyer O (1990) *Streptomyces thermoautotrophicus* sp. nov., a thermophilic CO- and H_2-oxidizing obligate chemolithoautotroph. Appl. Environ. Microbiol. 56:3727-3734

King GM, Weber CF (2007) Distribution, diversity and ecology of aerobic CO-oxidizing bacteria. Nat Rev Micro 5:107-118